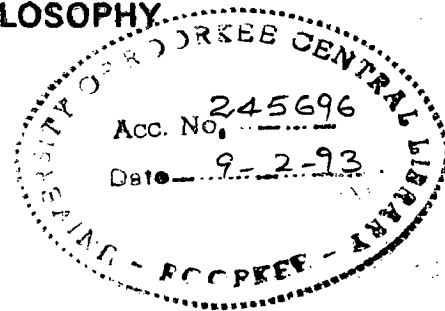


T  
F97-91  
GAU

# **CORROSION BEHAVIOUR OF STEEL IN AQUEOUS ENVIRONMENT OF BLEACH SECTION IN PAPER INDUSTRY**

**A THESIS**

submitted in fulfilment of the  
requirements for the award of the degree  
of  
**DOCTOR OF PHILOSOPHY.**



By

**BHUPENDRA GAUR**



**INSTITUTE OF PAPER TECHNOLOGY  
(UNIVERSITY OF ROORKEE)  
SAHARANPUR-247 001 (INDIA)**

**FEBRUARY, 1991**

UNIVERSITY OF ROORKEE

CANDIDATE'S DECLARATION

I hereby certify that the work which is being presented in the thesis entitled Corrosion Behaviour of Steel in Aqueous Environment of Bleach Section in Paper Industry in fulfillment of the requirement for the award of the Degree of Doctor of Philosophy, and submitted at the Institute of Paper Technology, Saharanpur of the University is an authentic record of my own work carried out during a period from March, 1987 to February, 1991 under the supervision of Dr.A.K.Singh and Professor N.J.Rao.

The matter presented in this thesis has not been submitted by me for the award of any other degree of this or any other University.



(BHUPENDRA GAUR)

Date 14.2.1991.

This is to certify that the above statement made by the candidate is correct to the best of our knowledge.




(A.K. SINGH)  
Lecturer  
Institute of Paper Technology  
Saharanpur, INDIA

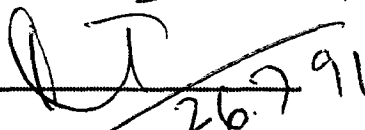


(N.J. RAO)  
Professor  
Institute of Paper Technology  
Saharanpur, INDIA

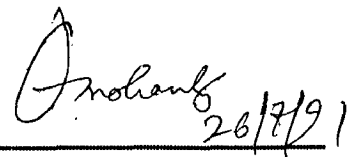
---

The Ph.D. Viva-Voce examination of Bhupendra Gaur, Research Scholar, has been held on 26.7.91.

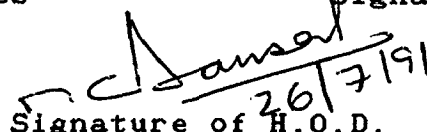
 26/7/91

 26.7.91

Signature of Guides

 26/7/91

Signature of External Examiner

 26/7/91

Signature of H.O.D.

## ACKNOWLEDGEMENT

A person, desirous to do investigations in an interdisciplinary area, always needs the support from various field personnels. I was initially introduced with the present subject by my supervisors. I express my sincere thanks, gratitude and indebtedness to my superiors - Dr. A.K. Singh and Prof. N.J. Rao (Ex-Director), for their valuable, inspirational, encouraging and meticulous guidance, creation of interest and thorough understanding of relevant fields. They provided me a lot of time in spite of their busy schedule. Of course, it is impossible for me to express my feelings in words for all kinds of help received from them throughout the duration of this work. Again, I am thankful to Dr. A.K. Singh for devoting long hours when I performed laboratory tests and analyzing results in every season in spite of his critical family circumstances.

I am highly obligated to Prof. M.C. Bansal, Director of the institute, for allowing me to avail all kinds of laboratory facilities and administrative helps during the research work.

I express, a lot of thanks and indebtedness to Dr. S. Kumar, Lecturer at the institute, for his guidance and fruitful suggestions in chemical analysis. I am also highly obliged to Dr.V.K.Tewari, Reader, Department of Metallurgical Engineering, of the University, for introducing me with the corrosion experiments and micro-structure determinations.

I also thankfully acknowledge the managements of M/S Seshasayee Paper and Boards Ltd., Erode, and M/S Ballarpur Industries Ltd., Yamunanagar, for permitting to perform mill studies, which form an important part of this dissertation. Dr.A.R.K.Rao, Vice-President (Technical) and Dr.M.B.Jauhari, Asstt. General Manager (R&D) of the respective mills provided all possible cooperations during mill tests, for which I am indebted to them.

Thanks are also due to Prof. Mohammed Ajmal, Department of Applied Chemistry, Aligarh Muslim University for extending their laboratory facilities for a part of the electrochemical studies.

Obligations are also due to Sri V.K.Singh, Assistant Manager, R&D, Steel Authority of India Limited, Ranchi, for helping in the determination of chemical composition of stainless-steels in their laboratory.

I express my appreciations to Prof. Desmond Tromans, Department of Metallurgy and Materials Science, University of British Columbia, Vancouver, Canada, for giving useful comments and suggestions on the electrochemical studies. Thanks are also due to Dr.L.Häggstrom, Uppsala University, Sweden for recording low temperature Mössbauer spectra.

During my stay at institute hostel, fortunately, I found an entertaining, encouraging and cooperating company of my juniors. Being missing many names, I would like to express my gratitude and affection to Susanta, Vijay, Pankaj, Mahesh, Raghavir, Sunil, Manoj, Anil, Chawla, Vipin, Saleem, Sanjay and Anan.

At last, but not the least, I am highly obligated to Department of Science and Technology, Government of India and Council of Scientific and Industrial Research, New Delhi, for providing me fellowships, and getting rid of worries of finance during the Ph.D. work. The credit of figures drafting goes to Mr.S.S.Thakur and typing to Mr. D.P. Singh.

*Bhupendra Gaur*  
(Bhupendra Gaur)

**Dedicated to the cherished feet  
of Sri Chen Sukh Gaur  
my beloved grandfather  
whose memory has been of  
continuous inspiration**

## S Y N O P S I S

The work presented in this thesis pertains to the corrosion behavior observed by commercial grades of mild steel and stainless steels in liquors of bleach section of paper industry. Other related aspects e.g. analysis of corrosion products formed in these metal-environment systems; cost-effective aspects of corrosion protection measures etc. have also been dealt with. The studies presented here involved laboratory tests and those performed in actual mill environment in two mills namely M/S Seshasayee Paper and Boards Ltd., Erode (Tamilnadu) (mill A) and M/S. Ballarpur Industries Ltd., Yamunanagar (Haryana) (mill B). Chapterwise summary of the thesis is presented in the following paragraphs.

### CHAPTER-1:

This chapter introduces the paper manufacturing process in brief. The process comprises of pulping, bleaching, recovery and paper making steps. In all integrated Indian paper mills Sulfate (Kraft) pulping process is used. Paper Industry in general is prone to corrosion attack which results in untimely loss or failure of machinery/equipment. A literature survey is given on corrosion in pulp and paper industry. The review includes calculation of annual cost of general corrosion and cost involved in adopting different corrosion control methods. On the basis of literature survey it was observed that bleach plant is responsible for approximately 50% of the total corrosion cost of

paper mill. Accordingly, the bleach plant was considered as an area for investigations.

Based on the above literature review, it is established that the washer section of bleach plant is one of the heavy corrosion areas and a little information is available on actual plant performances with respect to corrosion rates, the nature of corrosion and corrosion products etc. Accordingly, the following plan of work was proposed to be taken up.

i. To obtain well formulated data on corrosion in mill environment using different types of materials. The data generation will include weight-loss measurements, pitting and crevice corrosion assessment, analyses of corrosion products using modern techniques. The performance in the vats and in the gaseous phases is to be studied individually. In order to correlate the corrosion data to environmental parameters, analyses of various mill process parameters will be made.

ii. To generate data on corrosion reactions in the aqueous media, laboratory based experiments will be conducted. The electrochemical tests using bleach liquor of varying compositions will be used to evaluate the electrochemical behavior.

iii. The results from mill and laboratory based experiments will be analyzed to understand the nature of corrosion, the mechanism of corrosion and the influence of the various parameters on the nature and rate of corrosion.



iv. Above results will be used to draw inferences for possible methods of minimizing losses due to corrosion either by using a more suitable material or by control of process parameters, using possible protection methods etc.

## CHAPTER-2:

This chapter deals with the various experiments performed in the present study. The experiments were carried out at two mill locations and in the laboratory. The materials used in corrosion studies for both mill and laboratory experiments included mild steel and five different types of stainless steels. The composition of materials used in the studies was determined by chemical and optical emission spectroscopic methods. Rectangular coupons were prepared from plane sheets for weight-loss measurements and cylindrical samples were made from rods for electrochemical studies. These were suitably ground, polished, degreased and finally cleaned ultrasonically before mounting them. For mill studies the coupons were fitted in polymer racks while they were hung by a polymer thread in the flasks for laboratory studies.

Mill tests were conducted at two mills namely M/S Seshasayee Paper & Boards Ltd., Erode (Tamilnadu) and M/S Ballarpur Industries Ltd., Yamunanagar (Haryana). The studies were conducted by putting the coupons in the vats for aqueous media and near sprays for gaseous environment. The conditions maintained in the mill, the characteristics of liquors used and time of exposure were

carefully noted. It is interesting to mention that in one of the studied mills, the liquid environment had sulfamic acid additions. This required some experimentations for finding the effect of sulfamic acid on corrosion behavior.

For the laboratory tests, liquor was prepared from the bleach liquor available in a nearby paper mill to give a varying concentration of free available chlorine from 150-600 ppm. The pH was maintained  $\approx$  8-9 and in some experiments sulfamic acid was added to the tune of 10 - 30 ppm. The corroded coupons both from the mill and the laboratory exposure for varying durations were subjected to weight-loss determination. The rusts scraped from mill corroded coupons were analyzed for the product identification by X-ray diffraction and Mössbauer spectroscopy both at room and low temperature.

The above performed laboratory and mill studies give only the relative performance of tested materials, effect of various process parameters on corrosivity, corrosion rates and nature of attack but do not help in understanding the reaction mechanism undergoing on metallic surface. Therefore, it needed to carry out electrochemical polarization studies in the discussed metal-environment system. In these studies mild steel and four types of stainless steel namely, 304, 304L, 316 and 316L were tested in solution of sodium chloride and bleach liquor of varying free available chlorine concentration with and without sulfamic acid addition. Tafel plots and linear polarization measurements were

made using the experimental set-up consisting of corrosion cell, Potentiostat/Galvanostat, Logarithmic current converter, Universal Programmer and Saturated Calomel electrode etc. (all of E G & G PARC, U S A make).

### CHAPTER-3:

This chapter deals with (i) the tests performed on steels by exposing them in actual mill environments (ii) the analysis of corrosion products/scale formed on corroded coupons. Field corrosion studies were performed at two mills, mill A and mill B as indicated above. The fibrous raw materials used by the first mill are hard wood and non-wood (mainly bagasse) and that by the second mill are a mixture of eucalyptus, pine and bamboo. Bleaching section of mill A consists of three stages namely chlorination (C), buffered-hypo (B) and hypochlorite (H) while that of mill B are chlorination (C), hypochlorite-1 (H1) and hypochlorite-2 (H2). Rectangular coupons of mild steel were initially put for exposure in C, B and H stages inside vats (liquid media) and near shower pipes (gaseous media) for a duration of 15 to 45 days at mill A. The coupons experienced heavy corrosion loss at chlorination washer shower pipes while those exposed in hypochlorite vat minimum. In another mill test, mild steel and five types of austenitic stainless steel racks were put for exposure in C, H1 and H2 washers in vats and near shower pipes in mill B. The duration of exposure was three months. Similarly, racks of coupons consisting of five same types of stainless

steels were exposed in C, B and H stages in vats and near shower pipes of mill A for a duration of six months. The process parameters responsible for aggressiveness of environment were monitored continuously at regular intervals. Lastly, a mill exposure study was also conducted on mild steel and five same types of stainless steels in bleaching section of mill B in wet / dry cyclic exposure conditions for a duration of three months for comparison of results. After completing the exposure, the cleaned coupons were assessed for localized attack and corrosion rates were also calculated. Pitting, crevice corrosion and corrosion rates were the basis for comparison of corrosivity of various stages. Crevices were formed due to PVC spacers used in racks to separate coupons from each other. Aggressivity was compared with respect to the material composition and environmental parameters e.g. available chlorine, pH, chlorides and sulfamic acid. Comparison of liquid and gaseous phases, liquid and liquid phases for same and different stages were also made. The categorization of pitting and crevice corrosion was made on the basis of estimation of fraction of exposed surface area experiencing localized attack. A comparison of Indian mills with those of American and Scandinavian mills is also given although process sequence used by those mills is different from that of Indian mills. It has been discussed in terms of practice of recycling the filtrates by the latter mills. In chlorination stage mild steel corrosion rates have shown reverse trend in comparison to stainless steels. Generally chlorination gaseous phase is most corrosive in both the mills and none of the tested materials can

be used in this stage. Corrosion behavior of materials in wet/dry cyclic exposure are generally more closer to the vat conditions. If one compares the corrosivity at two mills, mill A is highly aggressive than mill B. This behavior has been explained on the basis of difference in process parameters. In general, 316L performs best in most of the stages of both mills.

The analysis of corrosion products/scales formed in various stages on mild steel on the basis of X-ray diffraction and Mössbauer spectroscopy (of room temperature and low temperature) shows iron oxides and oxyhydroxides. One stage of mill A shows the presence of calcite ( $\text{CaCO}_3$ ) only. All rust samples obtained from mild steel coupons exhibit superparamagnetism effect due to fine particle size. Corrosion products identified mainly are  $\text{Fe}_{3-x}\text{O}_4$  and  $\alpha\text{-FeOOH}$  ( $\approx 85\%$ ) while  $\gamma\text{-FeOOH}$  appears as minor phase. In one case mild steel exposed to chlorination washer shower pipe, the rust components are observed to be  $\text{Fe}_{3-x}\text{O}_4$  and  $\beta\text{-FeOOH}$ . An attempt has been made to find a correlation among corrosivity of environments and non-stoichiometry of  $\text{Fe}_3\text{O}_4$  and  $\alpha\text{-FeOOH}/\text{Fe}_{3-x}\text{O}_4$  ratio. Corrosion products obtained from stainless steel coupons show presence of Ni, Cr, and Fe compounds as analyzed by X-ray diffraction. The type of products obtained differ in case of the two mills.

#### CHAPTER-4

In this chapter, an account has been given of weight-loss and electrochemical tests performed in laboratory to understand

corrosion behavior of steels. To begin with, justification has been given for doing such tests and for selecting the particular liquid media. On the basis of process parameters values obtained from the two mills (during weight-loss test) their average ranges were assessed. Accordingly the conditions for laboratory tests were fixed. Most significant parameters were observed to be available residual chlorine and pH. Chloride has a secondary effect as it breaks the passive film formed by the oxidants and results in the increased corrosion. Therefore, mild steel coupons were initially exposed in chloride concentration of 200 to 3000 ppm, which did not show any significant change in corrosion rate in the studied range. Second test was performed in bleach liquor having free available chlorine concentration 150 to 600 ppm at constant 1000 ppm chlorides and pH 8 - 9 (the approximate pH value observed in hypochlorite washers). Test shows an increase in corrosion rate with concentration of free available chlorine. One of the studied mills is adding sulfamic acid as buffer and descalant. To show its own effect on the corrosivity of process liquor, weight-loss tests in bleach liquor having small contents of sulfamic acid were also performed which showed that corrosion rate decreases with concentration of sulfamic acid in presence of bleach liquor in the studied ranges. Weight-loss studies were also performed on stainless steels but because of very low corrosion rates it is difficult to visualize any trend on performance.

To understand the mechanism of corrosion reactions occurring on metallic surface electrochemical polarization studies i.e. Tafel plots and polarization resistance measurements were made on mild steel and four types of stainless steels in bleach liquors. Experiments were also done in presence of sulfamic acid in bleach liquor. Experimental Tafel plots are tried to be fitted for cathodic parts. Reactions responsible for cathodic polarization parts of Tafel curves are discussed and electrochemical parameters e.g. Tafel slopes, exchange currents, limiting currents and electrode potentials for those reactions have been predicted. With the help of polarization resistance measurements and Tafel plots, corrosion rates have been calculated for some cases. In case of mild steel, obtained rates from weight-loss and electrochemical polarization methods have been compared. In case of mild steel, obtained rates from weight-loss and electrochemical polarization methods have been compared. In case of stainless steels, metal is considered as one redox system. Mild steel does not give any Tafel slope region, even on stirring the solution, since concentration polarization interferes at the high current densities. Cathodic reactions in case of both mild steel and stainless steels are same. Tafel plots drawn from stainless steels show Tafel region when solutions are stirred. Polarization resistance measurements showed good linearity and their slopes have been calculated. Anodic part of the plots is not fitted since in most of the cases passive behavior region had started. Mechanism of mild steel and stainless steels seems to be signifi-

cantly different in terms of anodic reaction part. Observed equilibrium potentials of steels were positive in presence of hypochlorite liquors but currents were higher in comparison to the curves drawn in water and chloride environment. The effect of sulfamic acid addition in bleach liquor on polarization curves and hence on electrochemical reactions has also been discussed.

### CHAPTER-5

This chapter describes the conclusions drawn on the basis of different tests described in the thesis. Mill tests show highly aggressive environment in chlorination section. The tested steels experience severe localized corrosion in gas phase of all stages at mill A and chlorination stages at mill B, thus making them uneconomical for use. In liquid media (vats), however, even 304 can be used after taking due precaution against crevice attack. Analysis of corrosion products formed on mild steel in above environments, show  $Fe_{3-x}O_4$  and  $\alpha$ -FeOOH/ $\beta$ -FeOOH with  $\gamma$ -FeOOH as minor phase. It was possible to establish a correlation of the nature of corrosion products with corrosivity. Laboratory tests show that  $Cl^-$  ions do not affect the corrosivity of bleach liquor much but molecular chlorine does. Sulfamic acid shows inhibition effect in bleach liquor. Electrochemical tests performed in above metal-environment system help in generating electrochemical parameters and in understanding the corrosion behavior of steels.



This Chapter further discusses possibilities of working in this area in future. It is observed that in some stages even the best available steels are not economical to use. As such tests should be performed on other special alloys e.g. high Mo steel, nickel alloys etc. Tests should also be performed to see the suitability of different types of commercially available polymers/FRP's. This has to be done in view of the possibility of adopting filtrate recycling as a pollution control measure. Further, tests have to be performed in presence of chemicals of newer bleaching process e.g.  $\text{ClO}_2$ , peroxide, ozone etc. As an alternative corrosion protection mechanism, viability should be seen for developing the electrochemical protection system. Hence passivation behavior of various metallic materials should be tested in different bleach media.

## LIST OF RESEARCH PAPERS

1. A study of Steel Corrosion in Bleaching Environment of Pulp and Paper Industry.  
10th International Congress of Metallic Corrosion (Madras) Vol.III: Nov.7-11,1987 pp 2519-2528.
2. Investigations into Bleach Plant Corrosion Problems.  
IPPTA 24 No.3 (1987) pp 42-47.
3. Stainless-Steel Corrosion in Paper Mills Bleach Plant Washers.  
Presented and to appear in the proceedings of National Seminar on " Alloy Design and Development" held at Met. Engg. Deptt., University of Roorkee, Roorkee, March 10-11, 1989 .
4. Corrosivity of Environment and Material Performance in Bleach Plant Washers.  
Tappi Journal 73, No. 1 (1990) pp 67-71 (U.S.A.).
5. Analysis of Rusts Formed on Mild Steel in Pulp Bleaching Section.  
Corrosion Science (England)  
( In press for printing )
6. Steel Corrosion in Bleach Plant Washers.  
APPITA (Australia).(communicated)
7. Corrosion of Mild Steel in Hypochlorite Solution -  
An Electrochemical and Weight-loss study.  
Material Science and Technology (England) (communicated)
8. Electrochemical Study of Steel Corrosion in Bleach Liquor.  
Corrosion Science (England) (communicated)

**LIST OF CONTENTS**

<b>CHAPTER</b>	<b>PAGE NO.</b>
1. INTRODUCTION.	2
2. EXPERIMENTAL TECHNIQUES AND PROCEDURES.	51
3. ANALYSES OF CORROSION ON STEEL COUPONS EXPOSED IN BLEACH PLANTS.	90
4. ANALYSES OF CORROSION BY LABORATORY TESTS.	160
5. CONCLUSIONS AND RECOMMENDATIONS.	196

## **Chapter-1**

### **INTRODUCTION**

	<b>Page No.</b>
<b>1.1 Pulp and Papermaking Process.</b>	<b>4</b>
<b>1.1.1 Pulping.</b>	<b>5</b>
<b>1.1.2 Recovery.</b>	<b>7</b>
<b>1.1.3 Bleaching.</b>	<b>8</b>
<b>1.1.4 Papermaking.</b>	<b>13</b>
<b>1.2 Corrosion in Pulp and Paper Industry.</b>	<b>15</b>
<b>1.2.1 Kraft Pulping Process.</b>	<b>16</b>
<b>1.2.2 Chemical Recovery.</b>	<b>18</b>
<b>1.2.3 Paper Machine Section.</b>	<b>21</b>
<b>1.2.4 Bleach Section.</b>	<b>23</b>
<b>1.3 Definition of the Problem with Justification and Objectives.</b>	<b>30</b>
<b>1.4 Corrosion Phenomenon.</b>	<b>32</b>
<b>1.4.1 Types of Corrosion Damages.</b>	<b>32</b>
<b>1.4.2 Evaluation of Corrosion.</b>	<b>37</b>
<b>1.4.3 Electrochemical Principles.</b>	<b>40</b>

Corrosion is a reaction undergoing on a metal/non-metal surface due to the chemical media ( gaseous and liquid both ), temperature and pressure of surroundings. All three of these could be responsible independently or collectively for the observed degree of corrosion. Corrosion is of concern as it weakens the materials and hence is responsible for unscheduled shutdowns, maintenance ,repair and replacement costs, catastrophic failures etc. At the same time , corrosion reaction begins and continues, by nature, on its own not requiring any catalyst or external energy. Rate at which material is lost, due to corrosion, may not be always alarming. However, wherever this rate is significant , it is necessary to take precautionary measure to minimize its ill effects. In all such cases, taking these measures at right time results in saving of significant amount of money which otherwise would be drained due to corrosion reactions. However, it is necessary to have an adequate understanding of corrosion phenomenon for taking such precautionary steps.

Corrosion in process industry is a cause of concern. Paper industry is no exception to this observation. Corrosion in different sections of a paper mill has resulted in significant loss of money. This is also one of the first industries which started using stainless-steels widely in different sections - a parameter which indicates high corrosivity of media prevalent in this industry. The thesis deals with the work done on corrosion in bleach section of paper industry. The work of the thesis consists of both mill tests and laboratory tests. Mill tests were conducted in two representative Indian mills namely M/S Seshasayee Paper

and Boards Ltd., Erode and M/S Ballarpur Industries Ltd., Yamunanagar. Since a work of this nature needs an understanding of the process also, the initial part of this chapter gives a brief background of papermaking process. This is followed by an account of corrosion problems faced by different sections in brief and by bleach section in more detailed form as this forms the subject matter of the present dissertation. Based on this, the dissertation problem has been defined giving due justification and objectives. Lastly, some fundamental aspects of corrosion phenomenon have been discussed. Accordingly, this chapter has been divided into the following sections :

1.1 Pulp and Paper making Process.

1.2 Corrosion in Pulp and Paper Industry.

1.3 Definition of the problem with justification and objectives.

1.4 Corrosion Phenomenon.

These subsections are now discussed onwards.

### 1.1 Pulp and Paper Making Process

Paper is a felted sheet of fibers formed on fine screen from water suspension. These fibers are obtained from wood/non-wood species. The paper making process, therefore, essentially involves the pulping of wood/non-wood species in order to remove lignin, responsible for binding the fibers. Thus obtained delignified fibers after passing through several stages e.g. bleaching, beating, stock preparation etc. are spread into the form of felted

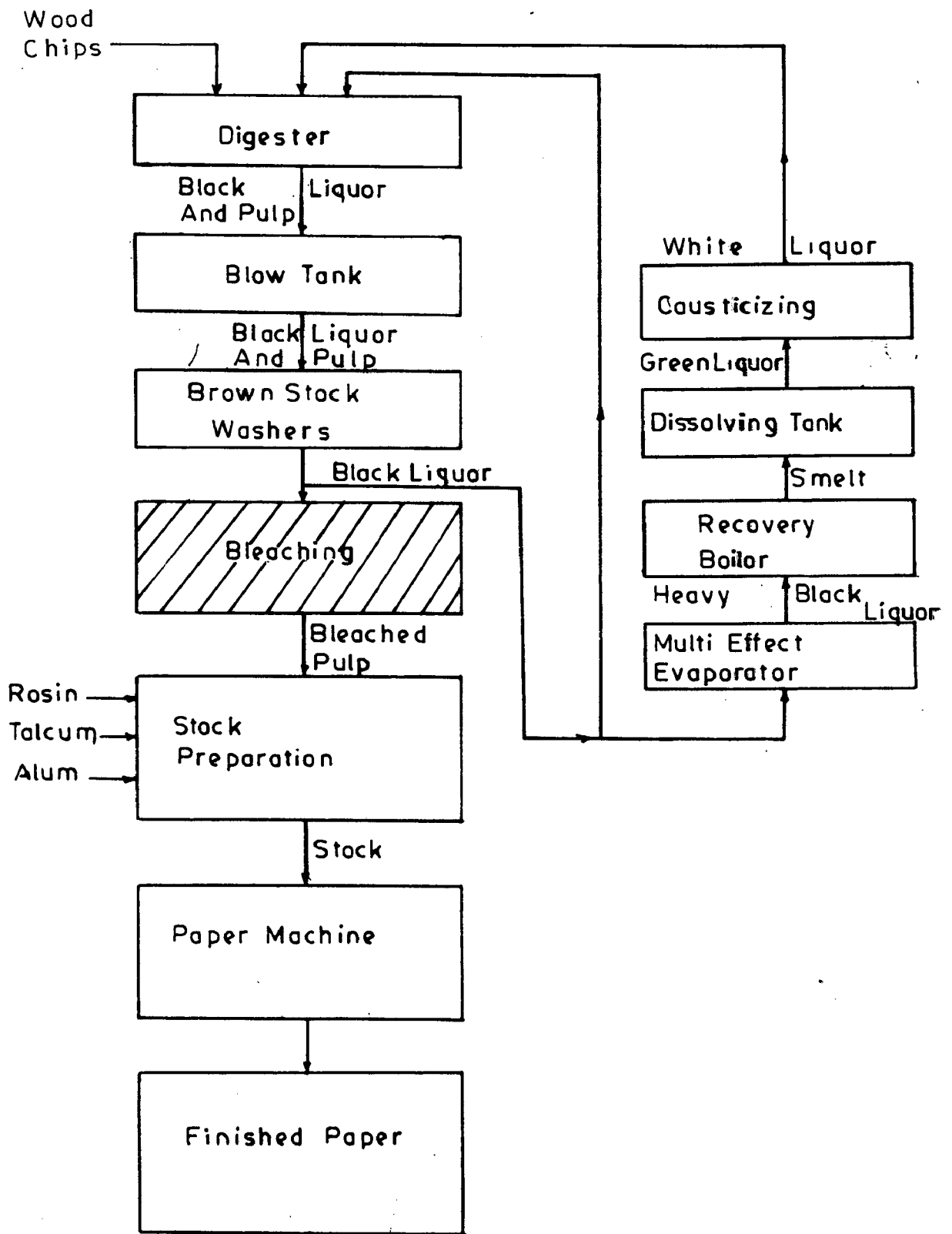


FIG.1.1: KRAFT PAPER MAKING PROCESS

sheet. This sheet after water removal in several stages, turns into the final product commonly known as 'paper'.

Major plant sources of fibers are coniferous woods (softwood), deciduous wood (hardwood) (amounting to 93%), straw and grasses, canes and reeds, bamboos, wood stalks with bast fibers, bast, leaf, and seed fibers (amounting to 7%) (1). In Indian paper industry, bamboo is used mostly (61%). Hardwoods (27%), agricultural residues (5%), waste paper (5%) and softwoods (2%) are used in various low percentages (2). Among hardwoods various types of eucalyptus are used.

The paper making process can be discussed in following parts with reference to Fig.1.1:

1.1.1 Pulping (1,3,4)

1.1.2 Recovery (1,3,4)

1.1.3 Bleaching (1,5,6)

1.1.4 Paper Making (1)

1.1.1 Pulping

After debarking, the logs are reduced to chip fragments. These chips are transported then for pulping, a process which selectively removes lignin with minimum deterioration of cellulose. Different types of pulping process are : kraft (sulfate) pulping, soda process and soda-anthraquinone pulping (chemical) and neutral sulfite pulping (semi-chemical).

The kraft process is the most popular among the pulping processes. White liquor, used for cooking chips, contains



sodium hydroxide and sodium sulfide in the approximate proportions (5 NaOH + 2Na<sub>2</sub>S) and has pH of 13.5 to 14.0. It also contains sodium sulfate, sodium thiosulfate, polysulfides etc. In aqueous solution the sodium sulfide reacts with water according to the equilibrium



NaSH thus formed involves in delignifying reaction together with NaOH.

Pulping is carried out in a vessel called 'Digester'. Generally two types of digester are in use (a) continuous and (b) batch types. In Indian mills mostly batch digestion is used. Batch digesters are normally vertical cylinders constructed of steel plate. The cooking cycle in the sulfate process requires about 3 to 4 hrs, using 14 to 20% active alkali, 20 to 30% sulfidity, and heating for 90 to 120 minute at 165 to 170°C at a pressure of around 6.5 - 7 Kg/cm<sup>2</sup>. The maximum temperature is typically reached after 1 to 1.5 hrs, which allows the cooking liquor to impregnate the chips. The cook is then maintained at maximum temperature (≈ 170°C) for 1 to 2 hours to complete the cooking reactions. After cooking, the softened chips are blown into a tank, where the force of ejection breaks up the chips into individual fibers. This is known as "pulp". The pulp is transferred to the brownstock chest and then to vacuum washers where it is washed thoroughly. Pulp then passes through various stages to remove large fragments such as knots and undercooked chips, and finally it goes to the stock tanks.

### 1.1.2 Recovery of Chemicals & Heat:

The steam and the other vapors from the blow-tank are condensed thus conserving heat in the form of warm and condensed water which is used in washing the pulp. The liquor obtained after washing of pulp is known as the black liquor. This liquor is evaporated to a solid content of 60 to 70%. The resulting viscous black mass is made up with chemicals usually sodium sulfate (salt cake), which is added in the range of 40 to 75 Kg per tone of pulp. The concentrated black liquor is fired to the recovery furnace, where the organic components from the wood burn and evolve heat to generate steam and produce carbon dioxide which is absorbed predominantly by alkaline residue to form sodium carbonate. Thus a molten mass of sodium carbonate and sodium sulfide remains. It contains as impurities small quantities of sodium sulfate, sulfite, and thiosulfate. The green liquor, produced by dissolving this mixture in water, is treated with a suspension of calcium hydroxide (slacked lime) to convert sodium carbonate back into sodium hydroxide, thereby producing white liquor for reuse in the pulping. The resulting precipitate of calcium carbonate is heated, in kiln to produce quicklime, which is slaked with water to furnish calcium hydroxide for further use. This is, however, not practiced in Indian mills. The white liquor produced by the recovery system is mixed with some black liquor (10-50%) before being charged to the digesters. Black liquor is used to attain the required liquor-to-wood ratio (bath ratio) without adding water.

### 1.1.3 Bleaching:

The main objective of bleaching is to increase the brightness of pulp and to make it suitable for the manufacturing of printing, tissue and several other grades of papers. Each bleaching stage essentially consists of three major steps (5): (i) mixing of the pulp with chemicals and heating, (ii) retention of the mixture and (iii) washing of pulp after reaction to remove the impurities released by the chemical reaction together with the excess of the bleaching chemicals. Bleach plants vary from a single stage to as many as nine or more stages. Different bleaching stages are chlorination (C), alkaline extraction (E), hypochlorite (H), chlorine dioxide (D), oxygen (O), peroxide (P), etc. The selection of a particular sequence is determined by: (i) the nature of the fiber species to be bleached, (ii) the pulping process, (iii) end use of bleached pulp, and (iv) the environmental limitations. In India, most of the integrated pulp and paper mills are using CEH or CEHH bleaching sequence. A complete bleaching flow diagram is shown in Fig. 1.2.

#### (a) Bleaching stages :

##### - Chlorination :

When chlorine is dissolved in water, it undergoes a reversible hydrolysis as per the following reaction:



HCl and HOCl dissociate as follows





whereas the dissociation of hydrochloric acid is completed in dilute aqueous solution, that of hypochlorous acid is only partial at the pH of chlorine water. The pH controlled changes in composition are as shown in Fig. 1.3. Thus molecular chlorine predominates only below pH 2, hypochlorous acid between 2 and 7.5, and hypochlorite ions ( $\text{OCl}^-$ ) above pH 7.5.

In the chlorination reaction major portion of residual lignin is degraded and converted into water or alkali-soluble products with little detriment to carbohydrates. Chlorination is usually carried out at relatively low consistency (2.5 - 3.5 %). Mills using fresh water carry out chlorination at 20 to 30°C, while those utilizing recycling, at 60°C. At higher temperature, less retention times are required. Most existing chlorination towers are of fixed retention time, requiring between 45 to 90 minutes under normal operating conditions. The chemical amount used is usually about 75 to 80% of the full "chlorine demand", as indicated by the permanganate or Kappa number. Hypochlorous acid is generally regarded as destructive to cellulose and therefore, bleaching within the pH range 2 to 9 is usually avoided. After chlorination, the pulp is washed thoroughly on rotary drum washer to remove HCl and water soluble lignin compound and sent to alkali extraction stage.

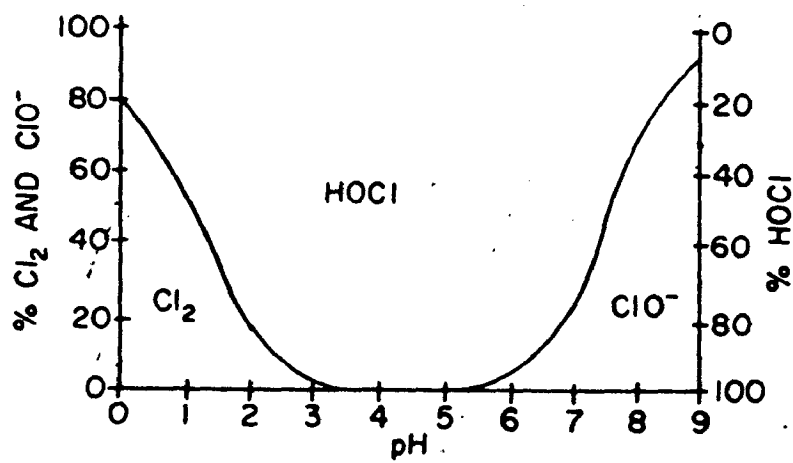


FIG.13: FORM OF CHLORINE AT DIFFERENT pH.

#### - Alkaline Extraction:

In this stage, removal of chlorinated and oxidized lignin, water insoluble organic acids is accomplished by solubilization. The extraction is carried out at high consistency (12 to 15%) at temperature between 60 and 80°C, and with the retention time upto 2 hrs. The final pH should be above 10.8, otherwise the solubilization will be incomplete. The caustic application is equal to 60% of the chlorine application. Efficient washing following chlorination is important to save alkali consumption. Alkaline extraction, at a later stage of a multi-stage sequence, serves to remove colored and degraded products and "open up" the fiber for more effective treatment in the subsequent oxidation stage.

#### - Hypochlorination:

Residual lignin not removed during the pulping process is largely responsible for the color of unbleached pulps. Chlorination and alkaline extraction remove a large amount of this lignin, but sufficient amounts of lignin and lignin derivatives still remain. In hypochlorite bleaching, pulp is brightened by the destruction and removal of the residual lignin and its derivatives. The ability of hypochlorite to remove lignin depends upon the wood species, pulping process and the degree of cooking. Hypochlorite bleaching is carried out at 35 to 45°C with a retention time of 1 to 2 hrs. Modern bleach plants operate at 10-12% consistency. Alkali is added with the hypochlorite solution to ensure that terminal pH is 9.0 or higher so that attack on cellulose is avoided. Calcium hypochlorite is used more extensively than

sodium hypochlorite for bleaching.

- Chlorine dioxide :

All high brightness kraft pulps are obtained by bleaching with chlorine dioxide. It is highly selective in destroying lignin without significantly degrading cellulose. Initially, chlorine dioxide stage was latter stage in multi-stage bleaching e.g. CEHDED or CEDED. Now it is also being used partly for replacing chlorine in the first stage to improve strength and color stability and reduce color effluents. In this stage, chlorine dioxide solution is mixed in heated stock at 70 - 75 °C. Retention time is controlled between 2 - 4 hours. Excess chlorine dioxide is usually neutralized with SO<sub>2</sub> or NaOH to eliminate toxic fumes and reduce corrosion during subsequent washing stages. Chlorine dioxide usually has 2.5 times more oxidizing power than that of chlorine. A terminal pH of 3.5 - 4.0 is recommended for optimum chemical usage in the first dioxide stage. However, a somewhat higher pH (5.5 - 6) has been found to provide highest brightness from second chlorine dioxide stage.

- Oxygen:

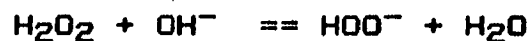
In this bleaching, alkaline oxygen stage delignification is used prior to bleaching with chlorine chemicals. Most commercial oxygen bleaching is carried out at high consistency ( 20 - 30% ) pulp when gaseous oxygen at 80 - 100 psig is continuously dissolved into liquid phase and reacted with pulp. Temperature is usually kept between 90 - 130 °C, retention varies from 20 - 60 minutes and application of NaOH is between 3 - 7% of pulp. Small



amount of magnesium salt is mixed (0.1 - 0.5% of pulp) to minimize the degradation of cellulose. The latter restricts delignification to only about 50%. Recently 'low consistency' oxygen pulping is in use. In this process, the hot stock at 110 - 150 °C and 3 - 5% consistency is mixed with gaseous oxygen and caustic. This process allows upto 80% delignification, without magnesium protector.

#### - Peroxide :

Peroxides are used in the bleaching of both high yield and chemical pulps. This type of bleaching is strongly affected by pH, which must be adjusted and buffered at  $\approx 10.5$  for best results. The concentration of active perhydroxyl ions increases with pH as per the following reaction :



pH is usually controlled by addition of NaOH and sodium silicate. Although high temperature accelerates bleaching reaction, but the stability of peroxide is severely affected. Peroxide bleaching of chemical pulps is expensive than chlorine dioxide and hence is not very popular. It appears to have an application in the brightening of high yield pulp.

#### (b) Bleaching Equipments:

There are four basic elements of each bleaching stage (i) conveyance of pulp (ii) equipment to mix pulp, chemicals etc. (iii) a retention vessel and (iv) washer (3).

- Pulp conveyance :For low consistency (upto about 5%) ordinary stock pumps are used.In case of high consistency , the pulp is conveyed by gravity from the washer of the preceding stage to the mixer of the following stage. Lately however, thick-stock pumps have found application.

- Mixers : Wobble plate unit, accomplishes the mixing by means of two rotating perforated plates mounted at angles on the drive shaft. The mixer utilizes a low head, high capacity pump.

- Retention vessel: Three types of towers made of concrete and tiles are in use. One of these is, an upflow launder discharge unit where the stock enters at the bottom and moves upward with the help of pumps.For high consistency retention downflow and upflow towers and combinations of both are in use.

- Washers :The stock is generally diluted to 0.5 to 1.5% consistency before entering the washer vat. On its way over the drum the mat is sprayed with fresh water, which may be heated, and then enters the shredder -conveyor at about 10 to 20% consistency, depending on whether or not press rolls are used. Each washer requires a seal box to act as a separator for entrained air and to serve as a filtrate reservoir.

#### 1.1.4 Paper Making

##### (a) Preparation of Stock:

The objective in stock preparation is to process the bleached pulps and non-fibrous components (additives) to convert

into papermaking furnish. The fibers are first subjected to beating and refining by mechanical action to develop their optimal papermaking properties. Afterwards the pulp components are metered into machine stock chest at a consistency level between 2.8 and 3.2%. Deflaking and refining are usually carried out at intermediate consistency levels. In the next stage, a wide variety of chemicals and mineral additives are mixed to impart specific properties to the paper product. These are (i) Alum for controlling pH, fixing additives onto fibers and improving retention (ii) Sizing Chemicals e.g. rosin, wax etc.- added to increase resistance of paper products to penetration by fluids (iii) for imparting internal strength to paper sheet e.g. starches and gums (iv) Wet strength resins e.g. urea formaldehyde, melamine formaldehyde etc.- to impart strength to paper when immersed in water or aqueous solution. Wet strength paper is defined as such if it retains more than 15% of its tensile strength, however, some papers may retain upto 50% strength while they are wet. (iv) Fillers or Loadings- added to improve the optical and physical properties of the sheet. These produce a denser, brighter, smoother and more opaque sheet. The most common papermaking filler are clay (Kaolin), calcium carbonate, talc and titanium dioxide (v) Control dyes etc.

#### (b) Paper Machine Section:

The 'stock', prepared as mentioned above, passes through various stages of water removal, which in turn helps in developing fiber-to-fiber bonding and thereby forming the paper sheet. Different stages in papermaking are (i) Low Spreads and Headboxes

to transform the pipeline flow of stock into a uniform, rectangular flow equal in width to the paper machine and to adjust its rate of flow and thickness of paper sheet (ii) Wire part (Four-drainer) - required for initial water removal by drainage, section (iii) Pressing - to remove water further to consolidate the web. Other objectives, may be to provide surface smoothness, reduce bulk, and promote higher wet web strength for good runnability in the dryer section (iv) Drying - to evaporate the residual moisture in the pressed sheet. Paper from the press section containing about 60% moisture (40% dryness) is dried upto a moisture content of about 3 - 10 % in this section (v) Calendering - general term meaning pressing with a roll. Primary objective to reduce sheet thickness to the desired level, even out caliper variations, and impart desirable gloss and other surface properties.

After drying and calendering the paper is collected in a convenient form for further processing. For this purpose, most modern machines are equipped with drum reels. From here paper is cut and wound in suitable sized rolls for dispatch to customer.

## 1.2. Corrosion in Pulp and Paper Industry (7,8)

Pulp and paper mills routinely face corrosive environments ranging from hot alkaline sulfide cooking liquors to acidic, highly oxidizing bleaching solutions. Molten salts attack water-wall tubes in chemical recovery boilers while condensates from flue gases attack electrostatic precipitator internals. Paper machine components are affected by localized corrosion,

fatigue and biological corrosion. Erosion-corrosion affects the life time of woodyard equipment, refiner plates and equipment for handling abrasive lime mud slurries. These mills are routinely challenged by virtually every known type of corrosion-related damage. The degree of corrosion is best illustrated by the fact that paper industry is one of the first industries which started using stainless steel extensively. In 1971, corrosion was estimated to cost the North American paper industry \$ 190,000,000/year (9) . A recent survey ,conducted in 1985 by NPC (10), shows an estimated loss, due to corrosion,of Rs. 100/- per ton of paper produced by Indian industry.To get a more detailed idea, we now discuss, specifically, various type of corrosion being faced in different sections of paper industry.

#### 1.2.1 Kraft Pulping Process:

The process equipment here include pressure vessels for batch or continuous digestion, rotary drum pulp washers, storage tank for various liquors, Ancillary equipment include pumps, valves, piping, heat exchangers, control instrumentation etc. Much of the equipment used in the kraft pulp mill is fabricated from plain carbon steel, although it has limited resistance to corrosion and cracking when exposed to kraft process liquors.

##### (a) Batch Digesters:

Corrosion damage in batch digesters appears in several forms, including uniform wastage, large gouges, pitting, and occasional cracking. In some cases, caused by steam impingement

during direct steam heating of the digester, by recirculating liquors, or by impingement of high velocity pulp slurries discharged at the end of cook. These include erosion corrosion of a blow target plate. Grooves are often found beneath blind nozzles and other areas where liquor/ saturated steam can lodge. Corrosion is often more severe in the bottom cone area where flow rates are higher during indirect heating and during blows. In some digesters, corrosion is most severe in the splash zone. Where cooking liquor splashes on the hot side walls during digester charging. Welds are often sites of preferential attack in batch digesters, including accelerated corrosion and occasional episodes of stress corrosion cracking (SCC). Digester life times were extended by the use of linings, and the specification of low-silicon steels.

The durability of stainless weld overlays has often been inadequate due to pitting, cracking and inter-granular corrosion. Consequently, mill operation often specify a higher chromium equivalent and lower carbon in the as deposited overlay.

#### (b) Piping and Ancillary Equipment:

Carbon steel piping is subject to corrosion and erosion corrosion in the kraft pulp mill, but is often chosen for economy. Elbow in blow lines and other areas of high abrasion are particularly susceptible to attack. SS-304L is effective in controlling corrosion damage in piping. Pump impellers, pump casings, and valves made from cast CF-8M are usually resistant to attack by kraft liquors. Corrosion and transgranular cracking have

been encountered in SS tubes in shell and tube heat exchangers used to heat recirculating liquors. Caustic cracking and chloride SCC have both been observed. Cracking has been eliminated in many cases by the use of a duplex SS-3RE60 liquor heater tubes. Inconel heater tubes have also been successfully used.

### 1.2.2 Chemical Recovery:

Each stage of the kraft pulping recovery and recausticizing is beset with severe corrosion because of the aggressiveness of the white, green and black liquors. Although 18Cr-8Ni Stainless steels are usually fully resistant to corrosion by kraft liquors, most of the equipment in contact with kraft liquors are of plain carbon steel for economic reasons. In critical locations (such as evaporator tubes in high-temperature evaporator) stainless steel is routinely used. Brick and tile linings as well as sprayed on concrete linings are often found in recausticizing equipment, particularly where abrasion is a concern.

#### (a) Black Liquor Processing:

Corrosion in multiple-effect evaporator is usually controlled by the use of stainless steels in critical, high temperature applications. The heat transfer surfaces are usually fabricated from 18-8 stainless steel in the highest temperature effects, with carbon steel finding applications in lower temperature effects (usually less than 95°C). Corrosion in evaporators usually occurs due to hot black liquor.

**(b) Chemical Recovery Boilers:**

Chemical recovery boilers experience severe corrosion of carbon-steel tubes in the water-wall above the char-bed at the bottom of the surface. Water cooled smelt spouts used to discharge molten salts from the bottom of the boiler are also subjected to severe corrosion and thermal fatigue failure. Water-wall corrosion has been reduced by the use of studded tubes, thermal sprayed coatings, and composite tubes. Composite tubes of 304L SS coextruded over a carbon steel substrate also provide a barrier against direct sulfidation of the carbon steel tubes. There are few instances of superheater tube corrosion. Superheated tube wastage in recovery boilers apparently occurs as a result of carryover of unburned black liquor droplets, and the development of reducing conditions that destroy the magnetite film that normally protects the tubes.

**(c) Reausticizing Equipment:**

In most cases clarifiers, storage tanks, piping, feedboxes and related equipments are fabricated from plain carbon steels. Stainless steel is used for some vulnerable equipment such as feedwells, clarifier rakes and rake arms and piping. Some mills have converted all reausticizing equipments to stainless-steel to avoid corrosion problems in this section.

The reausticizing plant provides a variety of corrosive media, including white and green liquors, lime mud slurries, lime mud wash waters, and lime kiln scrubber waters. White and green



liquors attack storage tanks, clarifiers, and piping fabricated from plain-carbon steel, but have a little effect on stainless-steel (in absence of abrasion). Erosion corrosion is frequently seen on equipment in contact with abrasive lime mud slurries, such as clarifier rakes, lime mud slurry pump casings and impellers, and lime mud discharge lines. Corrosion also occurs on lime kiln scrubber components.

The corrosivity of white liquor is mainly due to the presence of thiosulfates and low concentrations of polysulfide, which can increase the corrosion rate to more than 1.3 mm/yr (50 mils/year). Corrosion of carbon steel by white water is increased by a change from stagnant to laminar and then to turbulent flow conditions. Several corrosion control measures in effect are stainless steel fabrication, specifications of thick wall carbon steel at critical sites, controlling thiosulfate and polysulfide.

In some cases, clarifiers and storage tanks have been lined with epoxy or glass/epoxy composite.. Although these have fair resistance to direct attack by white and green liquors, a more severe problem is penetration of liquor behind the epoxy. A similar fate often befalls sprayed on, alkaline-resistant concrete linings applied to the wetted surfaces of tanks and clarifiers. Recently, anodic protection has been shown to be an effective and economical corrosion control measure for use in white liquor storage tanks and clarifiers. These have been found to reduce corrosion rates significantly.

#### (d) Electrostatic Precipitators:

Electrostatic precipitators are susceptible to the acid dewpoint corrosion. Severe corrosion is found on side walls, collector plates, inlet and outlet baffles and ductwork, and other surfaces where flue gases stagnate, cool below the acid dewpoint, and precipitate corrosive acid films. Plain carbon-steel and concrete are severely attacked by the sulfuric acid films. Insulation of precipitator side walls and elimination of in-leakage of cool air appear to be beneficial. Few stainless alloys are resistant, but some polymeric coatings (Furans and vinyl esters) have exhibited corrosion resistance. In spite of these control measures, precipitator corrosion continues to be a costly concern for the industry.

#### 1.2.3 Paper Machine Section:

Corrosion problem in paper machines are generally most severe in the wet end and in ancillary equipment handling white water. It causes rapid corrosion of bare carbon steel, appreciable corrosion of copper alloys and cast irons, and can even cause localized corrosion of SS. Cast iron machine structures and carbon steel roof sections are particularly susceptible to corrosion in the vicinity of the paper machine.

Paper machine components are susceptible to crevice corrosion under deposits resulting from fiber particles or biological growths. Critical equipment such as headboxes and headbox internals, is often electrodeposited to minimize hang-up of fibers and adhesion of slime deposits. Here growth of slimes and other

biological deposits should be prevented that can lead to crevice corrosion. FRP construction is effective in reducing crevice corrosion in piping and chests.

Thiosulfate anions also promote pitting and crevice corrosion of SS equipment used in manufacture of certain grades of pulp. Type 310 and 316L SS are more resistant, but are not immune from such pitting. Pitting is more severe in white waters containing dilute concentration of chloride in addition to thiosulfate. Thiosulfate induced pitting can be controlled by removal of aggressive anion or by use of more resistant 316L SS in white water application.

Suction roll cracking has continued as a serious problem in paper making applications. Cracking occurs by corrosion fatigue induced by the fluctuating stresses that are imposed during routine operations. Cracks typically begin on the inside surface of the roll at a drilled hole, and propagate from hole to hole to cause external failure of the roll. In many cases, multiple cracks have been initiated and are propagating in a roll at any given time. Increased white water corrosivity with increased closure also increase demands on suction roll alloys. Cast duplex suction roll have slow cooling heat treatments or aging heat treatment to minimize stresses. The alloys such as alloy 75 and VKA 378, have much greater resistance to cracking than earlier materials. However, these alloys have been used in suction roll application for less than ten years and it is premature to conclude that cracking has been eliminated.

#### 1.2.4 Bleach Section:

Corrosion is, perhaps, most severe in bleach section in comparison to others sections of a paper industry. This is evident from one of the surveys (11) which indicates that approximately half of the maintenance cost, incurred by the paper industry against losses due to or preventive measures for combating corrosion, goes into bleach section. Here various equipment show localized attack e.g. pitting, crevice corrosion, stress corrosion cracking and inter-granular corrosion (IGC) or weld decay. Pitting occurs on a flat metal surface which is uniformly exposed to the process solutions such as shower pipes, vat surface etc. whereas crevice corrosion occurs in an occluded region created by the design of equipment or by deposition of pulp (12). An example of this could be the grooved longitudinal ribs in a washer drum, fitted circumferentially with 'D' wires which create a natural crevice. Corrosion of weldments, due to IGC, is not a problem in bleach plant, but that due to preferential chloride pitting corrosion of weld metal in comparison to base metal is a cause of concern. This is particularly important when either no filler metal is used or when filler metal is close in composition to base metal (13).

Various factors responsible for corrosivity in different stages can be discussed in terms of chemical constituents, temperature and pH of liquors of the corresponding stages.

(a) Corrosion in different stages:

- Chlorination (C) Stage:

The aqueous media here contains low pH, moderate temperatures, significant amount of residual chlorine and  $\text{Cl}^-$  ion (Table 1.1). These conditions are responsible for excessive

Table 1.1 : Average filtrate conditions in typical Bleach Washers

Stage	pH	Temperature ( °C )	Residual $\text{Cl}_2$ ( mg/l )	Chloride ( mg/l )
C	2.0	35	90	1250
D1	2.4	58	56.5	576
D2	4.2	73	21.7	360
E	10.3	48	-	850
H	10.0	37	1.2Kg/ton	1450

localized attack in this stage, though  $\text{Cl}^-$  ion and temperature in the range normally observed in this stage play only a secondary role (12-15). One study (16) apprehends that mills that operate C stage at a pH < 1.5 are as corrosive as those that carry high residuals in vat but at 1.8 - 2.0 pH. In a study on Swedish bleach plants (17), crevice corrosion is indicated as major type of localized attack in liquid phase whereas in gas phase pitting and crevice corrosion attack is more prominent than weld metal pitting and IGC. It is also observed that gaseous phase is more

corrosive than liquid phase (13,17,18). This is mainly due to excess chlorination, where gaseous chlorine from vat filtrate makes small droplets of condensation highly corrosive (19). Another proposition is that perhaps non-volatile component of filtrate are showing inhibitive effect (18).

- Chlorine-dioxide (D) Stage:

Here the filtrate generally has comparatively higher, though acidic pH ( $\approx 2.5 - 4$ ),  $\text{Cl}^-$  ion, residual chlorine and higher temperature (Table 1.1). However depending upon the actual process conditions, in some mills D section is found to be more corrosive than C while in others it is reverse (13,14). In the former case, even 316L, 317L and 904L corroded at unacceptably higher rates (13). Residual oxidant ( $\text{ClO}_2$ ) concentration is primary cause of corrosion. It is observed that at a level of 25 ppm  $\text{ClO}_2$  or above, localized corrosion reactions occur more vigorously (17). Influence of temperature and  $\text{Cl}^-$  ion concentration is not so significant. pH when goes down to 1.5 or 1.2, corrosion rates increase dramatically. D stage washers are protected by adding NaOH (thereby raising pH) which makes  $\text{ClO}_2$  less corrosive by transforming it into  $\text{ClO}_2^-$  ions (11). Another common practice is to use  $\text{SO}_2$  as antichlor.  $\text{SO}_2$  should be added to the extent that  $\text{ClO}_2$  concentration drops to zero and a slight residual  $\text{SO}_2$  is maintained in the vat. Corrosion of non-wetted components (gaseous phase), e.g. shower pipes, metal vats above stock level etc., is not very severe unless  $\text{SO}_2$  used is in excess or it is badly mixed. In the presence of both  $\text{SO}_2$  and  $\text{ClO}_2$  in vapor phase, any condensation will contain HCl and  $\text{H}_2\text{SO}_4$  mixture

of which are highly corrosive ( 18,19).

- Hypochlorite (H) Stage:

Due to alkaline conditions, the corrosion attack is not as severe as observed in C and D-stage washer (19). Stainless steels are much less subject to pitting and crevice corrosion. Degree of corrosivity depends on pH and residual chlorine concentration. Corrosivity is observed to be highest at neutral pH (20) because at this point residual chlorine is in the form of  $\text{HOCl}$  which is more corrosive than  $\text{Cl}_2$  ( forming at lower pH). At higher pH ,  $\text{OH}^-$  acts as inhibitor. Most mills maintain pH  $\approx$  10-11 as most important corrosion-prevention measure in H-stages (18).

- Oxygen, Peroxide bleaching:

Oxygen bleaching involves use of highly alkaline solutions that may contain significant amount of  $\text{Cl}^-$ . Combined with high temperature ( $136^\circ\text{C}$ ) and mechanical stresses, there exists possibility of chloride SCC. At pH  $\approx$  11 in a solution containing 10 gpl  $\text{NaCl}$ , only mild pitting was observed on SS and no stress corrosion cracking (SCC) was observed (9). In gaseous phase, over these solutions, addition of carbon-monoxide reduces risk of SCC on Mo containing SS. Peroxide appears to present no more corrosion problems than  $\text{ClO}_2$ . It has been used for bleaching without corrosion consequences.

(b) Corrosion in Closed Bleaching System:

Since discharge of paper mills has lot of pollutants, mills

have been advised to recycle the filtrates in order to control pollution. It also helps in conserving energy indirectly. However, this strategy has led to increase in the corrosivity of bleach plants. As one can see from Table 1.2 (21), that as a consequence of filtrate recycling, during years, the liquors have increased concentration of dissolved solids (including residual oxidants), higher temperature and lower pH. All these

**Table 1.2 : Variation in conditions of Chlorination  
Washer Filtrate due to "Closure" of Mills**

Survey	Year	pH	Temperature (°C)	Residual Cl <sub>2</sub> (mg/L)	Chloride (mg/L)
CPPA	1964	2.0	16	110	-
CPPA	1973	2.0	25	110	917
TAPPI	1976	2.1	33	90	780
CPAR	1977	1.8	38	30	-
PAPRICAN	1979	2.0	39	90	1705
Proposed Closed Bleach Plants	-	2.0	60 - 75	?	3000-5000

factors enhance corrosivity of liquor. Hence as more and more plants approach full closure, it will become necessary to look for more corrosion resistant alloys rather than conventional ones such as 316, 317L etc.

**(c) Materials Selection/Performance:**

**- Metals:**

Looking at the highly aggressive nature of bleach plant,



specially the chlorination and chlorine-dioxide sections, tests have been conducted to find a more suitable alloy material for constructing process equipment (13,14,16-18). It is found that 316L (in case of Swedish Plants) and 317L (in case of Canadian Plants which are more corrosive) were considered to be widely used in handling and washing of chlorinated pulp during sixties (9,22). However, with the introduction of filtrate recycling, while Swedish mills started using 317L, use of same material in Canadian plants did not ensure long drum life. Performance of 316L and 317L was generally found to be poor whereas 904L, 254SMO were acceptable in two later surveys (13,18). With increased pollution control measures, corrosivity is bound to increase further. As such, in future bleach plants, for C & D stages, alloys will be chosen from 254SMO, Hastelloy, Carpenter 20 Mo-6, Cronifer 19/25 HMO, AL-6XN etc. In hypochlorite stages, 316 L and high Ni stainless-steel e.g. carpenter 20Cb-3 give satisfactory performance. 304 fails due to chloride SCC.

- Non-Metals:

Due to increasing corrosivity of bleach liquors, mills of late have been tending to use more and more of non-metallic materials. This is possible also because of the fact that most failures of non-metallic materials in bleach plants have been related to improper design/fabrication of the equipment.

Corrosion problems in bleaching towers have been overcome by the use of rubber, tile or brickwork lining of mild steel vessels. Extraction towers are usually lined with carbon/graphite brick

work, portland cement or polyester mortars. Since masonry lining are not usually impervious to the corrosive solutions, barrier linings e.g. elastomer coating on polyurethane or rubber latex in case of ClO<sub>2</sub> service are installed between ceramic and interior of steel vessel (23).

Thermoplastics find applications in different areas as shown in Table 1.3.

**Table 1.3 : Application of Thermoplastics in Bleach section of Paper Industry.**

Types	Usage location and conditions
HDPE	Sewer pipe, slip lining
PVC	Acid and alkali filtrates ( $\leq 60^{\circ}\text{C}$ ) Hypo not above ambient.
Polypropylene	Acid and alkali filtrates ( $\leq 60^{\circ}\text{C}$ ) Hypo $\leq 49^{\circ}\text{C}$ .
CPVC	Acid and alkali filtrates ( $\leq 85^{\circ}\text{C}$ )
Polyvinylidene fluoride (Kynar)	All acid and alkali filtrates Pump linings, wet Cl <sub>2</sub> and ClO <sub>2</sub> 50% NaOH to $52^{\circ}\text{C}$ Dilute H <sub>2</sub> SO <sub>4</sub> or H <sub>2</sub> O <sub>2</sub>
PTFE	Chemically inert in bleaching environment Temperature up to $260^{\circ}\text{C}$ .

For corrosion resistant applications in bleach section, Polyester and vinyl ester resins are generally used to make reinforced thermosetting plastics or FRP'S.

**(d) Electrochemical Protection:**

Increasing corrosivity, premature failures of polymer/FRP

equipment due to incorrect fabrication procedures have led many mills to select electrochemical protection as a cost-effective alternative in corrosion control strategy. This is evident from a recent survey (22), according to which around 50% of the surveyed mills are using this system, though it is available commercially only since about a decade (19,21,24) or so. Main principle behind this system is to polarize the stainless-steel washer anodically with respect to its redox potential or cathodically with respect to its corrosion potential in bleach liquor, so that, the washer potential is in passive region. Monitoring of corrosion rates and degree of localized attack on coupons exposed with/without protection system clearly indicates the usefulness of protection system (25). Electrochemical protection systems enhance the performance of 317 L to that of a higher alloy like 254SMO. Protection systems have been installed on washer made from 316L,317L,904L and 254SMO stainless steel. A protected 254SMO washer probably represents the present state-of-art for corrosion control in most severe washer environment.

### 1.3 Definition of the Problem with Justification and Objectives

The above sections indicate clearly that corrosion is most severe in bleach section of paper industry. This has led to a large amount of work done related to the corrosion problems in bleach section by various workers abroad, specially in developed countries. Indian mills also face similar degree of corrosion problems as is evident from a recent survey done on these mills (10). However, for the Indian mills, the data of North American

and Scandinavian mills can not be used due to difference in the local process conditions which, in turn, are due to the difference in the nature of fibrous raw materials. This survey (10) also reveals that practically no efforts have been done to monitor corrosion and hence to take preventive measures. As such data and knowledge related to corrosivity of environment and the performance of materials in the case of Indian mills should be generated. It is in this context, that present work was planned. Bleach section was chosen for study since this is the most corrosive of all sections in Pulp and Paper Industry. Further, since Indian mills use, in general, chlorination, extraction and hypochlorite stages as bleaching sequence, the studies were performed related to these stages only. Keeping in view the present state of affairs, with regard to corrosion problems in Indian paper industry, the work was done with the following objectives:

(a) To determine the corrosiveness of environment and to correlate it with the existing process conditions in bleach section.

(b) To evaluate the performance of commonly used steels in various stages and to see the dependence of corrosion attack on alloying elements and process conditions wherever possible.

(c) To characterize the nature of corrosion products formed on exposed coupons and to correlate it with the process parameters. This is an important aspect as the behavior of a material in an environment is also governed by the corrosion products.

(d) To do weight-loss and electrochemical studies to observe the

dependence of corrosion reaction on steels due to composition of bleach liquor and to understand the mechanism of corrosion reactions.

In order to undertake the above type of work, it is essential to have an understanding of the corrosion phenomenon and related aspects. These details are now given in the following subsection.

#### 1.4 Corrosion Phenomenon

Corrosion has been defined in several ways by different authors (26,27). A satisfactory definition could be -

**Destruction or deterioration of material because of chemical and/or electrochemical reaction with its environment .**

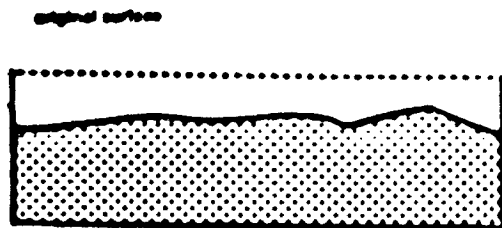
The nature and/or degree of corrosion attack may change in the presence of mechanical actions. 'Rusting' is the corrosion of iron or iron-base alloys, with formation of corrosion products consisting largely of hydrous ferris oxides(26,27).

##### 1.4.1 Types of Corrosion Damages:

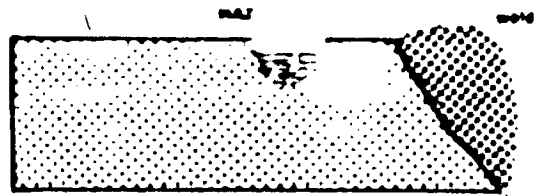
Various forms of corrosion (26-29) have been discussed in the following paragraph and shown in Fig.1.4.

##### (a) General (Uniform) Corrosion:

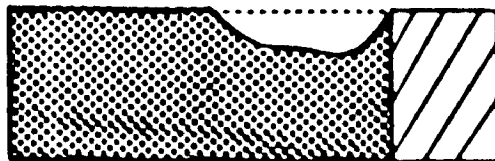
This is the most common form of corrosion. It proceeds uniformly over the entire exposed surface or over a large area. The metal becomes thinner and eventually fails. Examples are:



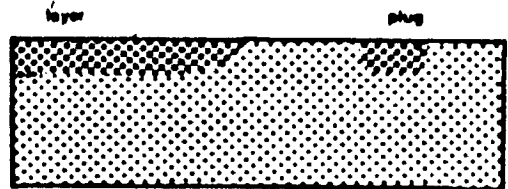
General Attack



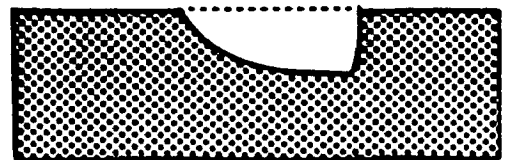
Intergranular Attack



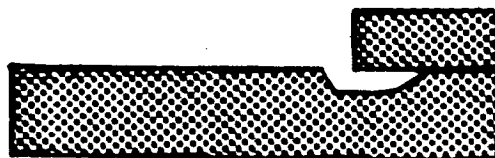
Galvanic Attack



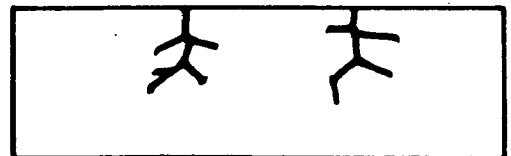
De-Alloying Attack



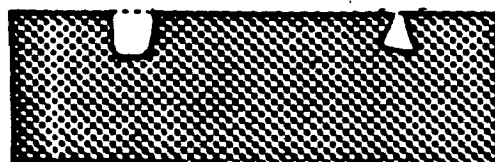
Erosion



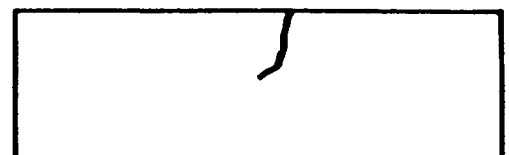
Crevice Corrosion



Stress Corrosion Cracking



Pitting



Corrosion Fatigue

FIG.14: TYPES OF CORROSION

rusting of steels in the atmosphere, the rapid attack on amphoteric metals ( e.g. Pb, Zn, Sn, Al) in many acids and alkalies etc.

(b) Galvanic or Bimetallic Corrosion:

A potential difference usually exists between two dissimilar metals when they are immersed in an electrolyte. If these metals are placed in electric contact , the potential difference produces electron flow between them. Corrosion of less resistant metal (anodic) is usually increased and that of the more resistant metal (cathodic) is decreased, as compared with the behavior of these metals when they are not in contact. The galvanic effect corrosion is greatest near junctions . Larger anode to cathode area ratio is preferred to control this type of corrosion.

(c) Crevice Corrosion:

Intense localized corrosion frequently occurs within crevices and other shielded areas on metal surface exposed to corrosive environments. This type of attack occurs due to stagnant solution caused by holes, gasket surfaces, lap joints, surface deposits, bolts and rivet heads. To function as a corrosion site, a crevice must be wide enough to permit liquid entry, but sufficiently narrow to maintain a stagnant zone. Metals or alloys which depend on oxide film or passive layers for corrosion resistance are particularly susceptible to crevice corrosion. This type of attack is observed quite often when metal crevice is immersed in acidic solution having chloride ions. A special types

of crevice corrosion is filiform corrosion. It is characterized by tunnel along the metal surface underneath an organic coating or passive protective film.

(d) Pitting:

Pitting is one of the most destructive and insidious forms of corrosion. This is an extremely localized type of attack, and results in pits/holes in metal. Pitting causes equipment to fail because of perforation with only a small percent weight-loss of the entire structure. It is often difficult to detect pits because of their small size and often covered with corrosion products. This may occur on an openly exposed surface, particularly with metals having a passive film. Pitting also occurs under deposits. Pits usually grow fast in the direction of gravity because chlorides are more easily retained under these conditions. Starting of pitting may be due to appearance of surface scratches, an emerging dislocation or other defects. All systems which show pitting attack are also susceptible to crevice corrosion, however, the reverse is not always true. Most pitting failures are caused by chloride and chlorine-containing ions. Hypochlorites are difficult to handle because of their strong pitting tendencies. Often, increase in solution velocity decreases pitting. Surface finish also affects pitting resistance.

(e) Inter-granular Corrosion (IGC):

Selective attack at or along grain boundaries, with relatively little corrosion of grains, is inter-granular corrosion. The alloy disintegrates and loses its strength and ductility.



The attack is often rapid, penetrating deeply into the metal, and sometimes causing catastrophic failures. Grain boundary areas may be intermetallic or be found by heat induced metallurgical changes such as welding ( weld decay ) or stress relief. It is most commonly experienced in the austenitic stainless steels and high nickel-chromium alloys and is known as sensitization. It is specific to certain environment/alloy combinations e.g. austenitic stainless steels in hot oxidizing acids .

(f) Selective Leaching (Dealloying):

Selective leaching is characterized by preferential dissolution of one component of an alloy by corrosion processes, typically leaving a weak pseudomorph of the original item. The most common examples are the selective removal of zinc in yellow brass alloys ( dezincification) and graphitization.

(g) Erosion Corrosion:

Erosion corrosion is the increase in the rate of deterioration on a metal because of relative movements between a corrosive fluid and metal surface. Metal is removed from the surface in the form of solid corrosion products or passive films, which are mechanically swept by fluid . Erosion corrosion ,in the appearance ,exhibits a directional pattern. Metals that are soft and readily damaged such as copper and lead are susceptible to erosion corrosion. It increases with suspended solid particles in fluid medium e.g. silica, pulp in pulp slurry etc. Equipments e.g. piping systems, bends, elbows, valves, pumps ,blowers , impel-

lers, agitators etc. Inlet Tube Corrosion, cavitation damage, impingement and fretting are the different types of erosion corrosion.

(h) Cracking:

There are following types of cracking in corrosive environments:

- Corrosion Fatigue:

Fatigue is defined as tendency of metal to fracture under cyclic stresses. When it cracks due to alternate tensile stresses in a corrosive environment it is called corrosion fatigue. Every metal is characterized by fatigue limit, which either lowers substantially or vanishes completely in corrosive environment.

- Stress Corrosion Cracking:

Stress corrosion cracking (SCC) refers to cracking caused over a period of time by the simultaneous presence of tensile stress and specific corrosive medium. The stress may be residual in the metal, such as the one appearing due to cold working or heat treatment undertaken by the it during fabrication, or it may be externally applied. Almost all structural metals ( e.g. steels, brass, duralumin, Ni alloys etc.) are subjected to SCC in some environments, for example stainless steels crack in chloride environments whereas brass cracks in the ammonia containing environment. Hydrogen damage is a general term referring to mechanical damage of a metal caused by presence of or interaction

with, hydrogen. This includes hydrogen blistering, hydrogen embrittlement, decarburization and hydrogen attack.

In a paper mill, one or the other type of corrosion is observable in different sections. In bleach Section, which is the section of present thesis work, types of corrosion generally prevalent are - uniform corrosion, pitting, crevice corrosion, IGC, stress corrosion cracking, and erosion corrosion.

#### 1.4.2 Evaluation of Corrosion:

Corrosion is a natural process which is under continuous action on every material in any environment. What is of concern is the degree of its attack. It is, therefore, of immense importance to know the severity of corrosion reaction, in some quantitative manner, before one decides whether it is worth considering, for a given metal-environment system, of preventive actions. Quantitative evaluation of corrosion depends on whether material is experiencing uniform corrosion or localized corrosion.

##### (a) Uniform Corrosion:

In this case the metal is lost uniformly with time from its surface exposed to corrosive environment. Change in the weight or thickness of the material should therefore give a good estimation of the severity of corrosion. This is denoted by a parameter called as 'Corrosion rate', defined in two ways. Firstly, it is 'Weight loss per unit exposed surface area of metal per unit exposure time in a corrosive environment'. Commonly used unit, in English and American literature for Corrosion rate as defined

above is 'mdd' i.e. milligram/dm<sup>2</sup>.day. Secondly, it has been defined from Engineering point of view. In this case rate of metal penetration (due to corrosion) or rate of thinning of material per unit time has been considered. Corrosion rate is represented as 'mpy' i.e. mils per year'. (1 mil = 10<sup>-3</sup> inch). Measurement of 'mpy' is done knowing weight loss as before. Thus 'corrosion rate' measured in 'mdd' is converted to 'mpy' using following equation-

$$1.44$$

$$\text{Corrosion rate (mpy)} = \frac{\text{corrosion rate (mdd)}}{\text{Density}} \dots (1.5)$$

Where density is represented in gm/cm<sup>3</sup>.

Measurement of corrosion rate (mdd/mpy) helps one in determining the utility/cost-effectiveness of a given material in a given environment, as is evident from following Table .

Relative Corrosion Resistance	Penetration (mpy)
Excellent	≤ 1
Very good	1 - 5
Good	5 - 20
Fair	20 - 50
Poor	50 - 200
Unacceptable	≥ 200

(b) Localized Corrosion:

Mass loss is generally not a good indication of the extent of localized attack e.g. pitting and crevice corrosion unless uniform corrosion is slight and pitting is fairly severe. Hence

generally these are not readily evaluated by the methods used for uniform corrosion. For this purpose following methods (30) are used :

- Identification and Examination of Pits:

Visual examination of the corroded surface can be performed with the unaided eye or a low power microscope. The corroded surface is usually photographed, and the size ,shape and density of pits is determined. Metallographic examination can be used to determine whether there is a correlation between pits and micro-structure.

- Determination of the Extent of Pitting:

This is done by pit depth measurement. It can be accomplished by several methods e.g. metallographic examination, machining, use of a micrometer or depth gauge, and the microscopical method. In the microscopical method, a metallurgical microscope is focussed on the lip of the pit and then on its bottom . The difference between the initial and final readings on the fine-focussing knob of the microscope is the pit depth.

- Evaluation of Pitting:

Standard charts (31) (Fig.1.5) can be used to classify pits in terms of density, size and depth. Column A and B in figure are used to rate the density ( number of pits per unit area on the specimen surface) and average size of pits respectively. Column C rates the average depth of attack. However it can be tedious and time consuming to measure all pits, and time spent on

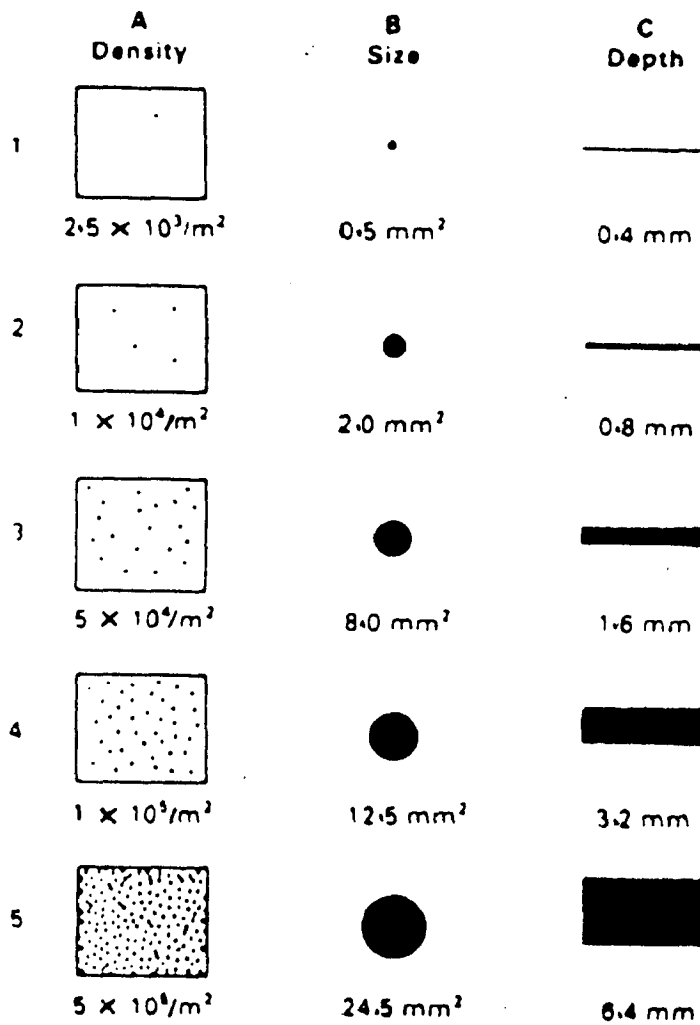


FIG.1-5: CHART FOR PITTING EVALUATION

such measurements is usually not justified, because maximum values (for example pit depths) are often more significant than average values. Therefore, the deepest pits are measured and metal penetration is expressed in terms of the maximum pit depth, an average of the ten deepest pits, or both.

Metal penetration can also be expressed in terms pitting factor, which is expressed by

$$\text{Pitting factor} = \frac{\text{Deepest metal penetration}}{\text{Average metal penetration.}}$$

A pitting factor 1 represents uniform corrosion. The larger the number, greater the depth of penetration.

### 1.4.3 Electrochemical Principles

Corrosion of metals in aqueous environments is generally electrochemical in nature. When a metal (Me) is immersed in an electrolyte, the metal gets oxidized as a result of the following reaction -



and the constituents of medium (electrolyte) are reduced following reduction reactions. Two of these reactions are -



Metal oxidation ( eqn.1.6) occurs spontaneously for most of the metals due to the fact that change in Gibbs's free energy ' $\delta G$ ', for this reaction, is negative. The magnitude of  $\delta G$  depends upon (i) nature of metal (ii) nature of electrolyte. The more negative is the value of  $\delta G$ , the greater is the tendency for metal to oxidize. For cases e.g. gold and platinum, where  $\delta G$  is positive, the oxidation reaction does not undergo spontaneously. However, the magnitude of  $\delta G$  does not indicate about the rate of oxidation. Thus it is not necessary that a metal, for which  $\delta G$  is more negative for oxidation, will oxidize at a faster rate.  $\delta G$  simply indicates whether the metal has a tendency to oxidize or not and how large is this tendency? Oxidation of metal does not continue indefinitely because not only metal is converting into metallic ion but some of the ions are reducing back to form metal. Initially the oxidation rate is more than the reduction rate but as more and more of  $Me^{n+}$  ions go into solution, the latter increases until a stage comes when both rates become equal. This stage is said to be equilibrium and equation (1) can be written as



(a) Electrode Potential:

Because in the above situation, the metal has some negative charge while electrolyte has positive charge, the metal electrolyte interface is said to have a potential called 'electrode' potential ( which has been defined later as half cell potential). The electrode potential,  $E$  is related to ' $\delta G$ ' according to the



following relation-

$$\Delta G = - n F E \quad \dots\dots(1.10)$$

Where  $\Delta G$  is in joules and  $E$  is in volts.  $n$  is oxidation state of metal and  $F$  is Faraday (96500 coulombs/equivalent). The electrode potential depends on the concentration of metal ions in the vicinity of metal electrode, according to Nernst equation, as given below -

$$E = E^{\circ} + 2.303 \frac{RT}{nF} \log \frac{Me^{n+}}{Me} \quad \dots\dots(1.11)$$

where  $E^{\circ}$  is standard electrode potential i.e. when all reactants and products are at unit activity.  $Me^{n+}$  and  $Me$  are activities of metallic ions and of metal respectively. The activity,  $a_L$ , of a dissolved specie 'L' is given by

$$a_L = T C_L \quad \dots\dots(1.12)$$

where  $T$  is activity coefficient,  $C_L$  is concentration of specie 'L' in moles/1000 grams of water. For a pure solid and homogeneous solutions, the activity is set equal to unity.

$E$  and  $E^{\circ}$  in equation (1.11) are the reduction potentials and throughout the thesis, reduction potentials will be reported.  $E^{\circ}$  is very useful in determining the tendency to corrode. As such this parameter, for various metals, has been determined and when put together form Standard EMF series. Metals with more negative potentials are at the active end (having more tendency to oxi-

dize) whereas those with more positive potentials are at the passive end ( having less tendency to oxidize ).

(b) Reference Electrode:

It is impossible to measure absolute potential of a metal electrode and so it is customary to choose some electrode with respect to which the potential of former is measured. The latter is then called as reference electrode. The universal reference electrode is standard or normal hydrogen electrode ( SHE/NHE ). Saturated calomel electrode, Ag/AgCl electrode etc. are also used as reference electrode. In the present studies, saturated calomel electrode has been used whose details have been discussed in next chapter.

(c) The Corrosion cell:

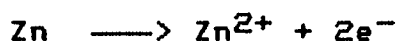
A combination of two electrodes immersed in an electrolyte is called a galvanic cell. The electrode at which oxidation occurs is called anode and the one at which reduction occurs is called the cathode. Corrosion of metal occurs at anode.

Another type of cell responsible for corrosion is called as concentration cell. Its formation can be understood from the Nernst equation ( eqn. 1.11 ). According to this equation, a metal having higher concentration of  $Me^{n+}$  ions behaves as cathode ( less negative potential ) whereas same metal surrounded by lower concentration of  $Me^{n+}$  ions acts as anode ( more negative potential ). Thus same metal surrounded by varying concentrations

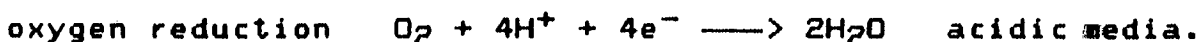
of  $Me^{n+}$  ions will behave as pairs of cathode and anode. In totality it will represent a concentration cell.

(d) Anodic and Cathodic Reactions:

In order that corrosion reaction proceeds, metal should continue to oxidize. This creates more and more of electrons on metal. If oxidation has to proceed further these electrons must somehow be removed by undergoing a reduction reaction. Hence whenever one is studying corrosion (oxidation) of metal, due consideration should also be given to reduction reactions. Whereas oxidation takes place at anode (anodic reaction), the reduction occurs at cathode (cathodic reaction). Various anodic reactions are metal oxidation e.g.



At cathode, several reactions may be encountered during corrosion. These are given below :



Some solutions may have highly oxidizing species e.g.  $Cl_2$  in acidic and  $OCl^{-}$  in alkaline media, in which case reduction reaction of these species will also be among the cathodic reactions.

### (e) Electrode Kinetics:

Some metals with pronounced tendency to oxidize (having more anodic potential) nevertheless corrode very slowly. From an engineering standpoint the major interest is in the kinetics or rate of corrosion. Here one studies reaction rates at the interface between an electrode and liquid in contact. At equilibrium, oxidation and reduction both are taking place with same rate so that no net current flows either from or to electrode. One measures, in this situation, what is termed as 'Equilibrium potential'. When electrode is no longer at equilibrium, either oxidation reaction dominates or reduction reaction, as such a net current flows to or from electrode surface. The measured potential of such an electrode is altered to an extent that depends on the magnitude of the external current and direction. The anode always becomes more cathodic and the cathode more anodic, the difference of potentials becomes smaller. This change in potential is called as polarization (27). It's magnitude (+ or -) is termed as overvoltage, measured with respect to the equilibrium potential. During corrosion the metal electrode may get polarized in three ways. This is due to activation polarization, concentration polarization and resistance polarization (IR drop).

#### - Activation Polarization:

For any given electrode process, charge transfer at a finite rate will involve an activation overpotential  $\eta_a$ , which provides the activation energy for the reaction to surmount the energy

barrier that exists between the energy state of the reactant and product (28). Thus, activation polarization refers to an electrochemical process which is controlled by the reaction sequence at the metal electrolyte interface. The activation polarization  $n_a$ , varies exponentially with the current density  $I$  (27) , in accordance with the Tafel equation -

$$n_a = \pm ( E - E^0 ) = \pm \beta \log \frac{I}{I_0} \quad \dots(1.13)$$

Where  $I_0$  is exchange current density indicating the rate of oxidation/reduction at equilibrium potential.  $\beta$  is Tafel slope indicating change in potential ( in milli volts) per unit decade current change. This is normally measured on  $E$  vs  $\log I$  curves (Figure 1.6).  $n_a$  is +ive (more positive potential than  $E^0$ ) for anodic process , and is -ive (more negative potential than  $E^0$ ) for cathodic processes. Activation polarization usually is a controlling factor during corrosion in case of (i) higher concentration of active species, (ii) turbulent electrolytes (iii) low applied current densities.

#### - Concentration Polarization:

In concentration polarization mass transfer i.e. transfer of cation from anode to solution and from solution to cathode, is the governing factor for corrosion reactions. At anode, due to oxidation reaction, more metal ions move into solution thereby tending to increase their concentration in solution near the electrode with respect to that in bulk. At cathode, due to

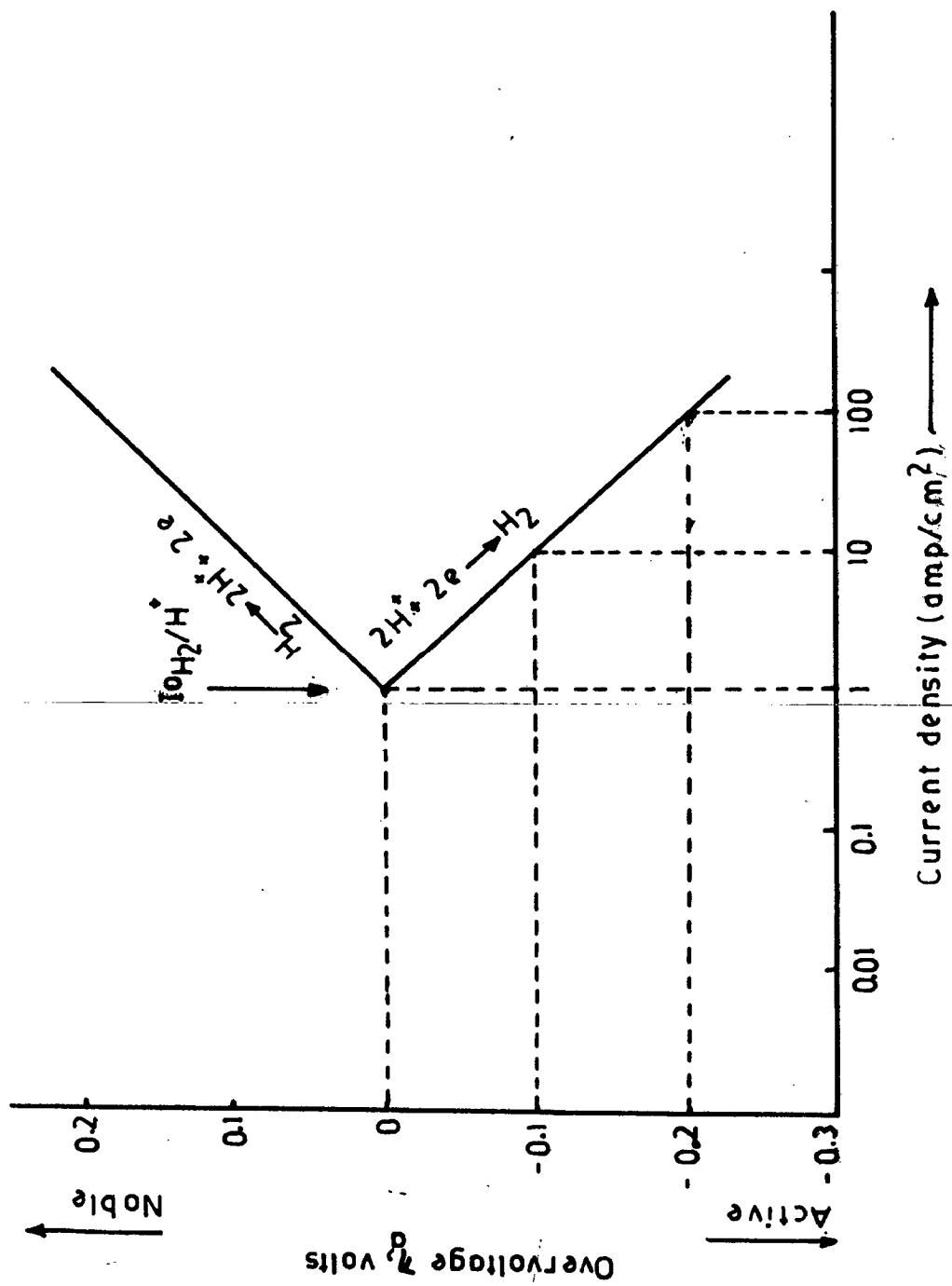


**FIG.1.6: ACTIVATION POLARIZATION**

reduction, more cations move towards electrode from solution thereby tending to decrease their concentration near electrode with respect to that in bulk. Consequently, the potential of anode and cathode both change guided by Nernst Equation. As long as applied currents are not large, these effects do not influence polarization much. But at large currents, specially at cathode, mass transfer effects dominate over the corrosion reaction leading to almost zero concentrations of cations. Consequently, potential changes sharply (Fig.1.7). The reduction current at which this effect is observed is called 'limiting current Density', denoted by  $I_L$ . It represents the maximum possible rate of reduction for a given metal-environment system. This type of effect is not observed at anode because there the concentration of cations does not change so enormously as to show a sharp change in potential. If one considers an electrode in which there is no activation polarization, then the equation for concentration polarization at an applied current  $I$  is given by

$$n_c = 2.3 \frac{RT}{nF} \log \left( 1 - \frac{I}{I_L} \right) \quad \dots\dots(1.14)$$

Thus at  $I=I_L$ ,  $n_c$  becomes infinite. In practice, however,  $n_c$  never reaches infinity, instead another electrode reaction establishes itself at more active potentials.  $I_L$  increases with increase in solution velocity, concentration and temperature. It can be evaluated from the following expression (27)

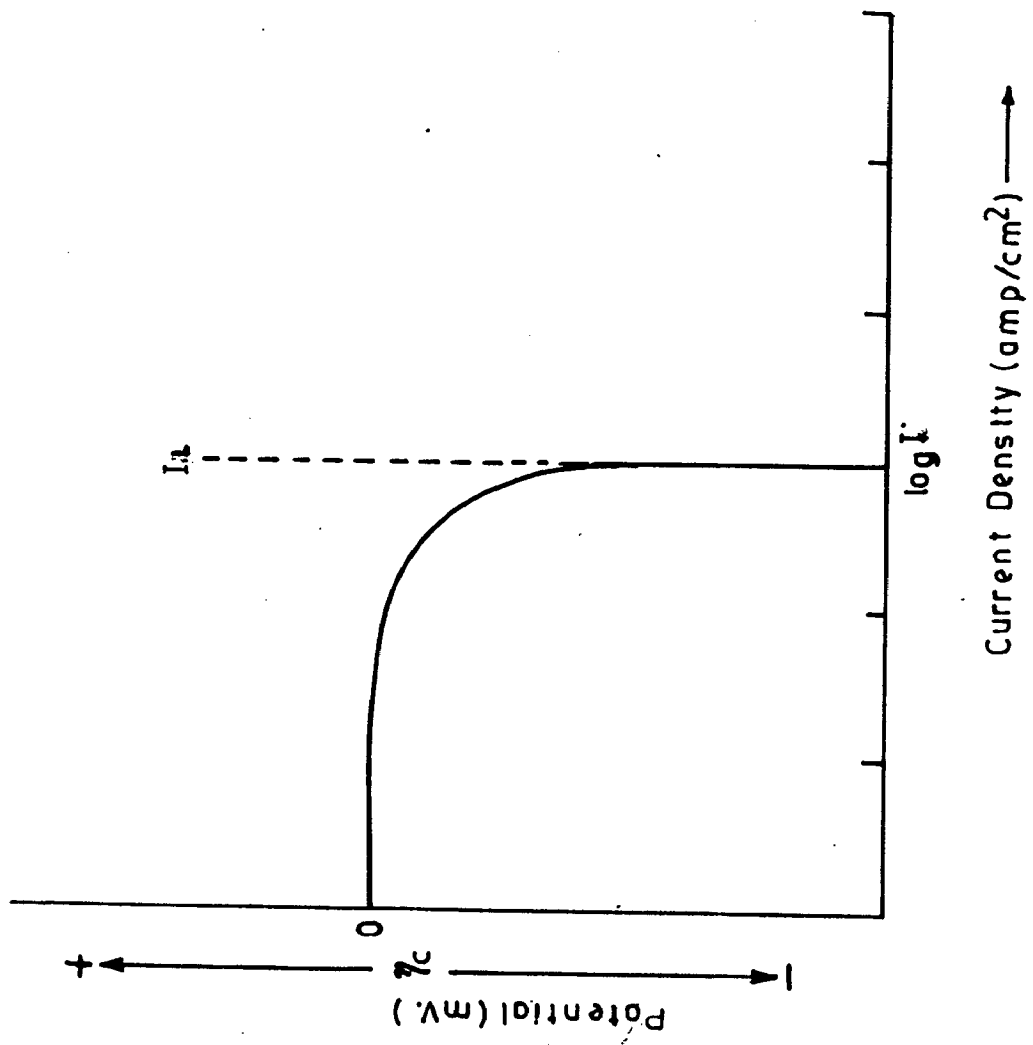


FIG.17: CONCENTRATION POLARIZATION



$$I_L = \frac{DnF}{\delta t} \times 10^{-3} \quad \dots\dots(1.15)$$

Where D is the diffusion coefficient for species being reduced,  $\delta$  is the thickness of the stagnant layer ( $\approx 0.05$  cm in unstirred solution) of electrolyte next to the electrode, t is the transference number of all species in the solution.

- Resistance Polarization or IR Drop:

An ohmic potential drop always occurs between the working electrode and the capillary tip of the reference electrode (27). Resistance overpotential is determined by factors associated with the solution or with the metal surface. Thus resistance overpotential may be defined as (28)-

$$\eta_R = I (R_s + R_f) \quad \dots\dots(1.16)$$

where  $R_s$  refers the electrical resistance of solution and  $R_f$  resistance for film or coating on the surface. Considering all polarizations, formula for cathodic polarization will be given as

$$\eta_{\text{cathodic}} = -\beta_c \log \frac{I}{I_0} + 2.3 \frac{RT}{nF} \log \left( 1 - \frac{I}{I_L} \right) - IR \quad \dots\dots(1.17)$$

In case of anodic polarization, since the effect of concentration polarization is not significant, therefore, the formula for anodic polarization is given by the following equation -

$$E_{anodic} = + \beta_a \log \frac{I}{I_0} + IR \quad \dots\dots(1.18)$$

(f) Anodic Polarization and Passivity:

The rate of an activation-controlled reaction (eqn.1.13) increases ~~(or increase in corrosion rate for anodic reaction)~~ with increase in potential. However, in certain metals and their alloys, in an anodic polarization experiment, the rate of corrosion first increases and then decreases considerably when the potential is raised above a critical value. The metal is said to have become passive. Passivity refers to the loss of chemical activity of certain metals and alloys when they start behaving like noble metals. The typical features of a metal/ solution system that exhibits an active to passive transition is shown in Fig.1.8. To determine this curve galvanostatic or potentiostatic methods are used. Part AB of the curve corresponds the active region. At B there is a departure from linearity that becomes more pronounced as the potential is increased ( becomes more noble) and at a potential C the current decreases significantly and remains essentially independent of potential over a considerable potential region ( upto D ). CD is termed as passive region. The critical current density and the potential at which transition from active to passive state occurs are represented as  $I_{crit}$  and  $E_{pp}$  ( passivation potential ) respectively. On further increasing potential, the metal transits from passive region and the corrosion current again starts increasing mainly due to destruction of passive film. This region is termed as transpas-

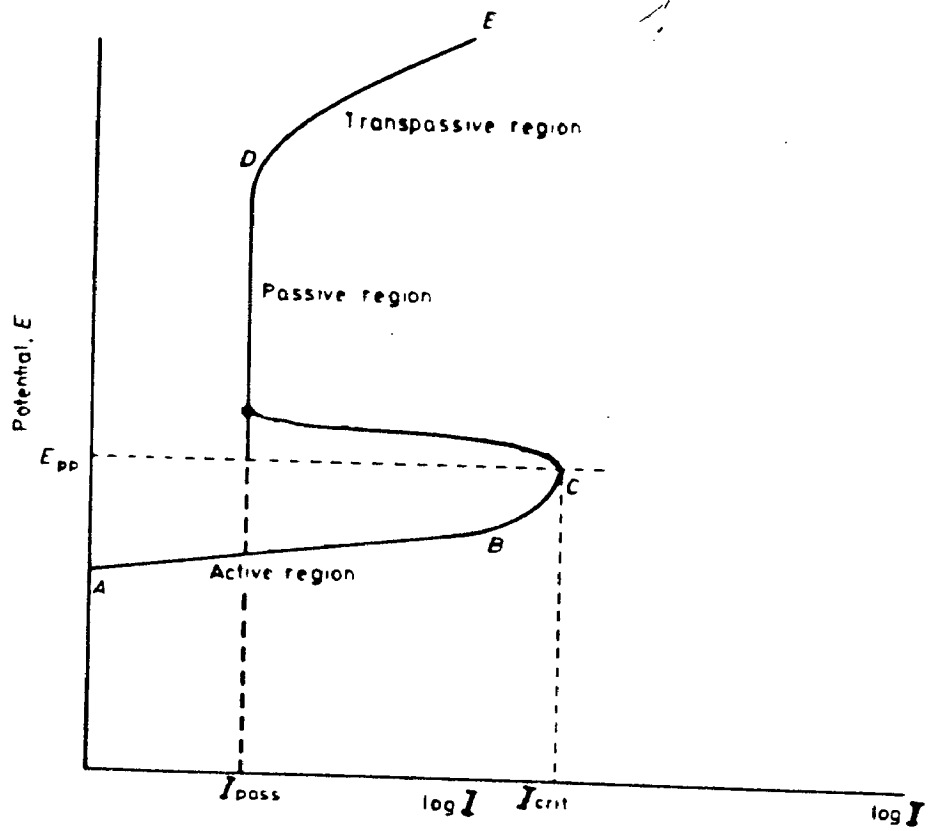
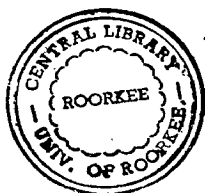


FIG.1-8: ACTIVE - PASSIVE TRANSITION

sive region ( part DE ). Potential at which this transition is observed is called as 'pitting potential', because in the trans-passive region, metals observe pitting. Iron can be passivated in reducing acids e.g.  $H_2SO_4$  by raising its potential into the passive region by means of external source of potential , a process that is known as anodic protection. The optimum potential for anodic protection is midway in the passive region. If iron is alloyed with metals e.g. Ni, Cr, etc, that passivate more rapidly,  $I_{crit}$  decreases .



245696

## Chapter-2

### EXPERIMENTAL TECHNIQUES AND PROCEDURES

	Page No.
2.1 Material Selection	53
2.2 Chemical Analysis	54
2.2.1 Mild Steel	54
2.2.2 Stainless-steel	56
2.3 Microstructure Examination	57
2.4 Coupon preparation	57
2.4.1 For Weight-loss measurements	57
2.4.2 For Electrochemical measurements	59
2.5 Mill Tests	60
2.5.1 Coupon exposure details	60
2.5.2 Analysis of vat liquors	61
2.6 Analysis of Corrosion	63
2.6.1 Degree and Nature of corrosion attack	63
2.6.2 X-Ray Diffraction	64
2.6.3 Mössbauer Spectroscopy	66
2.7 Laboratory Tests	74
2.7.1 Solution Preparation	74
2.7.2 Weight-Loss Tests	76
2.7.3 Electrochemical Tests	77

Coupon testing in field and laboratory are widely used to help engineers in selecting materials of construction for process equipment and to monitor the corrosiveness of process streams (26,32). In coupon testing, preweighed and dimensionally measured samples (coupons) of mild steel and stainless-steels were exposed to the mill and laboratory test environment for different periods of time. After exposure, the coupons were removed, cleaned and weighed. From weight loss, exposed surface area and density, the corrosion rate was calculated. The coupons were then examined for the type of corrosion attack and its degree of attack to complete the analysis. Rust scraped from corroded coupons and the surface of mill exposed coupons were also analyzed for identifying the corrosion products and for understanding the mechanism of corrosion reactions.

It has been well established that corrosion is an electrochemical phenomenon, therefore electrochemical measurements are helpful in understanding corrosion reactions. A particular type of electrochemical test help in developing electrochemical protection systems for process equipments. As such, polarization tests were performed on mild steel and stainless-steels in liquors having compatible composition with process liquors. The tests include mainly electrode potentials, Tafel plots and linear polarization measurements. The results have been used to investigate various redox systems active in the studied metal-environment system which help in understanding the corrosion behavior. This chapter has been divided into following sections for discussing various experiments performed during the course of

present dissertation work :

**2.1 Material Selection**

**2.2 Chemical Analysis**

**2.2.1 Mild Steel**

**2.2.2 Stainless-steel**

**2.3 Microstructure Examination**

**2.4 Coupon preparation**

**2.4.1 For Weight-loss measurements**

**2.4.2 For Electrochemical measurements**

**2.5 Mill Tests**

**2.5.1 Coupon exposure details**

**2.5.2 Analysis of vat liquors**

**2.6 Analysis of Corrosion**

**2.6.1 Degree and Nature of corrosion attack**

**2.6.2 X-Ray Diffraction**

**2.6.3 Mössbauer Spectroscopy**

**2.7 Laboratory Tests**

**2.7.1 Solution Preparation**

**2.7.2 Weight-Loss Tests**

**2.7.3 Electrochemical Tests**

**2.1 Material Selection :**

A commercial grade mild steel (MS), and five different types of austenitic stainless-steels (SS) namely 304, 304L, 316, 316L and 321 were selected for performing different tests. The former was selected due to its being the cheapest and mostly used for fabricating equipment. The latter were taken due to their good corro-

sion resistance, acceptable mechanical and fabrication properties which make them widely applicable in bleach sections.

## 2.2—Chemical Analysis :

Chemical composition of mild steel was determined by wet chemical methods (33,34) and those of stainless steels by optical emission spectroscopy ( OES ) (35,36). The latter analysis was got done at R&D Center, SAIL, Ranchi.

### 2.2.1 Mild Steel:

The estimation of carbon, silicon and manganese has been done by following procedures :

#### (a) Carbon:

In case of steels and ferroalloys ,carbon is present only in combined form and therefore in these materials total carbon is determined. This estimation is based on the principle that when a regulated stream of oxygen is passed over the heated iron/steel sample (at  $\approx 1000-1100^{\circ}\text{C}$ ) carbon and sulfur burn to  $\text{CO}_2$  and  $\text{SO}_2$  respectively. After removing  $\text{SO}_2$  gas , by absorbing in 50 gpl  $\text{KMnO}_4$ ,  $\text{CO}_2$  is absorbed in a soda-lime (passed through 20-30 mesh sieve) impregnated with  $\text{NaOH}$  ,followed by anhydrous  $\text{Mg}(\text{ClO}_4)_2$  to absorb the water formed during the reaction . The carbon was estimated by knowing the increase in weight of the absorbent.

#### (b) Silicon:

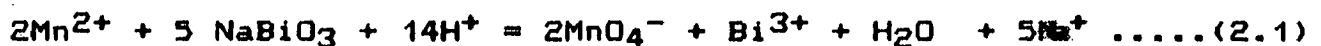
The gravimetric techniques are the standard methods for determination of silicon. In iron, steels and ferroalloys sili-



con is determined mainly by two methods (i) sulfuric acid method and (ii) perchloric acid method. The former method was used in our studies. In this method, sample is allowed to react with  $H_2SO_4$  (1 part acid, 4 parts water) by warming gently in covered conditions. After the reaction ceases, the cover is removed and rinsed. The solution is then evaporated to white fumes for 2-3 minutes. The contents are cooled to about  $60^\circ C$  and warm water is added with stirring. The contents are immediately filtered using a rapid whatman 41 filter paper and residue is washed with hot water and 5% HCl alternatively to remove iron salts. The paper along with residue is transferred to platinum crucible and the determination of silicon, is carried out by the weight of  $SiO_2$  found by ignition and HF treatment.

(c) Manganese:

Estimation of manganese was carried out by titrametric method named 'Bismuthate method'. The steel is dissolved in nitric acid and the resulting cooled solution is treated with excess sodium-bismuthate when permanganic acid is formed due to oxidation of Mn in steel.



Excess bismuthate is removed by filtration, a measured volume of a standardized ammonium iron (II) sulfate solution is added to reduce the permanganic acid into manganese state and the excess ammonium iron (II) sulfate is then determined by titration with standard potassium permanganate.

### 2.2.2 Stainless-Steel :

In the optical emission technique, determination of the elementary composition of a substance is done from optical atomic emission spectra excited in high-temperature sources. This is possible as each element has specific emission lines spectra, with which the element can be identified.

Generally, OES involves excitation of atoms and ions, to achieve emission, from the excitation source (in which, a sample becomes a vapor and is dissociated into atoms and ions), resolving the emitted radiation into a spectrum, and recording the intensities of the corresponding spectral lines. The excitation sources normally used are different types of electric gas discharge (e.g. arc or spark), the combustion flames and also certain special sources. Radiation is resolved into a spectrum by means of the dispersing components which are either prisms or diffraction gratings. When a flame is used, in many cases the required spectral lines are isolated by means of light filters with narrow spectral transmission bands. Spectra are recorded photographically or photoelectrically. The quantitative analysis is carried out with the help of standards. These usually are chemicals of the similar composition and properties as the specimens to be analyzed, but containing different known amounts of the elements to be determined. Standards make it possible to establish the relationship required by the analyst between the amount of an element in a sample and the intensity of its characteristic lines. This relationship is recorded in the form of a calibration curve. With the help of this curve, the amount of an

element in a sample is estimated. The other details relevant to theory, technique and evaluation of results have been discussed in ref.(36). Chemical analysis results for mild steel and stainless steels are given in Table 3.1 ( sheet specimens ) and 4.1 (rod specimens ).

### **2.3 Microstructure Examination:**

For characterizing the steel specimens , microstructure examination was done using metallurgical microscope. Mixture of HCl and FeCl<sub>3</sub> and Oxalic acid were used as etchant for mild steel and stainless-steel respectively to observe various phases. The specimens were examined with a magnification of 500 for mild steel and 375 for stainless steels. The results are shown and discussed in next chapter. The scanning electron microscope (SEM) was used for taking photographs of corroded specimens to analyze the nature of localized attack. These photographs were taken at magnification of 20x1, 20x1.1, and 40x1. Details about these photographs have been discussed in next chapter.

### **2.4 Coupon Preparation:**

#### **2.4.1 For Weight-loss Measurements:**

Coupon design is an important aspect of corrosion test program. The commonest coupons shape is rectangular, the reason is that most of the alloys are available in sheet form. For the convenience rectangular coupons of the size 2.5 cm x 3.75 cm were cut from plane sheets. Mild steel was treated at a temperature of 750°C for refining the structure of metal. Holes were drilled

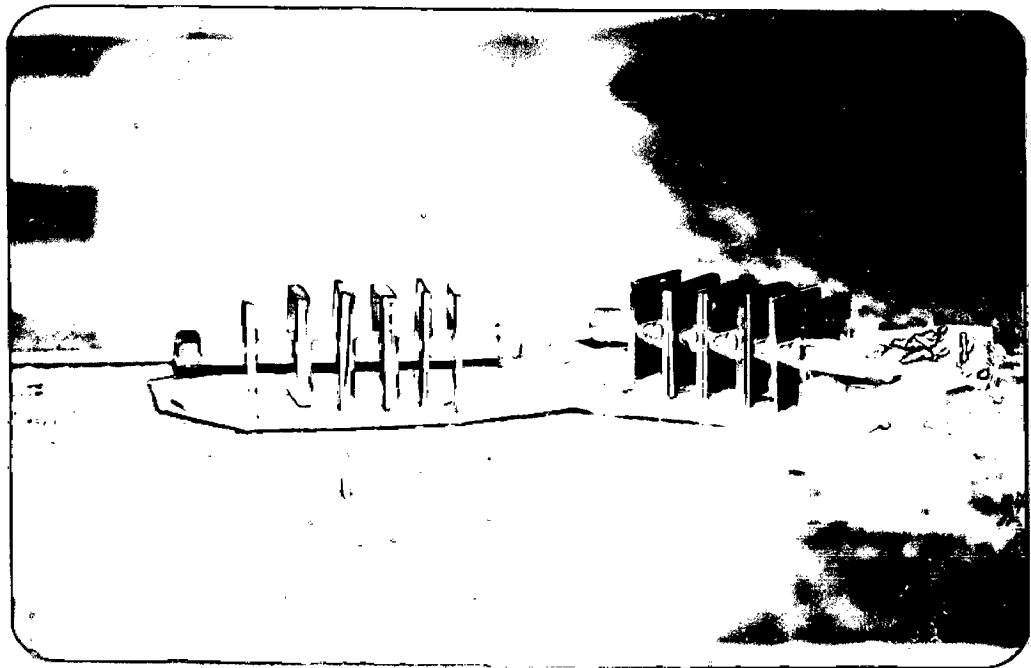
in samples for mounting in racks for mill tests and to suspend in flasks for laboratory tests before surface preparation.

The surface preparation of corrosion test coupon is viewed as a tedious process but it is of great importance and can markedly affect the results (37). An unprepared surface may have scratches non uniformities and hence may experience corrosion due to these factors. This will make difficult the comparison of corrosion attack due to difference in metallurgy alone, when one is intending to compare the performance of different materials. Standard methods of surface preparation have been discussed in details in several books (30,38,39). This process consists of mainly two steps- grinding and polishing. In grinding, the surface is abraded using a grit sequence starting from coarse towards fine, i.e. 120, 240, 320, 400 and 600 of emery or silicon carbide paper fitted on motor driven polishing wheels. Initial grit depends on the surface roughness. Silicon carbide abrasive paper is used because of its very high hardness (9.5 Mohs), reasonable cost, excellent cutting characteristics and less depth of damage than other (e.g. emery). In present case the polishing machine has two different speed ranges 300 rev/min and 600 rev/min respectively. The coupons were held by hand and between each step, these were rinsed under running water and rotated to 45° from previous orientation with continuous water falling. Wet grinding was used to avoid heat generated metallurgical damage, for lubrication, and to maximize grinding paper life. Moderate to heavy pressure was applied evenly. It was ensured that scratches from previous steps have been removed

completely. Sharp corners were also avoided during finishing. After grinding, the samples were polished to produce reasonably scratch free surface. There are several polishing methods, but here so called "universal method" has been adopted. Similar to grinding, polishing was also done from coarser to finer level on emery papers of grade 1/0, 2/0, 3/0 and 4/0 taking care to remove dust of specimen from time to time during polishing. As with grinding the sample orientation was varied. The applied pressure was moderate to heavy initially and was gradually reduced towards the end. The samples were washed and dried between each polishing step. Final polishing was done on self adhesive backed selvyt cloth sprinkled with fine polishing alumina (prepared as 1 part of alumina slurry and 10 parts of water) at speeds varying upto 300 rev/min. After completing the final polishing step, the specimen were degreased ultrasonically in bleach free detergent solution followed by thorough rinsing in 50% solution of acetone in distilled water and dried. Lastly weight and dimensions were accurately measured. The coupons used for laboratory weight-loss studies were suspended in polymer strings. For mill studies, coupons were fitted in racks having nylon axles and PVC spacers ( Photograph No.2.1 ) to avoid the galvanic effects.

#### 2.4.2 For Electrochemical Measurements:

For electrochemical studies, cylindrical samples of 1.0 cm length and 1.0 to 1.5 cm. diameter were cut from cylindrical rods. The cylindrical surface was finished and polished on



PHOTOGRAPH 2.1 : RACK USED IN MILL FOR CORROSION TESTS.

drilling machine by threading on one plane surface. Other types of preparation and cleaning are same as discussed previously for weight-loss tests. Final polishing level for these samples was 4/0 because selvyt cloth cleaning was not possible.

## 2.5 Mill Test:

### 2.5.1 Coupon Exposure Details:

Initially a weight-loss corrosion test was conducted on mild steel at M/S Seshasayee Paper and Boards Ltd., Erode, Tamilnadu, India. This mill has been referred in text as Mill A. The bleach section of this mill consists of three stages namely chlorination (C), buffered-hypo (B) (mixture of alkali and hypochlorite) and hypochlorite (H). The fibrous raw materials used by this mill are hardwood and nonwood (mainly bagasse). Test coupons were fitted above shower pipes (approximating gaseous phase) and at inlets of vats (liquid phase) in the washers of C, B and H stages. The process parameter of vats during test period were monitored carefully. Three set of coupons were put for exposure in bleach section of this paper mill. The first set of coupons from each stage was removed after 15 days, the second after 35 days and remaining set after 45 days. Second test was performed on austenitic stainless-steels by keeping them in a rack. This test was run for six months. After removal, coupons were visually inspected for type of rust and nature of corrosion products and attack etc. The loose rust was scraped with soft brush and was collected for corrosion product analysis.

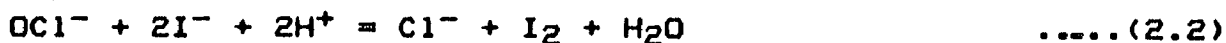
In another set of mill corrosion study, coupons of mild

steel and stainless-steels ( as tested in mill A ) , fitted in racks , were tested in bleaching section of M/S Ballarpur Industries Limited, Yamunanagar, India. This mill has been referred in text as Mill B. Bleach section of mill B consists of three stages - chlorination (C), hypochlorite-1 (H1) and hypochlorite-2 (H2). This mill uses a mixture of eucalyptus, pine and bamboo as fibrous raw material. Both the mills do not recycle the filtrates. For exposure in mill B , the racks were fitted above the shower pipes (approximating gaseous phase), at inlets of vats (liquid phase) and over the rotating washer drum ( wet/dry cyclic exposure) of all three C, H1 and H2 stages washers ( Fig. 2.1). The duration of test was 3 months . Vat liquor conditions for this mill also were monitored at regular intervals. This test was planned to compare corrosivity of both the mills.

### 2.5.2 Analysis of vat liquors:

#### (a) Free Available ( Residual ) Chlorine Determination:

This is determined by iodometric titration method (34,40,41). In this method, the chlorine containing solution (hypochlorite solution) is treated with an excess of a solution of potassium iodide. The resulting solution is then strongly acidified with acetic acid. Consequently following reactions take place :





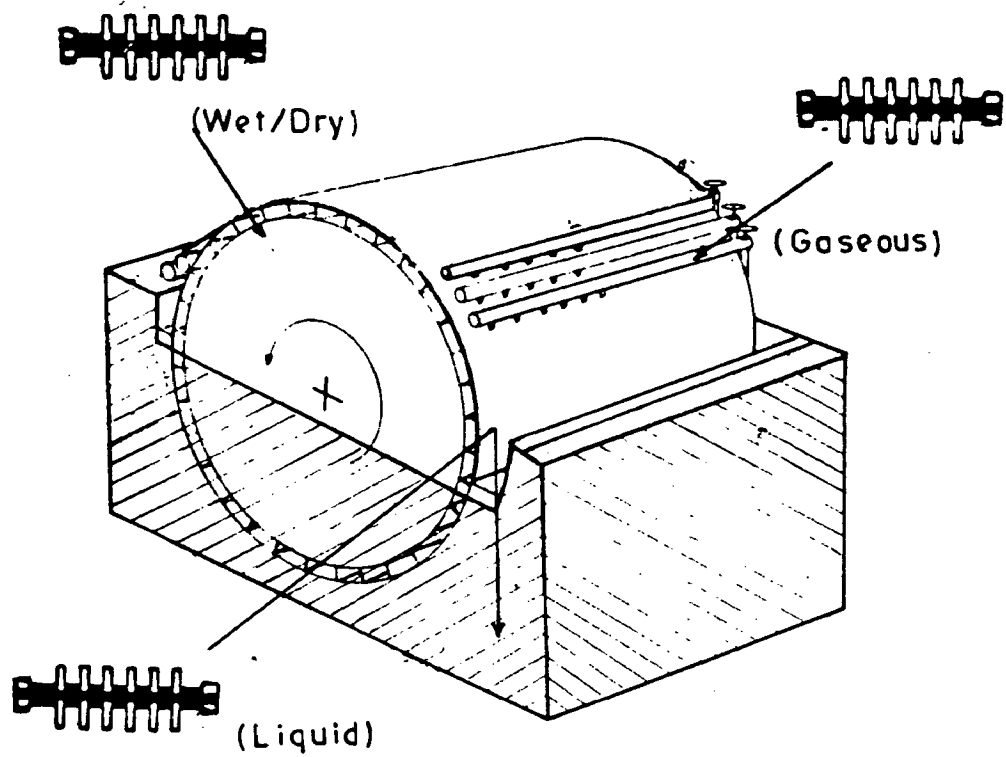


FIG. 2.1: WASHER WITH LOCATION OF COUPONS EXPOSED TO LIQUID, GASEOUS AND WET/DRY ENVIRONMENT.

The liberated iodine is titrated with the standard sodium thiosulfate using starch as indicator. The amount of iodine thus determined represents the corresponding amount of chlorine.

In case of liquor from chlorination vat, the procedure adopted is same except that in this case acetic acid is not mixed. This is so because chlorination vat liquor is already acidic in nature. Following reaction takes place in this case, in place of reaction (2.2) :



(b) Chloride ion Determination:

Determination of chloride ion is done by Volhard's method (34). The chloride ion containing solution is treated with excess standard silver nitrate solution. Silver chloride thus obtained as precipitate is filtered out. Residual silver nitrate, in the solution, is determined by titrating with standard ammonium thiocyanate solution. The used ferric indicator gives the end point.

(c) Sulfate ion determination:

Nephelometric method (34) was used for this purpose. In this method, standard solutions of sulfate ions are prepared by dissolving pure potassium sulfate in water. Then sodium chloride-hydrochloric acid reagent and glycerol-ethanol solution is mixed. Finally sieved barium chloride is dissolved in these standard solutions. These solutions are used to calibrate the nephelometer. The calibrated nephelometer was used to find out the con-

centration of sulfate ions in the liquors from vats of bleach plant. However, it was observed to be below the detectable limit (1ppm) in used instrument.

(d) pH Determination:

pH of the solution was measured by 'pH meter'. It was calibrated using buffer solution of 0.05M potassium-hydrogen phthalate for pH 4.0 and of 0.01M sodium tetraborate (borax) for pH 9.18 (at  $\approx 25^{\circ}\text{C}$ ).

2.6 Analysis of Corrosion:

2.6.1 Degree and Nature of Corrosion Attack:

After the exposure period, the corroded coupons were cleaned for finding weight-loss due to corrosion attack. Prior to chemical cleaning, loose rust was removed by brush for its analysis. Then coupons were treated with a cold solution of concentrated HCl acid, 50 gpl  $\text{SnCl}_2$  and 20 gpl  $\text{SbCl}_3$  (30,38) and were scrubbed until they were completely clean. Since some metallic part is also expected to be lost during chemical cleaning, fresh pre-weighed coupons of similar types were given cleaning treatment in similar conditions and accordingly correction in the weight-loss was made for tested coupons. Weight-loss thus obtained was used to calculate corrosion rate, in mils per year (mpy), using following formula:

$$\text{Corrosion Rate ( in mpy )} = \frac{1.44 \times (W_0 - W_f)}{\sigma \times A \times D} \dots\dots(2.5)$$

where  $W_0$  is original weight of coupon ( in mg ),  $W_f$  is weight of corroded coupon after cleaning ( in mg ),  $\rho$  is density of metal ( in gm/cc ) ,  $A$  is exposed surface area ( in  $dm^2$  ) , and  $E$  is duration of exposure ( in days ).

The cleaned coupons were examined for nature and degree of localized attack e.g. pitting and crevice corrosion. The severity of localized corrosion was assessed by estimating  $f_{loc}$ , the fraction of exposed surface of coupon experiencing localized attack. The categorization was done as per following gradation :

- (i) Excessive attack :  $f_{loc} > 0.05$
- (ii) Moderate attack :  $0.015 < f_{loc} < 0.05$
- (iii) Negligible attack :  $f_{loc} < 0.015$

#### 2.6.2 X-Ray Diffraction :

Analysis of corrosion products reveals an idea for reactions undergone in particular metal-environment system and the former's protective and non-protective nature. This idea is one of the most important basis for most of the corrosion protection methods. Therefore, rust obtained from corroded coupons, or the coupons itself in some cases were undertaken for the analysis of corrosion products using X-Ray Diffraction and Mössbauer Spectroscopy. In this part details are given about X-Ray diffraction whereas Mössbauer spectroscopy has been discussed in later section.

X-ray diffraction is one of the widely applied analytical

techniques for determination of components for crystalline powders, and has increased importance in scientific studies in recent years, consequently several (42-52) texts have appeared related to principles and practices of X-ray diffraction. The method depends upon the wave character of X-rays and the regular spacings of planes in a crystal.

Bragg's law is the main principle utilized in identification of unknown compounds. According to this law, when an X-ray beam strikes a material at some angle  $\theta$ , it is diffracted at the same angle ( Fig.2.2 ) governed by following equation :

$$n \lambda = 2 d_{hkl} \sin \theta \quad \dots\dots(2.6)$$

where  $d_{hkl}$  is inter-planar spacing ,  $\lambda$  wavelength of x-rays ,  $n$  is an integer indicating the order of the diffraction.

The Bragg's equation helps in recording diffraction pattern using powder camera /diffractometer. Sample is taken in the form of powder and it is put at the axis of diffractometer (Fig.2.3) . Monochromatic X-rays of given wavelength after passing through slit S falls on sample , say , at an angle  $\theta$  over a given set of atomic planes, characterized by inter-planer spacing  $d_{hkl}$ . It will be diffracted at angle  $2\theta$  ( along OB in Fig.2.3) with respect to direction of incidence , SO. The detector at 'B' records the diffracted intensity. When detector moves, at a given speed, from position A (corresponding to  $2\theta = 0^\circ$ ) towards B and beyond over a circular path, it will record intensities of X-rays diffracted at different angles. In this manner, one obtains a chart showing variation of intensities (I) of diffracted X-ray beams at

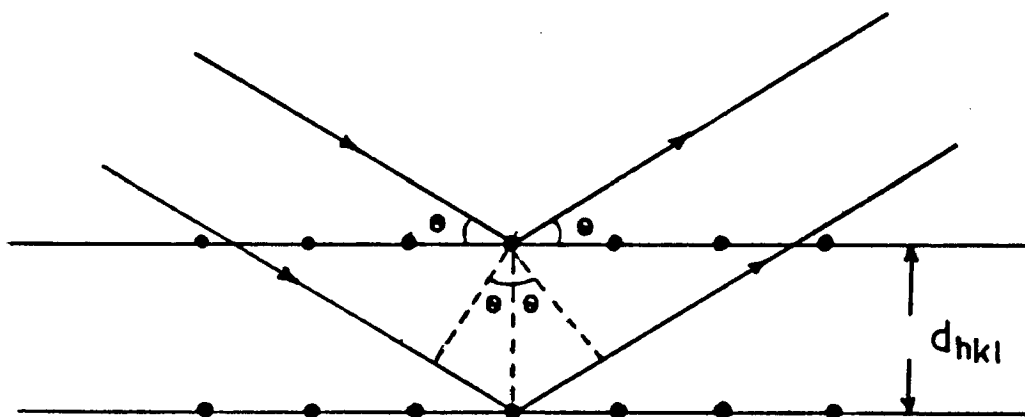


FIG.2-2: DIFFRACTION OF X-RAYS

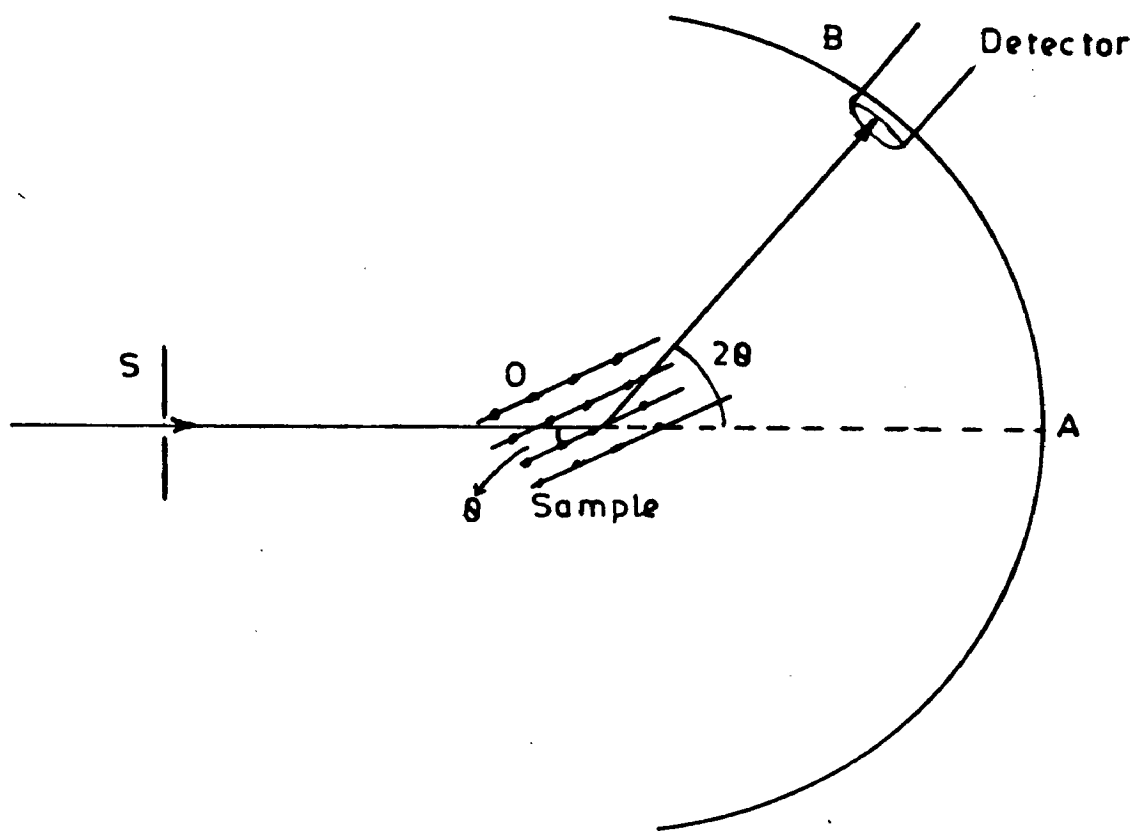


FIG. 2.3: PRINCIPLE OF X-RAY DIFFRACTOMETER

different angles  $2\theta$ . This I versus  $2\theta$  curve is called a powder diffractogram. Identification of particular species from a given diffractogram is done by comparing it with the diffractograms of standard samples. These diffractograms of standard samples show lines characterized by their intensity and  $d_{hkl}$  of planes from which the respective lines have diffracted (corresponding to a given  $\theta$  value) and have been compiled by several agencies. ASTM powder diffraction data file is one such compilation. In order to identify, first three lines with maximum intensities are compared with standard. After this matching, other lines (weaker) are also compared with standard to have an unambiguous identification of a specie.

In the present studies, for analyzing samples, the diffractograms were recorded on a Philips-Norelco X-ray diffractometer using Fe target with Mn filter (for analyzing ferrous compounds), and Cu target with Ni filter for stainless-steels (for non-ferrous compounds). From thus obtained diffractograms,  $d_{hkl}$  values were calculated from  $2\theta$  values using Bragg's equation. In this manner intensity (I) versus  $d_{hkl}$  variation was obtained which was then compared with ASTM X-Ray diffraction data files for identifying (qualitatively) the various compounds.

### 2.6.3 Mössbauer Spectroscopy:

Mössbauer spectroscopy, also called nuclear gamma resonance spectroscopy, has got its application in many disciplines of natural sciences (53-56) as well as corrosion science (57). Various review article and books have been written dealing with



its basic aspects and applications (58-65). In corrosion research, this is used for identification of corrosion products to get information about the structure and composition of products, phase composition of oxide films, deviation from stoichiometry and effect of ultrafine particles etc. (66-74). In the cases where the different corrosion products have roughly the same lattice parameters and could not be identified easily with the help of X-ray diffraction etc., Mössbauer spectroscopy clearly distinguishes by determining the hyperfine interaction parameters (75,76). It has got special application in corrosion of iron and its alloys (most common material used for fabricating process and other equipments and components) because  $Fe^{57}$  is the best suitable isotope for Mössbauer studies. In the present investigations, Mössbauer effect technique has been used to identify the corrosion products formed in paper mill's bleaching environment on steels by recording Mössbauer spectrum at room temperature and at  $\approx 80^{\circ}K$  along with the X-ray diffraction. The identified corrosion products have been correlated with the mill process conditions.

(a) Mössbauer Effect:

In 1958, R.L. Mössbauer (77,78) discovered and explained the phenomenon of nuclear gamma resonance popularly known as Mössbauer effect. In this effect the recoil free emission and resonant absorption of gamma rays is observed. If the chemical environment in the source and the absorber is different then either the emitted gamma rays will not be absorbed resonantly or

the resonance will be partial. In such a case, to make the resonant absorption possible, the energy levels of either the source or the absorber should be modified. Accordingly, an important part of a Mössbauer spectrometer is 'drive' which provides extra energy either to the source or to the absorber. A plot of the transmitted (or scattered)  $\gamma$ -photons (including resonantly absorbed ones) versus change in photon energy (in terms of Doppler velocity provided either to the source or the absorber) is called the Mössbauer spectrum. It may be singlet, a doublet, a sextet (Fig.2.4) or even more complicated depending on the types of interactions present. To make the technique more effective and draw certain important conclusion it is desirable to perform studies at lower temperature or higher temperature along with the room temperature studies. Application of external high pressure and magnetic field supplies additional information and thereby lead to better understanding of the specimen. Factors which should be considered for correct analysis of spectrum, detailed elsewhere (79-98), are (a) the line position / shift, (b) the line width, (c) line intensity and (d) the line shape.

#### (b) Hyperfine Interactions:

Main emphasis of the Mössbauer effect studies has been on the interactions between electrons of surrounding atoms/ions and Mössbauer nucleus, known as hyperfine interactions. These are electrostatic and magnetic in nature. Measurement of hyperfine parameters, in case of different iron chemicals, forms the basis of identifying and determining the structure of corrosion products. This is because these parameters differ significantly

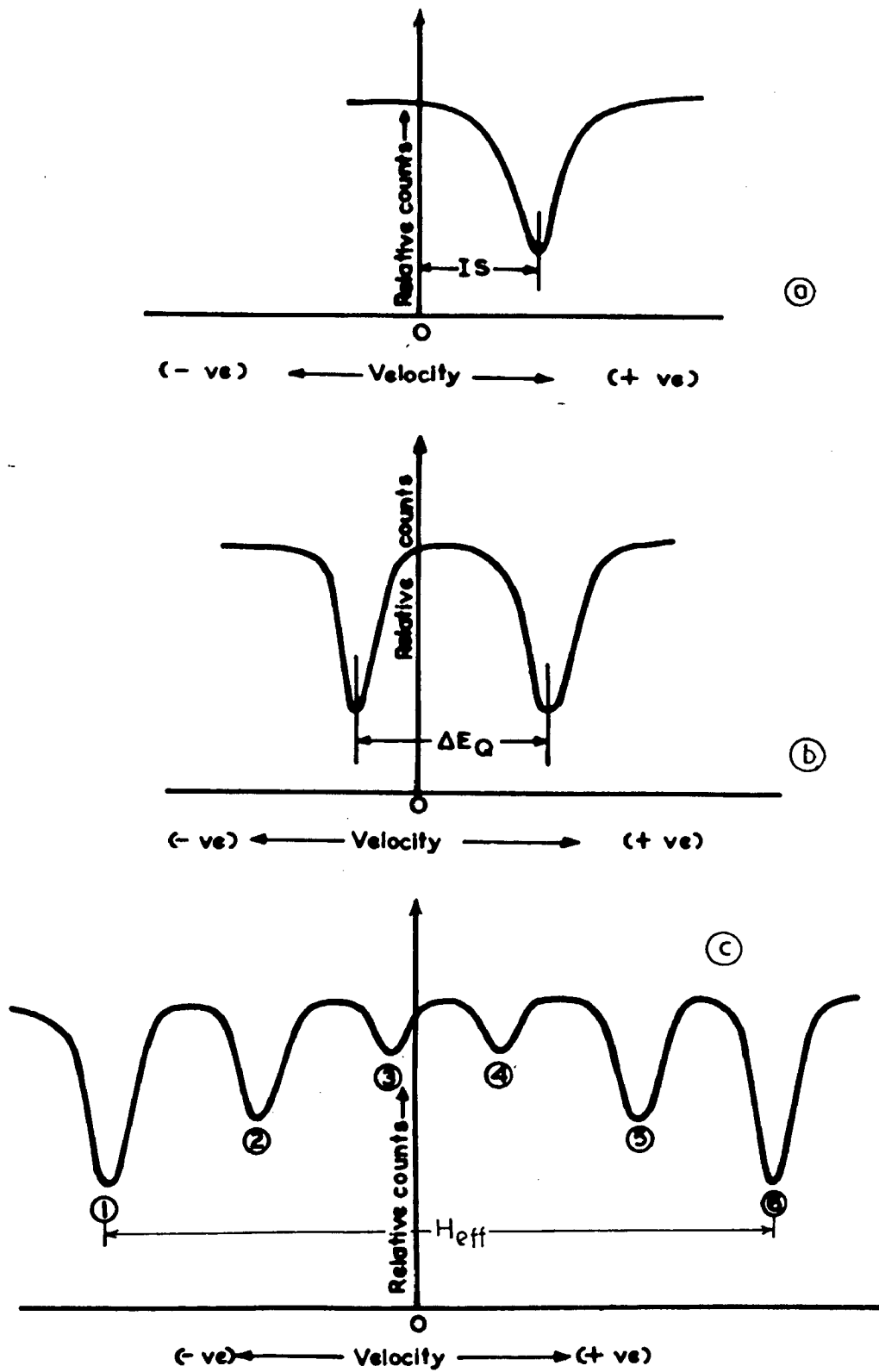


FIG.2.4 : BASIC TYPES OF MÖSSBAUER SPECTRA

- (a) SINGLET
- (b) DOUBLET
- (c) SEXTET

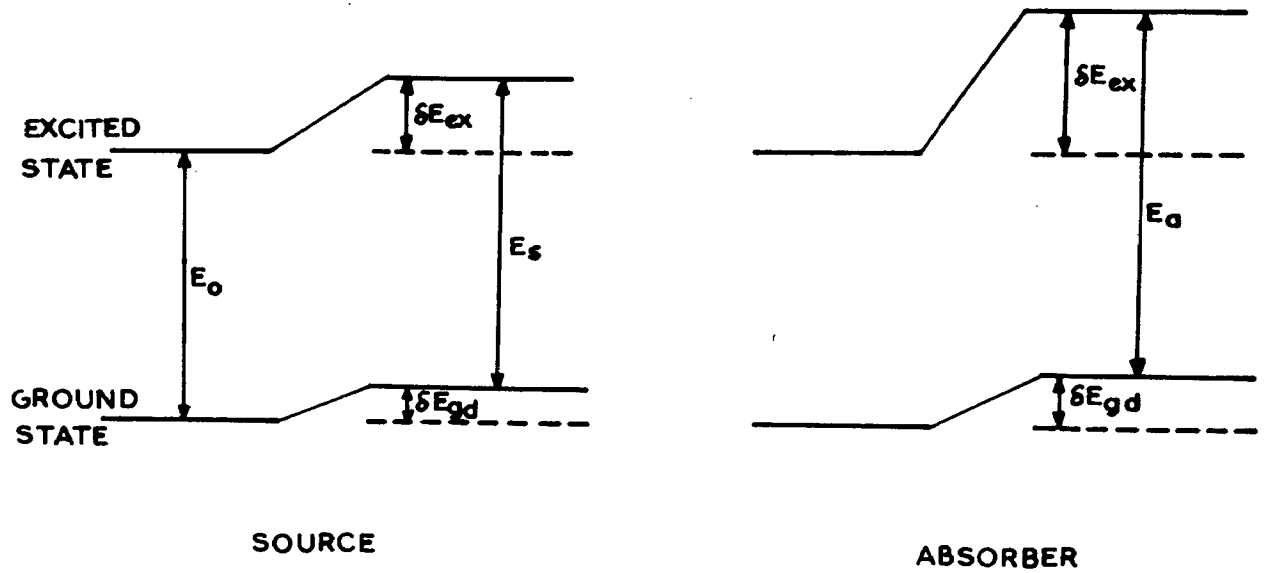
for many of the chemicals species produced as a result of corrosion reactions. The theory of these hyperfine interactions has been discussed in various books (79-86) and only a brief idea about these has been given below :

- Monopole Interaction or Isomer shift ( $\delta$ ):

The isomer shift arises from the electrostatic interaction between the charge distribution of the nucleus and those electrons which have a finite probability of being found in the region of the nucleus. This interaction causes a small energy shift of the nuclear energy levels. The isomer shift which denotes the shift of energy levels of the nucleus in the source relative to that in the absorber (Fig.2.5), can be written as

$$\delta = E_a - E_s = \frac{2\pi}{5} ze^2 \left[ |\psi_a(0)|^2 - |\psi_s(0)|^2 \right] (R_{ex}^2 - R_{gd}^2) \dots\dots(2.7)$$

where  $R_{ex}$  and  $R_{gd}$  represent the nuclear radii in the excited and ground states respectively,  $|\psi_a(0)|^2$  and  $|\psi_s(0)|^2$  denote the s-electron densities at the nucleus in the absorber and the source respectively. One can identify the oxidation state of iron with the help of isomer shift, however, it is difficult in spin paired (covalent) compounds. The isomer shift values can be used to obtain information about the electron configuration in metals and alloys (99) and also to study the ordering mechanisms (100) in alloys.



$$\text{ISOMER SHIFT} = (E_a - E_s)$$

(a)

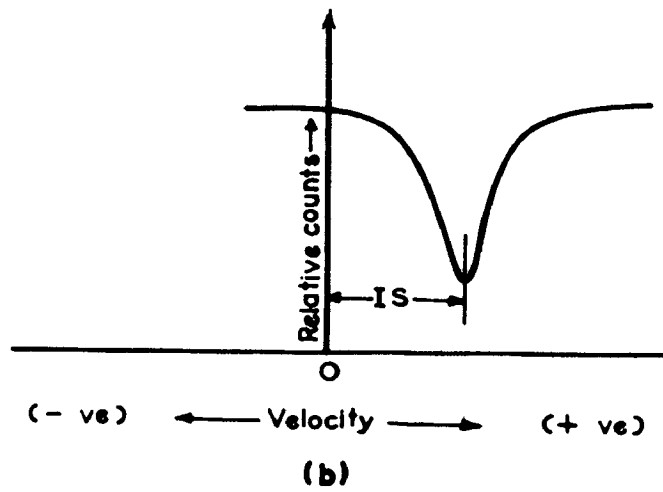


**FIG. 2.5 (a) SHIFT IN ENERGY LEVELS IN SOURCE AND ABSORBER**

**(b) MÖSSBAUER SPECTRUM SHOWING ISOMER SHIFT.**

- Electric Quadrupole Interaction or Quadrupole splitting ( $2\epsilon$ ):

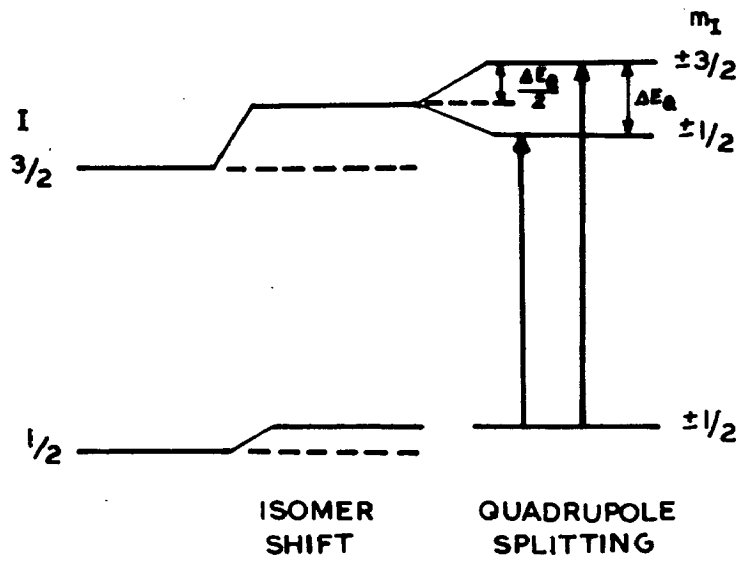
This arises from the interaction between the electric quadrupole moment  $Q$  of the nucleus and the electric field gradient (EFG), due to surrounding atoms/ions, at the nucleus. This interaction splits the excited state of  $Fe^{57}$  (constituent of absorber) ( $I^e = 3/2$ ) into two sublevels whereas the ground state ( $I_g = 1/2$ ) remains degenerate (Fig.2.6). Both the possible transitions between excited state and ground state are allowed and thus the use of single line Mössbauer source gives a characteristic two line pattern (Fig.2.6). The separation between these two lines gives the value of quadrupole splitting. For present case, quadrupole splitting can be expressed as

$$2\epsilon = \frac{1}{2} e^2 q Q \left[ 1 + \frac{\Omega^2}{3} \right]^{\frac{1}{2}} \dots\dots(2.8)$$

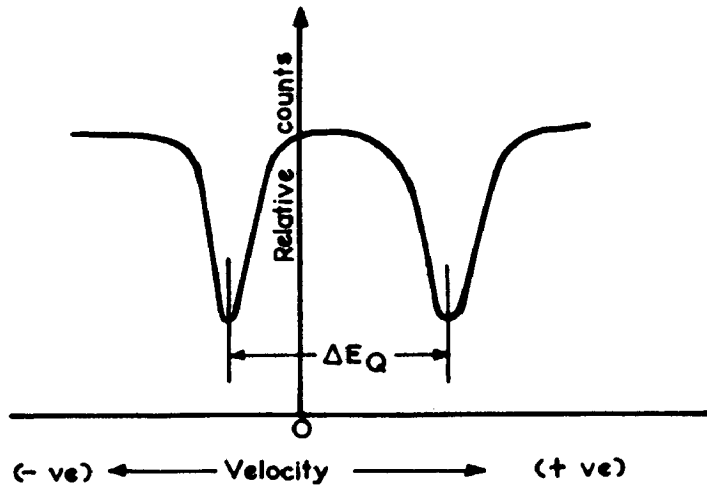
Where  $\Omega$  is the asymmetry parameter of the EFG tensor and  $q$  is the charge term responsible initiating EFG at nucleus. Thus, above equation suggest that measurement of  $2\epsilon$  can give information about the magnitude of  $q$  and  $\Omega$  and sign of  $q$ . The  $2\epsilon$  values are characteristic of ferrous and ferric compounds with further differentiation of low and high spins (54,80).

- Magnetic Dipole Interaction or Internal Magnetic field ( $H_{eff}$ ):

This interaction takes place between the effective magnetic field (due to surrounding atoms/ions) at the nucleus and its nuclear magnetic moment  $\mu$ . The magnetic field splits the nuclear



(a)



(b)

**FIG.2.6: (a) LEVEL SCHEME WITH QUADRUPOLE INTERACTION IN CASE OF  $Fe^{57}$ .**  
**(b) MÖSSBAUER SPECTRUM SHOWING QUADRUPOLE SPLITTING.**

energy levels of spin  $I$  into  $2I + 1$  equispaced non-degenerate sub-states. Thus is case of  $\text{Fe}^{57}$  (constituent of absorber) the excited state having spin  $I = 3/2$  splits into four non-degenerate sub-states and ground state  $I = 1/2$  into two sub-states (Fig.2.7). Since for magnetic dipole interaction, only transition with  $\Delta m_I = 0, \pm 1$  are allowed, six transitions between the ground and the excited states are possible (Fig.2.7). The values of the separation between ground state sublevels and excited state sublevels, and relative intensities of these transitions are discussed in literature (101,102).

- Combined Electric and Magnetic Interaction:

If the nucleus experiences both electric quadrupole and magnetic hyperfine interactions, the splitting of the states is not equally spaced and the spectrum is not symmetrical but is like the ones as shown in Fig.2.8.

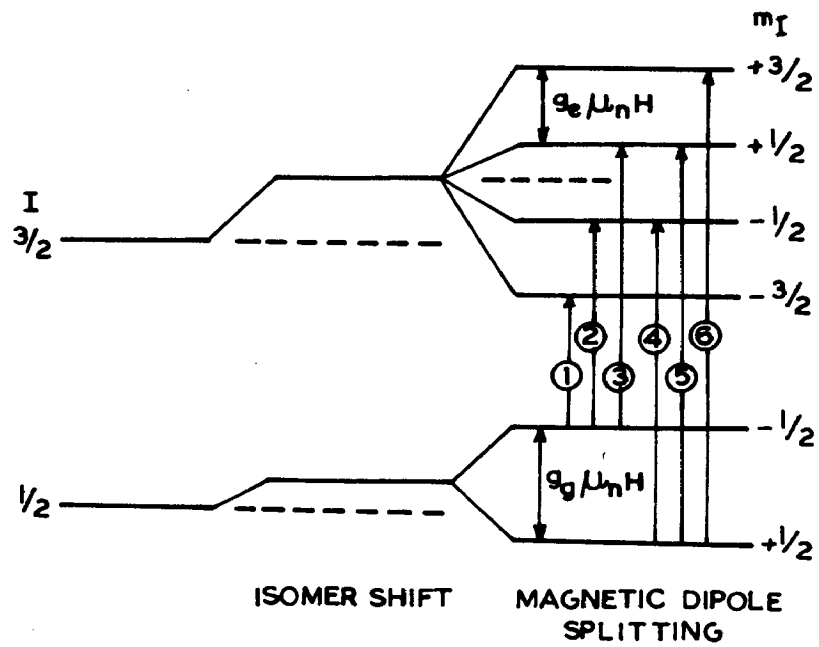
(c) Mössbauer Spectrometer:

Block diagram of Mössbauer spectrometer is shown in Fig.2.9. Its various components are discussed below :

- Mössbauer Source and Absorber:

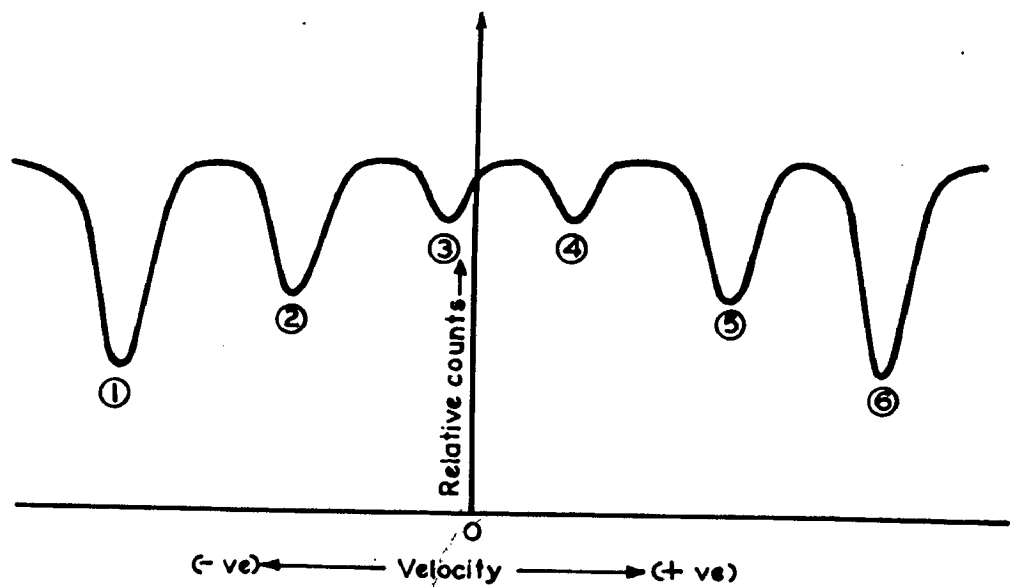
In the present work,  $\text{Co}^{57}$  diffused into rhodium matrix (host matrix) with an original activity of 50 mCi was used as Mössbauer source. Its energy level diagram is shown in Fig.2.10. According to this figure,  $\text{Fe}^{57}$  forms due to electron capture by  $\text{Co}^{57}$  and 14.4 KeV recoil free  $\gamma$ -rays, generated due to transition between  $I=3/2$  and  $I=1/2$  levels of  $\text{Fe}^{57}$ , are used as





( $g_e$  and  $g_g$  represents nuclear 'g' factor for excited and ground states respectively )

(a)



(b)

**FIG.2.7: (a) LEVEL SPLITTING IN  $\text{Fe}^{57}$  DUE TO MAGNETIC DIPOLE INTERACTION.**

**(b) MÖSSBAUER SPECTRUM SHOWING MAGNETIC HYPERFINE SPLITTING.**

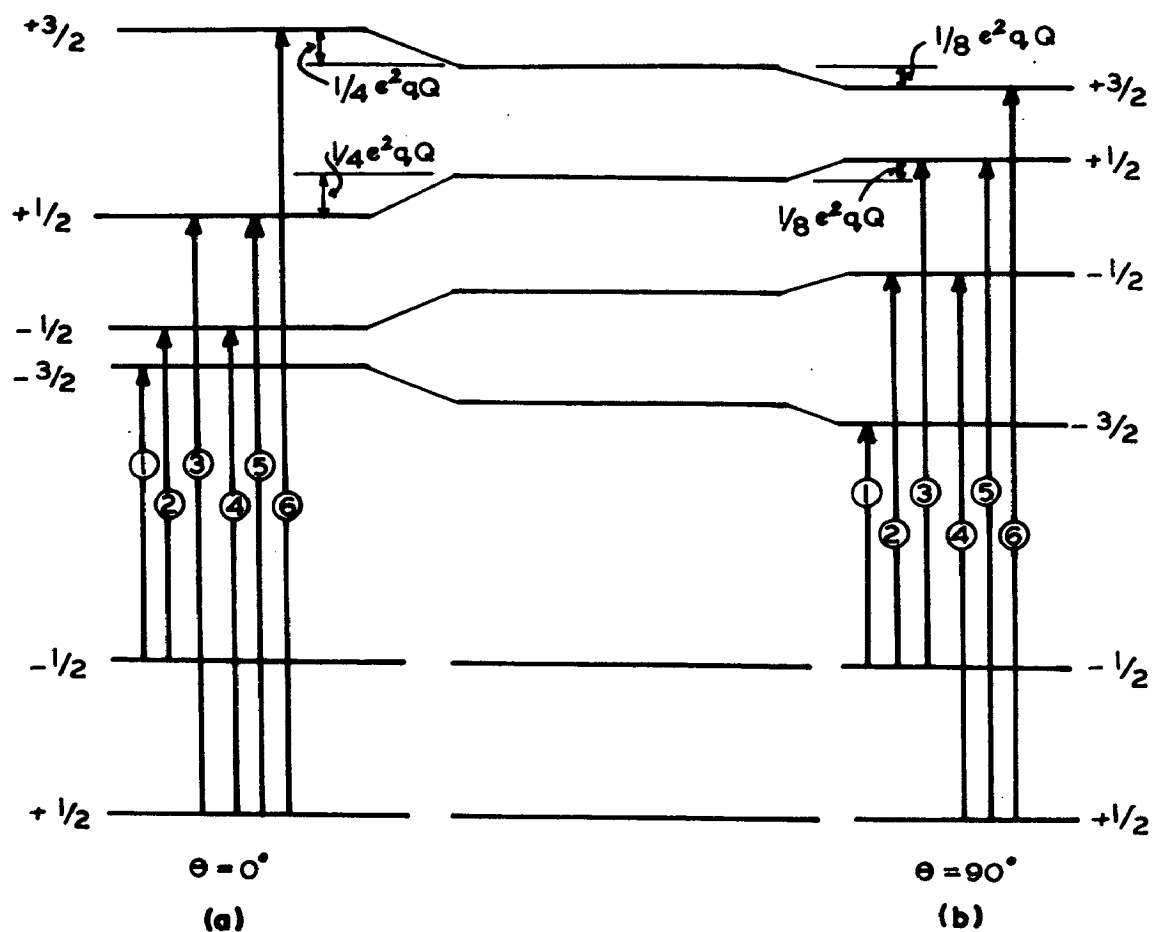


**FIG.2.8 : LEVEL SPLITTING IN  $Fe^{57}$  IN PRESENCE OF ELECTRIC QUADRUPOLE AND MAGNETIC DIPOLE INTERACTIONS WHEN (a)  $\theta = 0^\circ$  AND (b)  $\theta = 90^\circ$ .**

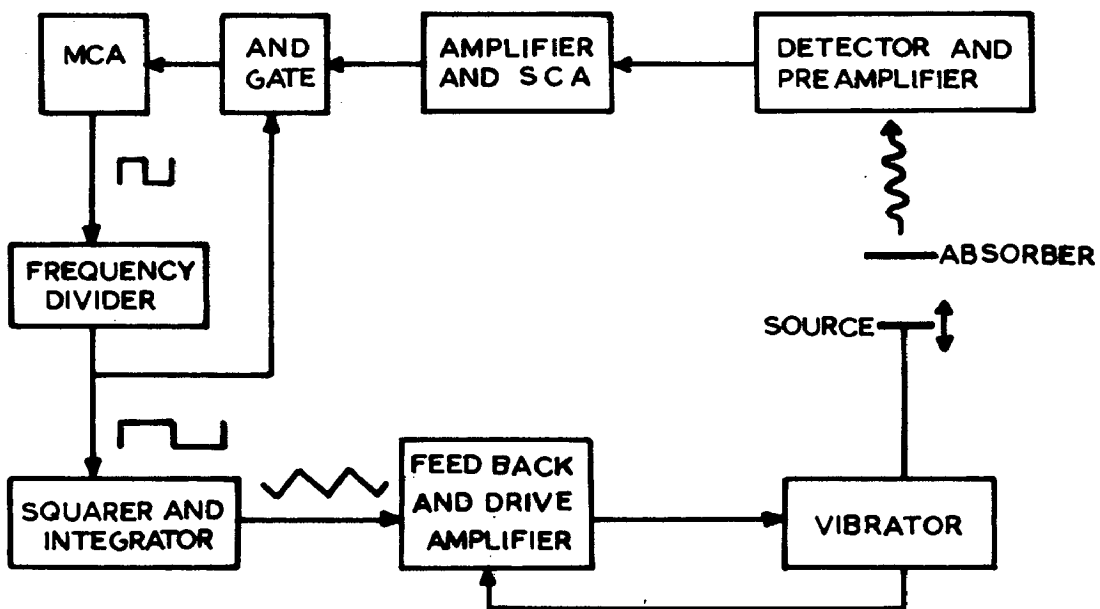
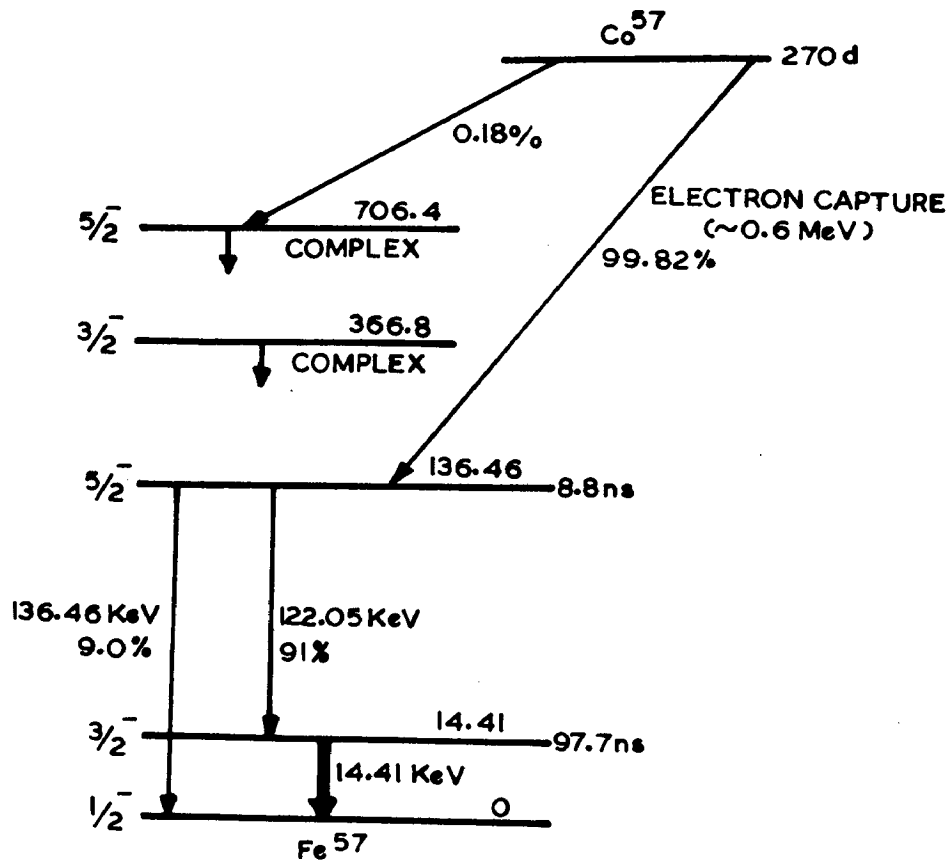


**FIG.2.9: BLOCK DIAGRAM OF MÖSSBAUER SPECTROMETER FOR RECORDING THE SPECTRUM IN TRANSMISSION GEOMETRY.**



(Thick line is indicating Mössbauer transition)

**FIG.2.10. DECAY SCHEME OF  $^{57}\text{Co}$  ISOTOPE.**

Mössbauer probe.

In the present studies, the experiments were performed in transmission geometry, which requires specimen in the form of absorbers. Therefore, rust specimens were made in pellet form by putting in perspex holder mountings, which acted as absorbers.

- Mössbauer Drive:

The problem of the partial or complete destruction of resonant absorption can be overcome by providing a relative Doppler velocity between the source and absorber. Thus, if the source is moved relative to the absorber with a Doppler velocity  $v$  then the change in energy of T-rays emitted from the source will be

$$\delta E = \pm \frac{v}{c} E_T \quad (2.9)$$

where  $c$  is the velocity of light and  $E_T$  is the energy of T-rays. The increased/decreased energy will make possible the resonance absorption. The amplitude, of Doppler velocities required, depends on the natural line width  $\Gamma$ , energy of T-rays, and the shift and splitting of various nuclear energy levels due to hyperfine interactions. For  $Fe^{57}$ , these velocities range within  $\pm 10$  mm/sec (corresponding to  $\delta E = 4.8 \times 10^{-7}$  eV energy modification). To provide a controlled and well defined velocities, of these magnitudes, to the source relative to the absorber, the source was made to move in constant acceleration mode. For this

purpose a triangular shaped pulse is given to drive circuit which moves the source back and forth in constant acceleration mode from  $-V_{\max}$  to  $V_{\max}$ . This pulse is obtained from the multi-channel analyzer itself as a square wave, which is then integrated to obtain triangular wave. The drive pulse is obtained from the multi-channel analyzer so that it has same frequency as that of the multi-channel scanning (MCS) sweep of the analyzer. This helps in achieving the resonance conditions between the source movement and the MCS sweep.

#### - Detection and Counting System:

Since Mössbauer effect is observed for gamma rays whose energies lie between few KeV to 150 KeV, one needs the low energy detection techniques. In general, three types of detectors which have been used in this range are (i) proportional counters (ii) Li drifted Ge counter ( semiconductor detector ) (iii) NaI (Tl) scintillation counter. For gamma-rays having energy below 20 KeV (in present case it is 14.4 KeV), proportional counter gives the best resolution (103). This is of the order of 10% with sufficient efficiency (104). In the present work, sealed proportional counters filled with mixture of 90% Ar and 10% methane was used. The operating voltage was of the order of 1900 V and the energy resolution obtained was  $\approx 14\%$ . The output of detector is fed to linear amplifier since the pulses obtained from detector are not sufficiently big. After amplification, the pulses are sent to single channel analyzer to select  $14.4 \pm 4.8 \times 10^{-10}$  keV T-rays. These are then fed to 512-channel analyzer for recording the spectrum in multi-channel scanning mode.

In addition to these basic components some other auxiliary system e.g. cryostat , to perform study at 80°K ,and temperature controller were also used.

## 2.7 Laboratory Testing:

Testing in the laboratory is an important phase of corrosion studies. These tests range from fundamental work to the procedures that attempt to simulate service or natural environments (38). Laboratory corrosion tests are used to predict corrosion behavior when service history is lacking and time or budget constraints prohibit service(field) testing. They can also be used as screening tests prior to service testing. Laboratory tests are particularly useful for quality control, materials selection, materials and environmental comparison, and the study of corrosion reaction mechanisms (105). The tests cover from simple immersion tests to various kinds of cabinet and autoclave controlled environments to sophisticated electrochemical tests.

In the present work, two types of laboratory tests were performed - (i) Weight-loss , (ii) Electrochemical polarization tests. These tests were performed in bleach liquor of varying concentration with and without addition of sulfamic acid . Prior to discussing two kinds of tests, a discussion is given on solution preparation.

### 2.7.1 Solution Preparation :

The following were the compositions of the test solutions.

(a) Sodium chloride solution containing  $\text{Cl}^-$  ions ranging from 200 to 3000 ppm, to observe the effect of  $\text{Cl}^-$  ion concentration on corrosion rate.

(b) Calcium hypochlorite solutions  $\text{Ca}(\text{OCl})_2$  having free available chlorine ( $\text{FACl}_2$ ) concentration ranging from 150 to 600 ppm at three different concentrations of  $\text{Cl}^-$  ions (1000, 2000 and 3000 ppm  $\text{Cl}^-$ ). These solutions were made to observe the effect of free available  $\text{Cl}_2$  on corrosion rate, in the presence of varying amount of  $\text{Cl}^-$  ions.

(c) (i)  $\text{Ca}(\text{OCl})_2$  solution of 300 ppm  $\text{FACl}_2$ , 1000 ppm  $\text{Cl}^-$  but varying sulfamic acid concentration from 10-30 ppm.

(ii)  $\text{Ca}(\text{OCl})_2$  solution of 300 ppm  $\text{FACl}_2$ , 3000 ppm  $\text{Cl}^-$  and same range of sulfamic acid as in (i) above.

(iii)  $\text{Ca}(\text{OCl})_2$  of 600 ppm  $\text{FACl}_2$ , 1000 ppm  $\text{Cl}^-$  and same range of sulfamic acid as in (i).

(iv)  $\text{Ca}(\text{OCl})_2$  of 600 ppm  $\text{FACl}_2$ , 3000 ppm  $\text{Cl}^-$  and same range of sulfamic acid as in (i).

Whereas the calcium hypochlorite solutions were prepared from bleach liquor (having 32 gpl  $\text{FACl}_2$ ) obtained from a nearby mill, other solutions were made with AR grade of respective chemicals. The concentration of chemicals in the above solutions were checked using the methods as mentioned in section 2.5.2. The above range of chemical concentration was selected to cover the concentration ranges which are normally observed in hypochlorite



stage washers of bleach section.

### 2.7.2 Weight-Loss Test :

Weight loss tests were performed on mild and stainless-steels in the different solutions as indicated in the above section to observe the corrosive effect of hypochlorite concentration and the effect of sulfamic acid on it. The latter part of the study was done to simulate with the process conditions in one of the mills in which corrosion tests were performed in the present programme.

For observing the corrosion rate, the coupons were completely dipped in the test solution. The volume of the test solutions should be large enough to avoid any appreciable change in its corrosiveness, during corrosion tests. From this point of view, for an exposed surface area of 1 square inch, 125 ml. of solution should be taken. In the present work it was preferred to have more than 250 ml. solution per square inch of specimen's surface.

Though duration of test will be determined by the purpose of the test, however, in general following practice is adopted. If anticipated corrosion rates are moderate or low, the following equation gives suggested test duration -

2000

$$\text{Duration of test (in hours)} = \frac{2000}{\text{Corrosion Rate (mpy)}} \quad \dots(2.10)$$

This method of estimating test duration is useful only as an

aid in deciding, after a test has been made, whether or not it is desirable to repeat the test for longer periods. In the present work test duration was 1 day for mild steel and 30 days for stainless-steel coupons.

The cleaning and corrosion rate determination methods have earlier been discussed. The tests on stainless-steels did not give significant and reliable information due to their having very low corrosion rates.

### 2.7.3 Electrochemical Polarization Tests:

The corrosion of metals in aqueous electrolytes occurs by an electrochemical mechanism. These techniques, with the help of potential-current relations, offer an easy way to accelerate the corrosion processes. For example they can be used to measure instantaneous corrosion rates (to compare metals and environments) without removing the specimen from the environment in a very short duration. They can be used to measure very small corrosion rates, which might take very long time ( $\approx$  few months) if we perform weight-loss tests. Such a situation is encountered while comparing performance of inhibitors and corrosion resistant materials. Similarly, these tests also help in telling whether a given material will suffer from localized corrosion in a given environment. They can also be used to increase or control the oxidizing potentials of an environment and thereby reveal specific characteristics of a material, such as passivity, without adding chemical oxidizing agents. However, there are some basic requirements for electrochemical testing. The corroding sample

must be in an electrolyte, environment must be continuous as least to the extent that all electrodes show semi-electrical continuity through the electrolyte and the primary corrosion mechanism must be electrochemical. Basic corrosion measurements include Tafel plot, linear polarization (also called polarization resistance), potentiodynamic polarization, corrosion behavior diagram etc. In the present investigations, Tafel plots and linear polarization measurements have been done, therefore only these will be emphasized in the forthcoming discussions.

(a) Basic Experimental Equipment:

The basic experimental equipment, used in the present work (Fig.2.11, photograph 2.2), for performing a variety of electrochemical tests include a cell, a potentiostat/galvanostat (potential/current controlling and measuring device) and a recorder. These components of Corrosion Measurements System of EG&G Princeton Applied Research Corporation, U.S.A. are discussed below :

- Corrosion Cell:

Corrosion cell system is shown in photograph 2.3. Electrochemical measurements of corrosion phenomena require a cell system that is versatile, convenient to use, and can provide reproducible conditions from one experiment to another. The above system fulfills these requirement. Different components of the cell are the working electrode (test metal) in the form of a small cylinder (Height and Diameter  $\approx$  1-1.5 cm.), reference

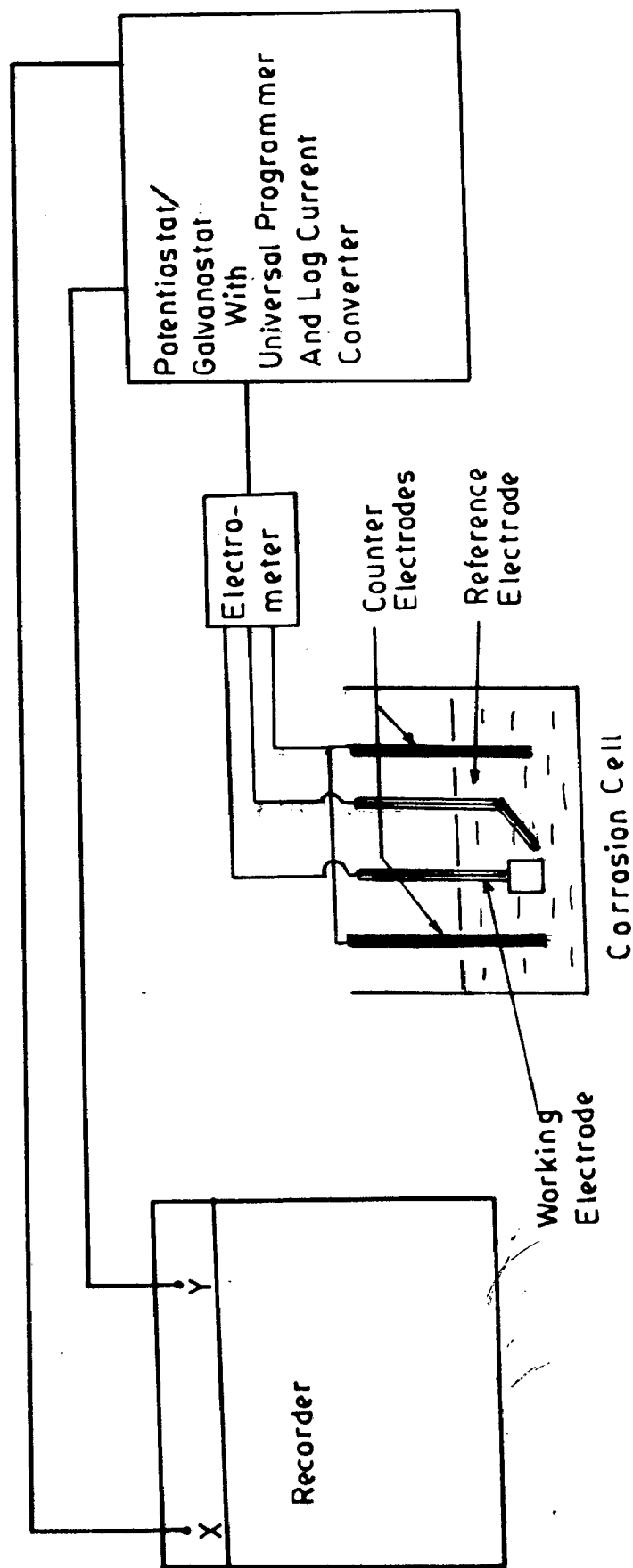
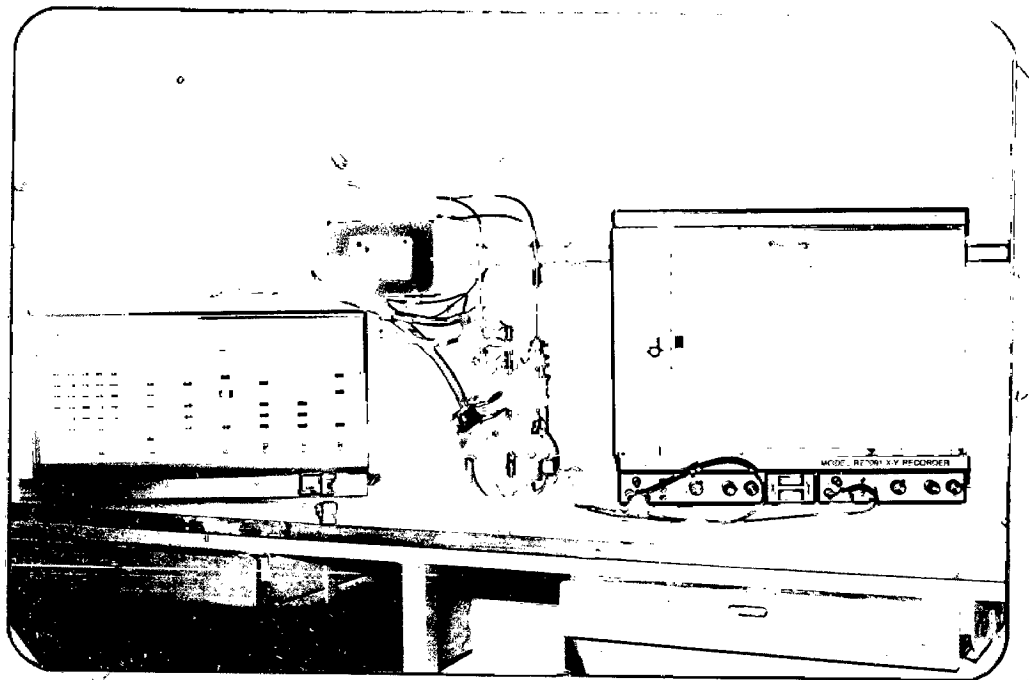
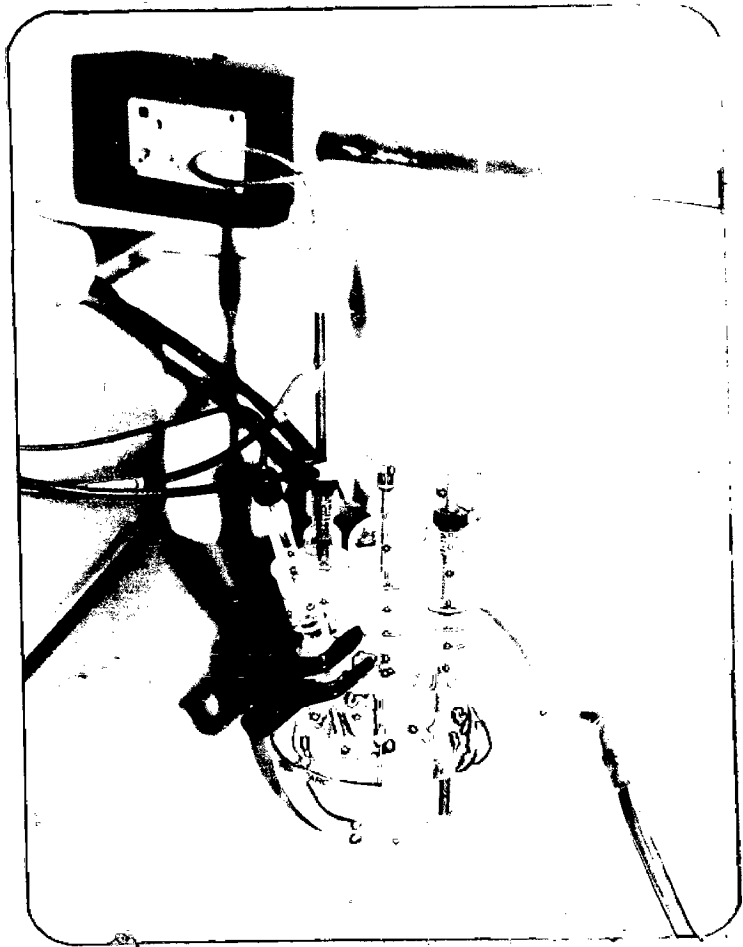


FIG. 2.11: BLOCK DIAGRAM OF CORROSION MEASUREMENT SYSTEM



PHOTOGRAPH 2.2 : ELECTROCHEMICAL EXPERIMENTAL SET-UP  
FOR CORROSION MEASUREMENTS.



PHOTOGRAPH 2.3 : CORROSION CELL

electrode and auxiliary or counter electrodes. One face of the working electrode is internally threaded at its centre for fitting the electrode holder. It is seated against the tubular glass holder using a threaded metal rod and a Teflon Gasket (Fig. 2.12). The reference electrode (saturated calomel electrode) rests in a luggin capillary, which is adjusted so that its other tip is closed to the test electrode (photograph no. 2.3). This reduces the error in measurement of the electrode potential due to I-R drop, or the potential drop associated with the passage of current through a resistive solution. There is a pair of counter electrodes in the form of graphite rods. During polarization tests, current flows between these counter electrodes, fitted symmetrically around the working electrode to provide the even current distribution. The corrosion cell also has an opening for inserting a gas purging tube. This tube is used to purge gases in the solution prior to / during the tests. Quite common is purging of Nitrogen gas which is used to remove oxygen from the corroding solution while performing electrochemical tests.

- Saturated Calomel Electrode ( SCE ) :

The saturated calomel electrode ( SCE ) has been used as the reference electrode. It is preferable over others in the sense that it is easy to handle and the potential of this electrode is fairly constant with time and temperature (  $dE/dT = -7.6 \times 10^{-4} \text{ V/}^\circ\text{C}$  ). The SCE is not easily poisoned or contaminated and is insensitive to the electrolyte's composition because of its design. In principle, it consists of mercury (Hg) in equilibrium with mercurous ions  $\text{Hg}^+$ . The half cell reaction is

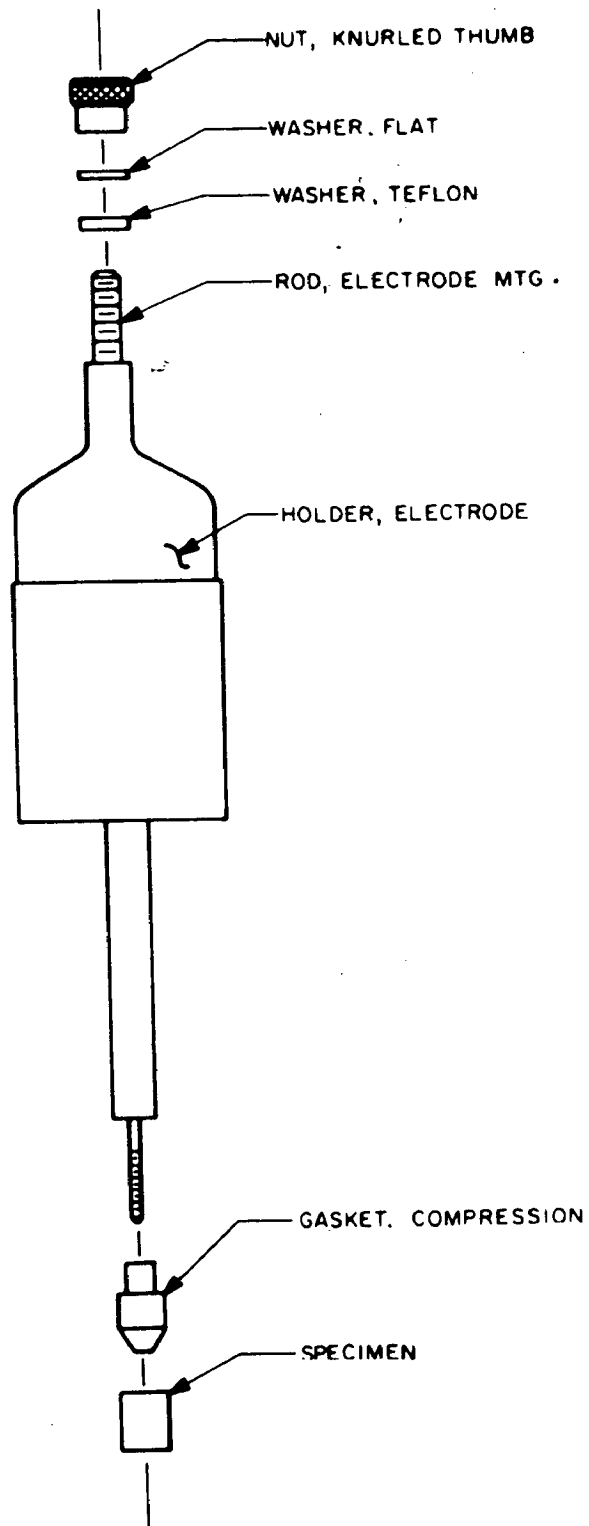


FIG.2-12: SPECIMEN HOLDER ASSEMBLY





.....(2.11)

For this reaction,  $E^0 = 0.268$  Volt. Pure mercury covers a platinum wire sealed through the bottom of a glass tube (Fig-2.13). The mercury is covered with powdered or pasted mercurous chloride, which is only slightly soluble in potassium chloride solution, the latter filling the cell. The potential on the standard hydrogen scale for saturated KCl concentration is around 0.242 Volt. The electrical contact with an electrolyte is maintained by an ultralow-leakage vycor tip of the electrode body. Liquid junction potentials are usually negligible in this case which is one of the main advantages of SCE electrode.

- Potentiostat/Galvanostat :

The potentiostat is a device which measures and controls the potential of the working (test) electrode with respect to a reference electrode. When it is controlling the current, it will be called as galvanostat. It controls the potential of working electrode, by supplying a current of the needed magnitude and polarity to the working electrode using counter electrodes. Therefore potential measurement is done between the working and reference electrodes, while potential adjustment is done by passing current between the working and the counter electrodes. Using a potentiostat, polarization may be accomplished either in steps (potentiostatic polarization) or continuously (potentiodynamic polarization). Similarly, when applied current is the controlling parameter the corresponding terms will be galvano-

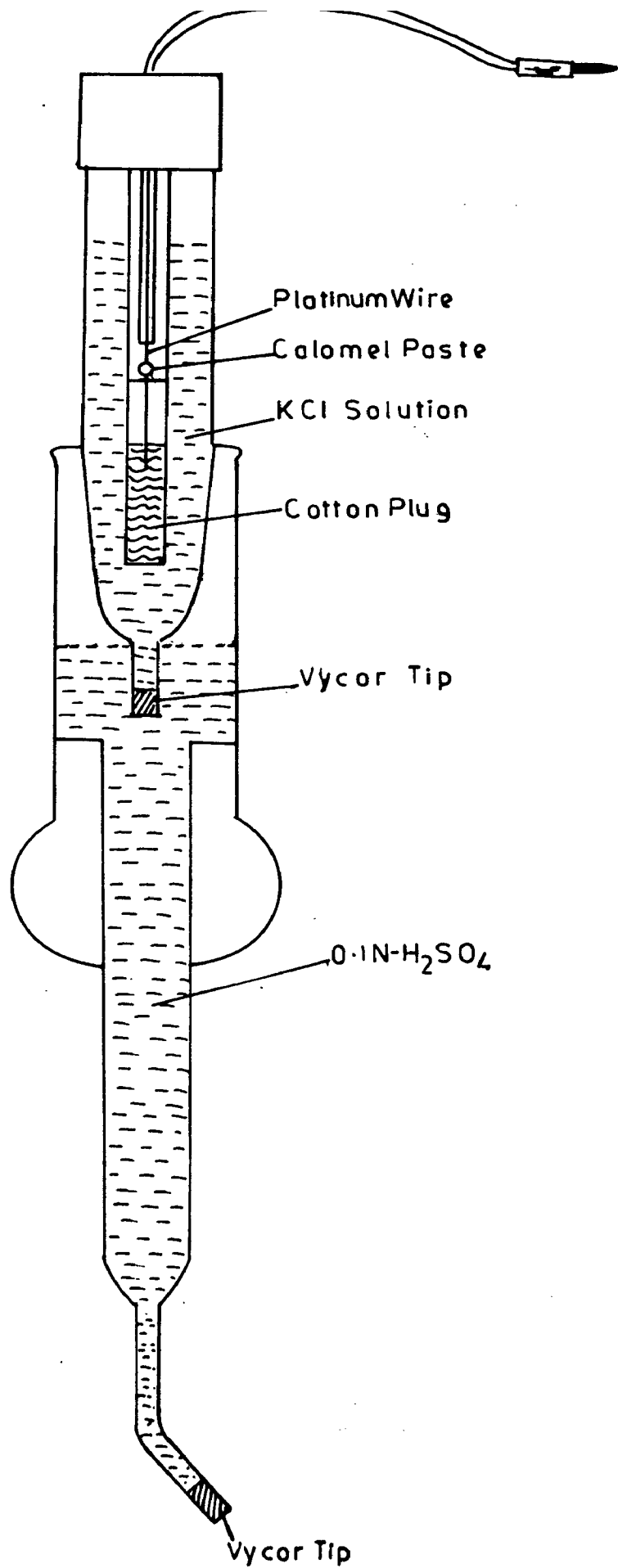


**FIG. 2.13: SATURATED CALOMEL ELECTRODE**

static and galvanodynamic. However, present investigations have been done only in potentiostatic mode, a preferred mode (27).

The potentiostat used in the present study, implements the very latest analog and microcomputer design to provide high performance, high sensitivity, ease of use and unlimited versatility in electrochemical measurements. Its 100 volt compliance voltage and 1 ampere output capability allows rapid, accurate, potential or current control which is important in controlling potential when working with higher resistance, dilute electrolytes or nonaqueous solvents. It has got inbuilt potentiostat/galvanostat, logarithmic current converter, universal programmer and voltage/current measuring unit. The electrometer is externally used. Thus the potentiostat is used for both to control the potential/current and note the corresponding current/potential on the working electrode immersed in an electrolyte.

#### - X-Y Recorder :

This is used to obtain current (or log current) versus potential variation in an electrochemical experiment. The current (linear or log scale) is selected on X-axis and applied potentials on Y-axis. One uses in these experiments semi-log graph paper (except linear polarization measurements) whose size is 15" for X-axis (which is log scale) and 10" for Y-axis. Y-axis sensitivity of 50 mV/inch is required since normally Tafel plots are recorded by polarizing the sample  $\pm 250$  mV about  $E_{\text{corr}}$ . The sensitivity of X-axis is determined by the ranges of currents that one expects to

measure in an experiment. For linear polarization measurements, the Y-axis is calibrated to measure 5mV/inch, since in these experiments the sample is polarized nearby  $E_{corr}$  only. The calibration of X-axis is done on a linear scale.

(b) Electrochemical Polarization Measurements:

The speed of electrochemical measurements is especially useful for those metals or alloys which are highly corrosion resistant (e.g. stainless-steels in present case). Long-term corrosion studies, such as weight-loss determinations, may take days or weeks or even several months while an electrochemical experiments will require at most a few hours. Much of modern corrosion analyses through electrochemical techniques are based on theoretical analyses of the shape of polarization curves by Stern and Geary (106). For representing the electrochemical data, ASTM recommendations have been adopted. According to these, a more negative reduction potential indicates an active metal whereas a more positive reduction potential represents a passive metal. In potentiostatic operation, making the applied potential more positive will make the current tend to be more anodic. Conversely, making applied potential more negative will make the current tend to be more cathodic. Positive current is cathodic, i.e., a current is defined as positive if reduction is taking place on the electrode. Negative current is anodic, i.e., a current is defined as negative if oxidation is taking place. Now the details are given about the different measurements performed in the present work.

- Corrosion Potential:

In all kinds of polarization studies, generally the first measurement is that of corrosion potential  $E_{corr}$  when the externally applied potential is zero. Once  $E_{corr}$  is known, the working electrode is then polarized either anodically (+ive going potential) or cathodically (-ive going potential) with respect to the  $E_{corr}$ . In the present set-up, the corrosion potential is measured by connecting the lead from working electrode to the electrometer, which in turn is connected to potentiostat. The reference electrode also has to be connected to the electrometer.

- Tafel Plot :

The purpose of determining Tafel Plot is to know kinetic electrochemical parameters so as to understand the corrosion mechanism and to determine the corrosion rates. One records the Tafel plots by polarizing the specimen cathodically as well as anodically. The anodic or cathodic Tafel plots are defined by following equation.

$$n = \pm \beta \log \frac{i}{i_{corr}} \quad \dots\dots(2.12)$$

Where  $n$  is overvoltage, the difference between the potential of specimen and the corrosion potential, i.e.,  $n = E_{appl} - E_{corr}$ ,  $\beta$  is Tafel constant and  $i_{corr}$  is the corrosion current.

To know Tafel constants, designated as  $\beta_a$  (for anodic curves),  $\beta_c$  (for cathodic curves) and  $i_{corr}$ , the  $n - \log i$

plots (Tafel plots) have to be experimentally obtained.

- Calibration of Axes :

Prior to start recording the Tafel plot, it is necessary to calibrate the current and potential axes. The calibration part becomes more important in view of the fact that one of the axes (representing current) is on log scale whereas the other (representing potential) is linear. Calibration of X-axis (current axis) is done with the help of a dummy resistor of  $100\text{ k}\Omega$  provided with the set-up. On application of 1 Volt to this resistor, a current of  $10^{-5}$  ampere (amp) ( $10\ \mu\text{A}$ ) flows in the dummy cell. It must be understood here that 1 decade of current (at chart paper) corresponds to 1 Volt of 'log reference voltage', with extreme right position ('f' in Fig.2.14) corresponding to 0 volt and extreme left ('a' in Fig.2.14) to -5 volt. The log reference voltage is set by potentiostat using command FUNCTION 12. These different functions (software controlled) have been provided in potentiostat to do specific jobs. For example when FUNCTION 12 = -3, say, log reference voltage of 0 volt will be generated by a current of  $10^{-3}$  amp which is fed to X-axis of recorder. Thus when FUNCTION 12 = 0,  $10^0$  amp will correspond to 0 (zero) volt. Since current in dummy resistor is  $10^{-5}$  amp hence an output of -5 volt will be generated. This is fed to X-axis of recorder when position of pen shifts by 5 decades of current or in other words pen will move to extreme left position (a in Fig.2.14) of the chart. This position will indicate  $10^{-5}$  amp on current scale. Now set FUNCTION 12 = -5. In this setting  $10^{-5}$  amp current will correspond to 0 (zero) volt. Because current in the dummy resistor is

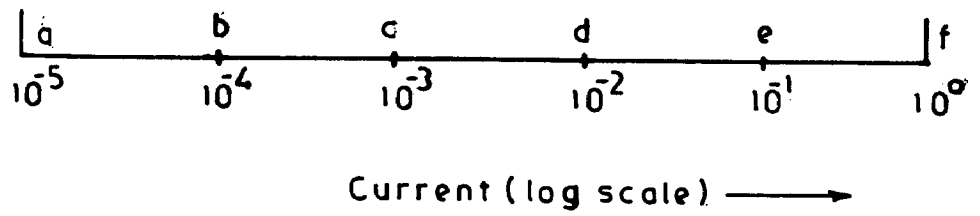


FIG. 2-14: CALIBRATION OF CURRENT AXIS ON LOG SCALE

still  $10^{-5}$  amp, an output of 0 volt is generated. This voltage when fed to X-axis of recorder, will move the pen to extreme right position ( f in Fig.2.14), because it will mean shifting from -5 to 0 volt. The intermediate positions of X-axis of chart ( i.e. b,c,d,e in Fig. 2.14 ) can be checked by setting FUNCTION 12 = -4, -3, -2, -1 respectively. Values of current, represented by these positions, depend upon value of FUNCTION 12. Thus if FUNCTION 12 = -1,  $10^{-1}$  amp will correspond to log reference voltage of 0 volt and hence will correspond to 'f' position. Positions e,d,c,b,a (Fig.2.14) then will represent  $10^{-2}, 10^{-3}, 10^{-4}, 10^{-5}, 10^{-6}$  amp respectively. Y-axis (linear axis here) is calibrated at a scale of 50 mV/inch. Since the size of chart paper is 10", this scale means the scanning of potential of specimen upto  $\pm 250$  mV about its corrosion potential.

- Measurements :

A Tafel plot measurement is done on a metal or alloy by polarizing the specimen by about 250mV ( or 300mV) anodically and cathodically from the corrosion potential  $E_{corr}$ , as shown in Fig.2.15. For recording the Tafel plot a five cycle semi-log chart paper is used. The potential axis ( Y-axis) is selected as linear having sensitivity of 50 mV/inch. The resulting current is plotted on a logarithmic scale, calibrated as mentioned above, and represented as X-axis. While recording Tafel plot, the electrometer is set at 'external' meaning for corrosion cell. The potential was scanned upto  $\pm 300$  mV about the corrosion potential with a scan rate of 2 mV/sec. The scan was started from the



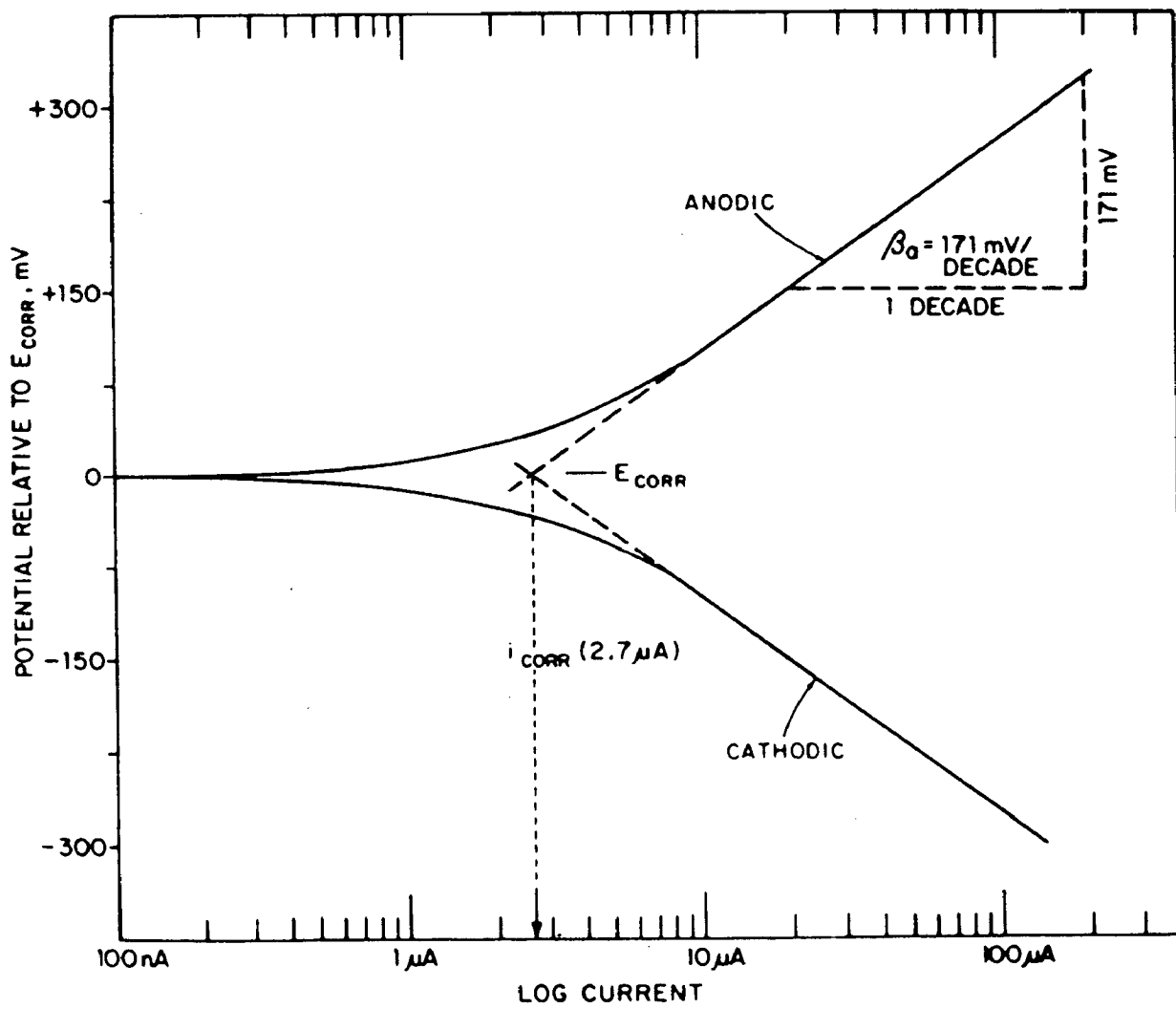


FIG. 2-15: POLARIZATION CURVE SHOWING TAFEL REGION

maximum cathodic potential.

Tafel slopes  $\beta_a$  and  $\beta_c$  are calculated by measuring the slopes of tangents to the anodic and cathodic polarization curves. These tangents are drawn on the linear part (Tafel region) of the curves. In order that one gets a reasonable tangent line and hence the value of slope, the length of Tafel region should extend to more than one decade of current at-least but normally it should be around two decades of current long (100). The unit of Tafel slopes is mV/decade of current change. In the present studies, the polarization curves didn't show linearity in anodic part hence only  $\beta_c$  could be measured. The corrosion current  $i_{corr}$  is obtained from Tafel plot by extrapolating the linear portion of the curve to  $E_{corr}$  as shown in Fig.2.14. It is important to note that usually (also in present cases) the extrapolation of anodic and cathodic linear region do not intersect at  $I_{corr}$ . In such cases  $I_{corr}$  is obtained only by intersecting tangent to cathodic polarization curve at  $E_{corr}$  axis.

Calculation of corrosion rate from the corrosion current density is done by the following formula ( which is obtained with the help of Faraday's law) -

$$\text{Corrosion Rate (mpy)} = \frac{0.13 \times I_{corr} \times E.W.}{d} \dots\dots(2.13)$$

Where  $I_{corr}$  = Corrosion current density,  $\mu\text{A}/\text{cm}^2$ .

E.W. = Equivalent weight of the corroding species, grams

d = Density of the corroding species,  $\text{gram}/\text{cm}^3$

In many cases, linear region of Tafel behavior may be shortened due to concentration and/or resistance polarization effects. These can be minimized by stirring the solution gently in the former case and compensating instrumentally for IR effects in the latter case. In cases where linearity of cathodic polarization curve is shortened due to dissolved oxygen, this could be avoided by purging  $N_2$  which removes the dissolved oxygen. In our experiments we have stirred the solutions and purged  $N_2$  gas through the solutions in an effort to increase the linear region.

- Linear Polarization (Polarization Resistance):

Stern and Geary (106) have provided a firm theoretical background for polarization resistance measurements. The electrochemical technique of polarization resistance is used to measure absolute corrosion rates. Excellent correlation can often be made between corrosion rates obtained by the polarization resistance and by conventional weight-loss determinations. These measurements are performed by scanning through a potential range which is very close to the corrosion potential,  $E_{corr}$ . (Fig.2.16). The resulting current is plotted versus potential, on linear scale because theoretically polarization potential varies linearly with current when the former is not very different than corrosion potential. Under the approximation, the corrosion current  $i_{corr}$  is related to the slope ( $\delta E/\delta i$ ) of the  $E$  vs.  $i$  curve as follows :

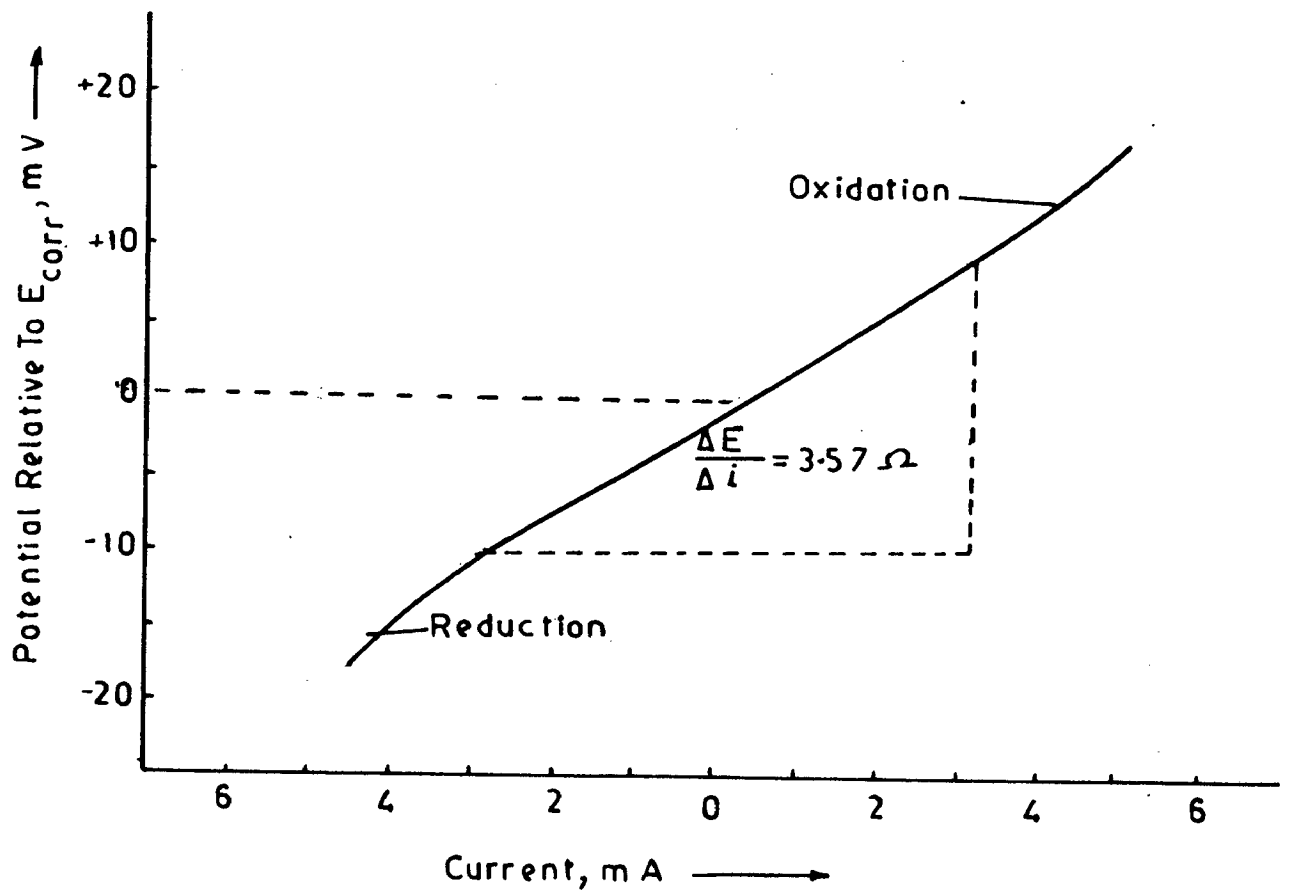


FIG.2-16: LINEAR POLARIZATION CURVE

$$\delta E / \delta i = \frac{\beta_a \beta_c}{2.3 (i_{corr}) (\beta_a + \beta_c)} \quad \dots (2.14)$$

Rearranging the above equation

$$i_{corr} = \frac{\beta_a \beta_c}{2.3 (\beta_a + \beta_c)} \frac{\delta i}{\delta E} \quad \dots (2.15)$$

Since the unit of slope  $\delta E / \delta i$  is resistance, determination of this slope by present method is also termed as polarization resistance method. The corrosion current and hence current density is related to the corrosion rate according to the equation 2.13. Some modifications in expression for corrosion rate and the range of validity have been discussed elsewhere (107,108).

- Calibration and Measurements :

Prior to starting measurements, it is necessary to calibrate the two axes namely current and potential axes. Since in this case current varies linearly with potential, unlike the case of Tafel plot, one takes here linear chart paper. The X-axis (current axis) sensitivity is set at, say, 10 mV/inch. Now if the current range set at potentiostat is, say, 100 mA, a full scale current in the corrosion cell will provide an output of 1 volt, which means that 10 mV will correspond to 1 mA. Since this voltage is fed to the X-axis of the recorder, the scale of this axis will be 1 mA/inch at the above mentioned setting. In

the present work X-axis was set at 0.1  $\mu\text{A}/\text{inch}$  and ~~10~~  $\mu\text{A}/\text{inch}$  (i.e. the selected current ranges were 10  $\mu\text{A}$  and 1 mA at X-axis sensitivity of 10 mV/inch). Y-axis is calibrated as usual, and it was set to a sensitivity of 5 mV/inch meaning that potential was scanned upto  $\pm 25$  mV about the corrosion potential with a scan rate of 1 mV/sec.

## Chapter - 3

### ANALYSES OF CORROSION ON STEEL COUPONS EXPOSED IN BLEACH PLANT

	Page No.
3.1 Weight-loss and Localized Corrosion Analyses.	91
3.1.1 Corrosivity of Environment.	105
(a) Assessment in different phases.	
(b) Assessment in different bleaching stages.	
(c) Comparison of corrosivity in mill A and B.	
3.1.2 Performance of Materials.	125
(a) Assessment of performance.	
(b) Comparison of material performance in mill A and B.	
3.2 Analyses of Corrosion Products.	132
3.2.1 Mild Steel.	133
(a) Mill A.	
(b) Mill B.	
3.2.2 Stainless-Steels.	150

Corrosion studies have been performed in bleach plants of two Indian paper mills to generate authentic data with regard to the corrosivity of environments and performance of materials, normally used to fabricate process equipments, in these mills. The rusts/scales scraped from the corroded coupons and in some cases the corroded surface itself were subjected to the analyses of corrosion products also. The subject matter of this chapter has been divided as follows :

3.1 Weight-loss and localised corrosion analyses.

3.2 Analyses of corrosion products.

3.1 Weight-loss and localised corrosion analyses:

The field coupon corrosion tests were performed at two integrated pulp and paper mills in India. Stainless-steels (SS) of type 304, 304L, 316, 316L and 321 and mild steel (MS), of commercial grade, were put through exposure in washers of bleach plant of both mills. The chemical composition and micro-structure of these steels are given in Table 3.1 and Photograph 3.1 respectively. The microstructure of all the stainless-steels show austenitic matrix. SS 316 shows coarse grains whereas carbide particles with recrystallised grains of austenite are observed in case of 316L. Mill A uses the bleaching sequence consisting of chlorination (C), buffered-hypo (B) and hypochlorite (H). Mill B has chlorination (C), hypochlorite-1 (H1) and hypochlorite-2 (H2) as the bleaching stages. The coupons in mill A were exposed in gaseous (G) phase (near shower pipes) and in liquid (L) phase (at pulp inlet of vats) while in mill B, the exposure was in gas



**Table 3.1: Analyses of Steels ( Wt% )**

Material	C	Si	Mn	Ni	Cr	Mo	Ti
Mild-steel	0.18	0.04	0.66	-	-	-	-
SS-304	0.04	0.59	1.92	11.52	18.10	-	-
SS-304L	0.02	0.59	0.91	9.25	19.15	-	-
SS-316	0.03	0.62	0.94	8.53	18.68	0.29	-
SS-316L	0.02	0.48	1.66	13.86	18.42	1.95	-
SS-321	0.05	0.69	1.30	9.38	18.63	-	0.41

SS - abbreviated for stainless-steel.



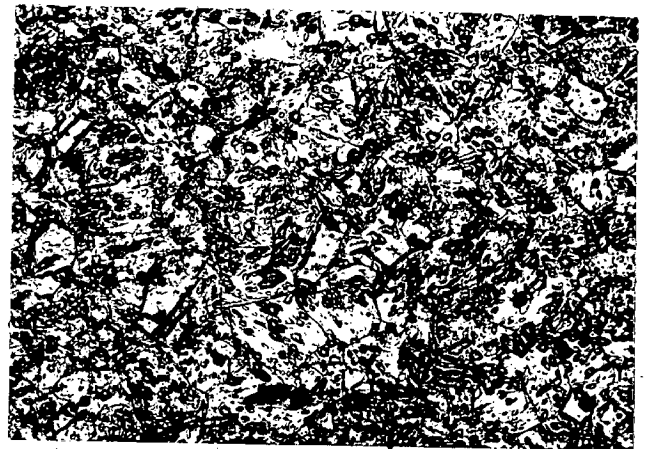
(a) SS-304 (x375)



(b) SS-304L (x375)



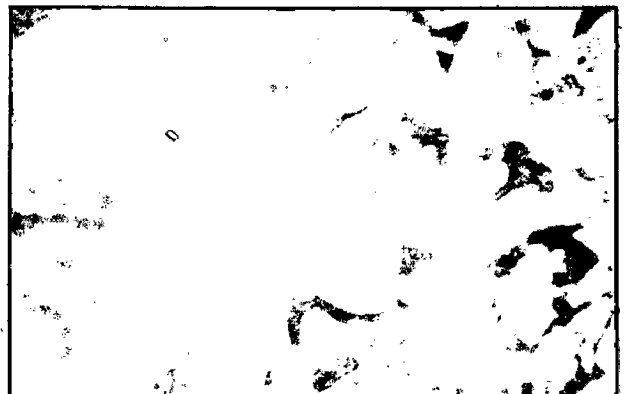
(c) SS-316 (x375)



(d) SS-316L (x375)



(e) SS-321 (x375)

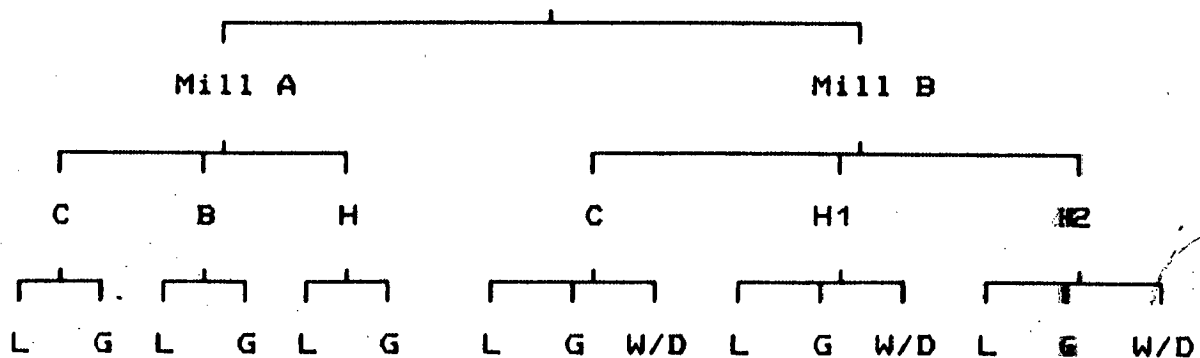


(f) MILD STEEL (x500)

PHOTOGRAPH 3.1 : MICROSTRUCTURE OF STEELS.

phase, liquid phase and in wet/dry (W/D) cyclic conditions (on rotating washer drum). These different positions are shown in Fig.2.1. Test duration for experiments in mill A, for mild steel was 15 days to 45 days and that for stainless-steels was 6 months . In case of mill B , the exposure was 3 months long. The conditions of vat liquors during exposure are given in Table 3.2, 3.3 and 3.4. The results of these tests, derived by measuring weight-loss and degree of localised corrosion , have been analysed to assess the corrosivity of environment and the performance of the steels at different parts of bleach plant of the two mills. However, as can be seen at next page that coupons have been tested in diversified media and that six different type of steels have been tested in these media, a meaningful comparison of the results and hence their analyses has to be done with precaution so as to avoid the confusion and intermixing of the results.

### Corrosion Tests



In each of the above shown fifteen different places (L,G and W/D) six different type of steels have been tested. We have tried to assess the corrosivity of environment in terms of weight lost by

**Table 3.2: Condition of liquors from bleaching stages of Mill A**  
 ( During mild steel exposure )

Parameters	Temperature	pH	Residual oxidant
Stages	(°C)		( ppm )
Chlorination	43	2.0	15
Buffered hypo	41	6.5	210
Hypochlorite	39	7.4	167

**Table 3.3: Condition of liquors from bleaching stages of Mill B**

Parameters Stages	Temperature (°C)	pH	Residual Oxidant (ppm)	Chloride ions (ppm)
Chlorination	29	2.8	0.0	621
Hypochlorite1	33	7.5	3.0	941
Hypochlorite2	32	8.1	20.0	450

**Table 3.4: Condition of liquors from bleaching stages of Mill A  
( During Stainless-steel exposure )**

Parameters Stages	Temperature (°C)	pH	Residual Oxidant (ppm)	Chloride ions (ppm)
Chlorination	44	2.1	17	899
Buffered-hypo	45	6.9	257	1907
Hypochlorite	41	7.4	220	911

materials (corrosion rate) and degree of localized attack e.g. pitting and crevice corrosion experienced by the coupons. The assessment of pitting and crevice corrosion has been done by estimating the fraction of exposed surface experiencing localized attack,  $f_{loc}$ . The severity of attack can be classified as defined in previous chapter. Consequently following experimental results have been obtained :

- Corrosion rates for mild steel (Table 3.5).
- Corrosion rates for stainless-steel in mill A (Table 3.6).
- Corrosion rates for stainless-steel in mill B (Table 3.7).
- Pitting on stainless-steel in mill A (Table 3.8).
- Crevice corrosion on stainless-steel in mill A (Table 3.9).
- Pitting on stainless-steel in mill B (Table 3.10).
- Crevice corrosion on stainless-steel in mill B (Table 3.11).

Vacant rectangle in Tables 3.8 to 3.11 indicate the absence of localized type of attack in the respective case. An idea about the degree of attack can be had from scanning electron microphotographs (Photographs 3.2 and 3.3). SEM photographs 3.2 a, b and c shows the excessive, moderate and negligible pitting attack respectively. The photographs have been taken at a magnification of 20x1.0, 20x1.0 and 40x1.1. Photographs 3.3 a, b and c show excessive, moderate and negligible crevice corrosion respectively. These photographs were taken at a magnification of 20x1, 20x1.1 and 20x1.1 respectively.

With the help of above mentioned results, an effort has been made to compare the corrosivity of environment and relative

**Table 3.5 : Corrosion rate for mild steel (in mpy)**

Mill	Exposure Duration (days)	Gaseous			Liquid			Wet/Dry		
		C	B	H	C	B	H	C	B	H
A	15	157	75	34	1121	49	-			
	35	107	89	94	-	-	20			
	45	72	49	24	-	27	-			
B	90	C	H1	H2	C	H1	H2	C	H1	H2
		9.4	6.1	8.2	39.9	4.3	16.3	17.7	2.5	6.8

C - Chlorination, B - Buffered hypo, H - Hypochlorite stages.

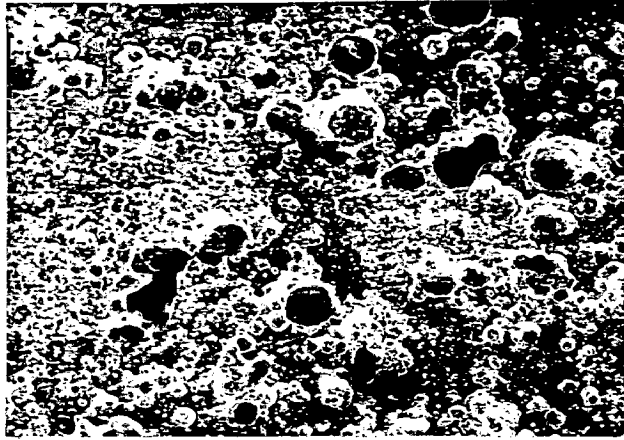


**Table 3.6 : Corrosion Rate ( in mpy ) ( Mill A )**

Stages Material	Gaseous			Liquid		
	C	B	H	C	B	H
304	34.85	4.22	3.9	0.35		0.06
304L	26.15	3.71	3.6	0.16		0.03
316	35.45	4.00	3.0	0.23		0.02
316L	38.61	1.90	1.7	0.07		0.02
321	23.66	2.50	3.0	0.18		0.05

**Table 3.7: Corrosion Rate ( in mpy ) ( Mill B )**

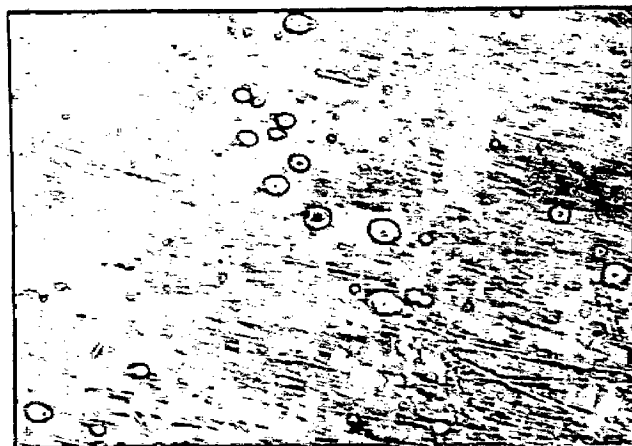
Stages	Gaseous			Wet/Dry			Liquid		
Material	C	H1	H2	C	H1	H2	C	H1	H2
304	6.97	0.28	0.06	0.02	0.16	0.44	0.10	0.07	0.86
304L	5.25	0.13	0.03	0.01	0.14	0.33	0.07	0.05	0.09
316	5.00	0.08	0.04	0.02	0.17	0.48	0.09	0.16	0.73
316L	2.57	0.05	0.03	0.01	0.12	0.23	0.03	0.12	0.65
321	4.56	0.12	0.05	0.03	0.16	0.32	0.07	0.11	0.74



(a) EXCESSIVE, SS-316 IN H-GASEOUS (MILL A)

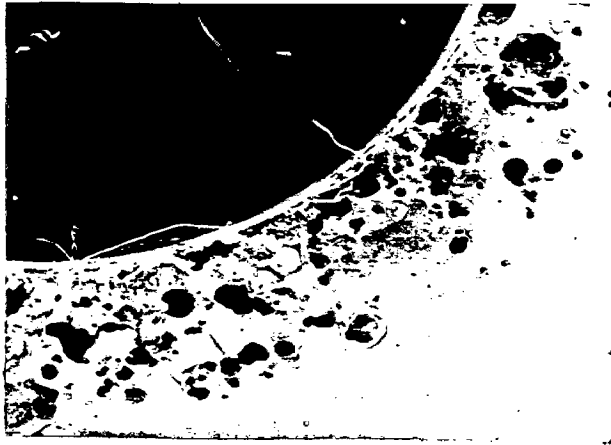


(b) MODERATE, SS-316L IN C-GASEOUS (MILL B)



(c) NEGLIGIBLE, SS-316L IN H1-GASEOUS (MILL B)

PHOTOGRAPH 3.2 : SCANNING ELECTRON MICROGRAPH SHOWING SEVERITY OF PITTING.



(a) EXCESSIVE, SS-321 IN H<sub>2</sub>-LIQUID (MILL B)



(b) MODERATE, SS-304L IN H<sub>1</sub>-LIQUID (MILL B)



(c) NEGLIGIBLE, SS-304L IN H<sub>2</sub>-LIQUID (MILL B)

PHOTOGRAPH 3.3 : SCANNING ELECTRON MICROGRAPH SHOWING SEVERITY OF CREVICE CORROSION.

**Table 3.8: Pitting on Stainless Steels ( Mill A )**

	GAS			LIQ		
	C	B	H	C	B	H
<b>304</b>	⊗	⊗	⊗	0		0
<b>304L</b>	⊗	⊗	⊗	0		0
<b>316</b>	⊗	⊗	⊗	0		0
<b>316L</b>	⊗	⊗	⊗	0		
<b>321</b>	⊗	⊗	⊗	⊗		0



**Excessive**



**Moderate**



**Negligible**

Table 3.9: Crevice Corrosion on Stainless Steels ( Mill A )

	GAS			LIQ		
	C	B	H	C	B	H
304	⊗	⊗	⊗	⊗		0
304L	⊗	⊗	⊗	⊗		
316	⊗	⊗	⊗	⊗		0
316L	⊗	⊗	⊗	⊗		
321	⊗	⊗	⊗	⊗		0



Excessive



Moderate



Negligible

**Table 3.10: Pitting on Stainless Steels ( Mill B )**

	GAS			W/D			LIQ		
	C	H <sub>1</sub>	H <sub>2</sub>	C	H <sub>1</sub>	H <sub>2</sub>	C	H <sub>1</sub>	H <sub>2</sub>
<b>304</b>	⊗	⊗	0						
<b>304L</b>	⊗	0	0						
<b>316</b>	⊗	0	0				0		
<b>316L</b>	⊗	0	0						
<b>321</b>	⊗	⊗	⊗				0		



**Excessive**



**Moderate**



**Negligible**

Table 3.11: Crevice Corrosion on Stainless Steels ( Mill B )

	GAS			W/D			LIQ		
	C	H <sub>1</sub>	H <sub>2</sub>	C	H <sub>1</sub>	H <sub>2</sub>	C	H <sub>1</sub>	H <sub>2</sub>
<b>304</b>	⊗				⊗	0	⊗	⊗	⊗
<b>304L</b>	⊗				⊗		⊗	⊗	0
<b>316</b>	⊗				⊗	⊗	⊗	⊗	⊗
<b>316L</b>	⊗				⊗	0	⊗	⊗	⊗
<b>321</b>	⊗				⊗	0	⊗	⊗	⊗



**Excessive**



**Moderate**



**Negligible**



performance of various materials . These in turn have been correlated with process parameters prevailing in the mills. The comparison has been made in the following manner :

### 3.1.1 Corrosivity of Environment

- (a) Assessment in different phases (L,G and W/D).
- (b) Assessment in different bleaching stages .
- (c) Comparison of corrosivity in mill A and B.

### 3.1.2 Performance of materials.

- (a) Assessment of performance.
- (b) Comparison of material performance in mill A and B.

### 3.1.1 Corrosivity of Environment:

The assessment of corrosivity of environment in different phases and in bleaching stages has been accomplished by analysing the corrosion attack on stainless-steels and mild steel in both the mills. Accordingly, the discussion will be given first on the degree of corrosion experienced by stainless-steels in both the mills and then that by mild steel in the two mills.

Austenitic stainless-steels have traditionally been employed in pulp mill bleach plants because of their combination of good corrosion resistance, mechanical , fabrication properties , weld-ability etc. (19). These steels contain chromium and nickel as main alloying elements and some others in lesser content e.g. molybdenum and titanium etc. in varying extents depending upon the rank of alloy, thus providing fair to excellent corrosion

resistance in various environments. The function of these constituents are mainly as follows (19):

**Chromium** enhances resistance to initiation of pitting and crevice corrosion and steels must have more than 12% of chromium to exhibit stainless properties.

**Nickel** also enhances resistance to pitting and crevice corrosion.

**Molybdenum** also enhances resistance to initiation and propagation of pitting and crevice corrosion. Its effect of improving corrosion resistance to bleaching environment is especially marked in the interval 4.5 to 6.1% (17). This is about three times as effective as chromium against localized attack but has solubility limit of 7% in stainless steels.

The main cause of using stainless-steels in aggressive environments is that they form a protective film of oxides of their constituents and thus avoid the contact of metal with the corrosive media ( electrolyte). A metal or alloy designed to be passive must be exposed to an oxidizing environment in order to form the passive film. Under most conditions, oxygen from dissolved air provides a sufficiently oxidizing environment for the film formation. Unfortunately, the passive films are very susceptible to localized breakdown in presence of halides (11) or highly oxidizing environments, as such localised corrosion attacks e.g. pitting , crevice corrosion etc. are observed.

Bleaching solutions are corrosive both because of the

strongly oxidizing chemicals e.g. chlorine and chloride ions, the latter accumulated as a product of bleaching reaction (23) as well as also due to its formation at the time of bleach chemical preparation and because of lower pH in chlorination stage.

Though oxidizing conditions were favorable to stainless steels because they cause passive film formation, the oxidants (chlorine or hypochlorite ions) and chloride bring about the localized film failure (11). High level of residual oxidants allow rapid corrosion because they are easily electrochemically reduced on the metallic surfaces, thus providing a sink for electrons produced in the localized corrosion reaction (109). As such, high levels of residuals raise the electrochemical surface potential of metal above the pitting potential which initiates localized attack. Also, cathodic reactions due to the residuals allow localized corrosion to propagate at rapid rate. Prior to initiation of localized attack, the solution in contact with the metal is relevant. However, after initiation, the corrosion processes inside pits and crevices take place in highly acidic solutions of metal chlorides e.g.  $\text{FeCl}_2$ ,  $\text{NiCl}_2$ ,  $\text{CrCl}_3$  and  $\text{MoCl}_3$  etc. These chemicals will hydrolyze to give solutions of very low pH ( $\approx 0$ ) (11). It has also been observed that most acidic, occluded solutions are produced by the dissolution of the alloying elements which are more resistant to localized attack (e.g. Ni, Cr, Mo etc.). Production of highly acidic solutions is explained by the fact that the activity coefficient of  $\text{H}^+$  ion in solutions of  $\text{FeCl}_2$ ,  $\text{NiCl}_2$  and  $\text{CrCl}_3$  etc. is not unity but increase exponentially with salt concentration in the range of

O - 2M (110). The final composition of this electrolyte ( in pit or crevice) is almost independent of the composition of the process solution (11). An important point to be noted is that crevice type of localized corrosion may be initiated under much less oxidizing conditions at a crevice site than would be required to cause pitting on an unshielded surface (109). Perhaps that is why one observes crevice corrosion more frequently than pitting in case of stainless-steels exposed to bleach solutions.

Mild steel, an Fe-C alloy ( C  $\approx$  0.2% ) is the material used mostly because of its low cost , acceptable strength, fabrication properties etc. However, because of its poor corrosion resistance, it is replaced by stainless-steels in the case of aggressive media such as those encountered in bleach section.

(a) Assessment in different phases:

In this section an assessment has been presented on the corrosivity of liquid, gaseous and wet/dry phases existing in different washers of the two mills. A general comparison of the corrosivity of these different phases has also been given. While doing assessment, first corrosion experienced by stainless-steels has been discussed and later discussion on mild steel has been given.

(i) Stainless-Steel:

- Pitting

Pitting is experienced by all coupons , exposed in both the

mills, to varying degree in gaseous phase only (Table 3.8 and 3.10). In liquid phase comparatively fewer coupons and no coupon exposed to wet/dry phase experience pitting (Wet/dry exposure was conducted only in case of mill B). Higher corrosivity of gaseous phase could be due to the following factors:

\* Formation of acidic fumes and liquids, in gaseous phase, due to the reaction of molecular chlorine with moisture giving following type of reaction



\* Higher accessibility of oxygen and chlorine in gaseous phase, since gases have limited solubility in vat solutions.

\* Formation of high concentration of chloride.

\* It is quite possible that solution forming on the coupons, exposed in gaseous phase, may have pH around 1.2 - 1.5 (19) in which case corrosion increases dramatically.

Thus limited solubility of dissolved oxidants ( $\text{Cl}_2$ ,  $\text{O}_2$  etc) in liquid media, comparatively higher pH in case of vat liquors ( $\approx 2$  for C-vat and 7 - 9 for B- and H-vats) are responsible for lesser tendency of pitting observed on coupons exposed in vats.

Another important factor may be the turbulent condition of vat liquors which continuously change the solution composition near metal and thus avoids stagnant conditions (26). This lowers stimulation in already formed pits. Turbulent solution may act as repairing specie by transporting the oxidants towards surface

and not allowing to concentrate chloride ions which breaks the oxide film. It is to be noted here that at gaseous phase of B and H-washers , solution formed on coupons will be acidic because these are basically representing the moist chlorine and there is no possibility of their removal . The environment near shower pipe (gas phase) is most stagnant, liquid phase is lesser stagnant due to incoming of stock whereas wet/dry phase is most turbulent as here coupons are rotating. Thus the observation is in accordance with general understanding that environment should be stagnant for observing pitting (26). Pitting is more severe in gaseous phase also due to the fact that the presence of  $Cl_2$  together with moisture results in condensation of highly acidic media having chlorides which are considered very aggressive from localized corrosion view point (109,111).

Pitting attack in case of gaseous phase and in liquid phase of mill A (Table 3.8) is more severe than that in respective phases of mill B. No pitting is observed for coupons exposed in wet/dry environment of this mill (Table 3.10).

#### - Crevice Corrosion:

Crevices in our case were formed due to PVC (poly-vinyl chloride) spacers used in racks for setting of coupons for exposure. This type of localized corrosion may be initiated under much less oxidizing conditions at a crevice site than would be required to cause pitting on an unshielded surface (109).

In case of mill A, crevice corrosion (Table 3.9) is experi-

enced on more number of coupons and to a higher degree for exposures in gaseous phase than liquid phase. It seems that chloride ion concentration is more and pH is less in the liquid forming in crevices of coupons exposed in gaseous phase in comparison to those which are completely dipped inside vats. Both these factors increase tendency of enhancing the crevice attack (39).

Excessive crevice corrosion experienced in C-washer gaseous phase can be attributed to the presence of chloride ion ( due to hydrolysis of molecular chlorine and metal chlorides e.g.  $\text{FeCl}_2$ ,  $\text{NiCl}_2$ ,  $\text{CrCl}_3$  etc.) and comparatively stagnant acidic solution. These factors have been suggested responsible for crevice corrosion ( 10,110,112 ). In case of B-and H-washers gaseous phase, the severity of crevice attack is lesser due to lesser amount of moist chlorine in surrounding environment.

In mill B, crevice corrosion (Table 3.11) is experienced by all coupons, though to varying extent , in liquid phase only. Perhaps while in dipped state, the crevices here are more probable of having depleted oxygen than when they are in gaseous phase. However lesser number of coupons are attacked by crevice corrosion in gaseous and wet/dry phases. Near shower pipes, the environment approximates gaseous type hence crevice corrosion is less likely to be expected. In wet/dry phase , due to least stagnancy of environment, the crevice attack appears on lesser number of coupons except those exposed in H1 washer. Erosion corrosion is also observed to some degree on coupons exposed to this last type of medium.

Comparison of results from both mills seems to indicate that where the environment is more corrosive, crevice attack depends upon concentration of  $\text{Cl}^-$  ions and it depends upon oxygen depletion in crevices in lesser corrosive media. Thus mill A, which overall is observed to be more corrosive (as concluded later) shows higher degree of crevice corrosion in gaseous phase (Table 3.9). In case of chlorination washer of mill B, observed to be more corrosive than H1 and H2 washers (as concluded later), crevice attack is more in gaseous phase than liquid phase. Whereas in H1 and H2 washers, crevice attack is more in liquid and wet/dry phases (Table 3.11) than in gaseous phase.

Crevice corrosion is observed even in those cases where pitting is not observed. This is expected on the basis of available information that occurrence of crevice corrosion requires lesser oxidizing environment than pitting.

#### - General Corrosion:

On comparison of corrosion rates experienced by different stainless-steels in different phases of mill A (Table 3.6), one observes that gaseous phase is more corrosive than liquid phase of the corresponding washers. Lesser tendency of corrosion in aqueous environments in comparison to gaseous phases may be considered due to less amount of oxidizing agents, limited solubility of oxygen and higher pH in former case.

Upon comparing corrosion rates experienced by steels in mill B (Table 3.7), gaseous phase is observed to be most corrosive among all phases in chlorination washer. This can be at-



tributed to the maximum amount of chlorine gas in this washer near shower pipe (gaseous phase) which condenses to form very low pH solution at the coupon. No clear trend is observed for different phases in H1 washer. However, in case of H2 washer, liquid phase is observed to be most corrosive. Perhaps the amount of residual chlorine in the liquid phase makes it more corrosive than the gaseous phase which is likely to have much less chlorine gas (emanating from C-washer's liquid phase) around shower pipe due to H2 washer being away from C washer.

Corrosion rates in wet/dry phase (Table 3.7) for C-washer are lower than those for both liquid and gaseous phases. SS-304L and 316L have lowest corrosion rate, although difference in corrosion rates are too less that consideration of material comparison is not important. In case of H1 washer corrosion rates in wet/dry phase are usually more than those for other two phases except for SS-304. In case of H2-washer, the values of corrosion rates in wet/dry phase are more than gaseous phase but less than liquid phase except in case of 304L which shows typically low corrosion rate in liquid phase.

(ii) Mild Steel:

So far the discussions regarding the corrosivity of environment have been based on the various types of corrosion attack experienced by stainless-steels. Now the corrosivity of different phases is being discussed on the basis of general corrosion experienced by mild steel during mill tests.

For both the mills, corrosion rates in chlorination are higher in liquid phase than for coupons exposed near the shower pipe (gaseous phase). This observation seems to be due to the dissolution of the corrosion products formed in the former phase at lower pH and due to turbulent condition of vat liquor. It has been observed earlier (13) that ferrous oxides (corrosion products) are generally soluble below, and insoluble above a pH of about 3.5. Since the iron oxide-oxyhydroxide film (rust) dissolves in acidic media, resulting in exposure of fresh metal surface, the corrosion rates for mild steel are higher in the liquid phase than gaseous phase in this stage (27).

In case of mill A, B- and H-washer liquid phases are lesser corrosive than their gaseous phases (shower pipe)(Table 3.5). This is possible because the liquors in vat of these stages have alkaline pH and therefore corrosion products formed over the metallic surface are not expected to dissolve. Although, amount of residual chlorine is more in these vats than chlorination vat (Table 3.2), its form is  $\text{OCl}^-/\text{HOCl}$  instead of  $\text{Cl}_2$ . The latter has higher oxidising power than the former.

In H1-washer stage, of mill B, corrosivity is more near shower pipe, than in vat (Table 3.5). This is inverse of what is observed in C-washer. The corrosion rate in gaseous phase will be due to reaction of metal with oxygen and some amount of chlorine being transferred from C-stage washer. This corrosion rate is more than liquid phase because the pH of liquor of H-stage is alkaline, in which corrosion products dissolve to lesser extent and so expect to have protective nature to some extent. Addition

of sulfamic acid, in this stage, also appears to be responsible for lower corrosion rate in vat. The sulfamic acid is added in hypochlorite bleaching stage to have the advantages such as : (i) reduction of pulp degradation as result of high temperature or low pH (ii) increased production by means of higher temperatures and lower pHs at the same level of pulp-strength and (iii) saving in chemical costs e.g. lower consumption of buffer, caustic soda and higher bleaching agents. Detailed discussion of reactions mechanism of sulfamic acid effects in bleaching section are given in ref.113. The other commercial applications of sulfamic acid are : it is used also for scale removing and chemical cleaning agent etc. It has also been indicated that it is compatible with corrosion inhibitors, wetting agents, pH indicators and dry-cleaning formulations. In H2-washer, liquid phase is more corrosive than gaseous phase, unlike H1-stage. Oxidation of metal in the gaseous phase, can be assumed due to oxygen and chlorine as in H1 stage. However, in liquid phase, though pH is alkaline but higher amount of residual chlorine (Table 3.3) than that in H1 and non-mixing of sulfamic acid results in its higher corrosivity.

Wet/dry cyclic exposure in chlorination stage shows more corrosion rate than gaseous phase exposure and lower than liquid phase exposure. This may be expected because in wet/dry exposure sample comes in contact with oxygen and gaseous chlorine which forms a film of corrosion products due to oxidizing nature of chlorine. When sample comes in contact with turbulent vat liquor, the film of rust gets dissolved leaving a fresh metal surface for

experiencing more corrosion . Coupon which is in contact with gaseous environment corrodes but after film formation corrosion rate decreases since the rust remains intact as it does not come in contact with liquid unlike wet/dry exposure. The coupons which are dipped completely in vat corrode but bears no rust film as it dissolves in vat liquor. During each cycle of wet/dry exposure , in H1 and H2 washer , the coupons after getting oxidised in gaseous media , pass through alkaline liquid media of vat. Consequently the rust formed over the coupons does not dissolve while passing through vat unlike the case of chlorination washer. As such least corrosion rates are observed on coupons exposed in wet/dry phase in these washers (Table 3.5).

If one compares the three phases (liquid, gaseous and wet/dry), in both the mills, of chlorination washer on the basis of general and localised corrosion experienced by stainless-steels, gaseous appears most corrosive, liquid phase lesser and wet/dry phase least corrosive. This behaviour is in accordance with earlier reported results in Canadian mills (13,19). However, for mild steel, gaseous phase of chlorination washer is less corrosive than its liquid phase.

In mill A, on the basis of general and localized corrosion both, gaseous phase appears more corrosive than liquid phase in hypowashers. In mill B, pitting is experienced more in gaseous phase and practically nil in liquid and wet/dry phase of hypowashers. Crevice corrosion is maximum in wet/dry phase in H1 washer. By and large, tests performed on mild steel also indicate

gaseous phase to be more corrosive than other phases, in buffered and hypochlorite washers, barring a few exceptions.

Over all, on the basis of general and localized corrosion both, gaseous phase appears more corrosive than liquid phase in all washers. The corrosivity of wet/dry phase in general appears intermediate between the two other phases, however, few variations have also been noticed.

(b) Assessment in different bleaching stages :

After assessing the corrosivity of different phases of respective washers (stages), attempt has been made to analyse the aggressiveness of different stages. For this purpose, details with regard to localised corrosion and then general corrosion have been given considering the attack first on stainless-steels and then on mild steel in both the mills.

(i) Stainless-Steel:

- Pitting:

Tables 3.8 and 3.10 show clearly that pitting is experienced widely by coupons exposed in gaseous phase of all washers of both the mills. Thus in case of mill A, excessive pitting is observed on coupons exposed to gaseous phase of all the three washers (Table 3.8), out of which those exposed in chlorination washer were so badly pitted that they were completely destroyed due to perforations. Extremely high pitting at C-washer and excessive pitting at B-washer and H-washer has been suggested to be due to the presence of moist chlorine (13,19,114), which is maximum in

C-washer. The corrosivity of B-washer and H-washer is less than C-washer because of lesser amount of moist chlorine in them. The required process conditions are such that there should be practically no molecular chlorine in these washers. However, because of uncontrolled conditions, a significant amount of chlorine reaches to B washer and slightly less than this to H-washer. This is due to closer proximity of B washer than H-washer to C-washer. Obviously B-washer shows more corrosivity than H-washer. Presence of chlorine creates, as previously discussed, highly oxidizing and chloride containing environment of very low pH. This solution breaks the passive film formed on steels by the earlier discussed reaction which results into formation of newer and deeper pits. In case of liquid phase, pitting experienced was approximately of the same degree in all the washers and it was much less than that experienced in gaseous phase of respective washers.

Pitting attack in H-washer vat is slightly lower than C-washer vat. This may be due to the fact that, although, concentration of residual chlorine is significantly higher in case of H-washer vat but due to alkaline pH of its liquor, the dominating form of chlorine is hypochlorite ion ( $\text{OCl}^-$ ) whose redox potential is less positive ( $< +0.9\text{V}$ ) in comparison to  $\text{Cl}_2$  ( $> +1.0\text{V}$ ). The redox potential for the  $\text{Cl}_2/\text{Cl}^-$  system is highly oxidising (115) and is expected to fall in the transpassive region of the anodic polarization curve of stainless-steels. The kinetic electrochemical parameters e.g. Tafel slopes and exchange current densities may also differ for these chemicals. Both these facts

will results in difference in electrochemical behavior of liquors of C- and H-vats. This in turn seems to be responsible for difference in pitting characteristics. Another possible reason for the difference in pitting could be due to formation of calcite ( $\text{CaCO}_3$ ) over coupons in, H-washer, which avoids direct contact of material surface with the liquor. Presence of calcite in hypochlorite stage may be because of impurities in lime by which calcium hypochlorite is prepared (116). The effect of temperature on penetration depth at concentration of chlorides which are encountered in our liquid case may not be considerable as per an earlier study (111), according to which the effect of temperature is less at smaller ( 0.05 mole/liter) chlorine concentration at pH 1.2.

In case of mill B, pitting attack is of lesser degree than in mill A (Table 3.8 and 3.10). Here too, in gaseous phase, coupons exposed in chlorination washer experience excessive pitting and moderate to negligible in hypochlorite washers. In liquid phase, barring two coupons exposed in chlorination washer, no pitting is observed (Table 3.10).

Thus on the basis of pitting attack, in both the mills chlorination washer appears to be most corrosive followed by buffered hypo and hypochlorite washers.

#### - Crevice Corrosion:

In mill A, excessive crevice attack is observed in chlorination washer and moderate to negligible attack in B- and H-washers

(Table 3.9). The attack is most severe in C-gas phase than gas phases of B- and H- washers due to highest chlorine concentration around shower pipes of former washer and its reduction from B- to H-washer. In vats also, coupons exposed in chlorination washer show higher degree of crevice attack than that in hypochlorite washer basically due to presence of  $Cl_2$  in former washer and formation of calcite scale on coupons in latter washer which avoids direct contact of vat liquor with coupons.

In case of mill B, coupons experience crevice corrosion (excessive) in chlorination washer only in gaseous phase (Table 3.11). Since in this mill, residual chlorine is almost negligible in chlorination washer (Table 3.3), chlorine gas emanating from the vat liquor is very little in amount. As such overall conditions are expected to be less corrosive than those observed in mill A, hence coupons hung in gaseous phases of hypochlorite washers do not experience crevice corrosion. In liquid and wet/dry phases, it appears that, due to lower corrosivity of bleach section in this mill, crevice corrosion is governed mainly by concentration of hypochlorite ion (present in H1 and H2 washers) rather than molecular chlorine (present in chlorination washer). Consequently, coupons exposed in liquid and wet/dry phases of H1 and H2 washers are observed to show higher degree of crevice attack than those exposed in the respective phases of chlorination washer.

On the basis of results on crevice corrosion, it is observed that chlorination washer, in both the mills, is more corrosive than others. However, in hypochlorite washers of mill B, liquid



and wet/dry phases appear to experience higher degree of attack.

- General Corrosion:

Comparison of corrosion rates, indicates highly corrosive conditions in C-washer of mill A (Table 3.6). As discussed earlier, higher corrosivity in this washer's gaseous phase is due to the presence of maximum amount of moist chlorine, which goes on decreasing from B- to H-washer thereby resulting in lesser corrosion rates in these washers. Higher corrosivity of C-washer aqueous phase than that of H-washer has been suggested (13,19) due to residual chlorine and acidic pH ( $\approx 2$ ) which are more detrimental factors while chloride and temperature have only a secondary effect as such the latter's influence is overshadowed by residual oxidants. Although concentrations of residual chlorine and chloride ions are more in H-washer but higher corrosivity in C-washer could be attributed to pH being acidic ( $\approx 2$ ), and also due to the fact that form of chlorine is molecular in nature. This is because molecular chlorine has higher oxidising power than hypochlorite ions as has been discussed earlier. Another possible reason of lower corrosion rate in H-vat may be the formation of calcite as scales on the coupons exposed in it, thereby, slowing down the corrosion reactions. Thus overall corrosivity of C-washer is maximum followed by that of B- and H-washers in mill A, on the basis of general corrosion.

Comparison of corrosion rates, in mill B, (Table 3.7) indicates that the gaseous phase of the chlorination washer is more corrosive than that of the H1 and H2-washers, because of the

higher concentration of moist chlorine present in the gaseous phase of C-washer as indicated previously. Further, in the H2 washer, the SS coupons experienced a lower corrosion rate, than in H1 washer, in the gaseous phase probably because there was lesser amount of moist chlorine in the gaseous phase of former washer.

In liquid media, however, coupons experience less corrosion in C- and H1-washer than in H2-washer. Lesser corrosion rates in C-washer could be attributed to almost nil concentration of molecular chlorine in C-vat. Possible reasons for maximum corrosion rates in H2-washer could be (i) higher amount of residual oxidant in H2 washer stage (Table 3.3). (ii) the addition of sulfamic acid in the H1 stage, which may be showing inhibitive action. Some hypochlorite ions may be consumed by sulfamic acid thus forming chloro-sulfamates (117). These sulfamates have lower oxidizing power than hypochlorite ions (118).

In wet/dry phase, coupons hung in H2-washer experience maximum general corrosion followed by corrosion experienced by steels in H1- and C-washer. Since corrosion rates, in general, in this phase show overall lower corrosivity, the former seem to be governed by same factors as prevailing in the case of liquid phase rather than gaseous phase.

#### (ii) Mild Steels:

So far the discussions on corrosivity were based on the test performed on stainless steels, now the results of weight-loss

studies performed on mild steel are given. Considering corrosion in both gaseous and liquid phases of respective washers, corrosion rates (Table 3.5) on steel samples, in mill A, show maximum corrosivity in chlorination washer. Buffered hypo washer shows lesser and hypochlorite washer shows least corrosivity. As described earlier, corrosion decreases with (i) increase in pH of liquor (in liquid phase), (ii) decrease in moist chlorine around shower pipes (in gaseous phase). Hence the above trend of corrosivity can be understood on the basis of prevailing conditions in these washers (Table 3.2). Another general observation is that the corrosion rate decreases with time (Table 3.5). This is normally observed fact and is due to the formation of corrosion products on sample after some time of exposure. The corrosion products avoid the direct contact between sample and corrodent. However, overall behavior will depend upon the nature of product whether it is protective or non-protective. In case of mill B, considering all the phases of respective washers, corrosion rates (Table 3.5) indicate maximum corrosivity in chlorination washer followed by H2- and H1-washer. As discussed earlier this trend can be understood on the basis of (i) lower pH ( $\approx 2.8$ ) in C-washer, (ii) higher residual chlorine in H2-washer and (iii) addition of sulfamic acid in H1-washer.

Thus both mills show maximum corrosion loss in chlorination washer stage than the other two washer stages. Lesser corrosion in buffered-hypo (in mill A) and hypochlorite washers (in both mills) is observed to depend upon the process conditions.

An important observation is that the corrosion rate for stainless-steels are more in H<sub>2</sub>-washer vat than in C-washer vat whereas for mild steel, corrosion rate is higher for exposure in C-vat and is as per normal expectations since C-vat liquor is acidic while that of H-vat is alkaline. Possible reasons for this observation could be (i) the difference in the nature of residual oxidants (e.g. Cl<sub>2</sub> in C-washer, OCl<sup>-</sup> in the H<sub>2</sub> washer), (ii) their varying amounts, and (iii) different electrode kinetics for mild steel and stainless-steel vis-a-vis the nature of chemicals present in liquors.

(c) Comparison of Corrosivity in Mill A and B:

Upon comparing corrosion rates, one observes that general corrosion in mill A is more than that in the respective stages of mill B whether we compare exposure in gaseous or liquid phase. Sole exception is hypochlorite vat liquor in mill A where general corrosion is less due to formation of scale (calcite) over coupons. Similar conclusions, one can draw when comparison is made of degree of pitting and crevice corrosion attack in respective stages of the two mills. Thus overall bleach section in mill A is more corrosive than mill B. It can be understood on the basis of process conditions (Table 3.2, 3.3 and 3.4) prevailing in two mills. The liquors of mill A are observed to have higher temperature, lower pH, higher residual oxidant and chloride ion concentration in the respective stages than in mill B. All these factors lead to enhanced corrosivity.

None of the coupons experience pitting when exposed to

liquid phase and crevice corrosion when exposed to gaseous phase of hypowashers of mill B. However these effects are observable in respective phases of mill A, whose bleach section is more corrosive. Since nature of aggressive environment is similar in both of the mills, it appears that a certain minimum degree of corrosivity (depending upon the concentration of residual oxidant, chloride ion and pH etc.) is required before the onset of localized attack on materials. Such a hypothesis has been put forwarded earlier also (11).

### 3.1.2 Performance of Materials:

#### (a) Assessment of Performance

In mill A, the general behavior of the tested materials is such that 316L experiences least corrosion except in chlorination shower pipe and 304 is affected most, while 321, 316 and 304L lie between them in all stages. Low carbon grade of steels e.g. 316L and 304L, show better performance than their higher carbon counterparts. Low hydrogen over-voltage of low-carbon steels (27) could be the possible reason for their experiencing low corrosion rate than the high carbon counterpart.

Upon analysing the pitting attack (Table 3.8), it is clear that exposed material in C-washer gaseous phase have suffered from localized corrosion excessively since some of the coupons were completely destroyed upto perforation. This behavior is quite similar to the one observed in American and Scandinavian mills (13,16,18,19) where 316L and 317L experienced severe pitting resulting into complete perforation after an exposure of

approximately three months. The situation in Indian mills seems only slightly better because the exposure was six months long in the presently referred tests instead of three months. It is worth mentioning here that the studied mill in the present work, does not recycle the filtrates, a practice which is normally adopted by the western mills and which enhanced the corrosivity appreciably due to increase in concentration of residual chlorine, chloride ions, temperature and lowering of pH. Similar situation is likely to emerge in near future in Indian mills as greater recycling of the filtrate to save energy and control pollution will be followed. Pitting experienced by B-washer and H-washer gaseous environment is excessive for all of the exposed alloys except 316L. Creation of aggressive environment and suffering from localized attack of FeCrNiMo alloys by chlorine has been discussed briefly in an earlier para and in details elsewhere (11,23, 109,119). Although process conditions are favorable to protect stainless steels due to passive film formation but, as discussed, the combination of oxidants and chlorides bring about the localized film failure. In C-washer liquid environment, pitting is negligible for all types of steels except SS-321 for which it is moderate. In H-washer liquid environment, except SS-316L, pitting attack observed on all type of exposed steels although to negligible extent.

Performance of 316L against pitting attack, in B-washer gaseous phase and H-washer liquid media is better among all of the tested steels which may be due to presence of molybdenum in it (13).

From Table 3.9, it may be observed that tendency of crevice corrosion in gaseous phase is excessive in case of C-washer, moderate in case of B and H washers. The behavior is almost uniform for all samples in a washer, except SS-316L exposed in B-washer which shows excessive tendency of crevice attack. In case of C-washer vat, different materials show different behavior for crevice attack e.g. SS-304L, 316L show moderate and SS-304, 316 and 321 excessive attack. In H-washer vat, 316L and 304L are not damaged by crevice at all, while other type of steels experience negligible crevice corrosion. In general, it appears that low carbon grade of stainless steels are prone to less severe crevice attack. Observation of very less crevice corrosion on coupons exposed in H-vat in comparison to those in C-vat could be due to alkaline liquors and to formation of calcite scale deposited on coupons exposed in former vat.

In the gaseous phase coupons are pitted so badly that materials of coupons can not be considered for their cost effective applications as suitable materials of construction for process equipments at all three stages. In liquid phase, stainless-steel 316L and 304L show better performance, perhaps, because the sum of chromium and molybdenum are more than that present in other steels. Overall, it may be stated that all types of steels show satisfactory performance in C-and H-washer vat provided crevices are avoided. It may be worth mentioning here that the construction of a washer drum is such that crevices simply can not be avoided, and so one has to consider a better resistant material.

On the other hand, none of the steels, tested in present study, can be used in gaseous phase of these washers.

In case of corrosion tests performed in mill B, except for the H1 and H2 liquid phase, 316L shows maximum corrosion resistance in all environments. Though the degree of localised attack in chlorination gaseous phase, even on 316L, is observed to be such that it can not be suggested for construction of process machinery for this bleaching stage. In the H1 and H2 liquid phase, 304L experienced least corrosion. 304L, 316L have better corrosion resistance than 304 and 316, respectively. The reason for this type of observation has been discussed in earlier (mill A) results.

In our study, for the C-washer, one can observe excessive pitting in gaseous phase, for all stainless steels except 316L. Nearly all materials experience excessive crevice corrosion in the gas phase. Thus for application in gaseous phase of chlorination washer of this mill also, none of the tested steels is suitable. In liquid phase of this washer moderate crevice corrosion and no pitting is observed for all the tested steels. Application of any of these steels in this phase will require cost-effective analysis before a particular grade is recommended. In wet/dry phase any of the tested steels is suitable to use since these do not experience observable localised attack.

Gaseous environments in H1 and H2 washers are less aggressive than in the chlorination washer with regard to the pitting



attack. On this basis different materials can be put in the following order of increasing tendency of pitting

SS 316L < SS 304L ≈ SS 316 < SS 304 < SS 321

This outcome is in accordance with the general understanding that an increasing amount of molybdenum in stainless steels improves their resistance against pitting (13). None of the tested steels experience crevice corrosion in these environments. Selection of suitable grade of steel will therefore be governed by the degree of pitting attack.

Pitting was not observed on any of the steels exposed to liquid phase of H1 and H2-washer. Crevice corrosion is generally more severe in H1 and H2-washer vats than in chlorination vat conditions. Here SS-321 experiences maximum crevice corrosion, while SS-304 and 304L experience minimum. No particular trend with regard to variation in the degree of crevice attack is observable in relation to varying amount of molybdenum and chromium in stainless steel. This could be the result of there being not much variation in the amount of molybdenum (Table 3.1) (17) and the lesser influence of chromium on crevice attack (20). SS-304 and SS-316 can be used economically in these environments if crevices are avoided. However, the possibility of failure of SS-304 as a result of chloride stress corrosion cracking attack should be accounted for (19).

In the case of wet/dry exposure, none of the tested materials have experienced pitting. However, excessive crevice corrosion has been experienced by all materials in H1 washer. In H2

washer 304, 316L and 321 experience negligible crevice corrosion while 304L and 316 remain unaffected. One also observes erosion corrosion on the coupons exposed to this phase, perhaps due to their movement as they are fitted on rotating drum .

Upon comparing the three phases, in the chlorination section, the gaseous phase appears to be most corrosive. This behavior is in accordance with earlier reported results in Canadian Mills (3). Overall none of the studied materials is suitable to use in the chlorination gas phase. SS-316L can be used in the chlorination liquor with the condition that crevice are avoided. However, as indicated earlier, the design of the washer drum is such that crevices do form due to winding of SS wire, which in turn support the filter mesh. Also 316L can be used in the H1 and H2 gaseous phases. SS-304L may be considered for use in H1 and H2 liquors.

(b) Comparison of Material performance in Mill A and B:

Degree of pitting in gaseous phase of all stages in mill A and of chlorination stage in mill B is such that none of the tested materials can be recommended for cost effective utilization. Crevice corrosion on coupons exposed to chlorination gaseous phase is also excessive. Performance of 304 and 316 comparable as far as pitting attack in H1 and H2 gas phase of mill B is concerned. Crevice corrosion is not noticeable in these environments.

Pitting on all materials is uniform and moderate in liquid phase of all washers of both the mills. However, crevice corrosion is severe in hypowashers of mill B. Here 304 and 304L appear to be better choice. In mill A, however, hypowasher liquid phase attack is either not noticeable or negligible on all materials. In chlorination washer liquid phase, with regard to crevice corrosion, all materials are moderately attacked in mill B whereas in mill A, SS-304L and 316L perform better than others.

As mentioned in earlier reports (11,13), the dependence of crevice corrosion/pitting on molybdenum content could not be observed. This could be due to lesser variation in amount of this element in tested steels and also that we could not consider steels with molybdenum content in them varying significantly.

It is found that performance of 316L is better than others in both mills. At some places 316L and 304L perform equally well. However in terms of general corrosion and crevice corrosion, performance of 304L is superior to 316L. This could be due to higher amount of nickel and chromium in former steel (Table 3.1). Better performance of 304/304L than 316/316L with regards to crevice corrosion in case of hypowashers of mill B is intriguing. Sum of nickel, chromium and silicon content in these materials indicates 316L should be best, but perhaps for the least value of silicon in it. It will, therefore, be worth looking in effect of silicon on crevice corrosion over steels in alkaline chloride solution.

In the context of present study, it may be worth considering the materials currently in use in bleach plants of Indian mills. In many of them, 316 and 317L are used as pipes for transporting stock, as washer wires and drum material, and for washed pulp in the chlorination stage, whereas hypochlorite washers are using 304 and cast iron as well (10). It appears that at some places materials with better corrosion resistance, than that required for the particular purpose, are being used whereas at other places materials having insufficient corrosion resistance are being used. In both the situations, the selection of material is not proper. In order to achieve appropriate material selection, it is therefore necessary to perform these type of tests.

### 3.2 Analyses of Corrosion Products :

To check the utility of a material, evaluation of its performance in the given corrosive environment is necessary. It is of equal importance to understand the mechanism of corrosion reactions undergoing on the surface of the exposed material. Both the above factors depend, to a large extent, on the nature of corrosion products formed over the exposed surface. Consequently, studies on understanding nature of corrosion products, formed in varying environments, have found interest among different workers (120-128). Until recently, mostly X-ray diffraction and Infra-Red spectroscopy were in use for analysis of corrosion products (120-122). In recent years, however, Mössbauer spectroscopy is being increasingly used for studying corrosion products formed on steels (123-128). Details of X-ray diffraction and Mössbauer spectroscopy, the techniques used in present

work for analyses of corrosion products , have been discussed in chapter 2.

This section deals with the rusts and scales , formed on corroded coupons, and their analyses by X-ray diffraction and Mössbauer spectroscopy . Nature of rusts and scales has been analysed by identifying the corrosion products. The form of corrosion products/scales has been discussed with respect to the process environment conditions. The details of corrosion products in terms of protective and non-protective nature, stoichiometry etc. have been discussed. Firstly details of corrosion products formed on mild steel will be discussed and later on an account of expected components of rusts obtained from stainless-steel coupons will be given.

### 3.2.1 Mild Steel:

#### (a) Mill A:

The present section deals with the investigations performed on rust obtained from mild steel coupons exposed in liquid and gaseous media of chlorination (C), buffered-hypo (B) and hypochlorite (H) stages of mill A. Details of chemical composition (Table 3.1), process conditions (Table 3.2) and exposed coupons have already been described earlier in this chapter. The selected coupons for the analysis were among those which were exposed from 4 to 5 weeks. The rusts scraped from these coupons have been named as given in Table 3.12. This Table also indicates the respective sites of exposure of these coupons. Thus obtained

**Table 3.12 : Location of Test Coupons**

Coupon No.	Location
1MS05	Chlorination Washer vat
2MS05	Chlorination Washer Shower pipe
3MS05	Bufferedhypo Washer vat
4MS05	Bufferedhypo Washer Shower pipe
5MS05	Hypochlorite Washer vat
6MS05	Hypochlorite Washer Shower pipe

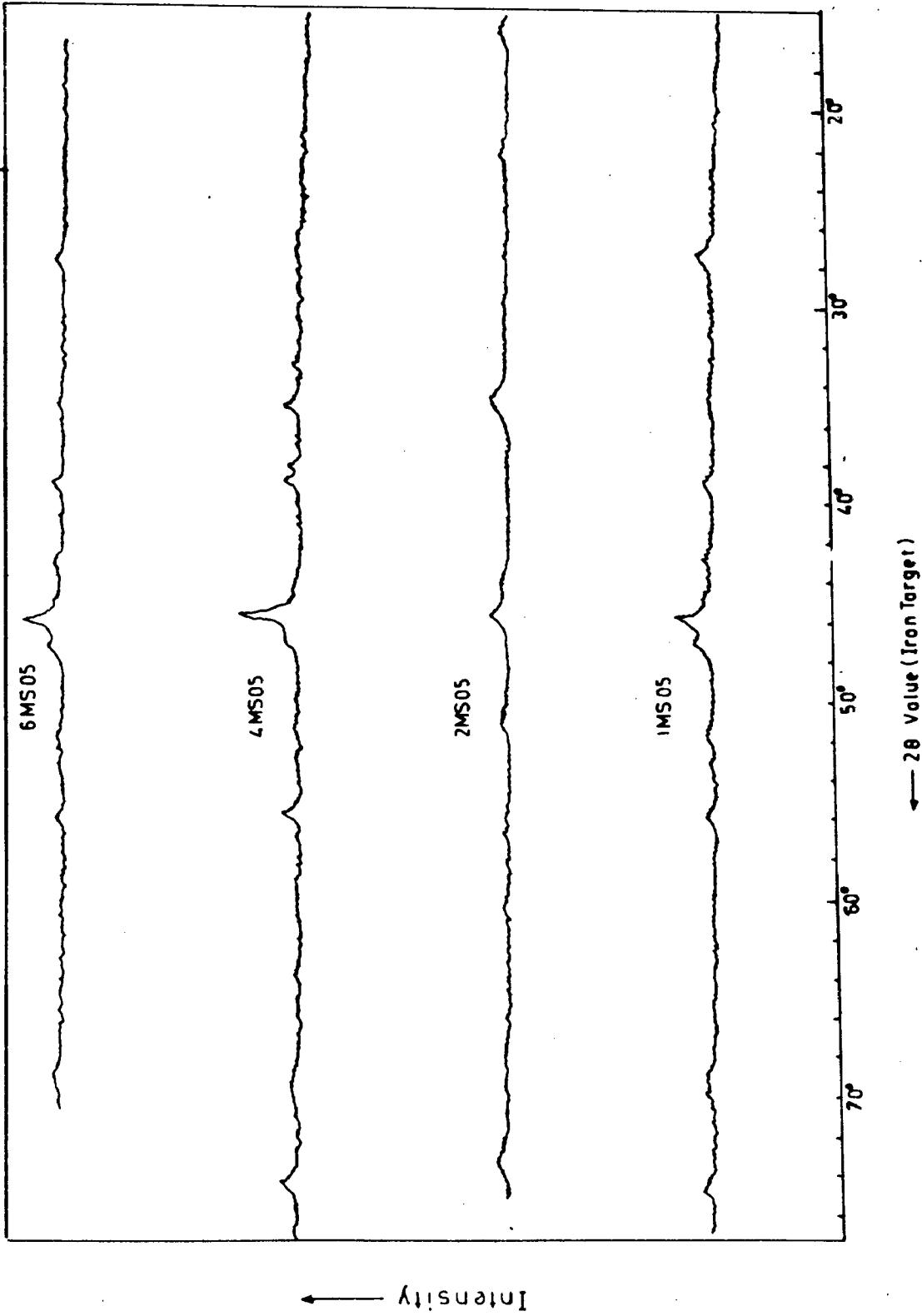


FIG.3.1: X-RAY DIFFRACTOGRAMS OF MILD STEEL RUST (MILL-A)

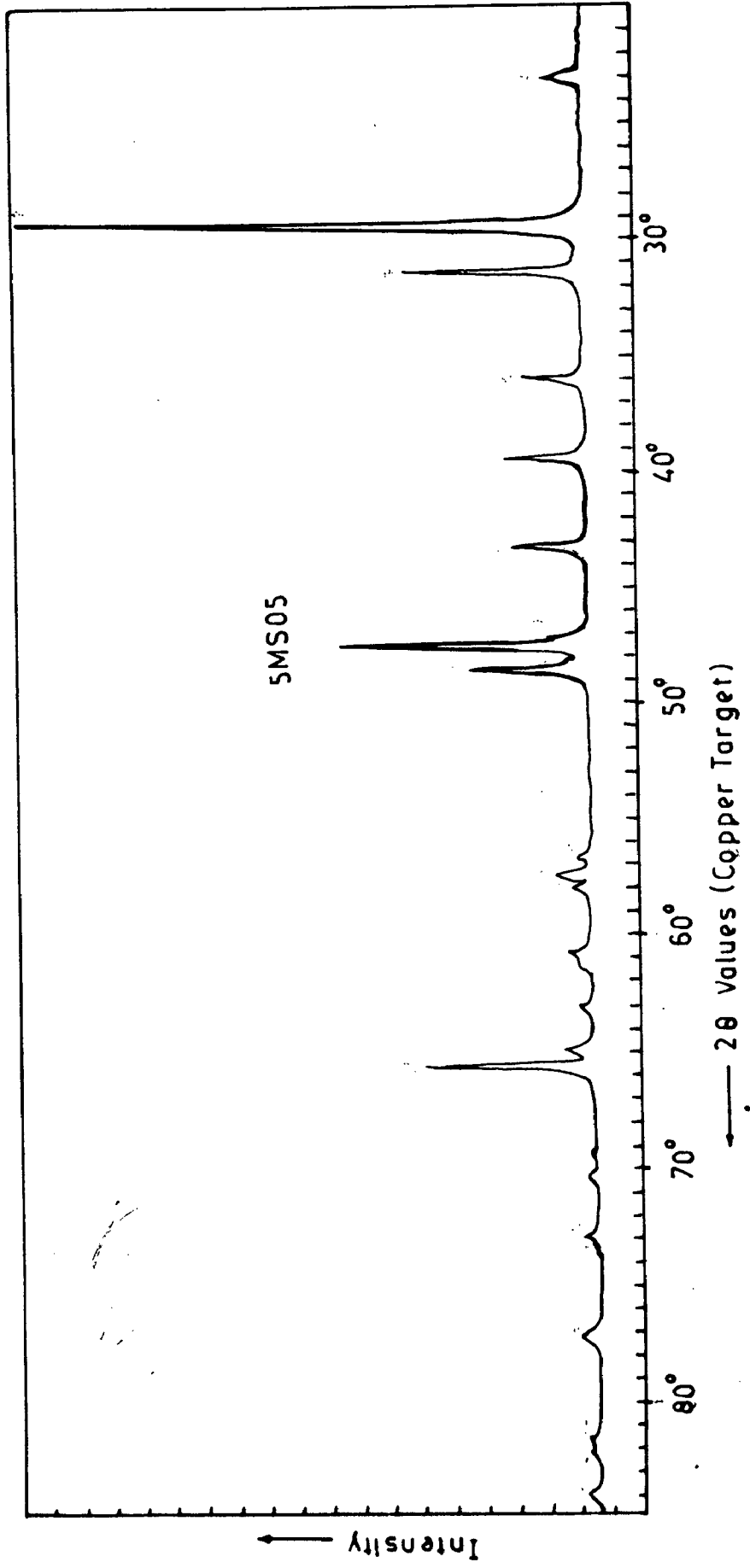


FIG. 3.2: X-RAY DIFFRACTOGRAM OF SCALE (MILD STEEL) (MILL-A)



rusts (except SMS05) appear dark brown/black in color. Film formed on coupon exposed to hypowasher vat (SMS05) is shining, light yellow colored and seemed to be more like a scale. In the first instance the rusts/scale were analysed by X-ray diffraction and then by Mössbauer spectroscopy.

(i) X-Ray Diffraction:

X-ray diffractograms of rust samples were first of all recorded with Fe target (Fig. 3.1). The diffractogram of SMS05 showed fewer and very weak lines at  $2\theta$  angles of  $37.5^\circ$ ,  $41.1^\circ$ ,  $46^\circ$ ,  $50.4^\circ$ ,  $55.4^\circ$ ,  $61^\circ$ ,  $62.5^\circ$  indicating at either the amount of iron in it to be very low and/or the components to be non-iron compounds. Consequently another diffractogram in this case was recorded with copper target shown in Fig.3.2, which gave strong and quite sharp peaks. The phases were identified for all samples including SMS05 from the diffractograms, on the basis of d-spacings from ASTM and from work of Suzuki et.al.(129), after converting them into respective  $2\theta$  values. 311, 110, 110, 104 were considered as the respective strongest line for  $Fe_{3-x}O_4$  ( non-stoichiometric  $Fe_3O_4$  ),  $\alpha$ -FeOOH,  $\beta$ -FeOOH and calcium carbonate. Table 3.13 shows  $2\theta$  angle values corresponding to different phases, derived from the diffractograms (Fig.3.1) for 1MS05, 2MS05, 4MS05 and 6MS05. Table 3.14 gives the  $2\theta$  values, from Fig.3.2, corresponding to different phases which are constituents of scale deposited on mild steel. Most of the obtained peaks correspond to calcium-carbonate and remaining for others e.g. silicates. Calcium silicate hydrate is also expected on the basis of its strongest line corresponding to d-values of 3.09 Å.

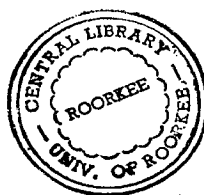
**Table 3.13 : 2  $\theta$  ( in degrees ) values for Iron compounds  
( components of mild -steel rusts from Mill A )**

Iron Compound	1MS05	2MS05	4MS05	6MS05
$\text{Fe}_3\text{O}_4$	38.8	-	38.5	38.8
	45.8	45.4	45.5	45.8
	55.8	-	55.4	56.0
	69.0	-	69.0	69.0
	74.6	73.0	74.2	-
$\alpha - \text{FeOOH}$	27.3		27.0	27.4
	42.6		42.4	42.8
	47.0		46.8	47.2
	51.6		-	-
$\beta - \text{FeOOH}$		15.6		
		22.0		
		34.4		
		43.8		
		50.8		
		60.2		

X-Ray Target - Fe

**Table 3.14 : 2  $\theta$  values (in degrees) for scale components  
(formed on steel in exposure at Mill A)**

Components	Mild Steel	Stainless-Steel
CaCO <sub>3</sub>	23.1	23.1
	29.6	29.5
	31.5	31.4
	-	32.2
	36.1	36.0
	39.5	39.4
	43.3	43.2
	47.3	47.2
	47.6	47.5
	48.6	48.5
	56.6	56.6
	57.5	57.4
	58.1	58.0
	60.8	60.7
	61.4	61.3
	63.2	63.1
	64.8	64.7
65.6	65.5	
70.2	70.2	
72.9	72.9	
77.1	77.1	
81.5	81.5	
83.8	83.8	
CaO.SiO <sub>2</sub> .5H <sub>2</sub> O	47.9	-
	69.2	-
	82.0	-



X-Ray Target - Cu

Identified phases in different rusts/scale are given in Table 3.15. Thus all rust samples are observed to have  $\text{Fe}_{3-x}\text{O}_4$  and  $\alpha\text{-FeOOH}/\beta\text{-FeOOH}$ . SMS05 shows the presence of mainly calcite ( $\text{CaCO}_3$ ) and silicates are also found, hence it appears as scale rather than rust.

(ii) Mössbauer Spectroscopy:

Representative Mössbauer spectra for iron compound containing rusts, recorded at room temperature  $\approx 25^\circ\text{C}$  and at low temperature  $\approx 80^\circ\text{K}$ , are shown in Fig.3.3, and 3.4 respectively. Low temperature Mössbauer spectra have been folded and fitted using a least square fitting program. All the samples exhibit superparamagnetism due to fine particle size.

Room temperature Mössbauer spectra (Fig.3.3) of five rust samples consist of either a doublet or a mixture of sextets and doublets. Spectrum of SMS05 didn't show any signal, indicating the amount of iron in this rust sample to be below the detectable limit. This was also in accordance with x-ray results (see Table 3.15). Appearance of asymmetric and broadened lines indicate the presence of superparamagnetic (spm) effects. These spm effects are due to ultrafine crystallites (100 Å) (130) which have been observed earlier also in the case of rust samples (121, 126-128).

The parameters of doublet (isomer shift,  $\delta$ , with respect to natural iron 0.4-0.5 mm/s and quadrupole splitting,  $2\epsilon$ , 0.47-0.85 mm/s) correspond to a  $\text{Fe}^{3+}$  site (85). This could be due to  $\beta/\text{T-FeOOH}$ ,  $\text{Fe}_3\text{O}_4/\text{T-Fe}_2\text{O}_3$  (130). These iron oxides and hydroxides, except  $\text{T-FeOOH}$ , have been identified in X-ray diffracto-

**Table 3.15 : Identified phases by X-Ray Diffraction ( Mill A )**  
 ( components of mild steel rusts/scale )

Rusts/Scale	Identified Phases
1MS05	$Fe_{3-x}O_4$ , $\alpha$ - $FeOOH$
2MS05	$Fe_{3-x}O_4$ , $\beta$ - $FeOOH$
4MS05	$Fe_{3-x}O_4$ , $\alpha$ - $FeOOH$
5MS05	$CaCO_3$ , $CaO.SiO_2.5H_2O$
6MS05	$Fe_{3-x}O_4$ , $\alpha$ - $FeOOH$

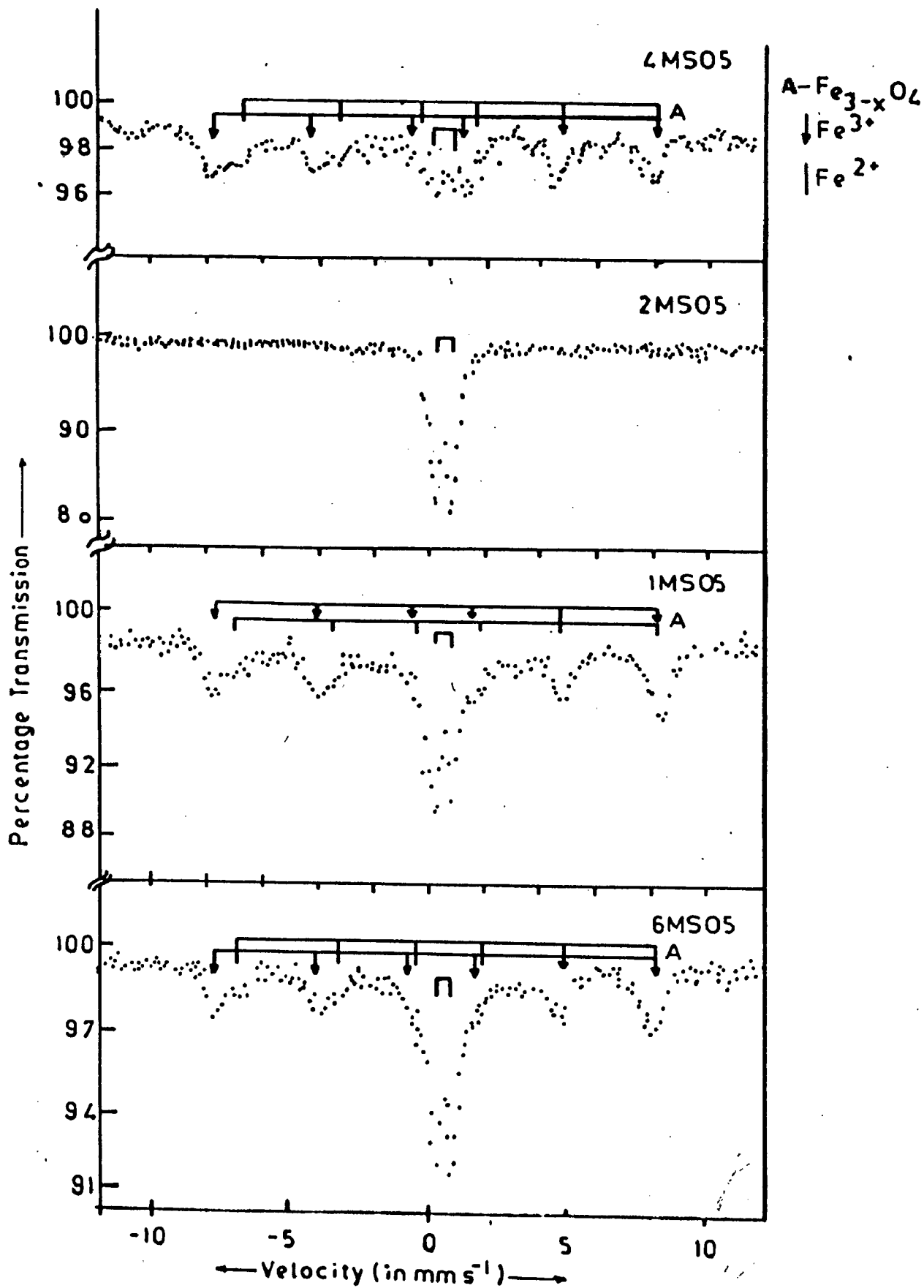


FIG.3.3: ROOM TEMPERATURE MÖSSBAUER SPECTRA OF MILD STEEL RUSTS(MILL-A)

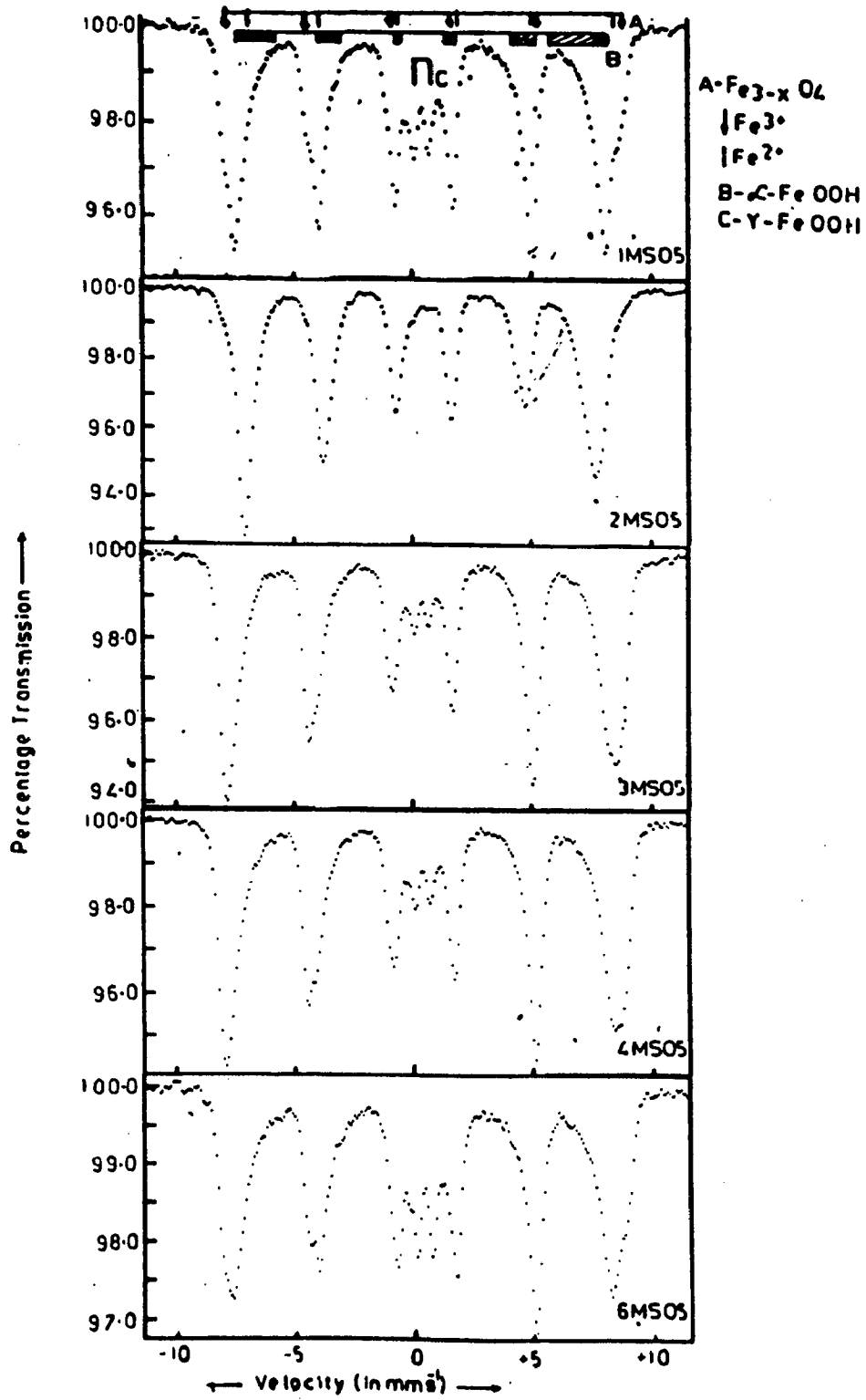


FIG.3.4: LOW TEMPERATURE MÖSSBAUER SPECTRA  
OF MILD STEEL RUSTS (MILL-A)

grams and they have also been suggested among the common corrosion products (123).

The parameters of one sextet ( internal magnetic field,  $H$ , 49.4 - 50.5 Tesla and  $\delta \approx 0.20 - 0.26$  mm/s) correspond to  $Fe^{3+}$  at tetrahedral site while those of the other ( $H \approx 47.3 - 47.8$  T and  $\delta \approx 0.58 - 0.70$  mm/s) correspond to ( $Fe^{2+} - Fe^{3+}$ ) at octahedral site of  $Fe_3O_4$  (133). The ratio of intensities of the two sextets is 1:2 in the case of stoichiometric  $Fe_3O_4$ . Variance of this ratio, in the spectra of present rust samples (Fig. 3.3), thus suggests the presence of non-stoichiometric  $Fe_3O_4$ . There exists a solid solution, represented in general as  $Fe_{3-x}O_4$ , whose end members are  $Fe_3O_4$  ( $x = 0$ ) and  $\gamma-Fe_2O_3$  ( $x = 0.33$ ) (133). While  $Fe_3O_4$  shows two sextets with intensity ratio as mentioned above, the other end member  $\gamma-Fe_2O_3$  or  $Fe_{3-x}O_4$  with  $x = 0.33$  shows at room temperature only one sextet corresponding to  $(Fe^{3+})_{tet}$  ('tet' represents tetrahedral site) and  $(Fe^{3+})_{oct}$  ('oct' represents octahedral site). The parameters of the two  $Fe^{3+}$  sites are so close to each other that their corresponding sextets are not resolvable until an external magnetic field is applied (134). Various members of  $Fe_{3-x}O_4$  series, for  $0 < x < 0.33$ , can be considered as mixture of  $Fe_3O_4$  and  $\gamma-Fe_2O_3$ , in varying amount, depending upon value of  $x$ . As such, for these members, there can be four possible iron sites e.g.

$(Fe^{3+})_{tet}$  and  $(Fe^{3+})_{oct}$  of  $\gamma-Fe_2O_3$

$(Fe^{3+})_{tet}$  and  $(Fe^{3+} - Fe^{2+})_{oct}$  of  $Fe_3O_4$

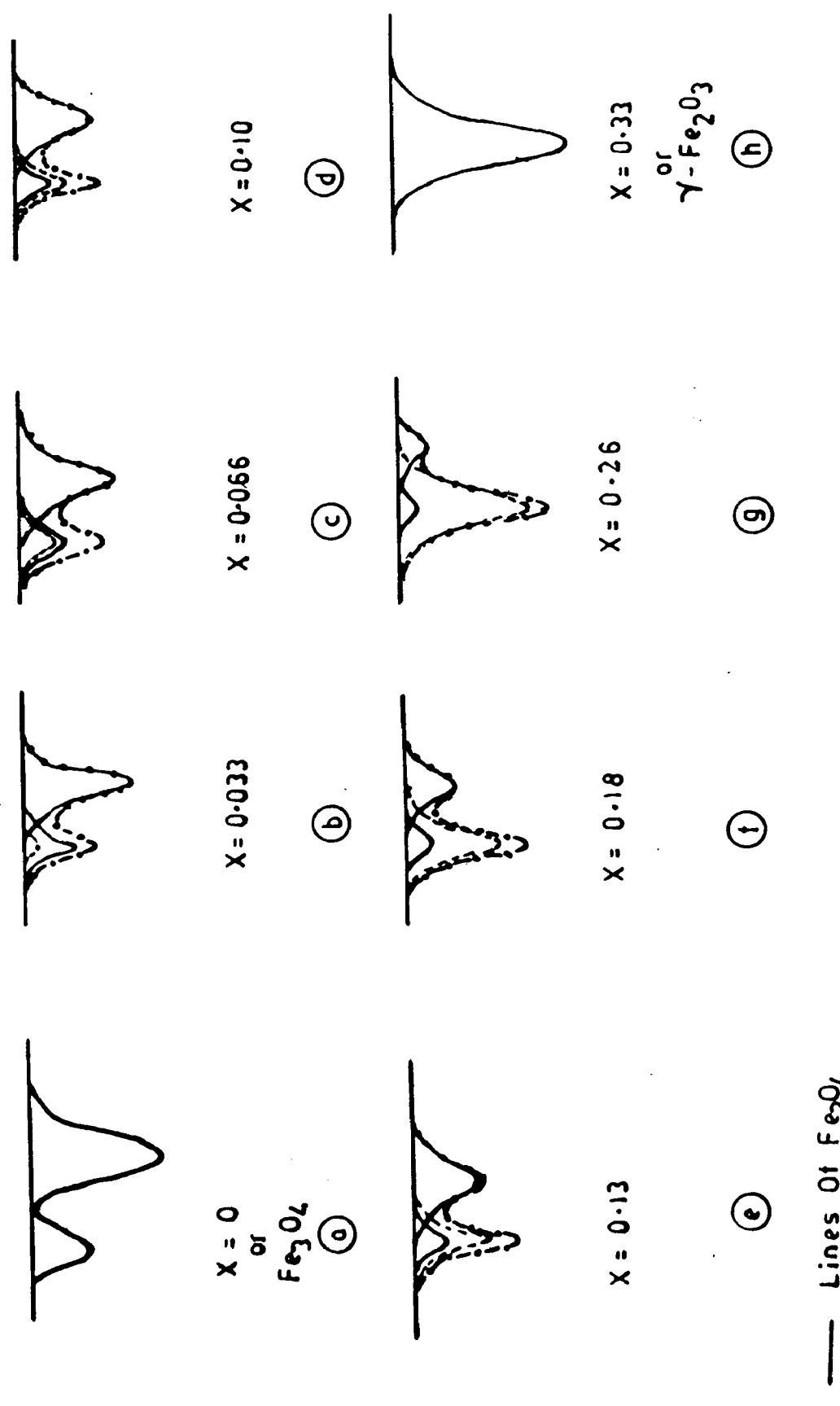
Thus a non-stoichiometric  $Fe_3O_4$  ( one of the members of  $Fe_{3-x}O_4$



series) will show two sextets at room temperature, one corresponding to  $(\text{Fe}^{3+})_{\text{oct}}$  and  $(\text{Fe}^{3+})_{\text{tet}}$  while other to  $(\text{Fe}^{3+}-\text{Fe}^{2+})_{\text{oct}}$ . Their relative intensities can be calculated to vary, with different values of  $x$ , in the manner as depicted in Fig.3.5 which shows first line of respective two sextets in different cases. These relative intensities are found to agree satisfactorily when compared with experimental spectra of  $\text{Fe}_{3-x}\text{O}_4$  for  $x = 0, 0.03, 0.09, \text{ and } 0.33$  (134). In this calculation, two assumptions have been made - (i) iron in  $\text{Fe}_3\text{O}_4$  structure is equally distributed as  $(\text{Fe}^{3+})_{\text{tet}}$ ,  $(\text{Fe}^{3+})_{\text{oct}}$  and  $(\text{Fe}^{2+})_{\text{oct}}$  sites, (ii) magnetic field of two sextets remain unaffected for different values of  $x$ . By comparing these intensity ratios with those observed in rust spectra, one finds that 1MS05 and 6MS05 have  $\text{Fe}_{3-x}\text{O}_4$  with  $x \approx 0.13 - 0.18$  while 4MS05 and 3MS05 consists of  $\text{Fe}_{3-x}\text{O}_4$  with  $x \approx 0.10$  and  $\approx 0.03 - 0.07$  respectively ( Fig 3.3 and 3.5 ).

Due to the presence of relaxation effects in the room temperature spectra, it is difficult to get further information on the nature of corrosion products and their relative amount. As such Mossbauer spectra were also recorded at  $80^\circ\text{K}$  where relaxation effects are almost absent.

$80^\circ\text{K}$  Mossbauer spectra were fitted into a doublet (except 2MS05) and five or six sextets. The parameters, derived out of fitted spectra, are shown in Table 3.16. The parameters of doublet correspond to  $\text{Fe}^{3+}$  iron in  $\tau\text{-FeOOH}$  (135,136). This is further supported by the fact that, among the possible corrosion products in present rusts, only  $\tau\text{-FeOOH}$  has Neel temperature lower than  $80^\circ\text{K}$  (132). Based on above, it is apparent that



X = 0  
or  
Fe<sub>3</sub>O<sub>4</sub>  
(a)

X = 0.033  
(b)

X = 0.066  
(c)

X = 0.10  
(d)

X = 0.13  
(e)

X = 0.18  
(f)

X = 0.26  
(g)

X = 0.33  
or  
γ-Fe<sub>2</sub>O<sub>3</sub>  
(h)

- Lines of Fe<sub>3</sub>O<sub>4</sub>
- - - Lines of γ-Fe<sub>2</sub>O<sub>3</sub>
- · · Lines of Fe<sub>3-x</sub>O<sub>4</sub>

FIG. 3.5: FIRST LINES OF TWO SEXTETS OF  $Fe_{3-x}O_4$   
( $0 < X < 0.33$ )

Table 3.16: 80° K Mössbauer Parameters of Mild Steel Rusts ( Mill A )

Rust	Site	$\delta$ (mm/s)	$\gamma$ -FeOOH $\delta$ (mm/s)	I (%)	H(T)	$\delta$ (mm/s)	H(T)	$\delta$ (mm/s)	I (%)	H(T)	$\delta$ (mm/s)	$\alpha$ -FeOOH $\delta$ (mm/s)	$\delta$ (mm/s)	I (%)	Width V (mm/s)	No. of Sextets
1MS05	Fe <sup>3+</sup>	0.48	0.68	10.2	51.7	0.44	0.03	17.4	46.5	0.47	-0.20	68	0.45	0+2+4		
	Fe <sup>2+</sup>				47.6	0.69	0.21	4.4								
2MS05					----- could not be fitted -----											
3MS05	Fe <sup>3+</sup>	0.47	0.61	5.5	52.1	0.46	0.04	25.1	48.3	0.45	-0.10	55	0.45	0+2+3		
	Fe <sup>2+</sup>				50.2	0.63	-0.09	10.4								
4MS05	Fe <sup>3+</sup>	0.48	0.65	6.6	52.3	0.46	0.00	31.4	48.1	0.46	-0.13	51.5	0.45	0+2+3		
	Fe <sup>2+</sup>				49.7	0.62	-0.08	10.5								
6MS05	Fe <sup>3+</sup>	0.50	0.70	13.0	52.2	0.46	0.02	24.0	47.1	0.48	-0.17	57.0	0.50	0+2+3		
	Fe <sup>2+</sup>				49.0	0.60	0.00	6.0								

$\gamma$ -FeOOH is undetectable in rust 2MS05 (Fig.3.4), its amount is lesser in 3MS05 and 4MS05 than in 1MS05 and 6MS05 (Fig.3.4 and Table 3.16). Since the amount of  $\gamma$ -FeOOH is very small in comparison to other corrosion products (Table 3.16), its peaks are not observable in x-ray diffractograms of rust samples.

To identify other corrosion products, the parameters of sextets were compared with those, given in literature, of  $\text{Fe}_3\text{O}_4$  and  $\alpha$ -FeOOH as their presence was indicated by X-ray diffraction results. For this purpose, a compilation of literature values has been done as the same are not in accordance with each other always. The values represent averages and the errors are estimated from the scatter in different references (137-145). Table 3.17 shows these compiled values.

The comparison indicates two sextets (Table 3.16) due to  $\text{Fe}^{3+}$  and  $\text{Fe}^{2+}$  sites of  $\text{Fe}_{3-x}\text{O}_4$  (non-stoichiometric  $\text{Fe}_3\text{O}_4$ ) respectively. Below transition temperature ( $120^\circ\text{K}$ ), the electron hopping between  $\text{Fe}^{2+}$  and  $\text{Fe}^{3+}$  ions at octahedral sites is slow enough to give significantly different parameters (137,146). As such in  $80^\circ\text{K}$  spectra, sextet with larger H and smaller  $\delta$  corresponds to  $\text{Fe}^{3+}$  at tetra- and octahedral sites while other one to  $\text{Fe}^{2+}$  at octahedral sites of  $\text{Fe}_3\text{O}_4$ .

The information obtained on the amount of vacancies present in  $\text{Fe}_{3-x}\text{O}_4$  (values of x) calculated on the basis of room temperature spectra, can be corroborated with the help of computer fitted parameters of  $80^\circ\text{K}$  spectra of rust samples. This is possible through  $\text{Fe}^{2+}/\text{Fe}^{3+}$  ratio in  $\text{Fe}_{3-x}\text{O}_4$ , obtained from  $80^\circ\text{K}$

**Table 3.17 : Mössbauer parameters at 80°K  
(compiled from literature Ref. 137-145)**

Rust component	Site	H (Tesla)	$\delta$ (mm/s)	$2\epsilon$ (mm/s)
Fe <sub>3</sub> O <sub>4</sub>	Fe <sup>3+</sup>	51.2 ± 1.8	0.47 ± 0.04	0
	Fe <sup>2+</sup>	48.0 ± 2.0	0.80 ± 0.15	?
$\alpha$ - FeOOH	Fe <sup>3+</sup>	49.4 ± 1.8	0.48 ± 0.04	?

**Table 3.18 : Values of 'x' in  $Fe_{3-x}O_4$**

Rust	Value of 'x'	
	Room Temperature Spectra	80°K Spectra
1MS05	0.13 - 0.18	0.16
6MS05		0.16
3MS05	0.10	0.11
4MS05	0.03 - 0.07	0.06

spectra. Table 3.18 compares values of 'x' for  $Fe_{3-x}O_4$  formed in different cases, obtained from room temperature and 80°K spectra.

Three to four sextets ( $H = 38.3 - 50 T$ ) were assigned to  $\alpha$ -FeOOH for complete interpretation of 80°K spectra. Attribution of more than one sextet to a single phase (here  $\alpha$ -FeOOH) can be understood to be due to wide particle size distribution including ultrafine particles (130). Thus smaller values of H can be assigned to fine particles of  $\alpha$ -FeOOH. Table 3.16 shows weighted average values of hyperfine parameters for  $\alpha$ -FeOOH. H value obtained thus is observed to be smaller than that for bulk  $\alpha$ -FeOOH (Table 3.17) showing that average size of  $\alpha$ -FeOOH grains in rust is smaller than that of bulk. Wider range of H values attributed to  $\alpha$ -FeOOH reflects fine dispersion, normally found for oxhydroxides as corrosion products (147), in comparison to  $Fe_{3-x}O_4$  where assignment of one sextet to each site ( $Fe^{2+}, Fe^{3+}$ ) was sufficient for interpretation of fitted spectra. The spectrum of ZMS05 could not be fitted due to its complex nature. It should be analyzed by recording the spectra at still lower temperature.

One thus observes that among the rusts, studied presently, only ZMS05 (steel exposed near chlorination shower pipe) shows the presence of  $\beta$ -FeOOH while  $\gamma$ -FeOOH is not detected. It is known that  $\beta$ -FeOOH forms in presence of chloride ion, lower pH solutions and as a result of aerial oxidation (148,149). In present tests, such conditions exist only in case of ZMS05 because the liquor in buffered-hypo and hypochlorite stages is alkaline. Though liquor in chlorination vat is acidic and chlo-

rine containing (Table 3.2), aerial oxidation of mild steel, exposed in C-vat, is not possible because it has undergone corrosion in completely immersed state.

Corrosion rates were also measured, given in section 3.1, for corroded specimens (1MS05-6MS05) from which present rust samples have been taken. It is found that mild steel experience more corrosion in chlorination stage than buffered-hypo and hypochlorite stages. In the latter two stages, corrosion is more near shower pipe than in vat. A correlation has been tried between nature and amount of corrosion products and corrosion rates. One observes from Table 3.16 and X-ray diffractograms that  $Fe_{3-x}O_4$  is least in amount in case of rusts obtained from chlorination stage. Further, the same is observed to be lesser in 6MS05 (hypochlorite shower pipe), where corrosion rate is higher than the rest. It thus appears that amount of  $Fe_{3-x}O_4$  is less and those of oxhydroxides ( $\alpha$ -,  $\beta$ - or  $\gamma$ -) is more in case of rusts formed on mild steel in more corrosive environments. It is also observed that  $Fe_3O_4$  is more non-stoichiometric (i.e.  $Fe_{3-x}O_4$  with  $x$  closer to 0.33) in case of rust formed in more corrosive environment, in accordance with an earlier work (147). This is evident from higher values of  $x$  in  $Fe_{3-x}O_4$  in case of 1MS05 and 6MS05 while lesser in 3MS05 (Table 3.18).

The above observations appear to support the model suggested earlier (147) for corrosion products formation. Thus the first detectable phase to form as rust seems to be  $Fe_{3-x}O_4$  (values of 'x' depending upon corrosivity), which later on changes to  $\beta$ -



FeOOH in case ZMS05, to  $\gamma$ - and then to more stable  $\alpha$ -FeOOH in other cases. Since  $\text{Fe}_3\text{O}_4$  to FeOOH transformation leads to increase in mole volume, it leads to disruption of oxide layer resulting in fine dispersion of FeOOH particles. Further, since this transformation is via the formation of  $\gamma\text{-Fe}_2\text{O}_3$  ( $\text{Fe}_{3-x}\text{O}_4$  with  $x = 0.33$ ) and that  $\text{Fe}_3\text{O}_4$  is more non-stoichiometric (closer to  $\gamma\text{-Fe}_2\text{O}_3$ ) when formed in more corrosive environment, the ratio of  $\alpha\text{-FeOOH}/\text{Fe}_{3-x}\text{O}_4$  should be more in rusts formed in these environments than in case of rusts formed in lesser aggressive conditions. In the latter case,  $\text{Fe}_{3-x}\text{O}_4$  formed is closer to stoichiometric  $\text{Fe}_3\text{O}_4$  (Table 3.18). This is in accordance with present investigations.

(b) Mill B

Now a brief discussion will be given with regard to the corrosion products formed on mild steel exposed in the bleaching environment of mill B.

X-ray diffractograms were recorded in this case only on Fe target. These are shown in Fig. 3.6. These diffractograms in general show less intensity and broadened peaks and in few cases practically no peak was observed. It is expected to be due to fine particle size and poor crystallinity that is normally observed in the iron compounds as a component of rusts. One significant difference observed in some of these diffractograms, in comparison to those of rusts from mill A, is the appearance of peaks corresponding to  $\gamma\text{-FeOOH}$  also. Table 3.19 shows the  $2\theta$  values, corresponding to different phases, in case of rusts

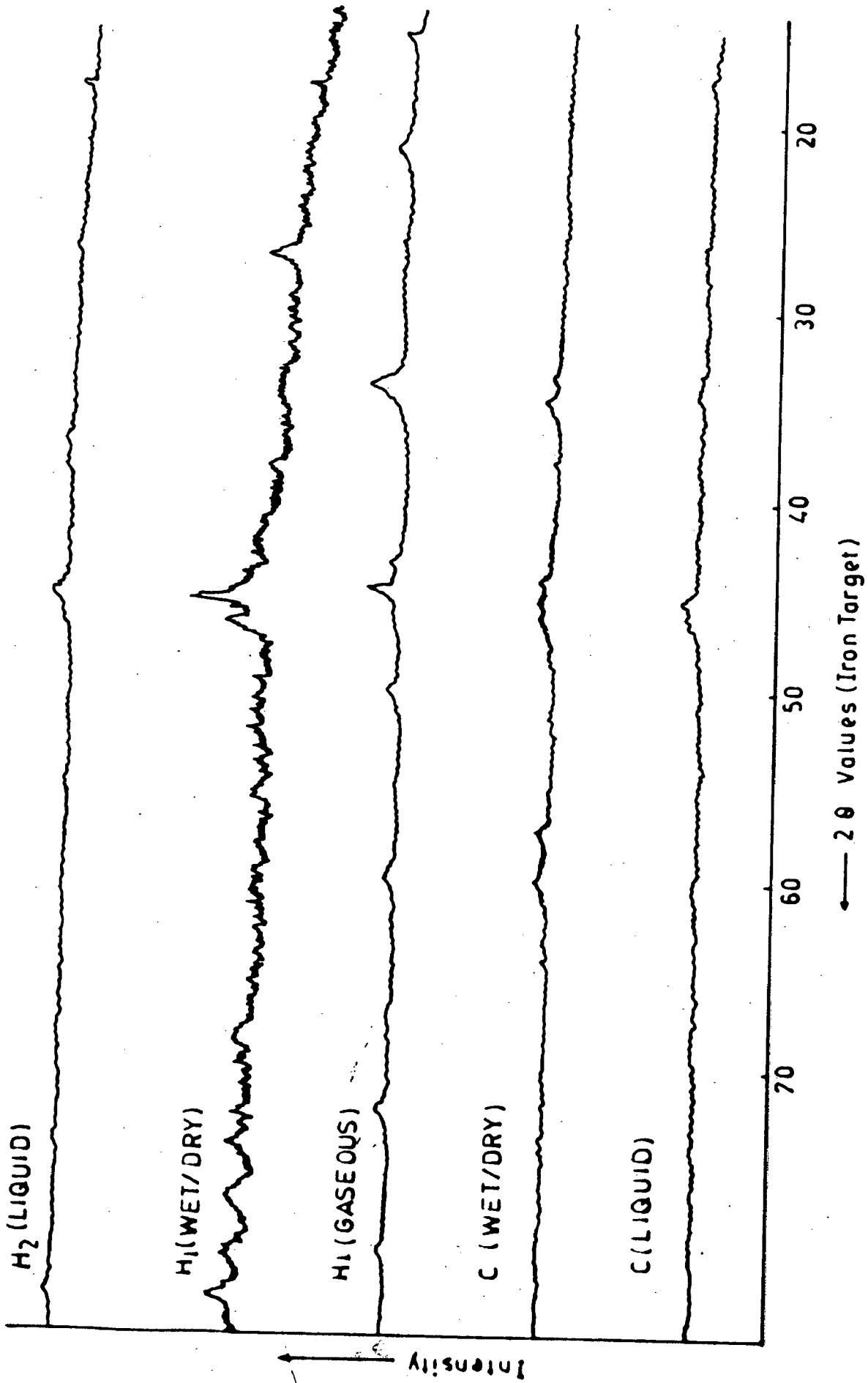


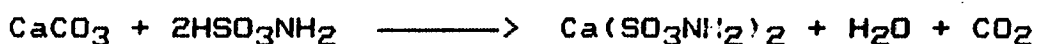
FIG. 3-6: X-RAY DIFFRACTOGRAMS OF MILD-STEEL RUSTS (MILL-B)

Table 3.19 : 2  $\theta$  values ( in degrees ) for Iron compounds  
 ( components of mild-steel rusts from Mill B )

Iron compound	C-liquid	H1-gas	H2-liquid	C-W/D	H1-W/D
$\text{Fe}_{3-x}\text{O}_4$	-	-	38.5		38.6
	45.2	44.8	45.3		45.5
	-	-	55.4		55.5
	74.0	72.4	74.2		75.3
	-	-	82.0		81.0
$\alpha - \text{FeOOH}$	26.7		26.8		27.0
	-		-		42.5
	46.4		46.0		46.7
	-		-		51.2
	-		-		68.8
$\tau - \text{FeOOH}$	34.2	33.9		34.4	
	46.0	46.3		45.5	
	60.1	59.6		-	
$\beta - \text{FeOOH}$		15.3			
		21.2			
		33.9			
		43.2			
		50.0			
		59.6			

X-Ray Target - Fe , W/D - Wet/Dry cyclic environment.

obtained from coupons exposed in C-liquid, H1-gaseous and wet/dry environment. These cases have been shown as they are different from the rusts of mill A. The identification of the different phases has been done as described earlier. Table 3.20 gives the components of different rust samples. These are observed to have  $Fe_{3-x}O_4$ ,  $\alpha$ -,  $\beta$ - and  $\gamma$ -FeOOH in varying amount. Another significant difference in the rusts obtained from coupons exposed to hypowashers, in comparison to those exposed in hypowasher of mill A, is the non-appearance of calcite etc. This could be attributed to use of (i) better quality of lime (ii) sulfamic acid which acts as descalant also, in mill B. Sulfamic acid readily forms various metal sulfamates (118) by reacting with the metal or the respective carbonate, oxides or hydroxide. The reaction with calcium carbonate ( calcite ) is given below:



Thus formed calcium sulfamate is water-soluble compounds. Scale helps in protecting steel to some extent but may also choke pipe lines etc.

### 3.2.2 Stainless-Steels:

The exposed coupons from both mills had three types of a appearance-

- i. those having loose, porous dark, coloured deposits on them (coupons exposed in gaseous phase of different washers).
- ii. those having scale deposition ( coupons exposed in liquid phase of H-washer of mill A) or shining violet/purple colored

**Table 3.20 : Identified phases by X-Ray Diffraction (Mill B)**  
 ( components of mild steel rusts )

Rusts	Identified Phases
Chlorination - G	$Fe_{3-x}O_4$ , $\beta$ - FeOOH
Chlorination - L	$Fe_{3-x}O_4$ , $\alpha$ - FeOOH , $\tau$ - FeOOH
Chlorination - W/D	$\tau$ - FeOOH
Hypochlorite1 - G	$Fe_{3-x}O_4$ , $\beta$ - FeOOH , $\tau$ - FeOOH
Hypochlorite1 - L	$Fe_{3-x}O_4$ , $\alpha$ - FeOOH
Hypochlorite1 - W/D	$Fe_{3-x}O_4$ , $\alpha$ - FeOOH
Hypochlorite2 - L	$Fe_{3-x}O_4$ , $\alpha$ - FeOOH
Hypochlorite2 - W/D	$Fe_{3-x}O_4$ , $\alpha$ - FeOOH , $\tau$ - FeOOH

G - Gaseous, L - Liquid, W/D - Wet/Dry cyclic environments.

film ( on coupons exposed in liquid and wet/dry phase of mill B).

iii. Almost clean.

Analysis of corrosion products formed on SS was done by X-ray diffraction using Fe target. The rusts from either of the two mills did not indicate much intense peaks ,therefore, X-ray diffractograms were also recorded using Cu target. The scale and the purple/violet coloured film were also investigated using Cu target. The identification of the phases in the rusts was done from the diffractograms recorded using both the targets. For this purpose, same procedure as described earlier for mild steel rusts, was followed. Some of the representative X-ray diffractograms of rusts from mill A, recorded using Fe target, are shown in Fig.3.7 .  $2\theta$  values corresponding to different phases are given in Table 3.21 and identified phases in different rusts are shown in Table 3.22. One observes  $Fe_{3-x}O_4$  and  $\beta$ -FeOOH in all the rusts with  $\gamma$ -FeOOH in case of SS-304 and 316 coupons exposed in hypo- and buffered-hypo washers' gaseous environment. The diffractogram of the scale ,observed on coupons exposed in hypo-vat, and  $2\theta$  values of the identified phase are given in Fig. 3.8 and Table 3.14 respectively. Thus the scale indicates the presence of calcite mainly, as in case of scale formed on mild steel coupon.

In the case of mill B, rust enough for X-ray analysis, was obtained from coupons exposed near shower pipe of C-stage only among all the gaseous phases. This is perhaps due to lesser corrosivity (compared to Mill A) of bleach plant of this mill. X-ray diffractograms of the rusts , in general, gave only weak

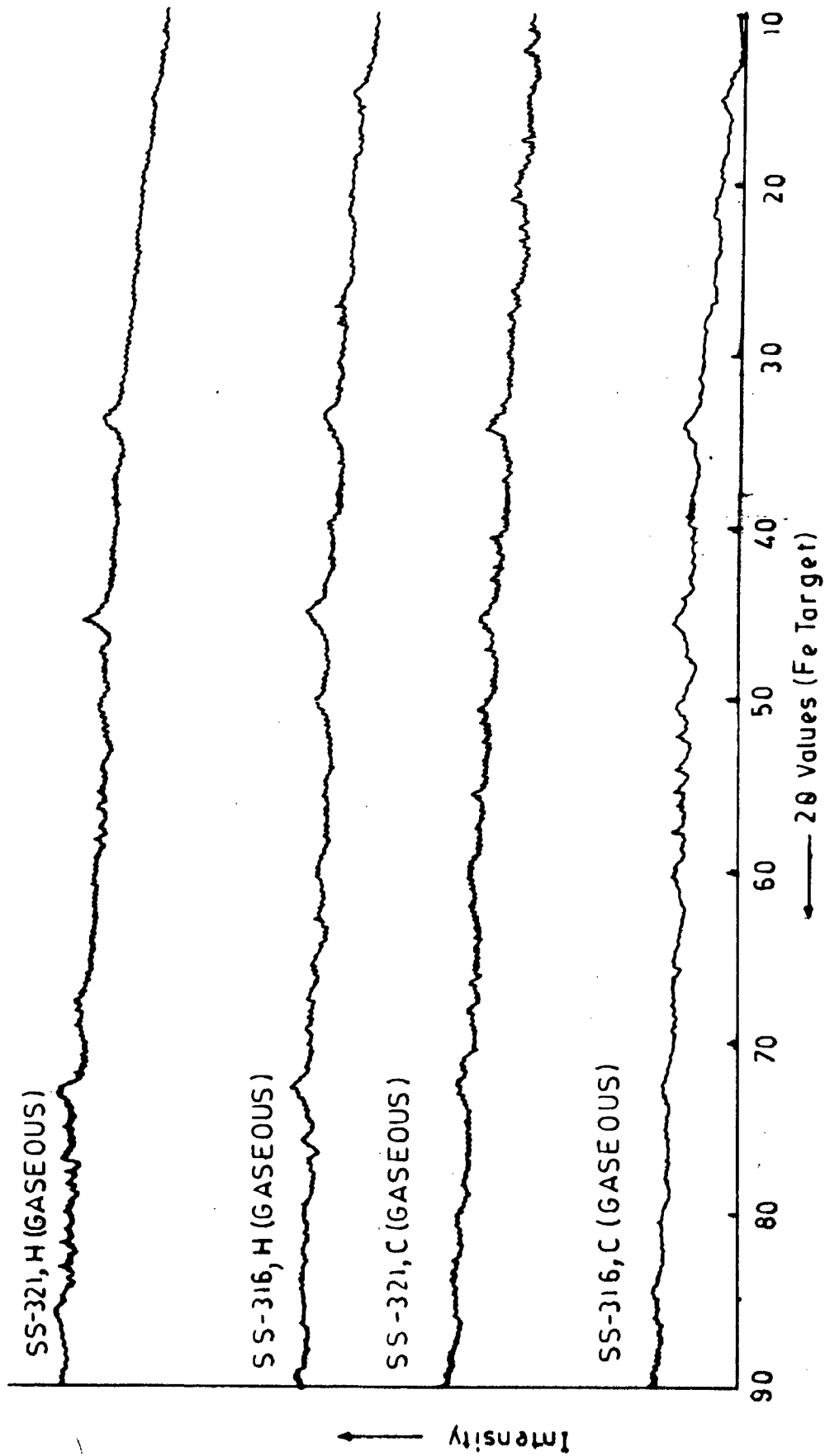


FIG.3.7: X - RAY DIFFRACTOGRAMS OF STAINLESS-STEEL RUSTS (MILL-A)

**Table 3.21 : 2  $\theta$  values (in degrees) for iron compounds  
(components of stainless-steel rusts from mill A)**

Iron compound	C-Gaseous Phase		H-Gaseous Phase	
	SS 316	SS 321	SS 316	SS 321
$\text{Fe}_{3-x}\text{O}_4$	-	37.8	-	-
	45	45.2	45	45.4
	53.7	-	-	-
	-	-	-	68
	72.6	72.3	72.5	73
	79.8	-	79.8	-
$\beta\text{-FeOOH}$	-	15.4	-	-
	-	20.4	-	-
	34	34	34	34
	50	50.4	50	50.5
	72.6	72.3	-	73

X-Ray Target - Fe



**Table 3.22: Components of Stainless-Steel Rusts/Scales formed in different environment ( Mill A )**

Rust/Scale	Components
304-CG	$Fe_{3-x}O_4$ , $\beta$ -FeOOH
316-CG	$Fe_{3-x}O_4$ , $\beta$ -FeOOH
321-CG	$Fe_{3-x}O_4$ , $\beta$ -FeOOH
304-BG	$Fe_{3-x}O_4$ , $\beta$ -FeOOH, $\tau$ -FeOOH (may be)
304-HG	$Fe_{3-x}O_4$ , $\beta$ -FeOOH, $\tau$ -FeOOH (may be)
316-HG	$Fe_{3-x}O_4$ , $\beta$ -FeOOH, $\tau$ -FeOOH (may be)
321-HG	$Fe_{3-x}O_4$ , $\beta$ -FeOOH
304-HL	$CaCO_3$

304,316,321 represents types of stainless-steels.

C - chlorination, H - hypochlorite, B - buffered hypo stages.

G - Gaseous and L - Liquid environments.

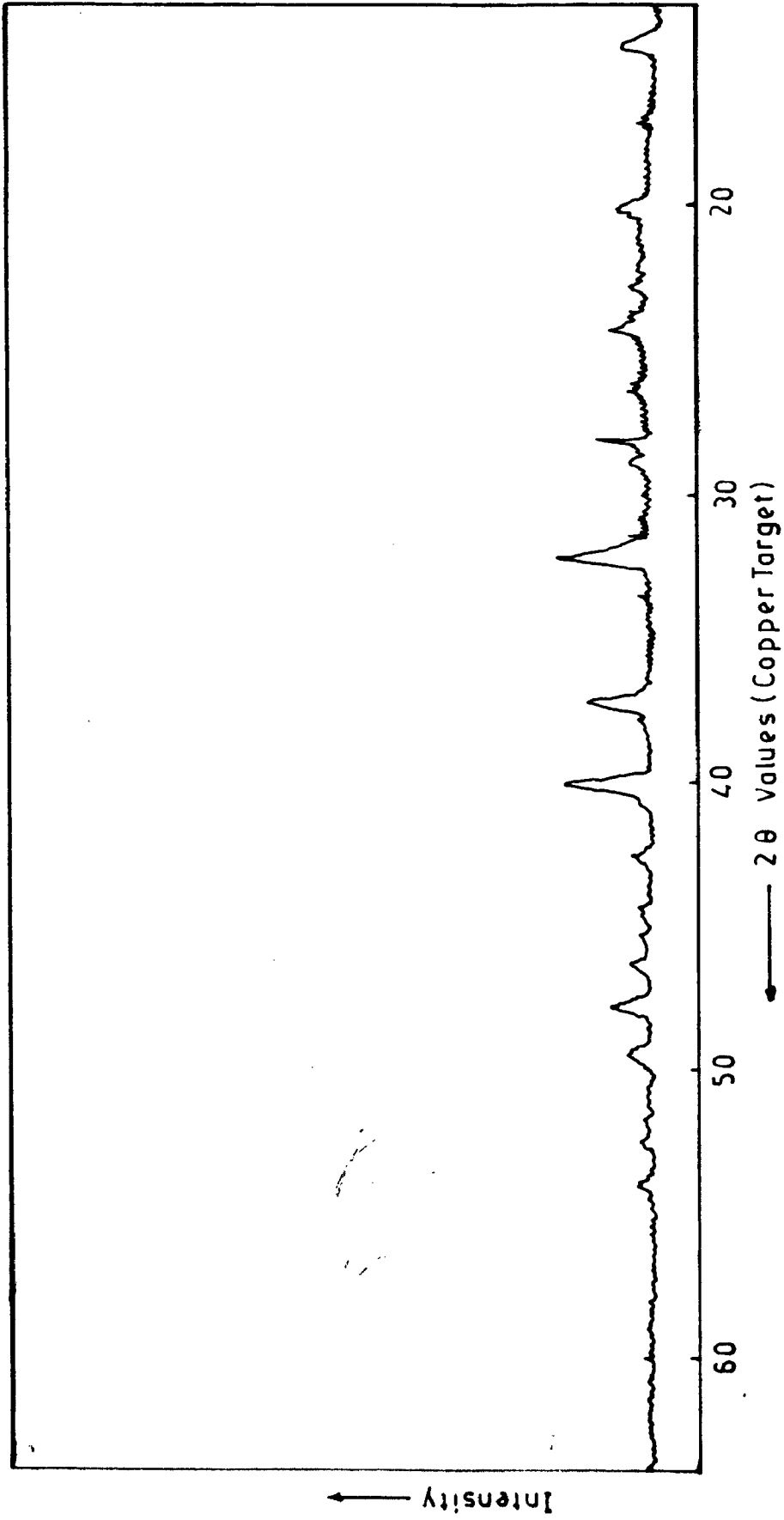


FIG. 3-8: X-RAY DIFFRACTOGRAM OF SCALE (STAINLESS-STEEL)(MILL-A)

peaks (like the case of mill A) at approximately same  $2\theta$  values as in the case of corresponding rusts of mill A. Table 3.23 shows the identified components in these rusts. These are mainly  $Fe_{3-x}O_4$  and  $\beta$ -FeOOH. X-ray diffractograms of film formed on coupons exposed in hypo-washer's liquid and wet/dry environment were recorded in some cases by directly incidenting X-ray beam on surface of corroded sample. While in others the film was scraped and then its X-ray diffractogram was recorded. In the former case one observes mainly the peaks of austenite phase (of SS itself) with very weak peaks of chromium oxide. In the latter case, mainly chromium compounds are observed (Fig. 3.9 and Table 3.24). However, many of the lines could not be identified.

A brief discussion of films and corrosion products in general are given in the coming paragraphs. Appearance of loose/porous deposits over coupon indicates that layer formed after exposure is not protective type. Hence it should form on coupons which are exposed to more corrosive environments. Because of the same reason large number of coupons (those exposed to gaseous phase of all the stages of mill A) show this type of layer. Such coupons (Table 3.22) show  $Fe_{3-x}O_4$  and  $\beta$ - and/ or  $\gamma$ -FeOOH. Formation of iron products was further confirmed by  $Fe^{57}$  Mössbauer spectroscopy as it was surprising to observe iron compounds instead of nickel/chromium compounds. This again hints about highly corrosive environment in bleach plant specially near shower pipes. Normally the first detectable phase to form as rust component is  $Fe_{3-x}O_4$  which later converts into  $\beta$ -/ $\gamma$ -FeOOH and finally to a more stable  $\alpha$ -FeOOH phase (147). Since  $\beta$ -FeOOH preferably forms

**Table 3.23: Components of Stainless-Steel Rusts/Scales formed in different environment ( Mill B )**

Rust/Scale	Components
304-CG	$Fe_{3-x}O_4$ , $\beta$ -FeOOH, $\gamma$ -FeOOH (may be)
304L-CG	$Fe_{3-x}O_4$ , $\beta$ -FeOOH
316-CG	$Fe_{3-x}O_4$ , $\beta$ -FeOOH
321-CG	$Fe_{3-x}O_4$ , $\beta$ -FeOOH
SS-H1W/D	$Cr_2O_3$ , Chromium Chloride (may be)
SS-H1 L (exposed coupon)	Austenite phase, $Cr_2O_3$

304,316,321 represents types of stainless-steels.

C - chlorination and H - hypochlorite stages.

G - Gaseous, L - Liquid, W/D - Wet/Dry cyclic environments.

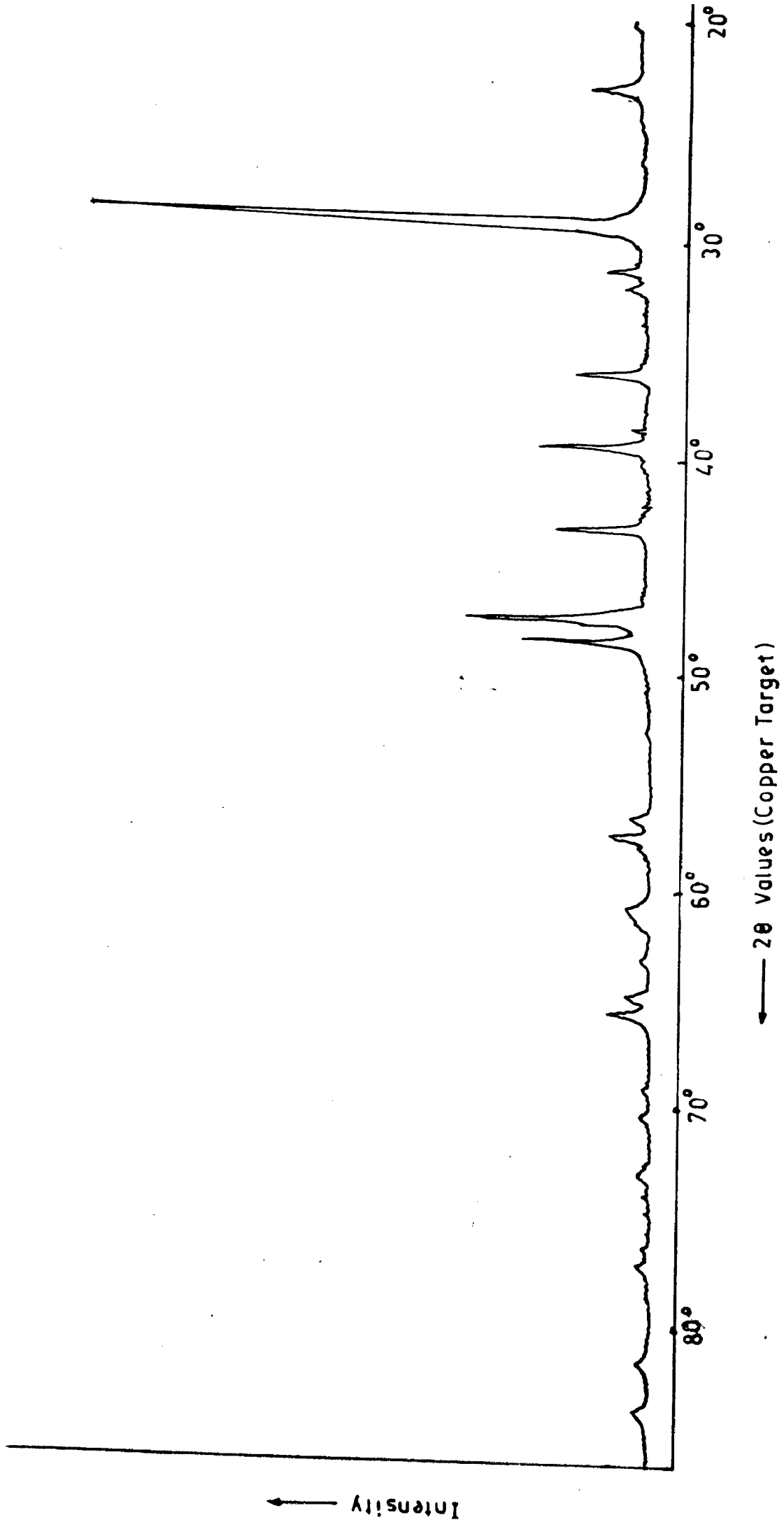


FIG.3-9: X-RAY DIFFRACTOGRAM OF CORROSION PRODUCTS FILM FORMED ON  
STAINLESS-STEEL (LIQUID AND WET/DRY EXPOSURE IN HYPOWASHERS  
OF MILL-B)

**Table 3.24 : 2  $\theta$  values ( in degrees) for components of film  
(formed on stainless-steel exposed in wet/dry  
cyclic phase of hypochlorite washers of mill B)**

Components	2 $\theta$
Cr <sub>2</sub> O <sub>3</sub>	24.2
	32.4
	37.4
	40.2
	44.6
	49.2
	54.0
CrCl <sub>2</sub>	65.4
	20.2
	32.4
Unidentified	42.6
	14.5
	28.2
	29.0
	31.8
	43.6
	45.4
	46.2
	47.8
	51.8
52.5	
66.8	

---

X-Ray Target - Cu

in presence of  $\text{Cl}^-$  ion, low pH solution and only as a result of aerial oxidation (149), rust scraped from coupons exposed to gaseous phases are found to contain mainly  $\text{Fe}_{3-x}\text{O}_4$  and  $\beta\text{-FeOOH}$ . Non-observation of  $\alpha\text{-FeOOH}$  phase in rust formed on stainless-steels perhaps is due to their better corrosion resistance.

Shining violet/purple film formed on coupons exposed to liquid and wet/dry phase in hypowasher of mill B appears to have nickel and chromium oxides together with some chloride whereas X-ray diffractogram of exposed coupon itself showed main peaks of austenite phase and weaker peaks of nickel and chromium oxides. It seems protective film formed on stainless steels has top most layer of nickel and chromium oxides. Presence of iron or its oxides is not noticeable.

It is thus seen that corrosion products, as a component of rusts or scale, can be identified using X-ray diffraction and Mössbauer spectroscopy. The latter technique, suitably assisted by X-ray diffraction, also helps in analysing the structure and stoichiometric details of the corrosion products. The analyses of corrosion products helps in understanding the nature of protective layer formed in many metal-environment system. The formation of this protective layer helps in passivating the steel in a given environment and hence enhancing the useful life of materials. It is therefore always desirable to understand the nature of protective layer and to know the alloying elements responsible for the development of this layer. This information in turn helps in developing corrosion resistant materials. Otherwise also, nature of corrosion products is important to know as it helps in pre-

dicting the behavior of a material in a given environment. This is because a material surface interacts with its surroundings through the rust/scale formed over it. The information on corrosion products and their nature also helps in understanding the mechanism of corrosion reactions proceeding over a surface.



## Chapter -4

### ANALYSES OF CORROSION BY LABORATORY TESTS

	Page No.
4.1 Weight-loss Tests.	163
4.1.1 Tests in High Concentration Solutions.	163
4.1.2 Tests in Low Concentration Solutions.	166
4.1.3 Effect of Sulfamic Acid.	170
4.2 Electrochemical Polarization Tests.	172
4.2.1 Tests on Mild Steel.	173
4.2.2 Tests on Stainless-Steels.	185

The present chapter deals with the corrosion studies performed on steels in liquors of bleach section in laboratory controlled conditions. These studies were performed by conducting the following two types of test:

4.1 Weight-loss Test.

4.2 Electrochemical Polarization Test.

The chemical composition of steels used in weight-loss tests is same as those of steels discussed in previous chapter while that of steels used in electrochemical studies are given in Table 4.1. In general, bleach section in Indian mills has three stages namely chlorination, alkali extraction and hypochlorite. Though variation is observed in process conditions from mill-to-mill, liquors mainly responsible for corrosivity of these stages are chlorine water, caustic solution and hypochlorite solution. As is widely known, caustic at room temperature is not very corrosive. Chlorine water though highly corrosive, is observed to show rapid variation, with time, in the concentration of chlorine in chlorine water at low pH ( $\approx 2$ , as observed in chlorination section) in open environment. This variation is so rapid that during the weight-loss test, it is difficult to maintain reasonably constant concentration of chlorine. Although it can be achieved by either closing the test-cell or decreasing the temperature of chlorine water, however, these do not simulate the actual mill conditions. Therefore, the laboratory tests were performed on steels in hypochlorite solutions at room temperature with varying chemical concentration. This liquor medium was chosen for laboratory tests, also because it was found that not much work on it

**Table 4.1: Analyses of Steel ( Wt% )**

Material	C	Mn	Si	Cr	Ni	Mo
Mild steel	0.18	0.66	0.04	-	-	-
SS 304	0.074	1.49	0.41	19.80	8.45	-
SS 304L	0.045	1.62	0.66	18.56	7.42	-
SS 316	0.071	1.90	0.48	19.25	12.70	1.77
SS 316L	0.019	1.71	0.49	17.56	11.66	1.79

has been cited in the literature. This is in spite of the fact that hypochlorite solutions too are responsible for the corrosion attack on the bleach plant machinery. In addition, the experiments were also done in chloride solution and in hypochlorite solution containing sulfamic acid as these two also are observed to affect the corrosion attack in the mills which have been considered for mill tests in the present work.

#### 4.1 Weight-loss Test :

The weight-loss tests were done to find the corrosion rate of commercial grade mild steel and austenitic stainless-steels of grade 304, 304L, 316, 316L and 321. Hypochlorite solution in two concentration ranges were taken for tests, namely higher concentration range ( free available chlorine  $\approx$  1 - 25 gpl ) and low concentration range ( free available chlorine  $\approx$  150 - 600 ppm ). Both solutions were prepared from bleach liquor (calcium hypochlorite solution) of pH  $\approx$  12 - 13, obtained from a nearby paper mill.

##### 4.1.1 Tests in High Concentration Solutions:

Calcium hypochlorite solutions of 1, 3, 6, 11, 15, 20 and 25 gpl free available (FA) chlorine concentration were prepared from the above mentioned bleach liquor. pH of these solutions was maintained around 11 whereas  $\text{Cl}^-$  concentration was not fixed. These pH and concentrations of FA chlorine simulate the conditions in hypochlorite towers, conveying pipes, valves etc. The study was aimed to provide information about corrosion effects on the above process equipment. In addition, it was expected to show

the effect of increased concentrations of FA chlorine on corrosivity of bleach liquor. After exposure in the hypochlorite solutions at ambient temperature, as described in Chapter 2, the samples were cleaned without giving any chemical treatment. This was unlike the case of mill exposed coupons which required such a treatment for cleaning. Table 4.2 and Figure 4.1 show the variation of corrosion rates with FA chlorine concentration. It is found that corrosion rate first increases, reaching a maximum value (213 mpy) at 6 gpl and then decreases with FA chlorine concentration. Corrosion of mild steel in these solutions is a function of (i) concentration of  $\text{OCl}^-$  ion (as per Fig.1.3, form of chlorine in hypochlorite solutions at the prevailing pH will be  $\text{OCl}^-$ ) (ii) dissolved oxygen content. Both the above factors affect corrosion in same direction. However, it has been observed that with increase in FA chlorine concentration, in case of neutral/alkaline electrolytes dissolved oxygen content decreases which leads to suppression of cathodic reactions. This results in decrease in rate of metal dissolution (154). In the present case, bleaching solution is alkaline, it appears that the observed behavior is due to decrease in dissolved oxygen with increase in FA chlorine concentration which has dominant effect beyond 6 gpl concentration in determining corrosion rate. In these solutions, the effect of  $\text{Cl}^-$  ion concentration has not been studied as it was not expected to give significant contribution in determining corrosion rate due to higher concentration of oxidants.

**Table 4.2 : Corrosion rate of mild steel in bleach liquor of higher concentration**

Free Available Chlorine (gpl)	Corrosion Rate (mpy)
1	108.5
3	156.5
6	212.8
11	163.6
15	130.3
20	108.2
25	108.5

---

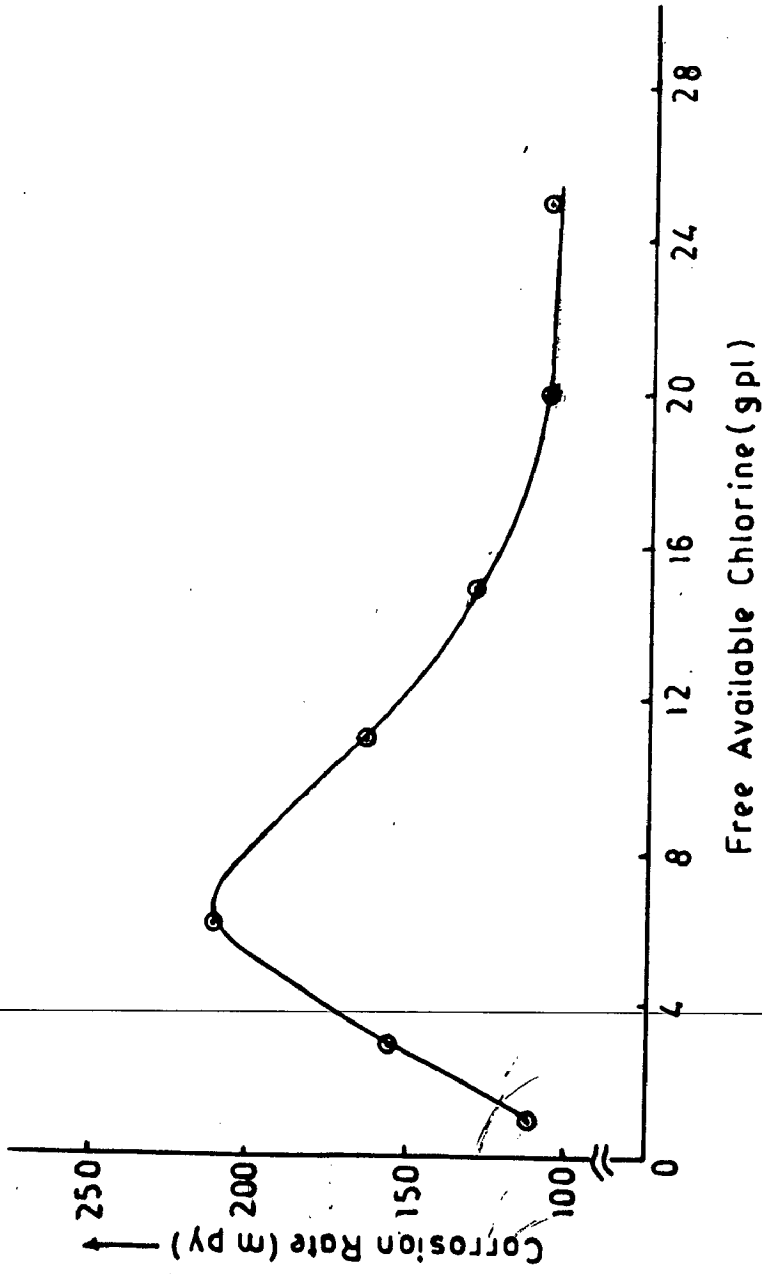


**FIG. 4-1: VARIATION OF CORROSION RATE WITH FREE AVAILABLE CHLORINE IN BLEACH LIQUOR**

#### 4.1.2 Tests in Lower Concentration Solutions:

Since the concentration of FA chlorine (as residuals) in bleach plant washers of mills ( Table 3.2 to 3.4 ) are controlled below around 600 - 700 ppm or so , it was planned to perform laboratory experiments in these concentration ranges so as to simulate the actual washer conditions. These concentrations are quite low in comparison to the earlier studied concentrations, it was suspected that  $\text{Cl}^-$  might have an important role in affecting corrosion . Therefore tests were performed in  $\text{Cl}^-$  solutions and in hypochlorite solutions maintaining constant concentration of  $\text{Cl}^-$  ions in them.

$\text{Cl}^-$  solutions were prepared by dissolving sodium chloride in distilled water. These solutions had  $\text{Cl}^-$  concentration ranging between 200 ppm to 3000 ppm and their pH was maintained at  $\approx 7$ . The selection of concentration range and pH was done on the basis of washer filtrate conditions encountered in the tested mills. The test was performed at ambient temperature. Fig. 4.2 and Table 4.3 show variation of corrosion rates in these solutions with  $\text{Cl}^-$  ion concentration. On an average, change in corrosion rate is observed as 0.5 mpy over the whole concentration range (200 - 3000 ppm) whereas error in the measurement of corrosion rate is  $\pm 0.15$  mpy. One , therefore, observes negligible variation in corrosion rate with  $\text{Cl}^-$  in the studied concentration range. These results are in accordance with the earlier observations (154). As indicated in Chapter 3, effect of  $\text{Cl}^-$  is to enhance the possibility of localized corrosion attack.



**Table 4.3 : Corrosion rate of mild steel in sodium chloride solution**

Chloride Ion (ppm)	Corrosion Rate (mpy)
200	3.52
400	3.28
600	3.54
800	3.45
1000	3.60
1500	3.68
2000	4.22
2500	4.26
3000	4.34

---

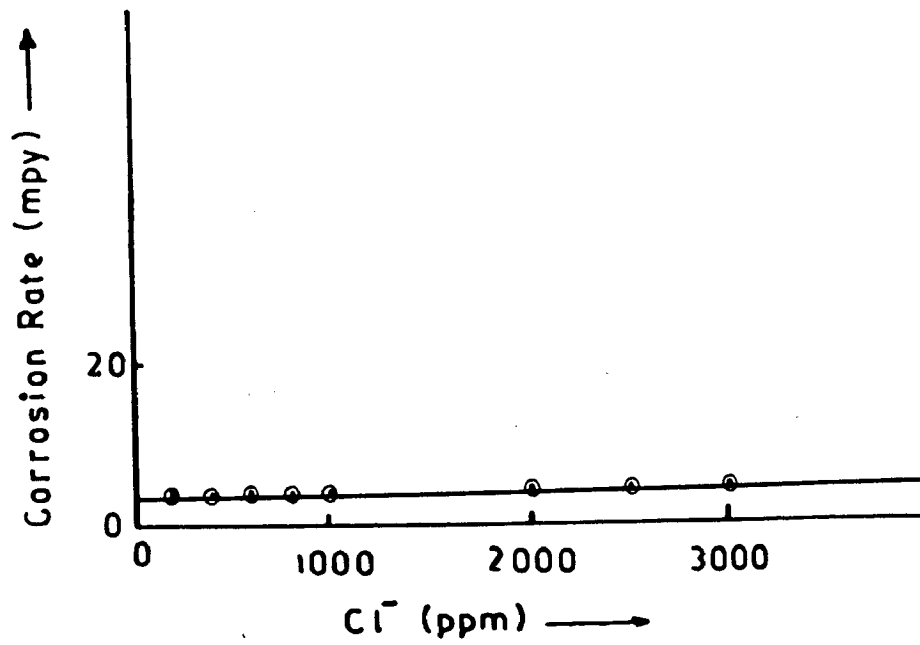


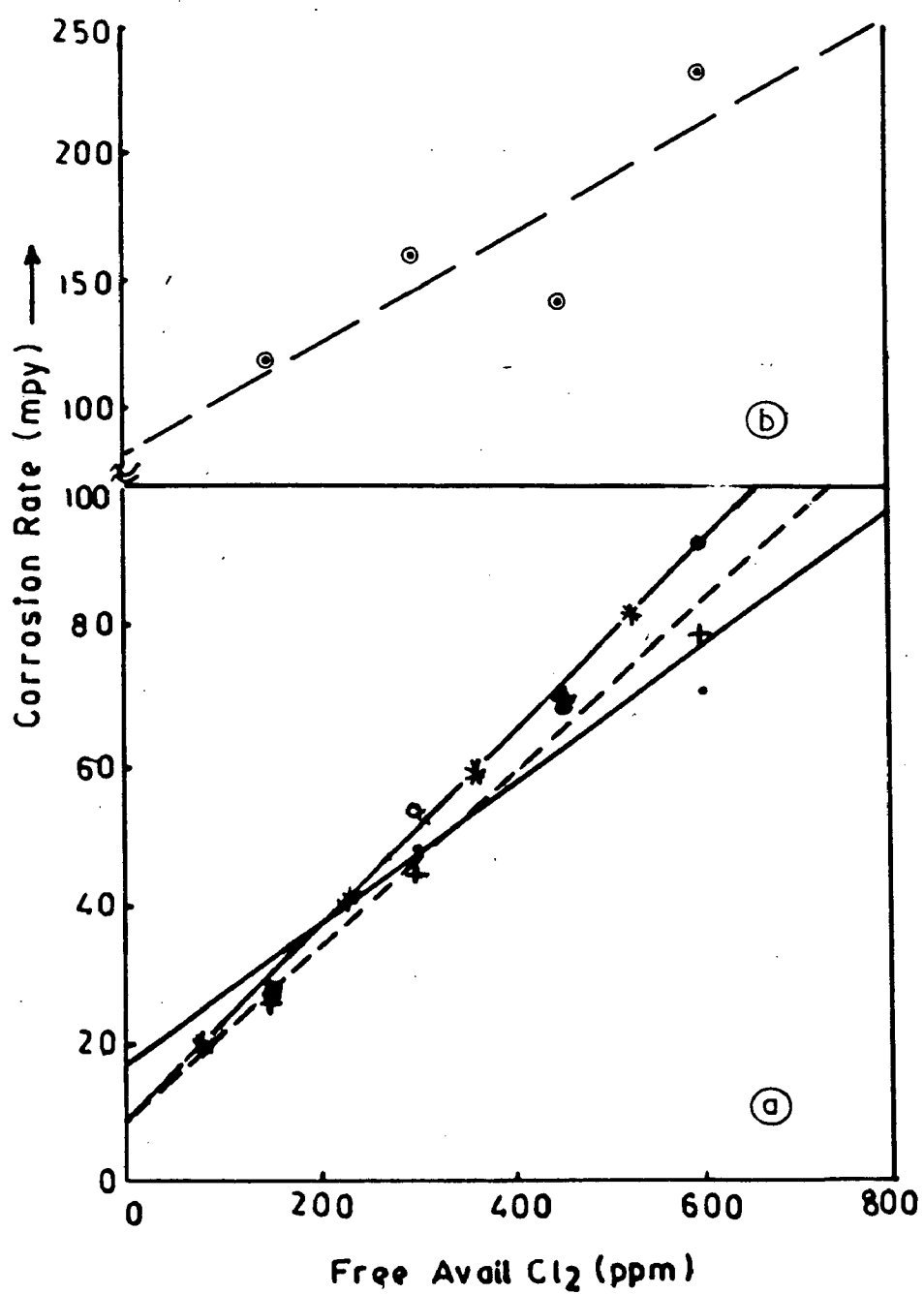
FIG. 4-2: VARIATION IN CORROSION RATE WITH Cl<sup>-</sup> ion CONCENTRATION IN SODIUM CHLORIDE SOLUTION

Hypochlorite solutions were prepared from bleach liquor having concentration of  $\text{OCl}^-$  ions as 150, 300, 450 and 600 ppm. pH of these solutions was maintained at  $\approx 8.5$  and  $\text{Cl}^-$  ion concentrations were fixed at 1000, 2000 and 3000 ppm.  $\text{Cl}^-$  concentration were taken as those which are normally observed in bleach plant washers. Amount of  $\text{Cl}^-$  was fixed to avoid variation in corrosion rate, whatsoever, due to these ions. The results of the weight-loss tests are given in Table 4.4 and shown in Fig.4.3. The corrosion rate is observed to increase with the  $\text{OCl}^-$  ion concentration. This variation is expected as  $\text{OCl}^-$  is an oxidant and hence an increased amount of it will increase the cathodic reaction rate which in turn will affect metal dissolution. It seems, at these low concentrations, change in dissolved oxygen content is not significant as has been observed in the case of high concentration solutions. Here again one does not observe a definite dependence of corrosion rate on amount of  $\text{Cl}^-$ . This is in accordance with the earlier obtained results (154).

Weight-loss tests were also performed on stainless-steels of the similar grades as used in mill tests. These steels were kept dipped in hypochlorite solutions, of same concentration as used in the case of mild steel, for 1 month. Corrosion rates measured after this duration were observed to be very low ( $\approx 10^{-1}$  mpy). These rates are of the same order as the error of the measurements. Hence, no clear trend is observed with regard to variation of corrosion rate with FA chlorine concentration for different steels.

**Table 4.4 : Corrosion rate of mild steel in Bleach liquor**

Free Available Chlorine (ppm)	Cl <sup>-</sup> ion concentration (ppm)		
	1000	2000	3000
	Corrosion Rate (mpy)		
150	28.0	25.5	27.4
300	47.2	44.3	52.4
450	70.2	70.2	68.6
600	70.1	78.5	91.0



○ — — — 1000 ppm Cl<sup>-</sup>                      Polarisation Data  
 • — — — 1000 ppm Cl<sup>-</sup> , + — — — — 2000 ppm Cl<sup>-</sup> } Weight-loss Data  
 ● — — — 3000 ppm Cl<sup>-</sup>

FIG. 4.3: VARIATION OF CORROSION RATE WITH FREE AVAILABLE CHLORINE IN BLEACH LIQUOR (a) WEIGHT-LOSS METHOD (b) POLARIZATION METHOD.

#### 4.1.3 Effect of Sulfamic Acid:

As indicated earlier, one of the mills (mill B) is adding sulfamic acid ( $\text{HSO}_3\text{NH}_2$ ) in one of the hypochlorite stages (H1 stage). The coupons exposed in the vat of this stage are observed to show less corrosion rates in comparison to those in the other hypochlorite stage (H2) in which sulfamic acid is not added. To assess the effect of sulfamic acid addition on corrosion behavior, tests were also performed on the hypochlorite solutions (low concentration) with addition of varying concentration of sulfamic acid. The addition of sulfamic acid was limited to 10 to 30 ppm, a range practically used in mills. The test solution, hypochlorite solution, had 300 and 600 ppm free available chlorine at two constant concentrations (1000 ppm and 3000 ppm) of chloride. Results of these tests are given in Table 4.5 and shown in Fig.4.4. These results indicate, in general, that the corrosion rate shows the trend of decreasing with addition of sulfamic acid at a given concentrations of free available chlorine and chloride ion. However, if one compares the corrosion rate in bleach liquor in presence of sulfamic acid (Table 4.5) with those without this acid (Table 4.4), in the corresponding concentration, it is observed that in some cases rates decrease while in others rates increase. This trend perhaps can be further checked if the added concentrations of sulfamic acid are increased to higher amount. The decrease is expected to be due to the reaction of sulfamic acid with the hypochlorite to form less active N-chloro-sulfamates (113,118). It was also observed that the nature of corrosion products changed when coupons were immersed in hypo-

**Table 4.5 : Corrosion Rate of mild steel in bleach liquor with addition of sulfamic acid**

Sulfamic Acid (ppm)	Free Available Chlorine (ppm)			
	300		600	
	Chloride Ion (ppm)		Chloride Ion (ppm)	
	1000	3000	1000	3000
10	50.5	50.9	104.4	106.6
20	45.0	48.2	94.5	98.6
30	45.9	47.3	88.6	94.8

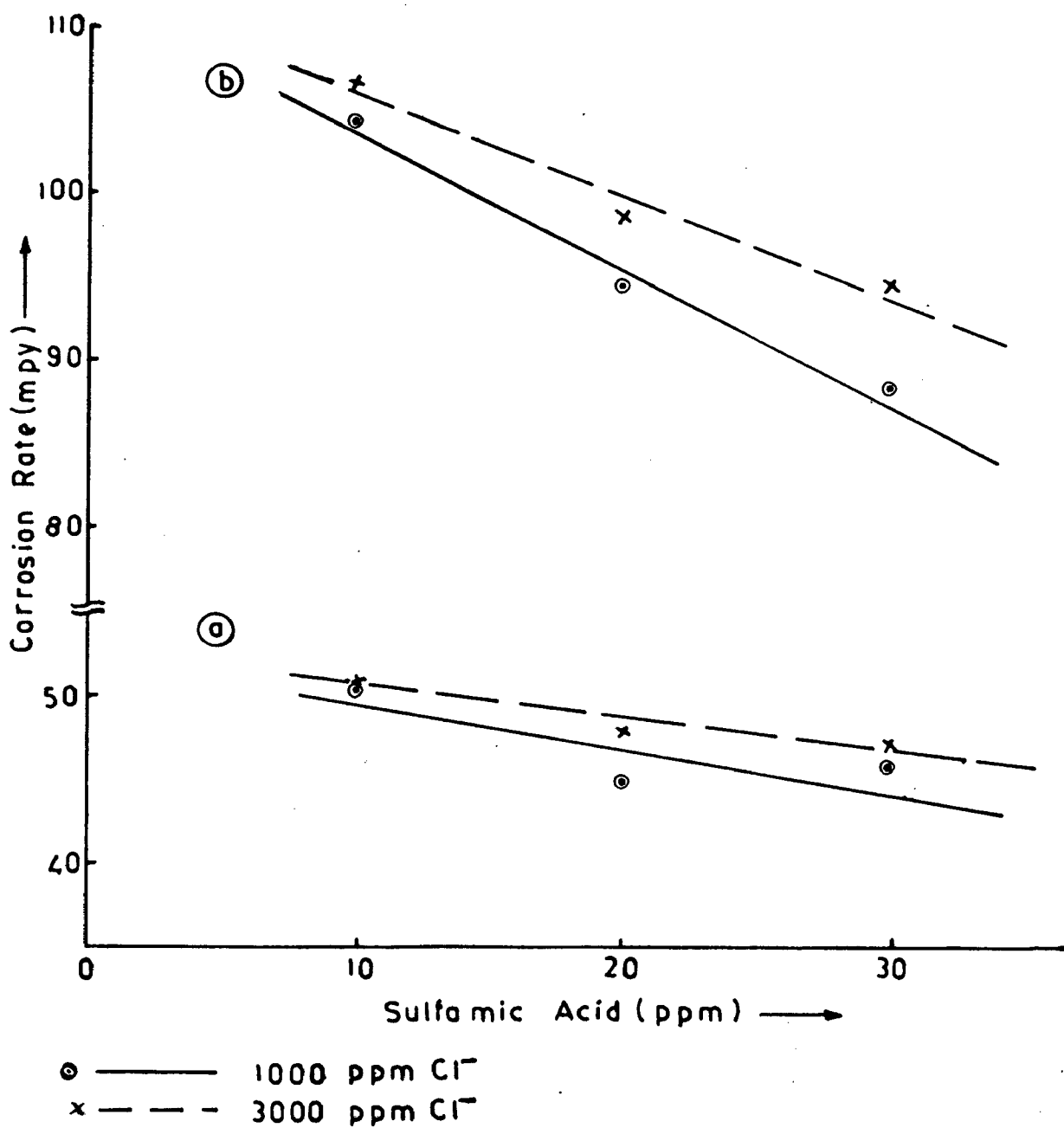


**FIG. 4.4: EFFECT OF SULFAMIC ACID ADDITION IN BLEACH LIQUOR HAVING (a) 300 ppm (b) 600 ppm FREE AVAILABLE CHLORINE.**



chlorite solutions having sulfamic acid. In these cases the color of products was black, characteristic of  $Fe_3-xO_4$ , whereas in the solutions without sulfamic acid the color was reddish brown, characteristic of  $FeOOH$  or  $Fe_2O_3$ . The former is protective in nature.

#### 4.2 Electrochemical Polarization Tests:

Adopting suitable corrosion protection measures requires better understanding of corrosion phenomenon vis-a-vis the given material-environment system. It is therefore desirable to understand the corrosion mechanism in the metal-environment systems in the tests, described in earlier section. Also due to higher corrosivity of media faced by steel equipments in bleach section, electrochemical corrosion control is emerging as a useful and economically viable alternative for protecting the equipments like washers (11,19,21,25,109). Both the above factors require electrochemical studies to be performed on steels, of the type as are normally used for making process equipment of bleach section of a paper mill, in the media as are normally observed in this section. It was with this intention that weight-loss tests, described in preceding section, were conducted. Electrochemical tests of steels in hypochlorite solutions become all the more necessary in view of the fact that literature on these solutions is scanty (152,153). As such electrochemical tests were performed on commercial grade mild steel and austenitic stainless-steels in hypochlorite solutions of varying concentration. These tests were also conducted in presence of sulfamic acid in bleach liquor. Some of the results were correlated with the weight-loss

measurements described in earlier section. These tests and results are described for mild steel and stainless-steels separately.

#### 4.2.1 Tests on Mild Steel

Electrochemical polarization tests were conducted on mild steel in (i) sodium chloride solution having 1000 ppm  $\text{Cl}^-$  concentration and (ii) calcium hypochlorite solutions with FA chlorine (mainly  $\text{OCl}^-$  ion) concentration maintained at 150, 300, 450 and 600 ppm at constant chloride concentration of 1000 ppm. pH of both type of solutions was kept around 8 to 9. These are the similar type of solutions as were used in weight-loss measurements. The electrochemical polarization measurements included cathodic polarization curves and polarization resistance measurements. Tafel plots could not be measured in these cases. The obtained cathodic polarization curves were fitted to get the electrochemical parameters of metal redox system and limiting diffusion current of the cathodic reaction responsible for polarization curves. Corrosion rates were calculated with the help of linear polarization measurements and these were compared with those calculated from the weight-loss measurements.

Corrosion reaction in calcium hypochlorite solution is influenced mainly by pH, free available chlorine and chloride ion concentration. Chloride ion in these solutions are present due to process of hypochlorite preparation. Since pH of these solutions is around neutral or slightly alkaline ( $\text{pH} \approx 8-9$ ), the dominating form of free available chlorine will be hypochlorite ion (114). An attempt, therefore, has been made to understand the

corrosion reaction in terms of hypochlorite and chloride ions. The effect of dissolved oxygen has also been considered in understanding the electrochemical mechanism.

In view of the above, corrosion rates of mild steel were measured in sodium chloride solutions. It was not possible to compare the present results with those cited in literature (27,154) as they correspond to studies performed at higher chloride ion concentration and show a different kind of behavior. The present observations, however, are supported by the fact that oxygen depolarization (cathodic reduction of oxygen) controls the corrosion rate in sodium chloride solution, though presence of chloride ion increases the exchange current density (decrease over voltage) for anodic dissolution of iron (27). Polarization curves drawn for mild steel in 1000 (Fig. 4.5), 3000 ppm chloride ion solutions can be understood by considering cathodic polarization of oxygen to be of concentration type in the measured current ranges ( $\approx 300 \mu\text{A}$ ). In such a situation, the corrosion current for iron dissolution will not vary significantly even if exchange current increases in case when dissolved oxygen is not varying significantly. It will result only in decrease in overvoltage for anodic dissolutions, as observed in present case.

Corrosion rate of mild steel is observed to increase with free available chlorine concentration (Fig.4.3 and Table 4.4.). To understand this behavior and the electrochemical mechanism in the existing metal-environment system, polarization curves of

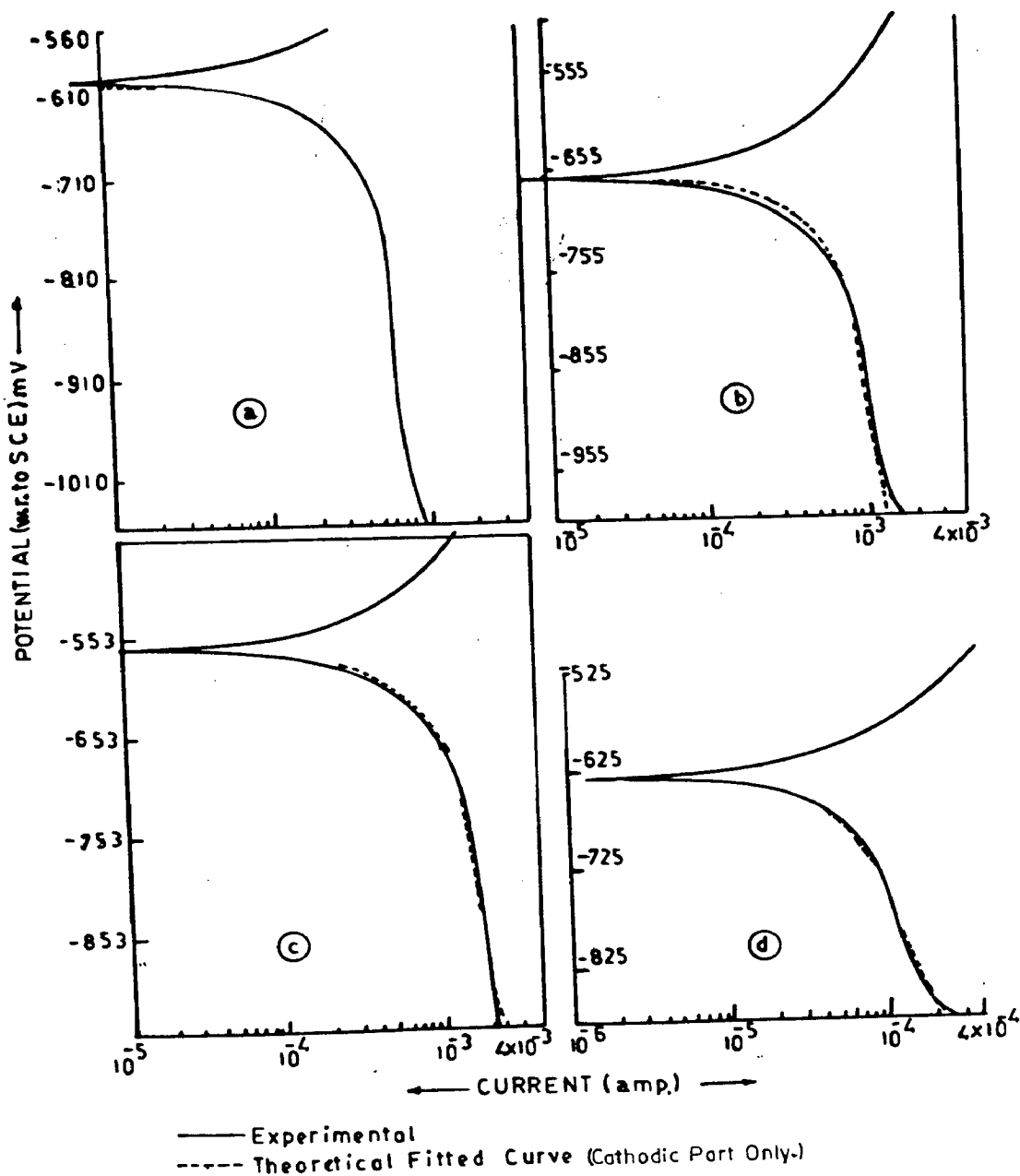
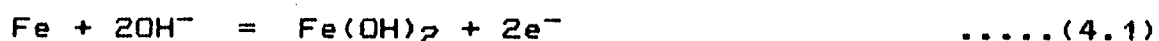


FIG. 4-5: (a), (b) AND (c) POLARIZATION CURVES OF MILD-STEEL IN BLEACH LIQUOR WITH 150 ppm, 300 ppm AND 450 ppm FREE AVAILABLE CHLORINE (d) IN NaCl SOLUTION ( $Cl^- \approx 1000$  ppm).

mild steel were recorded in calcium hypochlorite solutions. To understand the polarization behavior, it was tried to get the estimated value of electrochemical parameters e.g. electrode potential, Tafel slopes, and exchange current from literature, for different redox systems responsible for giving polarization curves. Then it was attempted to 'fit' the experimental curves by initially considering thus obtained parameters and changing them suitably around these values until a reasonable 'fit' was obtained. Once such a 'fit' is obtained, the values of parameters corresponding to the present system can be derived. Thus following redox systems may be considered in the present case:

First is the iron/iron hydroxide system [ Fe/Fe(OH)<sub>2</sub> ] which occurs, in alkaline solutions, with following reaction



This is responsible for anodic polarization part of present curves. In literature, for this system, value of standard reversible potential,  $E^0$ , is - 877 mV (with respect to SHE i.e. saturated hydrogen electrode) (116) and exchange current density,  $I_0$ , can be considered as around  $3 \times 10^{-5}$  amp/cm<sup>2</sup> (155). The variation of equilibrium potential with pH is governed by the following equation, derived on the basis of Nernst equation,

$$E_{\text{Fe/Fe(OH)}_2} = - 0.051 - 0.059 \text{ pH} \quad \text{.....(4.2)}$$

From the above, reversible potential for iron (with respect to SCE i.e. saturated calomel electrode) is expected to lie

between -794 to - 853 mV for present hypochlorite solutions ( pH  $\approx$  8.5 - 9.5 ). An earlier work (156) points that anodic Tafel slope  $\beta_a$ , for this reaction, in alkaline solutions may range between 200 to 320 mV/decade. Hence  $\beta_a$  for Fe/Fe(OH)<sub>2</sub> was considered to be 200 mV/decade.

Cathodic part of the experimentally obtained curves can be considered, in present solutions, due to the two system (i) O<sub>2</sub>/OH<sup>-</sup> (oxygen reduction to hydroxyl ion) (ii) OCl<sup>-</sup>/Cl<sup>-</sup> (hypochlorite reduction to chloride). O<sub>2</sub>/OH<sup>-</sup> system exists due to the presence of dissolved oxygen, in solutions, which reduces as per the following equation



E<sup>0</sup> (standard redox potential) for this system is + 401 mV (w.r. to SHE) and it varies with pH as given below

$$E_{O_2/OH^-} = 1.23 - 0.059 \text{ pH} \quad \dots\dots(4.4)$$

2

Other parameters for this system can be considered, for the purpose of fitting, as I<sub>0</sub>  $\approx$  10<sup>-10</sup> amp/cm<sup>2</sup>,  $\beta_a$  = 40 mV/decade and cathodic Tafel slope  $\beta_c$  = 110 mV/decade (157). Limiting current density, I<sub>L</sub> = 80  $\mu$ A/cm<sup>2</sup> considering (i) concentration of oxygen as saturated value in water at 25°C (ii) oxygen concentration varies only slightly with dissolved salts (28) e.g. chlorides.

Hypochlorite ions present in calcium hypochlorite solution are responsible for OCl<sup>-</sup>/Cl<sup>-</sup> system and they reduce as below



$E^0$  for this system is + 860 mV ( w.r. to SHE) and it varies with pH in the following manner :

$$E_{\text{OCl}^-/\text{Cl}^-} = 1.69 - 0.059 \text{ pH} \quad \text{.....(4.6)}$$

Other parameters for this system may be considered as  $\beta_c = 103$  mV/decade and  $I_0 \approx 10^{-12}$  amp/cm<sup>2</sup> (152,153).  $I_L \approx 10^{-4}$  amp/cm<sup>2</sup> for the concentration of  $\text{OCl}^-$  (153) as observed in present solutions.

The three redox systems, operative in the case of iron in calcium hypochlorite solutions, are shown together in Fig. 4.6, considering the kinetic electrochemical parameters as derived from literature above. The figure indicates that anodic dissolution of iron in present solutions is expected to be governed by the concentration polarization due to the presence of  $\text{OCl}^-$  and  $\text{O}_2$ . While in the case of sodium chloride solutions the same will be governed by the presence of dissolved  $\text{O}_2$  only.

From the estimated values of electrochemical parameters, for the above three redox systems, cathodic part of experimentally measured polarization curves were fitted by putting various values of kinetic electrochemical parameters for corresponding redox systems. To draw theoretical cathodic polarization curves, for the purpose of fitting, current densities were converted into currents since the experimental curves showed potential versus current variation in present case. The polarization curves (except that for mild steel in 600 ppm free available  $\text{Cl}_2$  calcium hypochlorite solution) fit well ( see dotted and continuous lines

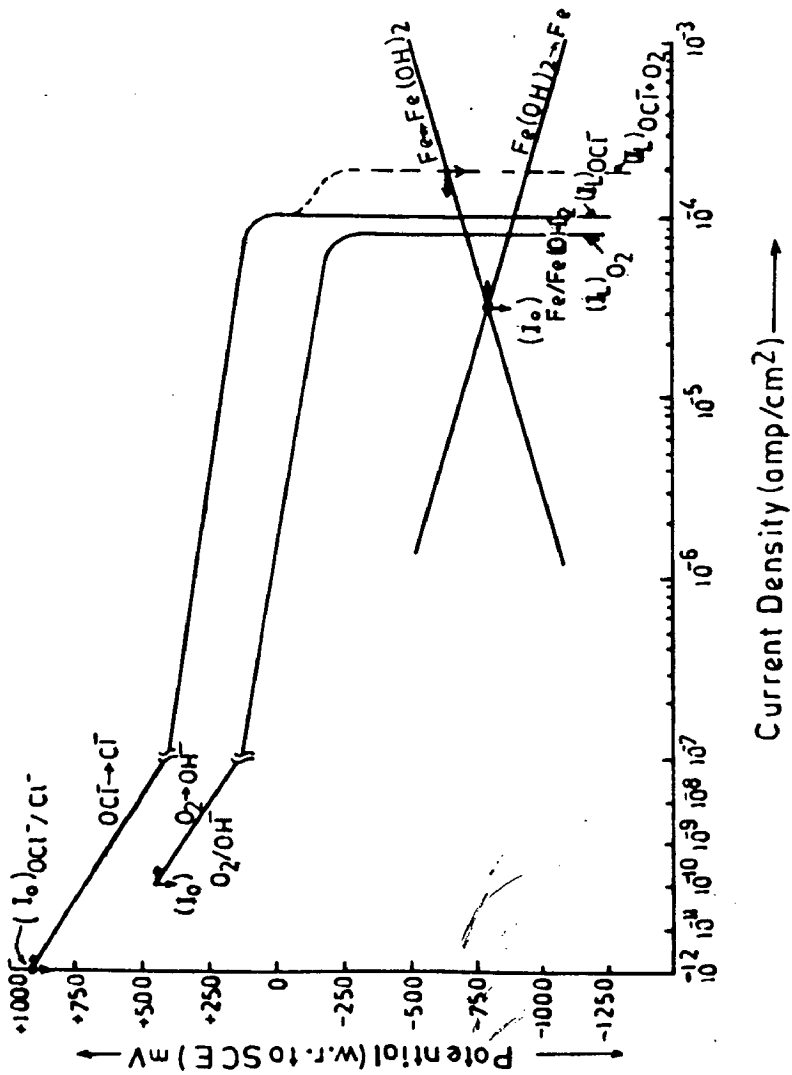


FIG. 4-6: REDOX SYSTEMS OPERATIVE IN CASE OF MILD-STEEL IN BLEACH LIQUOR.



in Fig. 4.7 ) if one considers reversible potential for iron around  $-825$  mV ( with respect to SCE). This value matches satisfactorily with the earlier considered value for this system. Table 4.6 gives the derived parameters, for the different redox systems, with the help of which a reasonable fit with experimental curves is achieved.

For Fe/Fe(OH)<sub>2</sub> system, the exchange current density increases with addition of OCl<sup>-</sup>. The anodic and cathodic Tafel slope values are 200 mV/decade except those for sodium chloride solution. The limiting current density ( due to presence of O<sub>2</sub> and OCl<sup>-</sup>) increases with addition of OCl<sup>-</sup>. Such an observation has been noticed earlier also (152) and is understandable in terms of basic electrochemistry (28). E<sub>corr</sub> (corrosion potential) value derived theoretically, after fitting, matches satisfactorily with those of the experimentally obtained values.

The values of electrochemical parameters (Fig.4.5,Table 4.6) indicates that difference in E<sup>0</sup> and I<sub>0</sub> values of Fe/Fe(OH)<sub>2</sub> and OCl<sup>-</sup>/Cl<sup>-</sup> systems are so large that I<sub>corr</sub> will be observed to be very high ( $10^{-2}$  amp/cm<sup>2</sup>). So the Tafel plot measurements will include high currents and solution has to be stirred to avoid mass transfer effects. It was therefore attempted to measure Tafel plots, for knowing Tafel constants of the present metal-environment system, by stirring the solution. However, stirring of the solution appears to change the metal surface characteristics in these cases so rapidly that no meaningful curve could be drawn. Values of the parameters also indicate that presence of

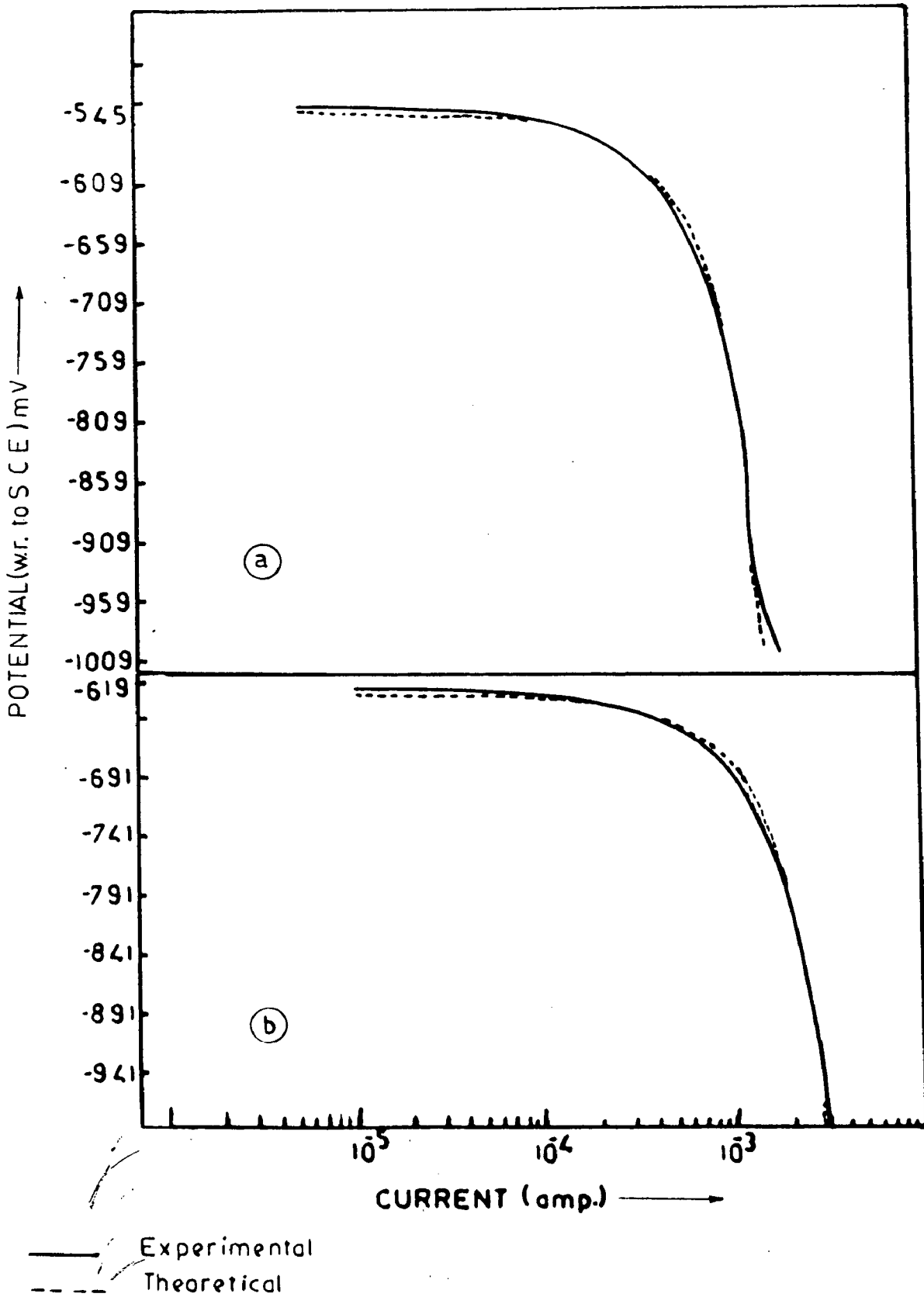


FIG.4.7: POLARIZATION CURVES OF MILD-STEEL IN BLEACH LIQUOR  
(a) 300 ppm (b) 500 ppm FREE AVAILABLE CHLORINE )

**Table 4.6 : Parameters of mild steel .**  
 ( derived after fitting the polarization curves )

Solution	Fe/Fe(OH) <sub>2</sub> redox system				i <sub>L</sub> ( amp. )	E <sub>corr</sub> (mV)	
	E <sup>0</sup> (mv)	i <sub>0</sub> ( amp. )	β <sub>a</sub> (mv/decade)	β <sub>c</sub> (mv/decade)		Theor	Expt
Cl <sup>-</sup> ≈ 1000 ppm							
Sodium Chloride	-773	0.2×10 <sup>-4</sup>	200	127	0.1×10 <sup>-3</sup>	-625	-634
Hypochlorite :							
FA chlorine							
150 ppm	-857	0.7×10 <sup>-4</sup>	200	200	1.2×10 <sup>-3</sup>	-617	-610
300 ppm	-857	0.9×10 <sup>-4</sup>	200	200	1.3×10 <sup>-3</sup>	-627	-667
450 ppm	-835	1.5×10 <sup>-4</sup>	200	200	1.7×10 <sup>-3</sup>	-600	-563

FA chlorine - Free available chlorine

E<sup>0</sup> and E<sub>corr</sub> measured with respect to SCE.

$$i_L = (i_L)_{O_2} + (i_L)_{OC1^-}$$

oxygen, in the tested hypochlorite solutions, is not expected to influence the corrosion reaction significantly. This was checked by recording polarization curve after purging N<sub>2</sub> gas which removes dissolved oxygen from solution. The measurement supports the above view.

Linear polarization measurements were performed to obtain the instantaneous corrosion rates. This was done by calculating the slope of potential E versus current i curves and relating it to corrosion current  $i_{corr}$  by the following equation (158)

$$i_{corr} = \frac{\beta_a \times \beta_c}{2.3 (\beta_a + \beta_c)} \times \frac{\delta i}{\delta E} \quad \dots\dots(4.7)$$

From earlier discussions, it has been seen that corrosion of iron in present solutions is controlled by the concentration polarization. In such cases  $\beta_c \rightarrow \infty$ , hence

$$i_{corr} = \frac{\beta_a}{2.3} \times \frac{\delta i}{\delta E} \quad \dots\dots(4.8)$$

Corrosion current  $i_{corr}$  is thus calculated by knowing  $\delta i/\delta E$  from linear polarization curves and considering  $\beta_a$  for iron in respective hypochlorite solutions. The corrosion rates (Table 4.7) obtained from polarization data are observed to be greater than those derived from weight-loss measurements. This is expected since corrosion rate is maximum in the beginning and it decreases, due to formation of corrosion products, with time to

**Table 4.7 : Corrosion Rate of mild steel calculated from polarization data**

Free Available Chlorine (ppm)	Corrosion Rate (mpy)
150	117.6
300	158.4
450	140.1
600	230.8

reach an equilibrium value. However, both types of corrosion rates are observed to increase with free available chlorine concentration (Fig.4.3). It can be understood in terms of electrochemical mechanism described earlier.

- Effect of Sulfamic Acid:

In view of the lower corrosion rates observed in hypochlorite washer of mill B, with sulfamic acid, weight-loss studies were performed in bleach liquor in presence of low concentrations (as are normally used in mills) of the sulfamic acid to verify its possible inhibiting effect. Results of these tests have already been discussed. To understand the observed behavior i.e. effect of sulfamic acid addition on corrosion behavior of bleach liquor, it was planned to perform the electrochemical tests. These tests were performed on mild steel in calcium hypochlorite solutions after adding sulfamic acid. The solution concentrations were among those as used in weight-loss measurements. Thus calcium hypochlorite solutions having 300, and 600 ppm FA chlorine ( $Cl^- \approx 1000$  ppm,  $pH \approx 8-9$ ) were mixed with 30 ppm sulfamic acid to observe the latter's effect.

In the solutions discussed above, Tafel plots could not be observed even after stirring them. This observation is same as was noticed in solutions without sulfamic acid and could be due to unstable oxide film forming over mild steel sample. The cathodic part of polarization curves was fitted as in the case of curves obtained without addition of sulfamic acid. Same redox systems as are operative in the hypochlorite solutions without

sulfamic acid, were considered for fitting. Although in the present solutions, redox system due to addition of sulfamic acid should also be considered, however, as an approximation the same has not been taken into account considering that the amount of sulfamic acid mixed is very less. Only the effect of addition of sulfamic acid on the electrochemical parameters of the considered redox systems was investigated. The kinetic electrochemical parameters obtained after fitting are given in Table 4.8 and fitted curves are shown in Fig. 4.7. As is clear from figure, the fitting of curves was satisfactory even though no additional redox system was considered. However, the kinetic electrochemical parameters of the considered redox systems gave different values in comparison to the respective values obtained in case of solutions in which sulfamic acid was not added.

Some important inferences can be drawn on the basis of Table 4.8. The corrosion potential and the  $\text{Fe}/\text{Fe}(\text{OH})_2$  redox potential both become more negative with increase in concentration of free available chlorine. A comparison of present results and those of the earlier case (when sulfamic acid was not mixed) indicates that  $E^0$  for  $\text{Fe}/\text{Fe}(\text{OH})_2$  becomes more negative (more active) and  $E_{\text{corr}}$  values become less negative upon addition of sulfamic acid (Table 4.6 and 4.8). The values of  $i_0$  in the both case (with and without addition of sulfamic acid) are not differing much (Table 4.6 and 4.8). Another important difference observed between the two cases is that the value of Tafel slopes for  $\text{Fe}/\text{Fe}(\text{OH})_2$  system increase significantly with addition of sulfamic acid.

**Table 4.8 : Parameters of mild steel - bleach liquor system in presence of Sulfamic Acid.**

( derived after fitting the polarization curves )

Solution	Fe/Fe(OH) <sub>2</sub> redox system				i <sub>L</sub> (amp)	E <sub>corr</sub> (mV)	
	E° (mV)	i <sub>o</sub> (amp)	β <sub>a</sub> (mV/Decade)	β <sub>c</sub> (mV/Decade)		Theor	Expt
Cl <sup>-</sup> ≈ 1000ppm							
S.A. ≈ 30ppm							
FA Chlorine							
300 ppm	-887	1.1x10 <sup>-4</sup>	320	262	1.2x10 <sup>-3</sup>	-550	-545
600 ppm	-938	2.7x10 <sup>-4</sup>	320	225	2.6x10 <sup>-3</sup>	-623	-619

S.A. - Sulfamic acid.

FA Chlorine - Free available chlorine.

E° and E<sub>corr</sub> measured with respect to SCE.

$$i_L = (i_L)_{O_2} + (i_L)_{OCl^-}$$



The observed differences may be due to the existence of another redox system in addition to those considered for fitting. This extra redox system, not considered presently, may be due to N-chlorosulfamates, which form as a consequence of reaction of hypochlorites with sulfamic acid (113). These sulfamates also have similar type of oxidizing effects as that of the hypochlorite ion but are comparatively lesser active. The differences observed above in the electrochemical parameters help to some extent in explaining the behavior of sulfamic acid as observed in weight-loss studies. Upon addition of sulfamic acid, the shifting of  $E^0$  to more negative values,  $\beta_a$  to higher values [For Fe/Fe(OH)<sub>2</sub> redox system] eventually leads to shifting of  $E_{corr}$ , for present metal-environment system, to less negative values (presuming that parameters of other redox systems are remaining unchanged). This, in turn, shifts  $i_{corr}$  to lesser values (Fig.4.8). In other words it means decrease in corrosion rates upon addition of sulfamic acid. This is what is indicated by results of weight-loss measurements described in an earlier section and give support to the suspicion that sulfamic acid might be acting as inhibitor in hypochlorite solutions.

#### 4.2.2 Tests on Stainless-Steels

With a view to understand the corrosion mechanism undergoing on stainless-steel in hypochlorite solutions (this material-environment system is observed in hypochlorite washers in mills) and also to obtain electrochemical parameters for this system which might help later in developing the electrochemical protection systems for bleach washers, the present tests were conducted.

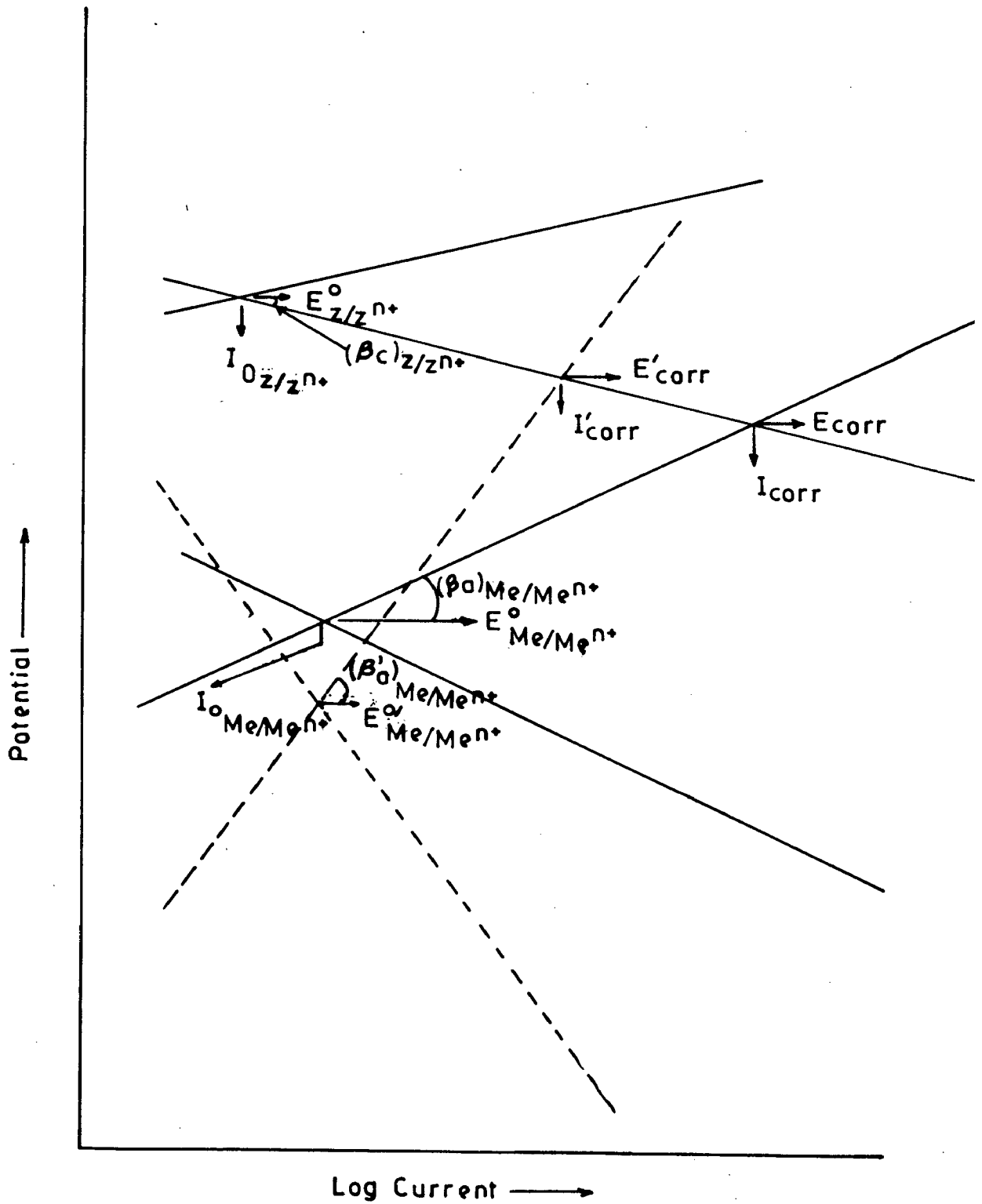
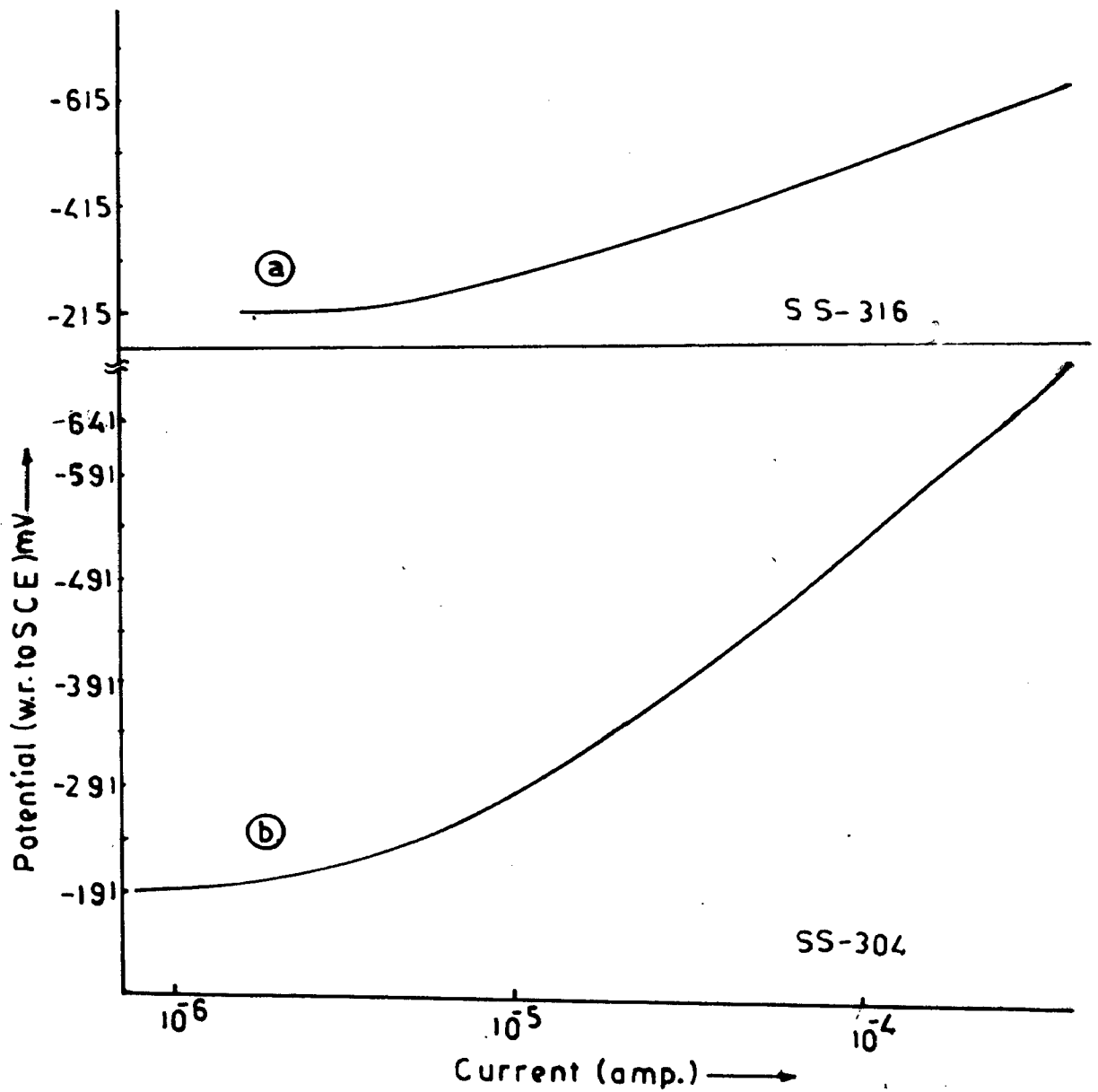


FIG.4.8: EFFECT OF SULFAMIC ACID ADDITION IN BLEACH LIQUOR ON ELECTROCHEMICAL PARAMETERS OF CONCERNED REDOX SYSTEMS.

These electrochemical studies were performed on austenitic stainless-steels, namely SS - 304, 304L, 316 and 316L , in solution of bleach liquor similar to those taken in tests with mild-steel . Tafel curves were plotted for these steels in sodium chloride solution of 1000 ppm chloride ion concentration, in bleach liquor having 150 - 600 ppm free available chlorine and finally in bleach liquor of 300, 600 ppm FA chlorine after adding in it 30 ppm sulfamic acid . The concentration of chloride ion and pH of the solutions were maintained at 1000 ppm and 8 - 9 respectively.

Reasonably acceptable linearity was shown by only cathodic Tafel plots when the solutions were stirred so as to avoid concentration polarization effects. The linearity obtained covers two decades of current range in some cases whereas in others it is slightly less. This is as per the normal practice adopted for acceptable Tafel plots (106). The anodic polarization curve did not give linearity for acceptance as Tafel plot.

Fig.4.9 shows the Tafel plots for stainless-steels in sodium chloride solution. Since anodic part of these plots do not show acceptable linearity , values of only  $\beta_c$  could be calculated from the cathodic Tafel plots. These values are given in Table 4.9.  $\beta_c$  is observed to vary between 115 - 138 mV/decade for the different steels tested here. These are in accordance with the earlier reported results (159) on austenitic stainless-steels in NaCl solution.



**FIG.4.9: CATHODIC POLARIZATION CURVES SHOWING TAFEL REGION IN CASE OF STAINLESS-STEELS IN NaCl SOLUTION (1000 ppm Cl<sup>-</sup>)**

**Table 4.9 : Parameters of Stainless Steel- Cl<sup>-</sup> system**  
 (measured from polarization curves)

Steel	Cl <sup>-</sup> (ppm)	E <sub>corr</sub> (mV)	β <sub>c</sub> (mV/decade)
SS-304	1000	-191	126
SS-304L	1000	-221	125
SS-316	1000	-215	115
SS-316L	1000	-238	138

---

E<sub>corr</sub> measured with respect to SCE.

Fig.4.10 and 4.11 shows the experimental polarization curves for SS-304 and 316 respectively in hypochlorite solutions . The polarization curves show that the corrosion reaction is governed by both activation and concentration polarization. Table 4.10 gives the values of  $\beta_c$ , cathodic Tafel slope, measured from the linear part ( Tafel region ) of the curves, and  $E_{corr}$  for the different metal-environment systems. Thus obtained Tafel slopes (cathodic), in these cases, lie between 100 and 120 mV/decade which is in accordance with the earlier observations (152,153). These values of cathodic Tafel slopes,  $\beta_c$ , are higher in sodium chloride solution (115 - 138 mV/decade) than hypochlorite solutions. A metal- environment system having higher Tafel slope will require higher polarization potential to experience same amount of oxidation/reduction current . In other words this might indicate a system which is less susceptible to corrosion than the one having less Tafel slope. From this point of view stainless-steel in NaCl solution is likely to experience lesser corrosion than that in hypochlorite solutions. This outcome is supported by the weight-loss measurements done with mild steel which indicate hypochlorite solutions to be more corrosive than sodium chloride solution.

The cathodic part of the polarization curves were fitted for obtaining electrochemical parameters of metal/metal ion ( $Me/Me^{n+}$ ) and other redox systems, in case of NaCl solution and hypochlorite solutions. Since linearity of Tafel region (obtained from cathodic linear part of experimental curves) is more for SS-304 and 316 than their low carbon counterparts ( 304L and 316L),

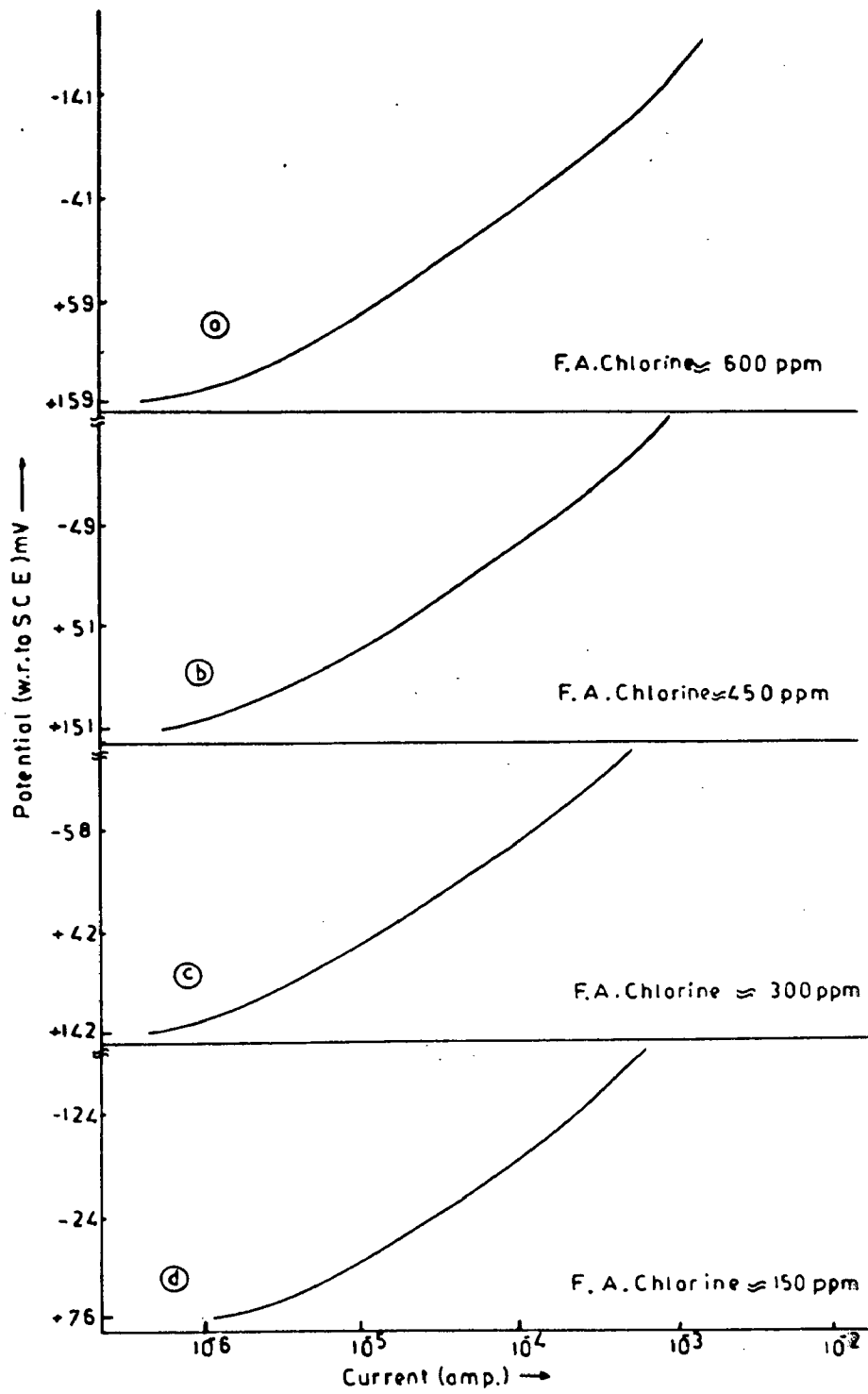


FIG.4.10: CATHODIC POLARIZATION CURVES SHOWING TAFEL REGION IN CASE OF SS-304 IN BLEACH LIQUOR

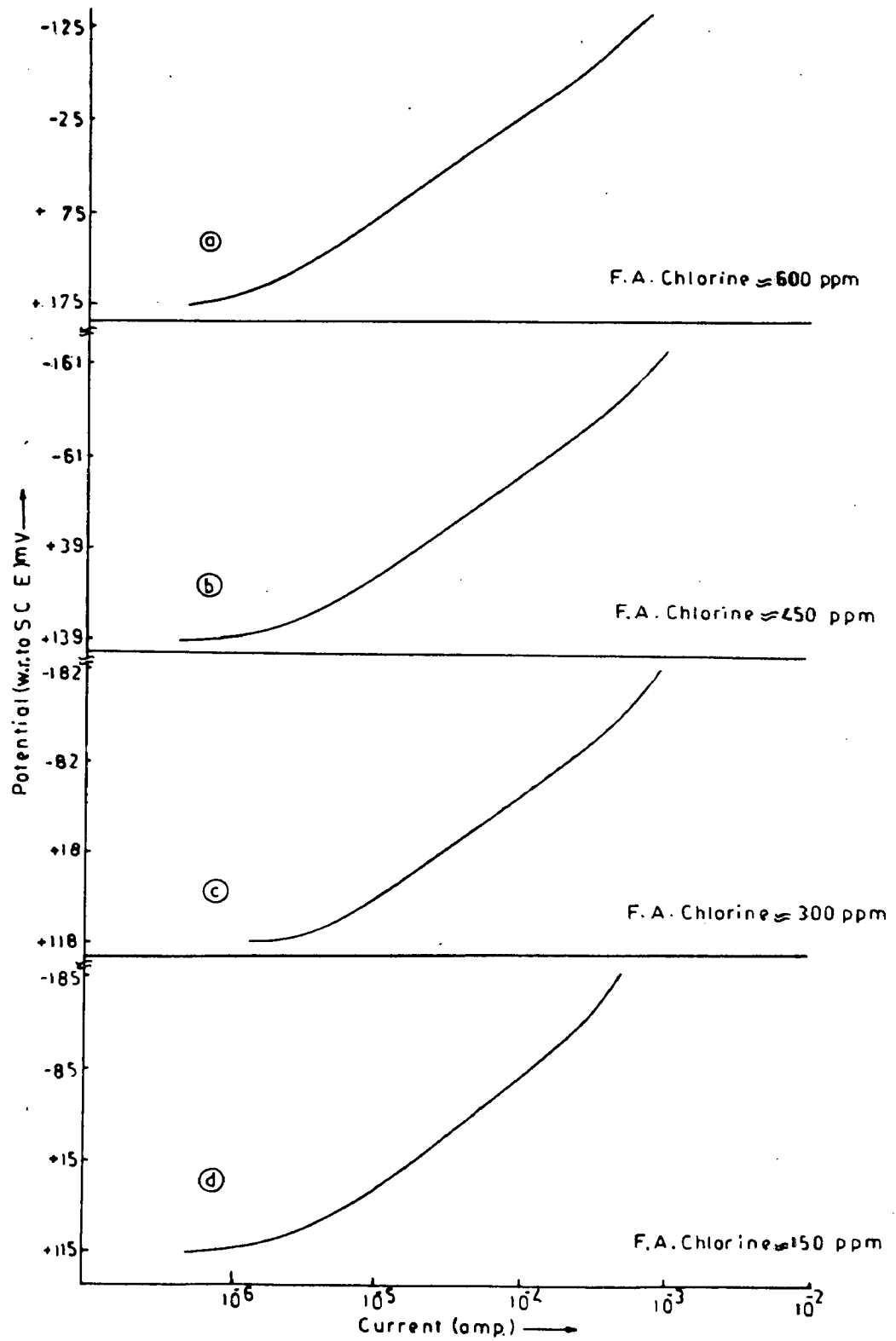


FIG. 4.11: CATHODIC POLARIZATION CURVES SHOWING TAFEL REGION IN CASE OF SS-316 IN BLEACH LIQUOR.



**Table 4.10 : Parameters of stainless steel-bleach liquor system**  
 ( measured from polarization curves )

Steel	F. A. Chlorine (ppm) (Cl <sup>-</sup> ≈ 1000 ppm)	E <sub>corr</sub> (mV)	I <sub>corr</sub> (μA/cm <sup>2</sup> )	β <sub>c</sub> (mV/decade)
SS-304	150	+76	0.53	108
	300	+142	0.23	108
	450	+151	0.26	108
	600	+159	0.27	110
SS304L	150	+100	0.27	100
	300	+91	0.51	103
	450	+98	0.72	108
	600	+123	0.36	100
SS-316	150	+115	0.34	120
	300	+118	0.50	118
	450	+139	0.37	118
	600	+175	0.16	109
SS-316L	150	+86	0.53	100
	300	+99	0.71	107
	450	+102	0.89	114
	600	+110	0.84	106

F.A.Chlorine - Free available chlorine  
 E<sub>corr</sub> measured with respect to SCE.

curves of 304 and 316 only were fitted. The redox systems responsible for cathodic part of the curves, in these cases, are same as those considered for polarization curves of mild steel. This is due to the same constituents of the electrolytes. However, in these cases  $Me/Me^{n+}$  redox system(s) has/have to be more than one because of different metal constituents in stainless steels. Accordingly one should consider  $Me/Me^{n+}$  redox systems for Fe, Ni and Cr, the main constituents of austenitic stainless-steels. Therefore, one needs to know the electrochemical kinetic parameters for these systems in similar solutions as the present ones. It was possible to get these parameters only for Fe. Also amount of Fe is much more in stainless-steels than Cr and Ni and hence is expected to be most influential in defining the polarization characteristics of steels. Therefore, for presently fitting of the experimental curves, parameters for  $Fe/Fe^{2+}$  redox system have been considered as starting parameters. Later on these have been modified so as to have the best possible 'fit' with the experimental curves. Because of the above strategy adopted for fitting the curves, the same was not as good as it was obtained for the case of mild steel. This is expected as the amount of iron in mild steel is more than 99%. Electrochemical parameters obtained as a consequence of fitting are given in Table 4.11.

The corrosion potential  $E_{corr}$  and  $(E^0)_{Me/Me^{n+}}$  (Table 4.9, 4.10, and 4.11) is significantly noble in case of hypochlorite containing solutions than in sodium chloride solution. This may be due to the presence of oxidants ( $OCl^-$  ions) in hypochlorite solutions, whose  $(OCl^-/Cl^-)$  redox potential is significantly more

**Table 4.11 : Parameters of stainless steel-bleach liquor system**  
(derived after fitting the polarization curves)

Steel	Solution	Me / Me <sup>n+</sup> redox system				E <sub>corr</sub> (mV)	
		E <sup>0</sup> (mV)	i <sub>0</sub> (amp)	β <sub>a</sub> (mV/decade)	β <sub>c</sub> (mV/decade)	Theor	Expt

Hypochlorite:

FA chlorine

SS-304	300 ppm	+117	7.3x10 <sup>-7</sup>	250	250	+155	+155
	450 ppm	+ 86	9.1x10 <sup>-7</sup>	250	250	+151	+151
	600 ppm	+ 44	1.1x10 <sup>-6</sup>	250	250	+134	+134
	Sodium chloride	-209	2.7x10 <sup>-6</sup>	300	300	-187	-187

Hypochlorite:

FA chlorine

SS-316	150 ppm	+ 26	1.1x10 <sup>-6</sup>	250	250	+115	+115
	300 ppm	+ 67	1.7x10 <sup>-6</sup>	250	250	+118	+118
	450 ppm	+ 62	9.8x10 <sup>-6</sup>	250	250	+137	+137
	600 ppm	+109	6.6x10 <sup>-7</sup>	250	250	+175	+175

E<sup>0</sup> and E<sub>corr</sub> measured with respect to SCE.

noble than that of  $O_2/OH^-$ . The later redox system is the only system present in case of sodium chloride solutions as the cathodic reactant. Stainless-steels, in general, have higher (theoretically derived)  $\beta_a$  and  $\beta_c$  values (250 mV/decade) for  $Me/Me^{n+}$  redox system in comparison to those of mild steel (200 mV/decade, see Table 4.6).

From Table 4.10 and Fig. 4.12, it is clear that corrosion potential,  $E_{corr}$ , for all materials become more and more noble with an increase in concentration of free available chlorine in hypochlorite solution. The shift in  $E_{corr}$  value is expected to be due to the formation of passive oxide film on metal surface (in case of SS), the passive state of any metal has more noble potential than that of metal in non-passive state. If we presume that kinetic electrochemical parameters ( $E^0$ ,  $I_0$  and Tafel slopes) for reducing species ( $O_2$  and  $OCl^-$  in present solutions) do not change, the shift in  $E_{corr}$  values can be attributed to decrease in  $I_0$  and/or  $E^0$  becoming more noble of  $Me/Me^{n+}$  redox system. However, the value of these parameters, obtained after fitting the curves (Table 4.11), do not indicate this pattern. This shows that the parameters for reducing species are also changing with the composition of the solutions. The corrosion current density  $I_{corr}$  obtained by extrapolating the Tafel line upto  $E_{corr}$ , does not show any specific trend with the solution composition. The  $I_{corr}$  obtained for stainless-steels are of very low order ( $\approx 10^{-6}$  amp) than those obtained for mild steel ( $\approx 10^{-3}$  amp).

We now give discussion about the parameters derived after fitting the polarization curves. The value of Tafel slope for

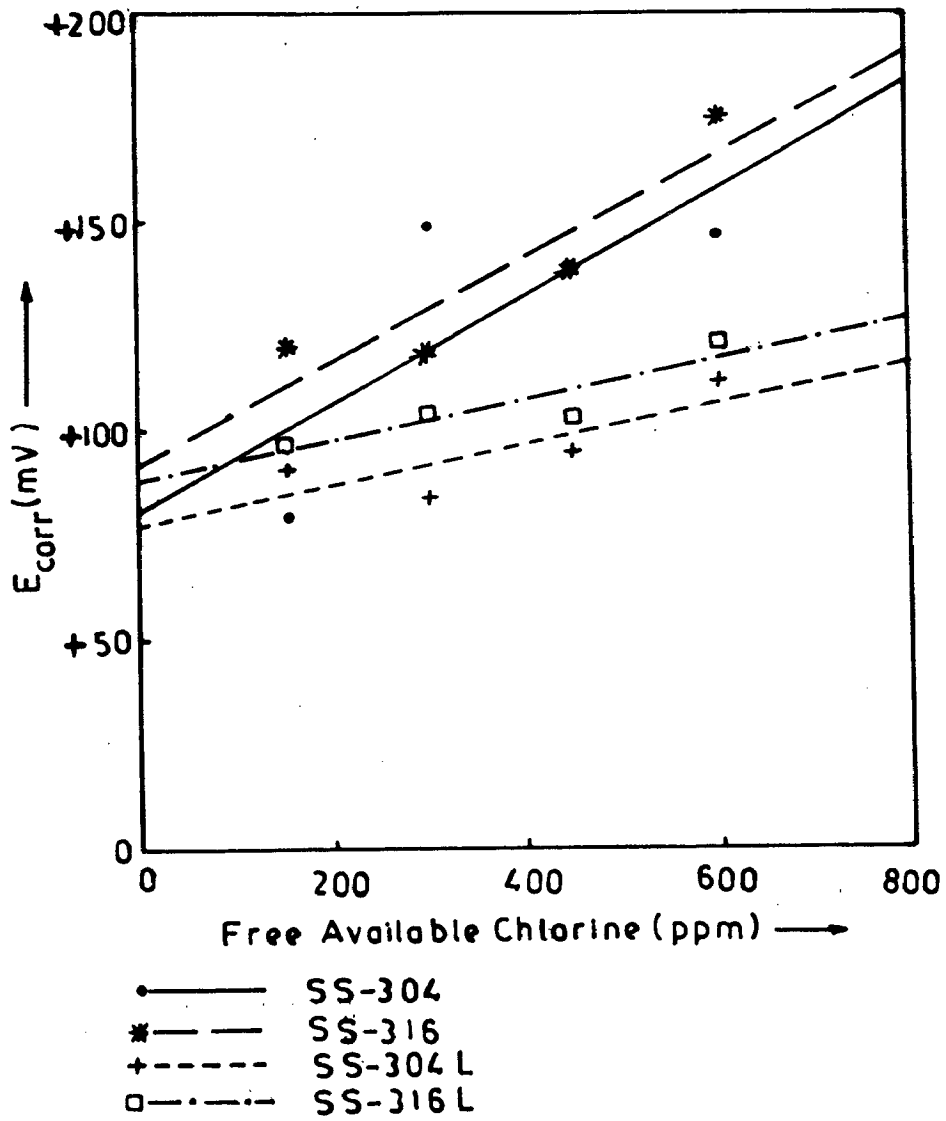


**FIG.4.12: VARIATION OF  $E_{corr}$  OF STAINLESS-STEELS WITH F.A.CHLORINE IN BLEACH LIQUOR**

Me/Me<sup>n+</sup> redox system ( $\beta_a$  and  $\beta_c$ ) in sodium chloride solution is more (300 mV/decade) than those obtained in hypochlorite solutions (250 mV/decade). This could be due to difference in characteristics of stainless-steels in oxidizing (hypochlorite) and non-oxidizing (NaCl) solutions. An attempt has been made to assess the value of exchange current density for hypochlorite redox system,  $(I_0)_{\text{OCl}^-/\text{Cl}^-}$ , by extrapolating the Tafel slope upto approximate  $(E^0)_{\text{OCl}^-/\text{Cl}^-}$  value, for SS-304 and 316 in these solutions. The observed values of  $(I_0)_{\text{OCl}^-/\text{Cl}^-}$  for SS-304 are the order of  $10^{-15}$  amp/cm<sup>2</sup> and those for SS-316 of the order of  $10^{-14}$  amp/cm<sup>2</sup>, these values are lower by two orders of magnitude than those reported earlier (152,153). Lower values of the exchange current densities in present cases may be due to comparatively lower concentration of active species and lower pH in the present solutions (152,153).

#### - Effect of Sulfamic Acid:

Sulfamic acid was added to a tune of 30 ppm in solution of 300 ppm and 600 ppm free available chlorine bleach liquor. Cathodic Tafel slopes measured from the linear portion (Tafel region) of polarization curves (Fig.4.13 and Table 4.12) lie between 109 to 120 mV/decade, almost similar range as one observes in case of bleach liquors without adding sulfamic acid. The variation of Tafel slope was also not expected to be very high since these slopes do not vary unless a significant change is made in metal-solution system. The value of corrosion potential,  $E_{\text{corr}}$ , is generally changing to more positive values

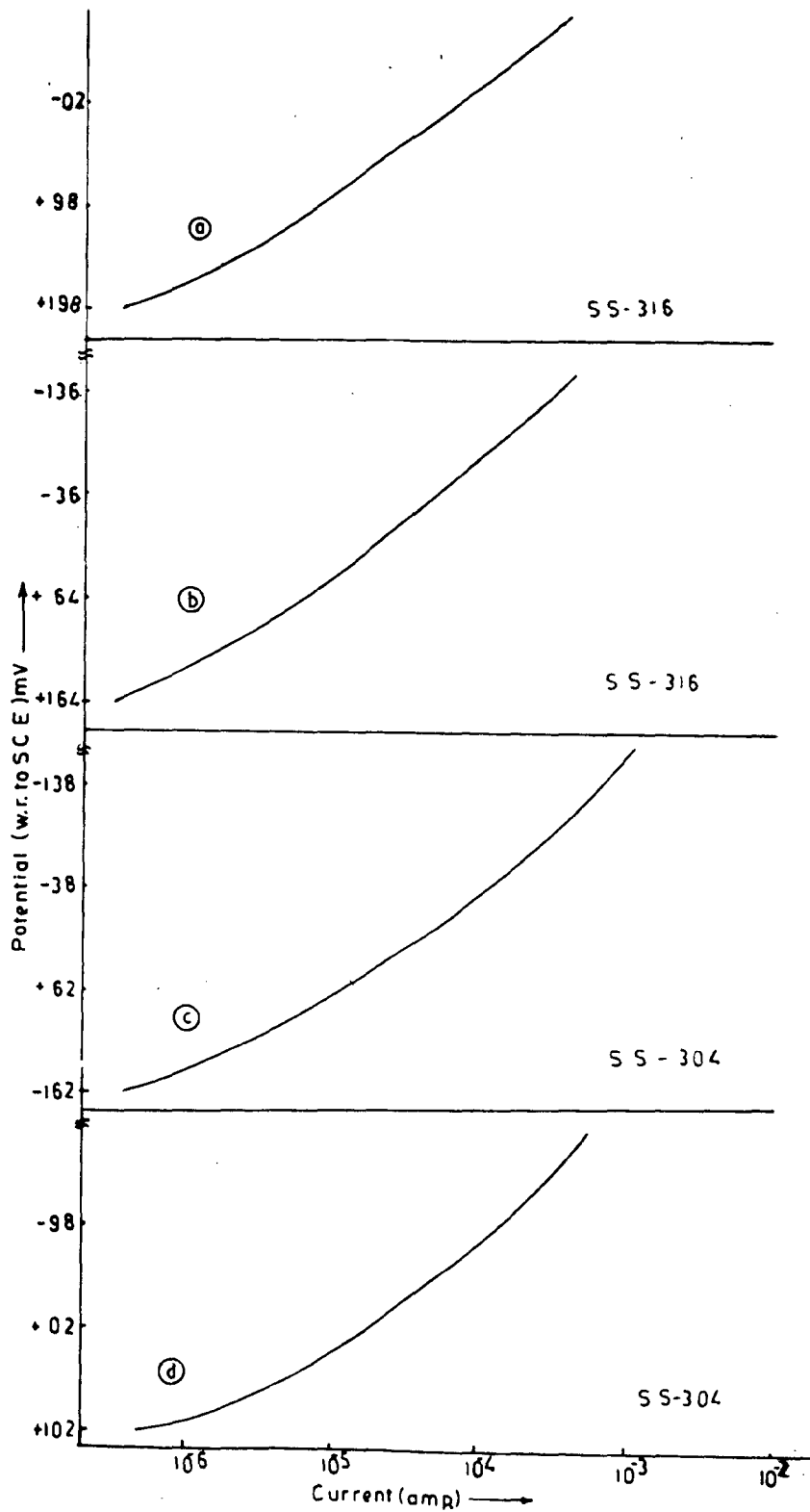


FIG.4.13: CATHODIC POLARIZATION CURVES SHOWING TAFEL REGION IN CASE OF STAINLESS-STEELS IN BLEACH LIQUOR ( (a) AND (c) 600 ppm; (b) AND (d) 300 ppm F.A. CHLORINE ) HAVING 30 ppm SULFAMIC ACID.

**Table 4.12: Parameters of stainless steel-bleach liquor system  
in presence of Sulfamic Acid.**  
(measured from polarization curves)

Steel	Solution Cl <sup>-</sup> ≈ 1000 ppm S.A. ≈ 30 ppm	E <sub>corr</sub> (mV)	I <sub>corr</sub> (μA/cm <sup>2</sup> )	β <sub>c</sub> (mV/decade)
F.A.Chlorine				
SS-304	300 ppm	+102	0.37	114
	600 ppm	+162	0.24	107
SS-304L	300 ppm	+94	0.35	109
	600 ppm	+128	0.37	101
SS-316	300 ppm	+164	0.11	118
	600 ppm	+198	0.13	112
SS-316L	300 ppm	+108	0.38	115
	600 ppm	+122	0.68	116

S.A.-Sulfamic acid  
F.A.Chlorine-Free available chlorine  
E<sub>corr</sub> measured with respect to SCE.



(noble) on addition of sulfamic acid in 600 ppm FA chlorine hypochlorite solution, whereas the reverse is observed in case of 300 ppm FA chlorine hypochlorite solution (Table 4.12). For most of the cases, the corrosion current density,  $I_{corr}$  is observed to decrease on addition of sulfamic acid. It appears as if sulfamic acid is acting as inhibitor in hypochlorite solutions for the tested steels, an observation in agreement with the weight-loss studies done on mild steel in hypochlorite solutions to see the effect of sulfamic acid. As the inhibition effect very much depends upon the solution composition, it remains to be explored the detailed conditions under which sulfamic acid will act as inhibitor in bleach liquors. It is, therefore, desirable to perform tests in bleach liquors in presence of this acid in other higher concentration ranges and also under the limitation of process conditions and chemical cost.

## Chapter - 5

### CONCLUSIONS AND RECOMMENDATIONS

	Page No.
5.1 Conclusions based on Mill Tests.	198
5.1.1 Corrosivity of Environment.	198
5.1.2 Performance of Materials.	200
5.1.3 Corrosion Products.	201
5.2 Conclusions based on Laboratory Tests.	203
5.2.1 Weight-loss Studies.	203
5.2.2 Electrochemical Studies.	204
5.3 Suggestions for Future Work.	206

Preceding two chapters deal with the corrosion tests performed on steels in mill as well as in laboratory conditions. The studies at paper mills were performed to assess the aggressiveness of various stages/phases and the performance of steels in these stages/phases of bleaching section. These in turn have been correlated with the process conditions prevailing in the concerned stages/phases. In some of the studied environments, the tested materials have shown satisfactory performance while in some of the cases none of the tested materials has been found suitable. The aggressivity is such that at some places use of even SS-316L is not advisable whereas at other places these, together with SS-304L, can be used by controlling carefully the process conditions, as is apparent when the results of the two mills are compared. Use of mild steel is almost ruled out as a fabrication material for these stages. This is basically due to the observation that steels have experienced significant crevice corrosion and pitting in the studied environments. The steels are observed to show crevice corrosion attack more frequently than pitting, in accordance with earlier studies on corrosion in bleach section. The aggressivity differs significantly in the two mills and the difference can be understood in terms of varying process conditions. Conditions in Indian Paper Mills appear less severe than those of American and Scandinavian mills because the former mills are not recycling the filtrates while latter follow this practice. The analysis of rusts with the help of X-ray diffraction and Mössbauer spectroscopy was done to have an idea of nature of corrosion products formed in mill conditions and to correlate them with process conditions. The analyses have

indicated that nature of corrosion product/scale is different in case of rusts formed in (i) the different stages of a mill, (ii) two mills obviously due to different process conditions. The laboratory weight-loss studies, done on steels in bleach liquor, indicated the dependence of corrosion rate on concentration of hypochlorite ions while it was found independent of chloride in the studied concentration ranges. Sulfamic acid, used in one of the studied mills as buffer and for increasing the viscosity of pulp, was also found, in mill and laboratory studies, to affect the corrosion reaction. The electrochemical tests e.g. Tafel plot, polarization measurements etc. were undertaken to understand the mechanism of corrosion reactions undergoing in the present metal-environment system, to understand the dependence of corrosion rate on solution composition and to derive the electrochemical parameters related with the studied system. In the following paragraphs, conclusions drawn on the basis of performed studies are given. Further an account of the work, which should be done as an extension of the presently reported investigations, is also given.

## 5.1 Conclusions based on Mill Tests:

### 5.1.1 Corrosivity of Environment:

(a) Among the different phases in washers, degree of corrosivity can be put in following order.

Gas phase > Liquid phase > wet/dry cyclic phase

Maximum corrosivity of gaseous phase may be assigned to the

condensation of moist chlorine (having very low pH) and higher concentration of chlorine and oxygen in comparison to that in vat.

However, some variations from the above observation are noticed.

(i) In case of mild steel, much higher corrosion rates are observed for coupons exposed in chlorination vat (liquid) than those exposed near shower pipe (gaseous). This is attributed to the fact that iron products dissolve in low pH solutions. However, reverse is observed in case of coupons exposed in buffered-hypo (B) and hypochlorite (H) washers. (ii) hypo-washers of mill B, where degree of crevice corrosion/ general corrosion is more in wet/Dry phase in H1 and in liquid phase in H2. To a large extent, this observation appears due to addition of sulfamic acid in H1 washer which affects corrosivity of its liquid phase. Further there is also possibility of coupons experiencing erosion corrosion when exposed to wet/dry environment.

(b) Degree of aggressiveness, among the various stages of washer, can be put in following order:

Chlorination > Hypochlorite

This may be assigned to acidic pH and molecular form of chlorine in liquid phase of chlorination washer.

Exceptions are Hypochlorite stages of mill B which are more corrosive when one compares general and crevice corrosion for coupons exposed to liquid and wet/dry phases.

In case of mill A , Buffered-hypo washer appears slightly more corrosive than hypochlorite washer when one compares the degree of general and localized corrosion. This may be due to ,overall, more corrosive process conditions in the former washer.

(c) Generally speaking bleach section of mill A is more corrosive than that of mill B. This behavior is evident from process liquors conditions which show lower pH, higher temperature, residual chlorine and chloride ion concentration in case of mill A. Higher degree and/or observation of localized attack experienced by coupons in mill A indicates that there is a minimum degree of corrosivity ( depending upon chemical condition of process liquors) which is required for the onset of localized attack. Thus it could be one of the ways to avoid localized attack by keeping degree of corrosivity to below this minimum limit (required for onset of localized attack) by controlling process parameters.

When one compares the corrosivity of the mills under question with those of the mills in North America and Scandinavia, the Indian mills are observed to be having less corrosive bleach section. Higher corrosivity of the western mills is attributed to the practice of greater filtrate recycling for pollution control and energy saving purposes. Filtrate recycling is yet to be adopted in most of the Indian mills.

#### 5.1.2 Performance of Materials:

(a) None of the tested materials is suitable for use in gaseous phase of all the stages of mill A and of chlorination stage of

mill B. In H1 and H2 gaseous phase of mill B , 304L/316L could be suitable choice.

(b) In liquid phase of both the mills, 304/304L appear better choice for hypo-washers. In chlorination washers, all materials are moderately attacked in mill B ,however, 304L/316L may be recommended for mill A. Overall performance of 304L and 316L are comparable in liquid phase.

(c) In wet/dry phase (test in this phase was performed only in mill B), tested materials are expected to fail by crevice attack in H1 washer whereas all except 316 may be recommended for use in H2 washer. This performance of 316 appears to be due to its sample having lesser amount of Cr and Ni than in other steels, used in present tests. Amount of Mo in 316, used in present tests, is also very small ( 0.29% ). Any of the tested materials may be used in chlorination stage.

### 5.1.3 Corrosion Products:

#### (a) Mild Steel

(i) Mild steel exposed to various stages, in mill A and B, showed formation of rust, except the coupon hung in hypochlorite washer vat of mill A, which is covered with scale consisting of calcium carbonate and silicate.

(ii) All rust samples, removed from mild steel coupons, show fine particle size of corrosion products which in turn exhibit super paramagnetic effect in room temperature Mössbauer spectra.

(iii) Rust samples from mild steel exposed to chlorination, gaseous phase, shows  $\text{Fe}_{3-x}\text{O}_4$  and  $\beta\text{-FeOOH}$ . Presence of chloride, lower pH and possibility of aerial oxidation in this stage are the factors responsible for formation of  $\beta\text{-FeOOH}$ .

(iv) Rusts formed in other stages consist of mainly  $\text{Fe}_{3-x}\text{O}_4$  ( $x \approx 0.16-0.06$ ) and  $\alpha\text{-FeOOH}$  while  $\tau\text{-FeOOH}$  is a minor phase.  $\beta\text{-FeOOH}$  is observed in steel exposed in H1 gaseous phase instead of  $\alpha\text{-FeOOH}$ .

(v) In case of rusts from coupons exposed in Mill A,  $\text{Fe}_{3-x}\text{O}_4$  formed in more corrosive environment (chlorination and hypochlorite gaseous phase) is closer to  $\tau\text{-Fe}_2\text{O}_3$ . Its conversion to  $\tau\text{-FeOOH}$  seems more rapid, which in turn transforms to stable phase  $\alpha\text{-FeOOH}$ . Consequently,  $\alpha\text{-FeOOH}/\text{Fe}_{3-x}\text{O}_4$  ratio is observed higher in rusts formed in chlorination and hypowasher gaseous phase in comparison to those formed in less corrosive environment.

#### (b) Stainless-Steels:

(i) In gaseous phase of both mills (except H1 and H2 stages of mill B) the environment is such that the rust deposited is porous, loose and therefore non-protective in nature. It consists of mainly  $\text{Fe}_{3-x}\text{O}_4$  and  $\beta/\tau\text{-FeOOH}$  as rust component.  $\beta\text{-FeOOH}$  is observed due to its preferential formation in low pH and chloride containing solution with aerial oxidation. Mild steel exposed in similar environments shows presence of  $\alpha\text{-FeOOH}$  in its rust. It seems  $\beta\text{-FeOOH}$  forms preferentially either in less corrosive environment or on comparatively passive surfaces.



(ii) In liquid phase of hypochlorite washer of mill A ,the exposed coupons show the deposition of scale which is identified as mainly calcite . This calcite comes from lime which is used to prepare hypochlorite solution. Calcite scale helps in protecting the steel to some extent but may choke pipe line. In liquid phase and wet/dry phase of both hypochlorite washers of mill B, the shining, violet/purple colored adherent film of nickel and chromium oxide is formed. This is protective in nature but dissolves in acidic solution therefore, it was not obtained in chlorination vat. Also it was not obtained in case of mild-steel which does not contain either Ni or Cr.

## 5.2 Conclusions based on Laboratory Tests:

### 5.2.1 Weight Loss Studies:

Following conclusions may be drawn on the basis of weight loss experiments performed on steels in calcium hypochlorite solutions:

- (i) In the higher concentration ranges ( 1 - 25 gpl ), corrosion rate increases , reaching a maximum and then decreases with free available chlorine concentration. This dependence can be explained on the basis of variation in concentration of  $OCl^-$  and dissolved oxygen with change in composition of studied solutions.
- (ii) In the lower concentration ranges (upto 600 ppm) , however, corrosion rate shows continuous increase with free available chlorine . Perhaps in these ranges variation in the amount of dissolved oxygen is not significant. The rates are found to be

independent of chloride ions present in the solution in the studied concentration ranges. Addition of sulfamic acid (10 - 30 ppm) in the bleach liquor shows decrease in corrosion rate with increase in amount of sulfamic acid .

(iii) The corrosion rates of stainless steels, in the low concentration ranges, were too low to show any observable trend with increase in free available chlorine.

#### 5.2.2 Electrochemical Studies:

These tests were conducted to understand the mechanism of corrosion reactions experienced by steels in bleach liquor and other solutions and also to know the electrochemical parameters of the metal-electrolyte systems prevailing in these solutions. Following inferences may be drawn on the basis of these experiments:

##### (a) Mild Steel

(i) The polarization curves in these experiments did not show Tafel region even on stirring the solution. Nitrogen purging through solution, to avoid the effects of dissolved oxygen, did not indicate any observable difference in the curves.

(ii) Polarization curves indicate that reaction can be understood in terms of three redox systems namely  $\text{Fe}/\text{Fe}(\text{OH})_2, \text{O}_2/\text{OH}^-$  and  $\text{OCl}^-/\text{Cl}^-$ . The rate of corrosion is controlled by the concentration polarization of the latter two systems, though the influence of dissolved oxygen is not observed to be significant. In the

case of curves measured in sodium chloride solutions, only first two systems are operative.

(iii) Electrochemical parameters have been derived by fitting the polarization curves. It is observed that exchange current density for  $\text{Fe}/\text{Fe}(\text{OH})_2$  and the limiting current density for  $\text{OCl}^-/\text{Cl}^-$  systems increase with free available chlorine concentration.

(iv) Instantaneous corrosion rates, calculated from linear polarization measurements also increase with free available chlorine. This variation is similar to the one observed in case of the measurement of corrosion rate by weight-loss method.

(v) The electrochemical cathodic polarization curves, obtained after adding sulfamic acid in bleach liquor, can be understood in terms of redox systems as considered with solutions without sulfamic acid. Upon addition of sulfamic acid, for  $\text{Fe}/\text{Fe}(\text{OH})_2$ ,  $E^0$  becomes more active,  $\beta_a$  and  $\beta_c$  increase. This change leads to more noble corrosion potential ( $E_{\text{corr}}$ ), also apparent from curves, provided parameters of other redox systems are not changing significantly. These eventually will shift  $i_{\text{corr}}$  (corrosion rate) to lesser value. This is a conclusion in agreement with results of weight-loss tests.

(b) Stainless-Steels:

(i) The polarization curves of these steels showed Tafel region when measurements were performed by stirring the solution. Best linearity of the Tafel region was obtained in case of curves of SS-304 and 316. Values of cathodic Tafel slope ( $\beta_c$ ) lie between

115 - 138 mV/decade in sodium chloride solutions and between 100 - 120 mV/decade in bleach liquor solutions.

(ii) The curves have been fitted by considering similar redox systems as in case of mild steel. Corrosion potential  $E_{\text{corr}}$  and  $\text{Me}/\text{Me}^{n+}$  redox potential  $(E^0)_{\text{Me}/\text{Me}^{n+}}$  is significantly noble in hypochlorite solutions than sodium chloride solution. This may be due to higher oxidizing power of hypochlorite ions.  $E_{\text{corr}}$  is also observed to become more noble on increasing free available chlorine concentration.  $I_{\text{corr}}$  for stainless steels are of very low order ( $\approx 10^{-6}$  amp) than those for mild steel ( $\approx 10^{-3}$  amp).

### 5.3 Suggestions for Future Work:

The studies discussed in the dissertation give an account of tests performed on commonly used austenitic stainless-steels in mill bleaching conditions and laboratory conditions. However, the results derived from these tests are only of the limited help in selecting the suitable material for different washers, since a large group of potential candidate materials have not been tested in the present investigation. It is important to notice here that both the studied mills do not recycle the filtrate. Further process conditions in mill A are observed to be more aggressive than those in mill B, as is evident from the corrosion tests of the present program. A comparison indicates that process conditions of North American and Scandinavian mills are more aggressive which in turn is due to filtrate recycling. Adoption of filtrate recycling by mill B might enhance the corrosivity to the level of that of mill A or even beyond that, similarly mill A is

also likely to become more corrosive than what it is at present. Increased corrosivity due to filtrate recycling, in western mills, resulted in outdateding of conventionally used materials e.g. SS-316L, 317L and replacing of these materials by stainless-steels having higher amount of Ni, Cr and Mo and by Ni based alloys. Even at the present level of corrosivity in mill A and B, one finds even SS-316L to be unsuitable in some phases. With the adoption of filtrate recycling by these mills, therefore, it is highly likely that SS 304L and 316L become outdated and newer materials may be required for fabricating process machinery. Also the laboratory experiments do not give idea about different type of protection procedures, if and wherever they are applied. As these two are amongst the possible ways to avoid the ill effects of corrosion, further work should be done on the following aspects at mill as well as in the laboratory.

Corrosion tests like the present ones should be conducted to check the performance of the higher grade austenitic stainless steels e.g. SS-317, 317L, 317LM, 904L, Avesta 254SMD etc. and nickel based alloys e.g. Incoloy 825, Inconel 625, Hastelloy-C etc. in the currently prevailing and in environment with filtrate recycling. This will help in analyzing economic feasibility of the possible changes to newer materials of construction specially in more corrosive conditions which result from filtrate recycling. Further, tests should also be done to know the suitable machinery material for bleach plants incorporating future bleaching processes namely chlorine-dioxide, peroxide, ozone etc. Besides these tests, some studies should also be done on lower

grade steels e.g. mild steel SS 304,316 etc. by coating/ lining them by metals of higher grade or non-metals like polymers e.g. PVC,kynar etc. These experiments should help in selecting more economic alternative for minimizing corrosion and to control crevice/pitting which have been encountered in most of the phases. There is also need of conducting the tests in bleach solution preparation and reaction towers because the components in these sections suffer from high corrosion and erosion.

Potentiostatic anodic polarization and other related studies should also be done in the bleach liquor, chlorine water and vat liquor to know the passivation characteristics of the tested materials. These tests help in developing electrochemical protection system , another alternative for minimizing corrosion losses. The possible inhibitive effect of reducing corrosion in bleach liquors , by addition of sulfamic acid is also to be further investigated and understood. The other studies, which will help in understanding the corrosion reaction mechanism for chlorination washer are to conduct tests in chlorine water of various chlorine content at pH normally observed in these washers. In addition to the discussed studies, the performance of steels in chlorine waters should be evaluated with addition of varying amount of sulfamic acid .